

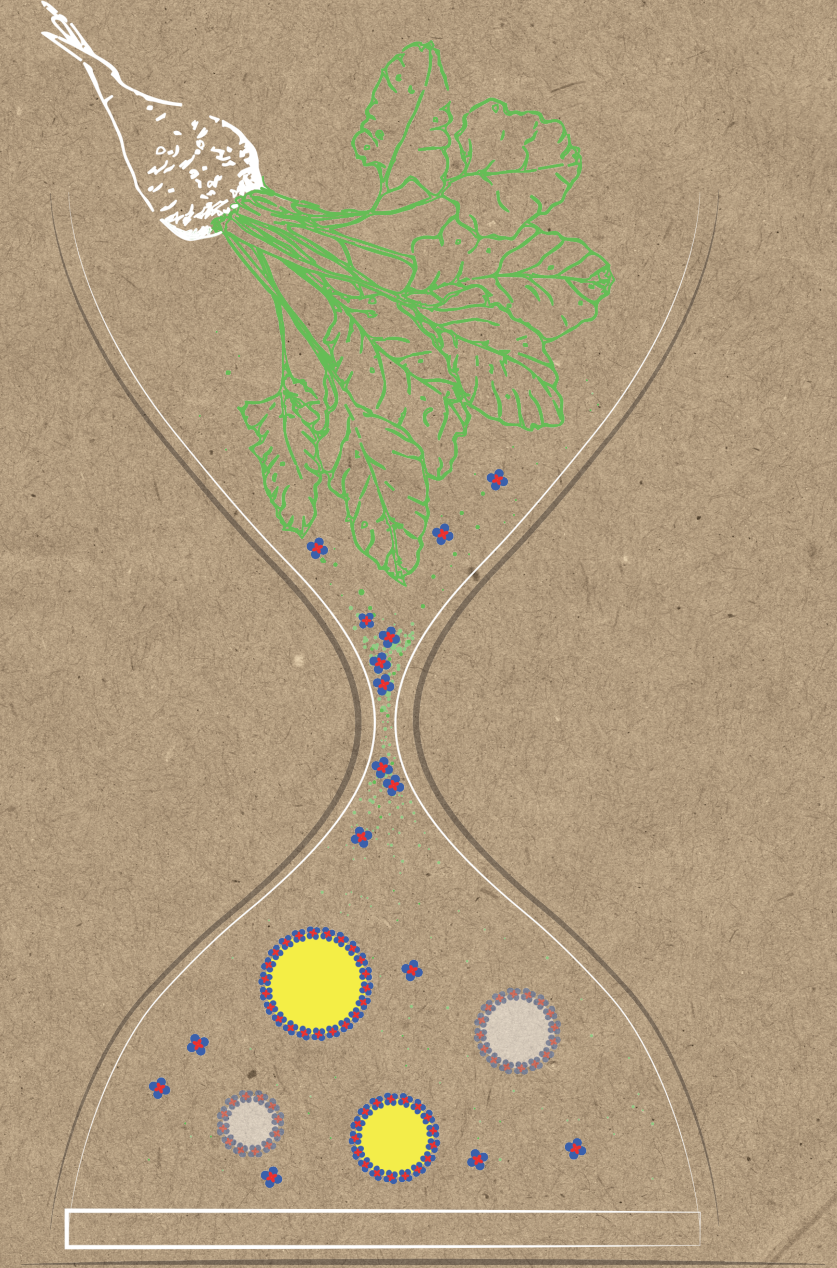
*Sugar Beet Leaves* : FROM BIOREFINERY TO TECHNO-FUNCTIONALITY

ALEXANDRA KISKINI

2017

# *Sugar Beet Leaves*

FROM BIOREFINERY TO TECHNO-FUNCTIONALITY



ALEXANDRA KISKINI



## Propositions

1. Plant age related differences in the chemical composition of leaves lead to increased PPO-mediated browning in leaves of old plants. (*this thesis*)
2. The formation of stable emulsions can be forecasted by using the molecular properties of the dominant proteins in non-pure protein mixtures. (*this thesis*)
3. Promoting gluten-free diet for improvement of irritable bowel syndrome symptoms is misleading.
4. The Heisenberg uncertainty principle extends to experimental social sciences when human subjects are incentivized to self-report their beliefs.
5. To improve gender equality at work, men and women must be obliged to take equal amounts of parental leave.
6. The number of meetings does not correlate positively with the amount of progress.

Propositions belonging to the thesis, entitled  
**Sugar beet leaves: from biorefinery to techno-functionality**

Alexandra Kiskini  
Wageningen, 13 October 2017

**Sugar beet leaves:**  
**from biorefinery to techno-functionality**

**Alexandra Kiskini**

## **Thesis committee**

### **Promotor**

Prof. Dr H. Gruppen  
Professor of Food Chemistry  
Wageningen University & Research

### **Co-promotor**

Dr P.A. Wierenga  
Assistant professor, Laboratory of Food Chemistry  
Wageningen University & Research

### **Other members**

Prof. Dr E. van der Linden, Wageningen University & Research  
Prof. Dr M.H.M. Eppink, Wageningen University & Research  
Dr L. Pouvreau, NIZO, Ede  
Dr A.C. Alting, Friesland Campina, Wageningen

This research was conducted under the auspices of the Graduate School VLAG (Advanced studies in Food Technology, Agrobiotechnology, Nutrition and Health Sciences).



# **Sugar beet leaves: from biorefinery to techno-functionality**

**Alexandra Kiskini**

## **Thesis**

submitted in fulfilment of the requirements for the degree of doctor

at Wageningen University

by the authority of the Rector Magnificus,

Prof. Dr A.P.J. Mol,

in the presence of the

Thesis Committee appointed by the Academic Board

to be defended in public

on Friday 13 October 2017

at 4 p.m. in the Aula.



Alexandra Kiskini

Sugar beet leaves: *from biorefinery to techno-functionality*,  
141 pages.

PhD thesis, Wageningen University, Wageningen, the Netherlands (2017)  
With references, with summary in English

ISBN: 978-94-6343-679-3

DOI: 10.18174/421994



*To  
Makis*





---

## Abstract

---

Sugar beet leaves (SBL), which are a side stream of the sugar beets cultivation, are currently left unexploited after sugar beets have been harvested. The general aim of this thesis was to study the biorefinery of SBL, with a special focus on the isolation of proteins. To reach this aim the research was divided into three sub-aims: 1) to determine whether there is variability in the chemical composition of the leaves due to pre-harvest conditions (plant age), 2) to evaluate the variability of the techno-functionality of leaf soluble protein concentrate (LSPC) due to system conditions and 3) to extend current product and process synthesis approaches to enable the design of biorefining process. To address the first aim, SBL collected at different time points were used. Despite a small variation in the chemical composition of the leaves of different plant ages, a large effect of the plant age on the quality of LSPC was observed. In particular, LSPC from old plants was brown (indicative of polyphenol oxidase - PPO - activity), whereas LSPC from young plants was yellow. Based on these data, samples extracted with sodium disulfite (to inhibit PPO-mediated browning) were used for further experiments. The obtained LSPC consisted mainly of protein (69.3% w/w db (N·5.23)) and carbohydrates (5.1% w/w db; half of which was charged carbohydrates). The main protein present in LSPC was Rubisco. The emulsion and foam properties of LSPC were studied as a function of protein concentration ( $C_p$ ), pH and ionic strength (I). The minimal  $C_p$  of LSPC needed to form a stable emulsion ( $C_{cr}$ ) was comparable to that of other widely used plant proteins, such as soy protein isolate. A critical  $\zeta$ -potential ( $\zeta_{cr} \sim 11$  mV) was identified, below which flocculation occurs. At pH 8.0 and high I (0.5 M) the  $C_{cr}$  was higher than at low I (0.01 M), which relates to a higher protein adsorbed amount at the interface ( $\Gamma_{max}$ ). The foam ability (FA) of LSPC increased with  $C_p$  at all conditions tested. The FA was related to the soluble and not to the total  $C_p$  in the bulk. Interestingly, the minimal  $C_{p,i}$  i.e.  $C_{crFA}$  needed to reach highest FA was constant as a function of pH. At high I (0.5 M) LSPC had higher FA than at low I (0.01 M), which was related to the faster adsorption of proteins at the interface. A minimum  $C_p$  was required to form stable foams. At pH 3.0 and 5.0 the foam stability of LSPC was higher than at pH 8.0. This was postulated to be due to formation of aggregates (between proteins or between proteins and charged carbohydrates). From these data it was shown that the techno-functional properties of LSPC could be linked to the molecular and interfacial properties of the dominant proteins in the concentrates. Thus, predictions for the techno-functional properties of impure systems, such as LSPC, can be made using only the known molecular properties of the dominant proteins and a small set of experiments. The knowledge acquired through the previous studies was used to adapt an existing methodology; namely the product-driven-process synthesis (PDPS) methodology, to extend its use in biorefinery. The adapted PDPS contained 4 novel steps, which facilitated its use in biorefinery. To illustrate how this new approach can be used in practice, a case study of a sugar beet leaves biorefinery was presented.





---

## Table of contents

---

<b>Chapter 1</b>	General Introduction	<b>1</b>
<b>Chapter 2</b>	Effect of plant age on the quantity and quality of proteins extracted from sugar beet ( <i>Beta vulgaris</i> L.) leaves	<b>23</b>
<b>Chapter 3</b>	Emulsion properties of sugar beet ( <i>Beta vulgaris</i> L.) leaf and soybean ( <i>Glycine max</i> ) proteins	<b>43</b>
<b>Chapter 4</b>	Foam properties of sugar beet ( <i>Beta vulgaris</i> L.) leaf and soybean ( <i>Glycine max</i> ) proteins	<b>65</b>
<b>Chapter 5</b>	Using product driven process synthesis in the biorefinery	<b>83</b>
<b>Chapter 6</b>	General Discussion	<b>109</b>
<b>Summary</b>		<b>129</b>
<b>Acknowledgements</b>		<b>133</b>
<b>About the author</b>		<b>137</b>





---

## General Introduction

---

To ensure sustainability in food processing the large volume of the waste or side streams needs to be valorized. In this thesis sugar beet leaves, which are a side stream of sugar beets (*Beta vulgaris* L.) cultivation, has been considered for its potential for recovery of valuable compounds, such as proteins. In the past, several studies have described extraction of proteins from leaves, but typically harsh conditions, e.g. use of heat during protein isolation, were used (1-4). In many reports, the obtained protein concentrates/isolates were further assessed for their use as functional ingredients in a variety of food products, such as emulsions and foams (5-8). From these reports, it becomes evident that the techno-functionality of the obtained protein concentrates/isolates depends on the intrinsic properties of the proteins. The latter can be affected by the presence of other non-protein compounds, e.g. presence of charged carbohydrates. Therefore, a variation in the chemical composition of the raw material and a variation of the protein isolation method that can both influence the chemical composition of the final protein concentrate/isolate, can ultimately affect the techno-functionality. Furthermore, the conditions of the system where the protein concentrates/isolates will be applied in can affect the techno-functionality. The aim of this thesis is to assess the variability of the soluble proteins isolated from sugar beet leaves (LSPC) due to a variation in the chemical composition of the raw material and to a variation in the isolation method. In addition, the effect of system conditions on the techno-functionality of LSPC is evaluated. Lastly, considering the techno-functionality of proteins, but also of other compounds present in an agricultural feedstock, and their sensitivity to various factors, a methodological approach for the design of a biorefining process is described.

### SUGAR BEET LEAVES

Sugar beet leaves are a side stream of the sugar beets cultivation. In the Netherlands in 2014 the sugar beets cultivation area was 75,094 ha (9). This translates to approximately 6.8 Mt beets (9) and 2.7 Mt leaves. Currently, after the sugar beets are harvested, the

sugar beet leaves are embedded in the soil. The dry matter composition of leaves comprises mainly proteins, carbohydrates, lipids and minerals, whereas other compounds, such as phenolic compounds, are present in smaller amounts (**Table 1.1**). Therefore, by embedding the leaves in the soil, a plethora of potentially valuable compounds, are left unexploited. It needs to be noted that due to the high water content of leaves (~ 90% (10)) the actual content of these compounds is rather low. However, given the high abundance of sugar beet leaves their exploitation for the extraction of valuable compounds is well justified. In a biorefinery process such compounds will be extracted and further used in various applications.

### CHEMICAL COMPOSITION OF (SUGAR BEET) LEAVES

Proteins are one of the main compounds present in leaves, accounting for 25-35% (5, 10, 11) of their dry matter (**Table 1.1**). Other major compounds commonly present in leaves include carbohydrates, ash and lipids.

**Table 1.1** Gross chemical composition (% w/w dry weight basis, db) of various leafy materials.

source	protein <sup>c</sup>	carbohydrate	ash	lipids
<i>Beta vulgaris</i> L. <sup>a</sup> (10)	28.7	30.7	16.2	10.6
<i>Medicago sativa</i> L. <sup>b</sup> (11)	24.9	22.5	9.6	4.8
<i>Solanum Africana</i> (5)	34.5	28.1	17.4	10.0
<i>Amaranthus hybridus</i> (5)	32.3	30.4	19.5	9.1
<i>Telfaria occidentalis</i> (5)	34.6	34.7	13.0	9.4
<i>Vernonia amygdalina</i> (5)	31.7	38.6	12.1	9.2

<sup>a</sup> Average values for leaves collected at 60, 80 and 100 days after sowing

<sup>b</sup> Average values for leaves grown in warm and cool growth chambers/ carbohydrate content refers to: total sugars, starch and crude fiber

<sup>c</sup> Protein is expressed as N\*6.25

It needs to be noted that often the values reported in literature for carbohydrate content are calculated by difference; i.e. subtraction from the total determined dry matter weight (10, 12). This might lead to an overestimation of the real carbohydrate content in the leaves. In addition, this method of calculation always leads to an apparent 100% characterization of the total dry matter of a sample, which is not always the case (13, 14).

The protein content of leaves reported in literature might also be often an overestimation of the true protein content. This is because the protein content is typically calculated by multiplying the total nitrogen content of the leaves by the conventionally used nitrogen-to-protein conversion factor (N-Prot factor) of 6.25. This is based on the assumption that all nitrogen present in leaves derives from proteins and that in these proteins the nitrogen content is 16%. However, leaves contain considerable amounts (~20%) of non-protein nitrogen (NPN) in the form of betaine (15), inorganic nitrogen, nucleic acids, free amino acids, ammonium salts, chlorophyll



and other organic nitrogen (16). In addition, the reported values of nitrogen in the proteinaceous amino acids from leaves range from 15.8 to 19.2% (16, 17). Thus, indeed the use of the conventional 6.25 N-Prot factor results in an overestimation of the true protein content. To determine the true protein content of leaves N-Prot factors need to be calculated based on the amino acid composition of the leaves. Based on the amino acid analysis and nitrogen determination two N-Prot factors; i.e.  $k_a$  and  $k_p$  (18) can be determined. The  $k_a$  is the ratio of the sum of amino acid residue weights, determined by amino acid analysis, to nitrogen weight from the recovered amino acids. The  $k_p$  is the ratio of the sum of amino acid residue weights to total nitrogen ( $N_T$ ) weight determined by, for instance, Dumas or Kjeldahl. The ratio of  $k_p/k_a$  gives an estimate of the NPN present in the samples. Based on the average of N-Prot factors ( $k_p$ ) determined for different leaves, a N-protein factor of 4.44 ( $\pm 0.22$ ) (16, 17) appears to give a much more accurate estimate of the true protein content in leaves.

### PROTEIN IN (SUGAR BEET) LEAVES

The proteins in leaves consist of both water soluble (50%) and insoluble (50%) fractions (19). Almost half of the soluble fraction consists of the enzyme ribulose-1,5-bisphosphate carboxylase oxygenase (Rubisco) (19). Rubisco plays an important role during photosynthesis; i.e. it catalyses the initial reaction during the conversion of inorganic  $CO_2$  to organic matter. In leaves, Rubisco is typically present in a hexadecameric form (Figure 1.1) by the association of 8 large ( $\sim 55$  kDa) and 8 small ( $\sim 15$  kDa) polypeptide chains (subunits), resulting in a total molecular mass of around 560 kDa (19, 20).

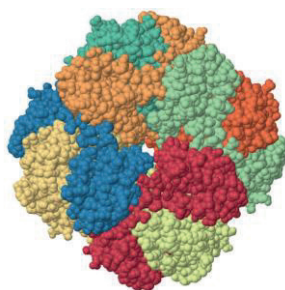


**Figure 1.1** Space filling model of the crystal structure of Rubisco obtained from spinach consisting of 8 large and 8 small subunits. All subunits are depicted with different colors (21).

Based on the amino acid sequence, the theoretical isoelectric point (pI) of Rubisco is around pH 6.0 (average of theoretical pI of large subunit; 6.33 and of small subunit; 5.84 (22)). The insoluble fraction mainly consists of membrane proteins of the chloroplasts. These proteins are associated with chlorophyll, carotenoids and lipids (19).

### PROTEIN EXTRACTION FROM LEAVES

The extraction of proteins from leaves typically consists of three steps: (1) cell disruption, (2) filtration and (3) isolation, i.e. separation or fractionation of proteins

(**Figure 1.2**). In the first step, the cells of the leaves are usually mechanically ruptured to release the cellular material. To this end, typically a homogenizer (e.g. blender, mill) or a press is used (5, 23-27). If blending or milling is used, the leaves are subsequently either squeezed (through a cheese cloth or a screw press) or filtered to remove the insoluble/fibrous material. After removal of the insoluble material, two different approaches are used to obtain protein concentrates/isolates. In one approach, the proteins are separated from the non-protein material to obtain a “whole protein concentrate” (whole leaf protein concentrate; WLPC). In the other approach, the proteins are fractionated into a “chloroplastic” or green fraction (green leaf protein fraction; GLPF) and a “cytoplasmatic” or white fraction (white leaf protein fraction, WLPF).

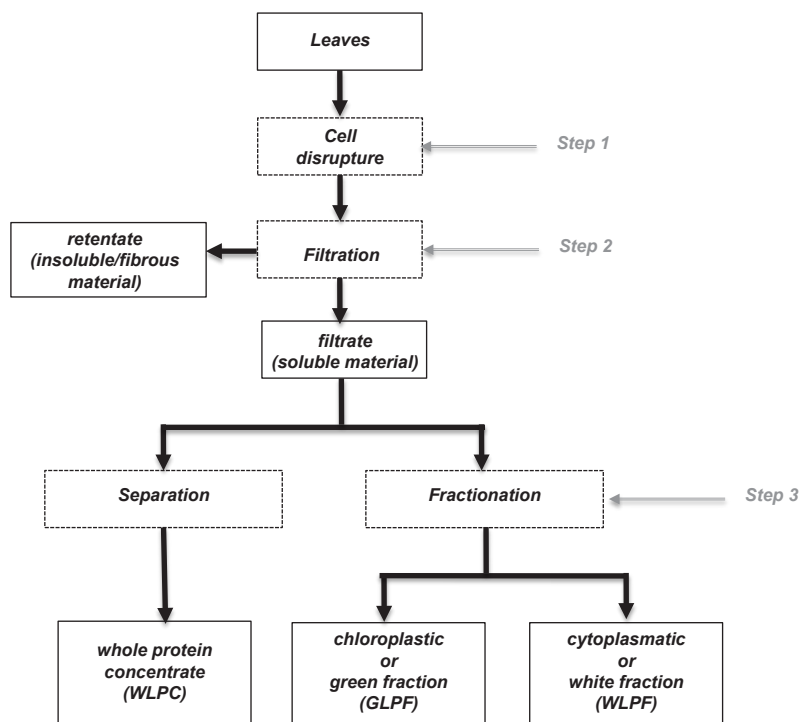


**Figure 1.2** Main steps in protein extraction from leaves to obtain either a whole protein concentrate (WLPC) or a green fraction (GLPF) and a white fraction (WLPF).

The most common methods described in literature for the isolation of WLPC are heating at 80-85 °C (4, 28), acid precipitation (26), ultrafiltration (4) or combination of the above (1, 28). A white leaf protein fraction (WLPF) can be obtained after removal of the green protein fraction (GLPF) using a two-step fractionation. The first step is typically achieved by heating at 50 – 60 °C (29-32), use of flocculants (33) or use of organic solvents (34). The final products of this step are an insoluble fraction (GLPF), which is typically obtained after centrifugation or filtration, and a soluble fraction. The soluble fraction can be further treated to obtain the white fraction (WLPF). The white

fraction is obtained by precipitation, which is commonly achieved by heating at high temperatures (80-85 °C) (29), use of acid (32) or combination of the above (33, 34) (**Table 1.2**).

**Table 1.2** Examples of the main methods described in literature for the separation or fractionation (step 3) of proteins from leaves. Data obtained from (1, 4, 29, 30, 33-35).

	Source	Isolation method	Fraction obtained	Protein content (% w/w db) in fraction <sup>a</sup>	Protein recovery %
Separation	<i>Medicago sativa</i> L.	heating 85°C (pH 8.5)	WLPC	61.9	42 of total
	<i>Beta vulgaris</i> L.	acid precipitation and heating pH 4.5 / 70°C, 5 min	WLPC	n.d.	n.d.
Fractionation	<i>Medicago sativa</i> L.	heating 60 °C, 20 s	GLFP	47.2	(15.1% based on total protein)
		heating 80 °C	WLFP	88.7	26.1 (8.7% based on total protein)
	<i>Medicago sativa</i> L.	heating 60°C, 20 s	GLFP	n.d.b	n.d.
		acid precipitation pH 3.5	WLFP	69.9	83
	<i>Medicago sativa</i> L. <i>Festuca arundinacea</i> L. var. Alta <i>Lolium multiflorum</i> L. var. RVP	organic solvents	GLFP	55 (50% true protein)	n.d.
		acid precipitation pH 4.0 (40 °C)	WLFP	60 (55% true protein)	n.d.
	<i>Medicago sativa</i> L. <i>Festuca arundinacea</i> L. var. Alta <i>Lolium multiflorum</i> L. var. Melle	floculants	GLFP	50 (45% true protein)	n.d.
		acid precipitation pH 4.0 (40 °C)	WLFP	65 - 75 (60 - 72% true protein)	n.d.
	<i>Beta vulgaris</i> L.	acid precipitation pH 5.3 (32 °C, 20 min)	GLFP	n.d.	n.d.
		acid precipitation and heating pH 4.5/ 70°C, 5 min	WLFP	58.9±1.4	54 (25% based on total protein)
	<i>Beta vulgaris</i> L.	heating 50°C, 5 or 10min / 55°C, 5 or 10min	GLFP	31.1 – 37.6	n.d.
		acid precipitation pH 3.0	WLFP	43.6 – 47.7	n.d.
	<i>Beta vulgaris</i> L.	heating 55°C, 5 min	GLFP	37.6	n.d.
		2 steps acid precipitation 1. pH 5.0 -5.6 2. pH 3.0	WLFP	54.2 – 63.2 66.1 – 82.1	n.d.

<sup>a</sup> Expressed as N\*6.25

<sup>b</sup> not determined

Regardless of the isolation method, and the source of the leaves, the main protein recovered in the final concentrate/isolate is Rubisco (3, 20, 32). The isolation method does, however, affect both the protein recovery and the protein purity of the final protein concentrate (**Table 1.2**). From an economical and an application point both protein recovery and protein purity of the final protein concentrate/isolate are important when extracting proteins from leafy materials. Moreover, special attention needs to be given on the (techno-)functionality of the isolated proteins, given that the (techno-)functionality determines the range of applications of a protein concentrate/isolate. Harsh conditions applied during protein extraction, e.g. extreme pH values and high temperatures, can negatively affect the protein techno-functionality. From example, as discussed below, heating at 80 °C during protein isolation from leaves leads to protein concentrates that are completely insoluble over the whole pH range (**Figure 1.3**). Therefore, in this thesis a mild isolation method; i.e. no use of a heating step, is employed.



## **AGRONOMIC AND ENVIRONMENTAL FACTORS AFFECTING QUANTITY AND QUALITY OF PROTEIN EXTRACTED FROM LEAVES**

In addition to the isolation method, various agronomic and environmental factors have been reported to affect the quantity of the extracted proteins. For example, for kale it was shown that the protein yield ( $\text{g/m}^2$ ) increased from 11.5 to 26.2% when a combination of nitrogen-phosphorus-potassium (NPK) fertilizer was used (4, 36). At the same time the ratio of protein nitrogen to total nitrogen in the extracted juice increased from 64.6 to 67.7%. Critical parameters regarding fertilization are the type and amount of fertilizer and the application time (36). Weather conditions during plant growth also play a key role in the amount of extractable leaf proteins. For example, a well irrigated soil allows plants for a more efficient nitrogen usage and also prevents nitrogen losses to the soil due to leaching. A 32% higher protein yield ( $\text{kg/ha}$ ) was obtained from kale grown in an irrigated than in a non-irrigated soil (36). Also, the age of the plant has been shown to influence the quantity of protein extracted from leaves. For winter wheat leaves, the protein yield decreased from 800  $\text{kg/ha}$  for leaves collected 60 days after sowing to ~600  $\text{kg/ha}$  for leaves collected 90 days after sowing (36). This decrease in protein yield was attributed to an increase in the NPN to protein nitrogen ratio (36). Other researchers have also reported effects of the plant age on the overall chemical composition of the leaves (10, 37, 38). Such effects are expected to influence not only the quantity of the extracted proteins but also the quality. For example, the total content of phenolic compounds in sugar beet leaves collected 100 days after sowing was approximately 1.5 times higher than that in leaves collected after 60 days (10). It is known, that the naturally present phenolic compounds in leaves can, upon cell disruption, be oxidized by endogenous polyphenol oxidases (PPOs). This reaction leads to quinones that can polymerize with other phenolic compounds (39) or covalently link to proteins (40). Protein modification can negatively affect the quality of the proteins, e.g. decrease their solubility (40), as is discussed in more detail below. Thus, in addition to the variation of the protein content, the variation of the overall chemical composition of leaves due to differences in plant age is of importance.

## **TECHNO-FUNCTIONAL PROPERTIES OF PROTEINS**

Proteins are often used as ingredients in food products because of their techno-functional properties, such as solubility, emulsion and foam properties. These properties depend on the intrinsic properties of the proteins, which in turn can be influenced by various parameters such as (1) the conditions (temperature;  $T$ , pH,  $I$ ) applied during protein isolation, (2) the conditions in the final system (termed here system conditions), and (3) the interaction with other compounds (e.g. other proteins and/or non-protein compounds). The major effects of these three parameters on solubility, emulsion and foam properties are discussed below.

### **Solubility**

Typically, the solubility of a protein is defined as the amount of protein that remains in solution under certain conditions, e.g. protein concentration ( $C_p$ ), pH and ionic strength,

relative to the initial amount of dispersed protein. Proteins have usually minimum solubility around their isoelectric point (pI). This relates to the fact that under these conditions the net charge of the protein, often measured as  $\zeta$ -potential, is zero, and thus there is no electrostatic repulsion between the protein molecules. Various factors related both to processing (e.g. conditions during protein isolation, purity of final protein concentrate) and to system conditions (e.g. pH, I) can affect the solubility of a protein. These factors are discussed in detail below.

Protein denaturation is one of the main problems encountered when temperatures higher than the denaturation temperature ( $T_d$ ) of the protein is used during protein isolation. Unfolding of the protein structure ultimately causes changes to the physico-chemical characteristics of the protein that subsequently lead to a decrease in protein solubility. **Figure 1.3** shows the differences in protein solubility as a function of pH for a protein concentrate obtained from alfalfa leaves using either acid or heat precipitation (2). When acid precipitation was used for the protein isolation, the solubility of the alfalfa protein concentrate showed a typical U-shape curve in the pH range from 2.0 to 10.0. However, when heating at 80 °C ( $> T_d$  of Rubisco (41)) was applied, the alfalfa protein concentrate was insoluble over the whole pH range. This is due to the denaturation of the proteins present in the alfalfa protein concentrate.

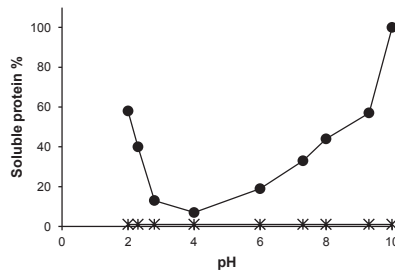


**Figure 1.3** Protein solubility at  $C_p = 7$  g/L (calculated from % soluble N) as a function of pH for acid precipitated (●) and heat precipitated (\*) alfalfa (*Medicago sativa* L.) proteins. The 100% protein solubility refers to 7 g/L (reproduced and adapted from (2)).

The ionic strength of the system can also affect the solubility of a protein. For example, an increase in ionic strength from 0.03 M to 0.25 M led to a decrease in solubility of helianthin from  $> 40\%$  to almost 0% in the pH range from 2.0 to 3.5. However, no effect on solubility was observed at pH  $> 4.0$  (**Figure 1.4 A**) (42). In this case, the loss of protein solubility was attributed to a reduced electrostatic repulsion energy that allowed the proteins at pH 3.0 to approach each other and form aggregates. In the same study it was shown that a change in ionic strength leads to changes in the association state of the protein; i.e. at pH 8.5 and  $I = 0.03$  M helianthin was present as 50% 11S and 50% 7S, whereas at pH 8.5 and  $I = 0.25$  M it was present as 70% 11S and 30% 7S (42). Whether such a difference in the association state of the protein at high and low ionic strength leads to a difference in the solubility of the protein cannot be derived from this study because the solubility of helianthin at each ionic strength was defined as % of protein dissolved at pH 8.5.

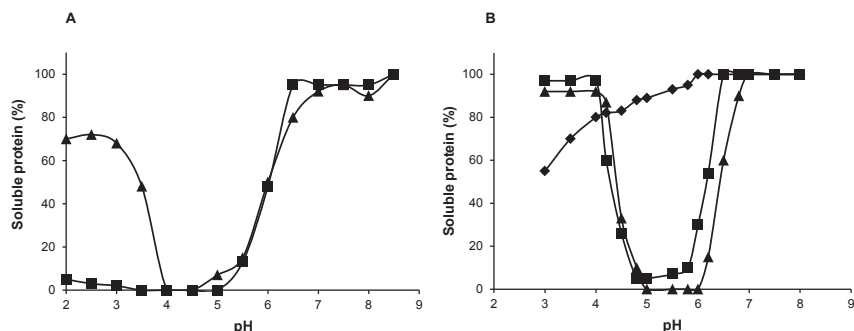


**Figure 1.4** Protein solubility as a function of pH for (A) helianthin at  $I = 0.03$  M (▲) and  $I = 0.25$  M (■) at  $C_p = 4$  g/L. and (B) glycinin at  $I = 0.03$  M (▲),  $I = 0.2$  M (■) and  $I = 0.5$  M (◆) at  $C_p = 6$  g/L. The protein solubility is expressed as protein solubility relative to the protein solubility at pH 8.5 (A) or pH 7.6 (B), hence the protein solubility at pH 8.5 (A) or pH 7.6 (B) is set at 100% (reproduced and adapted from (43, 44)).

Different proteins show different sensitivity to changes in ionic strength. An increase in ionic strength similar as described for helianthin had only a minor effect on the solubility of the soy protein glycinin (**Figure 1.4B**). However, for the same protein an increase in ionic strength from 0.03 M to 0.5 M led to a significant increase in the solubility in the pH range from 3.0 to 6.0 (**Figure 1.4B**). Furthermore, it was shown that the ionic strength affects the association state of glycinin (43). At pH 7.6 and  $I = 0.5$  M, glycinin is present as hexamer (45, 46), whereas at  $I = 0.03$  M it is predominantly present as hexamer, while a small part of it (15–20%) is present as trimer (43). Thus, the ionic strength of the system is of importance especially when multimeric proteins, e.g. Rubisco, are to be studied. With respect to Rubisco, to our knowledge, there is no literature available regarding the effect of ionic strength on the association/dissociation state of the protein. Typically, urea (47) or SDS (48) are applied to effectively dissociate Rubisco into its subunits.

In the case of complex mixtures, e.g. protein concentrates, a change of the association state of the protein due to ionic strength could lead to a change in the state of complexation between the protein molecules and the charged carbohydrates. The latter can ultimately lead to differences in protein solubility of the protein(s) present in the protein concentrates as a function of ionic strength. These effects might not be similar to the effects of ionic strength on the solubility of the pure protein(s). For example, for algae juice (24.5% w/w protein) at pH 5.5 the solubility (relative to the solubility at pH 8.0) at  $I = 0.03$  M and  $I = 0.5$  M was 60% and ~ 38%, respectively (13). For a more pure algae concentrate (ASPI; 64.4% w/w protein), the solubility (relative to the solubility at pH 8.0) at pH 5.5 was similar between the two ionic strengths tested (100%). Another interesting observation derived from this example is that the solubility of algae juice at pH 5.5 ( $I = 0.03$  M) was ~ 60%, whereas the solubility of algae concentrate was 100% (**Figure 1.5A**).

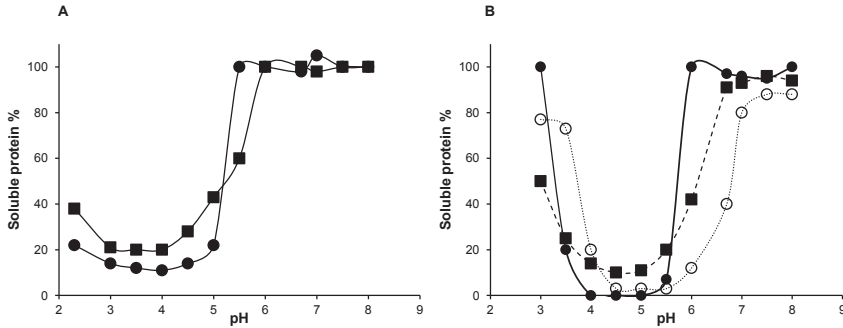


**Figure 1.5** Protein solubility as a function of pH for (A) for algae juice (i.e. ASPI before acid precipitation) (■) and purified ASPI (i.e. ASPI after acid precipitation) (●) and (B) glycinin (○),  $\beta$ -conglycinin (●), and SPI (64 glycinin, / 36  $\beta$ -conglycinin) (■) at  $C_p = 8$  g/L and  $I = 0.5$  M. The protein solubility is expressed as protein solubility relative to the protein solubility at pH 7.6 (A) or 8.0 (B), hence the protein solubility at pH 7.6 (A) or 8.0 (B) is set at 100% (reproduced and adapted from (13, 49)).

The difference in solubility between algae juice and algae concentrate might due to the overall difference in the chemical composition, e.g. difference in charged carbohydrates content, of algae juice and algae concentrate. However, the charged carbohydrate content for algae juice was not reported in this study (13). Charged carbohydrates and proteins can form complexes, which have a different overall charge than the pure proteins (50). Such complexation of proteins and charged carbohydrates will also shift the overall pI, and eventually alter the solubility profile of the protein. The presence of different proteins in a protein concentrate can also alter the solubility pattern of the protein concentrate as compared to the individual proteins. For example, glycinin and  $\beta$ -conglycinin, the main proteins of soy protein isolate, when fractionated were soluble up to 100% at pH 3.0, whereas their mixture (SPI) was only 50% soluble at the same pH (43) (**Figure 1.5B**). In the case of protein concentrates from leaves, the main protein present, as discussed earlier, is Rubisco, while other proteins such as photosystem II protein D1 (PSII) and chlorophyll a/b binding protein can also be found. Based on the amino acid sequence of Rubisco its theoretical pI is 6.1 (22). This pI is different from the apparent pI (pH where the minimum solubility is observed) of various Rubisco-containing protein concentrates. The reported apparent pI was around pH 4.5 (2). This apparent discrepancy can be due to the contribution of different proteins as well as the presence of charged carbohydrates in the protein concentrates.

The cross-linking of proteins with phenolic compounds can also influence the solubility of a protein. As discussed earlier, phenolic compounds that are naturally present in leaves can, upon cell rupture, be oxidized by endogenous polyphenol oxidase (PPO) into respective quinones (51). Once quinones are formed, they can polymerize with other phenolic compounds (39) or covalently link to proteins (40). The reaction products are brown (**Figure 1.6A**), and thus the color can be an indication of protein modification. Such protein modification can lead to decreased protein solubility (**Figure 1.6B**). The extent of modification and the effects of this modification on protein

functional properties may differ from protein to protein (40) as shown in **Figure 1.6B** for  $\alpha$ -lactalbumin and lysozyme.

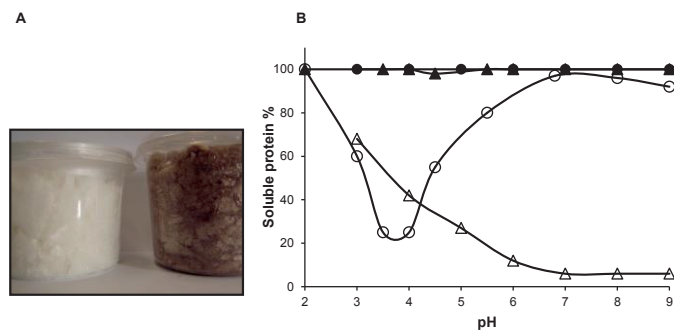


**Figure 1.6** (A) Protein obtained from *Solanum tuberosum* L. in the presence (white) or absence (brown) of ascorbic acid. (B) Protein solubility as a function of pH for unmodified (closed symbols) and PPO-modified (open symbols)  $\alpha$ -lactalbumin ( $\bullet$ ,  $\circ$ ) and lysozyme ( $\blacktriangle$ ,  $\triangle$ ) at  $C_p = 5$  g/L and  $I = 0.02$  M (reproduced and adapted from (40)).

To prevent the oxidation of phenolic compounds, and thus the cross-linking of proteins with phenolic compounds, typically ascorbic acid or sulfite is added in the protein extraction solvent. The anti-browning effect of ascorbic acid stems from its ability both to reduce quinones to their precursor phenolic compounds and to lower the pH of the material, which leads to PPO inactivation. Sulfite is known to prevent enzymatic browning, by inactivating the PPO and/or by formation of sulfo-adducts that do not contribute to browning (52).

### Formation of protein stabilized emulsions and foams

Emulsions and foams are colloidal systems in which oil (in emulsions) or air (in foams) is dispersed in a continuous liquid phase, e.g. water (53). Proteins tend to adsorb at the oil-water or air-water, respectively, interface and thus facilitate the formation of emulsions and foams, or else prevent the separation of the two phases (53). For emulsions, historically, a common way to characterize the emulsifying ability of a protein was to determine its emulsifying capacity (EC). The EC, which is widely used in literature, is typically expressed as the amount (mL) of oil emulsified by a certain amount (g) of protein. The results obtained from this method were qualitative and they could not be linked to the physico-chemical characteristics of the tested protein. Later, the emulsifying activity index (EAI) was introduced. The EAI was based on the turbidity of the emulsion after homogenization, which was directly related to the average droplet size ( $d_{3,2}$ ). A more quantitative description for the emulsifying ability of a protein has been more recently introduced (54, 55). In this approach, the emulsifying ability is characterized by the critical concentration ( $C_{cr}$ ); i.e. the minimum protein concentration needed to form a stable emulsion under given processing conditions (e.g. homogenization pressure, homogenization time, oil concentration). Below the  $C_{cr}$  (protein poor regime), there is not sufficient protein to fully cover the oil-water interface within the timescale of emulsification. As a consequence, the oil droplets coalesce



directly after homogenization. As the protein concentration increases more protein is available to cover the oil-water interface, and thus less coalescence is observed. This can be followed by measuring the average droplet size ( $d_{3,2}$ ) (**Figure 1.7A**).

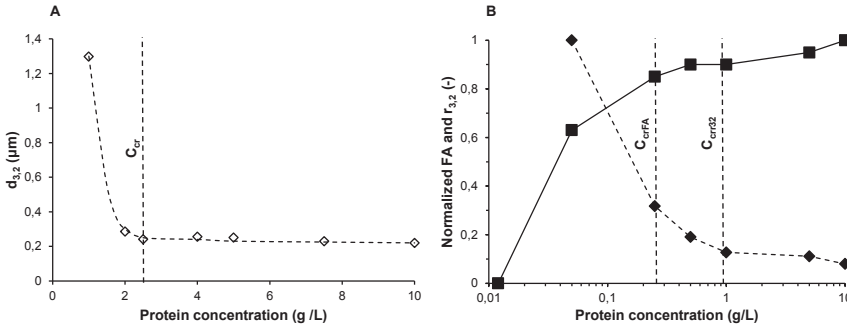


**Figure 1.7** (A) Average droplet diameter ( $d_{3,2}$ ) as a function of protein concentration for  $\beta$ -lactoglobulin at pH 7.0,  $I = 0.01$  M and  $\Phi = 0.1$ . Critical concentrations indicated by dotted lines (reproduced and adapted from (56)) (B) Normalized foam ability ( $\blacksquare$ ) and bubble radius ( $r_{3,2}$ ) ( $\blacklozenge$ ) as a function of protein concentration for  $\beta$ -lactoglobulin at pH 7.0. Critical concentrations indicated by dotted lines (reproduced and adapted from (57)).

In the protein poor regime the  $d_{3,2}$  decreases with increasing protein concentration. At  $C_p = C_{cr}$  the  $d_{3,2}$  reaches its minimum size ( $d_{3,2min}$ ), and becomes, thereafter, independent of protein concentration (at  $C_p > C_{cr}$ ; i.e. at the protein rich regime). The  $d_{3,2min}$  is determined by mechanical parameters, such as homogenization pressure, homogenization time etc.

Similarly to emulsions the foam ability (FA); i.e the amount of foam formed after sparging gas, of a protein increases with increasing protein concentration. In the case of foams, two critical concentrations have been identified; i.e.  $C_{crFA}$  and  $C_{cr3,2}$ , which demarcate the shift from the protein poor to the protein intermediate and the shift from the protein intermediate to the protein rich regime, respectively (**Figure 1.7B**). In the protein poor regime ( $C_p < C_{crFA}$ ) the foam ability increases with increasing protein concentration up to a maximum value ( $FA_{max}$ ), reached when  $C_p = C_{crFA}$ . In this regime, the bubbles are large, but their mean radius ( $r_{3,2}$ ) decreases with increasing protein concentration. In the intermediate-protein regime ( $C_{crFA} < C_p < C_{cr3,2}$ ) no further increase in foam ability is observed; i.e.  $FA = FA_{max}$ . In this regime the  $r_{3,2}$  still decreases with increasing protein concentration until  $C_p = C_{cr3,2}$ . At  $C_p = C_{cr3,2}$  the  $r_{3,2}$  reaches a minimum value and thereafter becomes independent of protein concentration (at  $C_p > C_{cr3,2}$ ; protein-rich regime).

### ***Effect of intrinsic properties and system conditions on protein stabilized emulsions and foams***

As described above, the adsorption of proteins at the interfaces is crucial for the formation and stability of emulsions and foams. Two main parameters of the adsorption play an important role in this process; the maximum amount of adsorbed protein ( $\Gamma_{max}$ ) and the adsorption rate. The latter was shown to be affected by the exposed hydrophobicity and the electrostatic repulsion (58, 59).

Before moving forward discussing the effect of intrinsic properties and system conditions on the stability of emulsions and foams we need to clarify some differences between these two colloidal systems. Typically, emulsions are made using multiple passes through the homogenizer. Therefore, in this case after the emulsification the emulsion droplets (at  $C_p > C_{cr}$ ) are stable against coalescence. Regarding foams, there are various ways to create bubbles, e.g. by whipping, sparging gas, fermenting yeast (60). Among these methods, the sparging of gas through porous plates or disks was shown to be one of the most reliable methods to form foam in a reproducible way (60). Therefore, this method is used for foam formation in this thesis. In this case, the bubbles are formed once (as opposed to "multiple passes" in case of emulsions). Therefore, after foam formation the bubbles can still coalesce.

*Emulsions.* Recently, Delahaije *et al.* (55) proposed a model for pure protein systems that links the adsorbed amount of protein ( $\Gamma_{max}$ ), which is needed to stabilize the oil-water interface, and the adsorption rate constant  $k_{adsorb}$  to the  $C_{cr}$ , the volume fraction of oil ( $\Phi_{oil}$ ) and the minimum average droplet size ( $d_{3,2min}$ ) (56). It was shown that for pure protein stabilized emulsions the values of  $\Gamma_{max}$  and  $k_{adsorb}$  can be estimated from the protein charge (related to electrostatic interactions), the relative exposed hydrophobicity and the protein radius (56). As expected proteins with different molecular characteristics were shown to have different  $C_{cr}$  at a given pH / I. For example, at pH 7.0, I = 0.01 M and 10% (v/v) sunflower oil the  $C_{cr}$  of lysozyme, ovalbumin and  $\beta$ -lactoglobulin were > 25 g/L, ~ 10 g/L and ~2 g/L, respectively (55). The difference in  $C_{cr}$  was attributed to the difference in the relative exposed hydrophobicity of these three proteins; 0.06, 0.19 and 1.00, respectively.

After the formation of an emulsion that is stable against coalescence, the system conditions can change, e.g. decrease of pH or ionic strength. At pH values close to the pI of the protein flocculation occurs. The latter is due to low electrostatic repulsion; i.e. there is not sufficient charge on the adsorbed layer to dominate over the attractive interactions (e.g. van der Waals and hydrophobic) between emulsion droplets. This can be observed by an increase in  $d_{3,2}$ . In this case the  $d_{3,2}$  reflects the diameter of the flocculate and not the droplet diameter (**Figure 1.8**). When there is sufficient amount of protein to fully cover the oil-water interface the flocculation is reversible as soon as the pH is brought away from the pI (61). In other words, in protein poor regime ( $C_p < C_{cr}$ ) the stability against flocculation is determined by the change in adsorbed amount. In protein rich regime ( $C_p > C_{cr}$ ) the stability against flocculation is mostly due to fact that repulsion becomes too low (61).

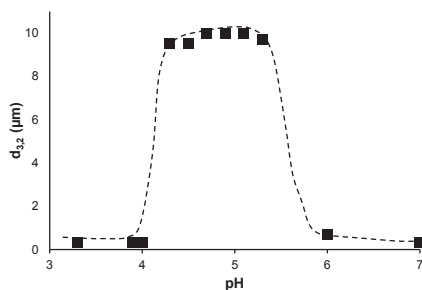


**Figure 1.8** Average droplet diameter ( $d_{3,2}$ ) of whey protein isolate (WPI) stabilized emulsions (10% oil,  $I = 0.03 \pm 0.01$  M,  $C_p = 10$  g/L) made at pH 8.0 and then adjusted to various pH values (reproduced and adapted from (61))

At high ionic strengths a decrease of the electrostatic repulsion between the proteins leads to a decrease of the effective radius of the protein at the interface. As a consequence, more proteins have to adsorb to completely cover the oil-water interface, and thereby prevent flocculation (**Figure 1.9**). This explains the observation that at high ionic strength the  $C_{cr}$  is higher than at low ionic strength (62).

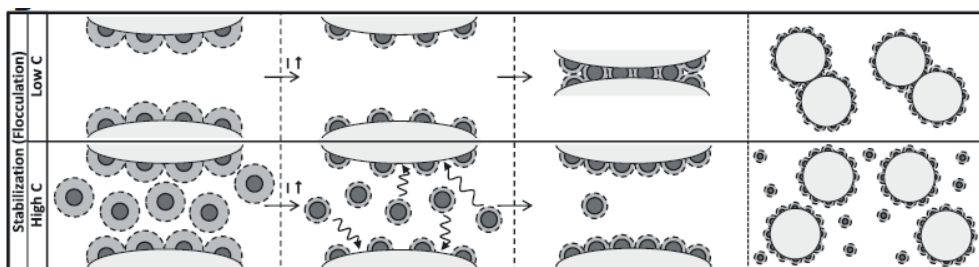


**Figure 1.9** Effect of high and low protein concentration on the emulsion stability against flocculation after formation (dark grey and light grey circles represent the protein and the Debye double-layer, respectively) (adapted from (55)).

The stability of protein stabilized emulsions against flocculation can be improved by the presence of charged carbohydrates. Anionic carbohydrates can form complexes with proteins, and co-adsorb at the oil-water interface. As a consequence a more charged layer is created at the oil-water interface, and thus the electrostatic repulsion is higher. For example, in pure  $\beta$ -lactoglobulin stabilized emulsions flocculation was observed in the pH range 4.0 – 5.5, which is around the pI of  $\beta$ -lactoglobulin ( $pI = 4.9$  (57)), whereas in mixed  $\beta$ -lactoglobulin-pectin stabilized emulsions no flocculation was shown at the same pH range. This was attributed to the higher electrostatic repulsion in this pH range for mixed  $\beta$ -lactoglobulin-pectin than for pure  $\beta$ -lactoglobulin, as shown by droplet  $\zeta$ -potential measurements (62). A similar effect; i.e. protein-charged carbohydrates stabilized emulsions are stable around the iso-electric point of the protein, while the pure protein stabilized emulsions are not, was also observed for ASPI

(14). In addition, the complexation of proteins with carbohydrates can lead to the formation of a thicker adsorbed layer, and thus steric stabilization.

*Foams.* Foam stability describes the stability (against coalescence and/or disproportionation) of the foam in time. A measure of foam stability is the half life time ( $t_{1/2}$ ), which is the time at which half of the initial foam volume (or height) has collapsed. As described above, at  $C_p > C_{cr32}$  (protein-rich regime) the bubble radius decreases with increasing protein concentration (57). The decrease of  $r_{3,2}$  is expected to decrease drainage rate and increase foam stability. However, for several proteins, e.g.  $\beta$ -lactoglobulin (57) and  $\alpha$ -lactalbumin (63) the foam stability was found to decrease at  $C_p > C_{cr32}$  even though one might expect either a constant, or increasing foam stability with increasing protein concentration.

The pH of the system was shown to affect foam stability. Typically, a protein is expected to have maximum foam stability at pH values close to its pI. That was shown for a number of proteins, such as alfalfa protein concentrate (8) and egg white albumin (EWA) (64). The high foam stability under these conditions was attributed to the fact that the electrostatic repulsion between the protein molecules is minimal, and subsequently the adsorption of the protein at the air-water interface is maximal. However, other researchers found different effects. For example, Kuropatwa *et al.* (65) found that the stability of whey protein isolate (WPI) stabilized foams was the lowest at pH 5.0 (pI of WPI). The latter was attributed to the formation of  $\beta$ -lactoglobulin octamers. Another factor that affects foam stability is the ionic strength of the system. For some proteins, e.g. WPI, the foam stability at pH 5.0 was higher at high ( $I = 0.2$  M) than at low ( $I = 0.01$  M) ionic strength, whereas for other proteins, e.g. EWA, no effect of ionic strength was observed under these conditions (64). For complex (non-pure protein) systems, such as protein concentrates, the composition of the concentrate has an effect on the foam properties. For example, it was shown that the foam stability of protein-charged carbohydrates complexes was higher than the foam stability of pure protein systems (66). This was attributed to the more rigid interface formed in the presence of protein-carbohydrates complexes. However, it needs to be noted that the role of aggregates on foam stability is controversial. In some studies, it was shown that the presence of aggregates had a positive effect (63), while in some others it was shown that large aggregates can negatively affect foam stability (67).

## DESIGNING OF A BIOREFINERY PROCESS

From the previous sections it becomes clear that proteins isolated from leaves can be used in a variety of applications as functional ingredients. However, to further increase the economic revenue from the exploitation of leaves, a biorefinery approach needs to be followed. The design of a biorefining process is challenging due to the high number of products (i.e. compounds) that can be obtained from one feedstock and the plethora of possible pathways that can lead to these products. Therefore, a systematic approach for the process design is needed. Typically, in literature the main focus of such approaches is on the identification and selection of the optimum processing pathway given certain objectives, such as yield maximization, energy minimization, or economic

performance (68). However, to design an optimal biorefining process also the specific physico-chemical properties of the individual final products need to be considered. The latter has been the focus of the product design methodologies (69-72). Thus, both product and process design methodologies need to be used. In the last years, a number of methodologies that integrate product and process design were published.

The product driven process synthesis (PDPS) methodology combines both the product and process design and can be used for this purpose. PDPS was first introduced as a structured approach towards the synthesis of a process in the food sector, where several raw materials are combined to produce one final product (72). Later, it was also successfully applied for the design of the separation process of one compound from a feedstock, e.g. the isolation of isoflavones from okara (73), the separation of oleosomes from soybeans (74), and the separation of polyphenols from tea (75). The use of PDPS in a separation process is not as straightforward as in the case of structured products. Some of the challenges, which have been already identified by Jankowiak *et al.* (73), are due to the complexity induced by the interaction among the different compounds present in the feedstock, which hinders the isolation of pure compounds. Moreover, in contrast to the production of a structured product, in the case of a separation process the raw material; i.e. the feedstock, may be less well defined or even less constant with respect to the composition. In other words, various factors, such as weather, soil, fertilizers, plant age, as discussed above, can lead to changes in the chemical composition of the feedstock, and as a consequence induce changes to the quantity and quality of the final product. The isolation process itself can influence the quantity, quality and composition of the final products. Finally, the composition and the state (e.g. native/denatured) of the final product define the applications in which the final product can be used. In the case of a biorefinery process, where multiple products are to be separated (extracted) simultaneously or consecutively the design of the process becomes even more complicated. To address all these challenges PDPS in its current form needs to be adapted.

## AIM OF THIS THESIS

The aim of this thesis is to study the biorefinery of sugar beet leaves, with a special focus on the isolation of proteins. The research is therefore divided into three sub-aims. The first sub-aim is to determine whether there is a variability in the chemical composition of the leaves, and thus in the quantity and quality of the extracted proteins, due to pre-harvest conditions (plant age). The second sub-aim is to evaluate the variability of the techno-functionality of LSPC due to system conditions, and the third sub-aim is to extend current product and process synthesis approaches to enable the design of a biorefining process.



## THESIS OUTLINE

The outline of this thesis is schematically shown in **Figure 1.10**.

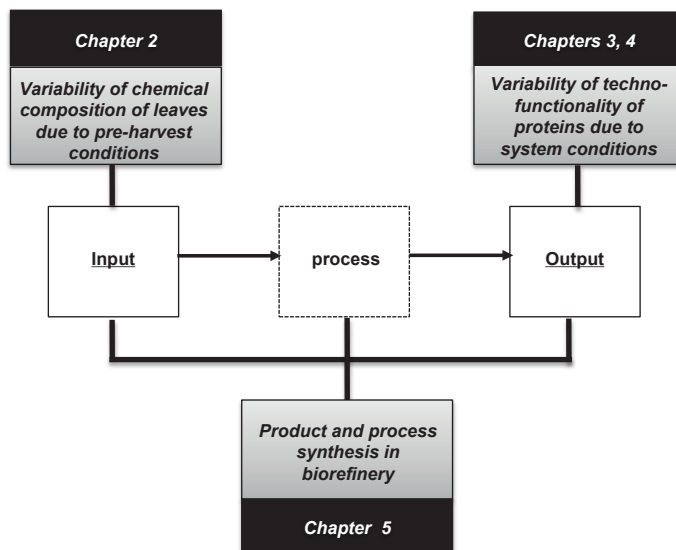


**Figure 1.10** Schematic representation of the thesis outline.

First the variation in the chemical composition of sugar beet leaves, due to variation in plant age (i.e. harvesting time), is studied (**Chapter 2**). For this, leaves from sugar beets grown in a field and in a greenhouse are used. The effects of this variation on the subsequent quantity and quality (color) of the extracted protein concentrate (LSPC) are determined. In the next two chapters, the effect of various system conditions on the techno-functional properties of LSPC is described. This is done using two approaches recently developed to describe the emulsion and foam properties of pure protein stabilized systems, and link them to the molecular properties of the protein. These approaches are used to obtain a quantitative characterization of the techno-functional properties of sugar beet leaf proteins and also link these properties to the molecular properties of the main proteins present in LSPC. More specifically, **Chapter 3** focusses on the effect of protein concentration, pH and ionic strength on the emulsion properties of LSPC. **Chapter 4** extends this work by studying the effect of the same conditions on the foam properties of LSPC. In both chapters, soy protein isolate (SPI) is used as a reference. SPI is selected as a reference protein because of its origin (plant-derived) and because, similarly to LSPC, it is a mixture of a (multimeric) protein and other non-protein compounds. In **Chapter 5**, an existing methodology, namely the product driven process synthesis (PDPS) that was developed for structured products, is adapted for use in biorefineries. A case study of a sugar beet leaves biorefinery is shown as an example. In the last chapter (**Chapter 6**), the main results obtained in the previous chapters are discussed with respect to data shown in literature. The chapter ends with

an outlook of how the knowledge acquired through this thesis can be further implemented in literature.

## References

1. Merodio, C.; Sabater, B., Preparation and properties of a white protein fraction in high yield from sugar beet (*Beta vulgaris* L.) leaves. *Journal of the Science of Food and Agriculture* **1988**, *44*, 237-243.
2. Betschart, A. A., Nitrogen solubility of alfalfa protein concentrate as influenced by various factors. *Journal of Food Science* **1974**, *39*, 1110-1115.
3. Koschuh, W.; Povoden, G.; Thang, V. H.; Kromus, S.; Kulbe, K. D.; Novalin, S.; Krotscheck, C., Production of leaf protein concentrate from ryegrass (*Lolium perenne* x multiflorum) and alfalfa (*Medicago sativa* subsp. sativa). Comparison between heat coagulation/centrifugation and ultrafiltration. *Desalination* **2004**, *163*, 253-259.
4. Kohler, G.; Knuckles, B., Edible protein from leaves. *Food Technology* **1977**, *31*, 191-195.
5. Aletor, O.; Oshodi, A. A.; Ipinmoroti, K., Chemical composition of common leafy vegetables and functional properties of their leaf protein concentrates. *Food chemistry* **2002**, *78*, 63-68.
6. Sheen, S. J., Comparison of chemical and functional properties of soluble leaf proteins from four plant species. *Journal of Agriculture and Food Chemistry* **1991**, *39*, 681-685.
7. Knuckles, B. E.; Kohler, G. O., Functional properties of edible protein concentrates from alfalfa. *Journal of Agriculture and Food Chemistry* **1982**, *30*, 748-752.
8. Lamsal, B.; Koegel, R.; Gunasekaran, S., Some physicochemical and functional properties of alfalfa soluble leaf proteins. *LWT-Food Science and Technology* **2007**, *40*, 1520-1526.
9. FAOSTAT Production of sugar beets in Netherlands. (09/06/2017)
10. Biondo, P. B. F.; Boeing, J. S.; Barizão, É. O.; Souza, N. E. d.; Matsushita, M.; Oliveira, C. C. d.; Boroski, M.; Visentainer, J. V., Evaluation of beetroot (*Beta vulgaris* L.) leaves during its developmental stages: a chemical composition study. *Food Science and Technology* **2014**, *34*, 94-101.
11. Smith, D., Yield and chemical composition of leaves and stems of alfalfa at intervals up the shoots. *Journal of Agriculture and Food Chemistry* **1970**, *18*, 652-656.
12. Teixeira, E. M. B.; Carvalho, M. R. B.; Neves, V. A.; Silva, M. A.; Arantes-Pereira, L., Chemical characteristics and fractionation of proteins from *Moringa oleifera* Lam. leaves. *Food Chemistry* **2014**, *147*, 51-54.
13. Schwenzfeier, A.; Wierenga, P. A.; Gruppen, H., Isolation and characterization of soluble protein from the green microalgae *Tetraselmis* sp. *Bioresource Technology* **2011**, *102*, 9121-9127.
14. Schwenzfeier, A.; Wierenga, P. A.; Eppink, M. H.; Gruppen, H., Effect of charged polysaccharides on the techno-functional properties of fractions obtained from algae soluble protein isolate. *Food Hydrocolloids* **2014**, *35*, 9-18.
15. Mäck, G.; Hoffmann, C. M.; Märlander, B., Nitrogen compounds in organs of two sugar beet genotypes (*Beta vulgaris* L.) during the season. *Field crops research* **2007**, *102*, 210-218.
16. Milton, K.; Dintzis, F. R., Nitrogen-to-protein conversion factors for tropical plant samples. *Biotropica* **1981**, *13*, 177-181.

17. Yeoh, H.-H.; Wee, Y.-C., Leaf protein contents and nitrogen-to-protein conversion factors for 90 plant species. *Food Chemistry* **1994**, *49*, 245-250.
18. Mosse, J., Nitrogen-to-protein conversion factor for ten cereals and six legumes or oilseeds. A reappraisal of its definition and determination. Variation according to species and to seed protein content. *Journal of Agriculture and Food Chemistry* **1990**, *38*, 18-24.
19. Fiorentini, R.; Galoppini, C., The proteins from leaves. *Plant Foods for Human Nutrition* **1983**, *32*, 335-350.
20. Barbeau, W. E.; Kinsella, J. E., Ribulose biphosphate carboxylase/oxygenase (rubisco) from green leaves-potential as a food protein. *Food Reviews International* **1988**, *4*, 93-127.
21. <http://www.rcsb.org/pdb/home/home.do>. (31/03/2017)
22. UniProtKB <http://www.uniprot.org/> (08/05/2017)
23. Carroad, P. A.; Anaya-Serrano, H.; Edwards, R. H.; Kohler, G. O., Optimization of cell disruption for alfalfa leaf Protein Concentration (Pro-Xan) Production. *Journal of Food Science* **1981**, *46*, 383-386.
24. Betschart, A.; Kinsella, J. E., Extractability and solubility of leaf protein. *Journal of Agriculture and Food Chemistry* **1973**, *21*, 60-65.
25. Tamayo Tenorio, A.; Gieteling, J.; de Jong, G. A. H.; Boom, R. M.; van der Goot, A. J., Recovery of protein from green leaves: Overview of crucial steps for utilisation. *Food Chemistry* **2016**, *203*, 402-408.
26. Ghazi, A.; Metwali, S.; Atta, M., Protein isolates from Egyptian sweet potato leaves. *Molecular Nutrition & Food Research* **1989**, *33*, 145-151.
27. Devi, A. V.; Rao, N.; Vijayaraghavan, P., Isolation and composition of leaf protein from certain species of Indian flora. *Journal of the Science of Food and Agriculture* **1965**, *16*, 116-120.
28. Pandey, V.; Srivastava, A., A simple, low energy requiring method of coagulating leaf proteins for food use. *Plant Foods for Human Nutrition* **1993**, *43*, 241-245.
29. Edwards, R. H.; Miller, R. E.; De Fremery, D.; Knuckles, B. E.; Bickoff, E.; Kohler, G. O., Pilot plant production of an edible white fraction leaf protein concentrate from alfalfa. *Journal of Agriculture and Food Chemistry* **1975**, *23*, 620-626.
30. Miller, R. E.; De Fremery, D.; Bickoff, E.; Kohler, G. O., Soluble protein concentrate from alfalfa by low-temperature acid precipitation. *Journal of Agriculture and Food Chemistry* **1975**, *23*, 1177-1179.
31. Hernandez, A.; Martinez, C.; Alzueta, C., Effects of alfalfa leaf juice and chloroplast-free juice pH values and freezing upon the recovery of white protein concentrate. *Journal of Agriculture and Food Chemistry* **1989**, *37*, 28-31.
32. Lamsal, B. P.; Koegel, R. G.; Gunasekaran, S., Some physicochemical and functional properties of alfalfa soluble leaf proteins. *LWT - Food Science and Technology* **2007**, *40*, 1520-1526.
33. Bray, W. J.; Humphries, C., Preparation of white leaf protein concentrate using a polyanionic flocculant. *Journal of the Science of Food and Agriculture* **1979**, *30*, 171-176.
34. Bray, W. J.; Humphries, C., Solvent fractionation of leaf juice to prepare green and white protein products. *Journal of the Science of Food and Agriculture* **1978**, *29*, 839-846.
35. Jwanny, E. W.; Montanari, L.; Fantozzi, P., Protein production for human use from sugarbeet: Byproducts. *Bioresource Technology* **1993**, *43*, 67-70.

36. Arkcoll, D. B.; Festenstein, G. N., A preliminary study of the agronomic factors affecting the yield of extractable leaf protein. *Journal of the Science of Food and Agriculture* **1971**, *22*, 49-56.
37. Addy, T. O.; Whitney, L.F.; Chen, C.S. , Mechanical parameters in leaf cell rupture for protein production. In *Leaf protein concentrates*, Telek, L. G., H. D. , Ed. AVI Publishing Co., Inc. : 1983.
38. Chutichudet, B.; Chutichudet, P.; Kaewsit, S., Influence of developmental stage on activities of polyphenol oxidase, internal characteristics and colour of lettuce cv. grand rapids. *American Journal of Food Technology* **2011**, *6*, 215-225.
39. Cheynier, V.; Owe, C.; Rigaud, J., Oxidation of grape juice phenolic compounds in model solutions. *Journal of Food Science* **1988**, *53*, 1729-1732.
40. Prigent, S. V.; Voragen, A. G.; Visser, A. J.; van Koningsveld, G. A.; Gruppen, H., Covalent interactions between proteins and oxidation products of caffeoylquinic acid (chlorogenic acid). *Journal of the Science of Food and Agriculture* **2007**, *87*, 2502-2510.
41. Tomimatsu, Y., Macromolecular properties and subunit interactions of ribulose-1, 5-bisphosphate carboxylase from alfalfa. *Biochimica et Biophysica Acta (BBA)-Protein Structure* **1980**, *622*, 85-93.
42. González-Pérez, S.; Vereijken, J. M.; Merck, K. B.; van Koningsveld, G. A.; Gruppen, H.; Voragen, A. G., Conformational states of sunflower (*Helianthus annuus*) helianthinin: effect of heat and pH. *Journal of Agriculture and Food Chemistry* **2004**, *52*, 6770-6778.
43. Lakemond, C. M.; de Jongh, H. H.; Hessing, M.; Gruppen, H.; Voragen, A. G., Soy glycinin: influence of pH and ionic strength on solubility and molecular structure at ambient temperatures. *Journal of Agriculture and Food Chemistry* **2000**, *48*, 1985-1990.
44. González-Pérez, S.; Vereijken, J. M.; Van Koningsveld, G. A.; Gruppen, H.; Voragen, A. G., Physicochemical properties of 2S albumins and the corresponding protein isolate from sunflower (*Helianthus annuus*). *Journal of food science* **2005**, *70*, C98-C103.
45. Badley, R. A.; Atkinson, D.; Hauser, H.; Oldani, D.; Green, J. P.; Stubbs, J. M., The structure, physical and chemical properties of the soy bean protein glycinin. *Biochimica et Biophysica Acta (BBA) - Protein Structure* **1975**, *412*, 214-228.
46. Iyengar, R.; Ravestein, P., New aspects of subunit structure of soybean glycinin. *Cereal Chemistry* **1981**, *58*, 325-330.
47. Voordow, G.; Vies, S. M.; Bouwmeister, P. P., Dissociation of ribulose-1, 5-bisphosphate carboxylase/oxygenase from spinach by urea. *European journal of biochemistry* **1984**, *141*, 313-318.
48. Ru, Q.-H.; Luo, G.-A.; Li, S.; Lu, W.; Li, G.-F.; Gong, Y.-D., Dissociation of ribulose-1, 5-bisphosphate carboxylase/oxygenase (Rubisco) observed by capillary electrophoresis. *Analyst* **2000**, *125*, 1087-1090.
49. Kuipers, B. J.; van Koningsveld, G. A.; Altling, A. C.; Driehuis, F.; Voragen, A. G.; Gruppen, H., Opposite contributions of glycinin- and  $\beta$ -conglycinin-derived peptides to the aggregation behavior of soy protein isolate hydrolysates. *Food Biophysics* **2006**, *1*, 178-188.
50. Benichou, A.; Aserin, A.; Lutz, R.; Garti, N., Formation and characterization of amphiphilic conjugates of whey protein isolate (WPI)/xanthan to improve surface activity. *Food Hydrocolloids* **2007**, *21*, 379-391.
51. Pourcel, L.; Routaboul, J. M.; Cheynier, V.; Lepiniec, L.; Debeaujon, I., Flavonoid oxidation in plants: from biochemical properties to physiological functions. *Trends in plant science* **2007**, *12*, 29-36.

52. Kuijpers, T. F.; Narváez-Cuenca, C. E.; Vincken, J. P.; Verloop, A. J.; van Berkel, W. J.; Gruppen, H., Inhibition of enzymatic browning of chlorogenic acid by sulfur-containing compounds. *Journal of Agriculture and Food Chemistry* **2012**, *60*, 3507-3514.
53. Hailing, P. J.; Walstra, P., Protein-stabilized foams and emulsions. *Critical Reviews in Food Science & Nutrition* **1981**, *15*, 155-203.
54. Tcholakova, S.; Denkov, N.; Lips, A., Comparison of solid particles, globular proteins and surfactants as emulsifiers. *Physical Chemistry Chemical Physics* **2008**, *10*, 1608-1627.
55. Delahaije, R. J.; Gruppen, H.; Giuseppin, M. L. F.; Wierenga, P. A., Towards predicting the stability of protein-stabilized emulsions. *Advances in Colloid and Interface Science* **2015**, *219*, 1-9.
56. Delahaije, R. J.; Gruppen, H.; Giuseppin, M. L.; Wierenga, P. A., Quantitative description of the parameters affecting the adsorption behaviour of globular proteins. *Colloids and Surfaces B: Biointerfaces* **2014**, *123*, 199-206.
57. Lech, F. J.; Delahaije, R. J.; Meinders, M. B.; Gruppen, H.; Wierenga, P. A., Identification of critical concentrations determining foam ability and stability of  $\beta$ -lactoglobulin. *Food Hydrocolloids* **2016**, *57*, 46-54.
58. Wierenga, P.; Gruppen, H., New views on foams from protein solutions. *Current Opinion in Colloid & Interface Science* **2010**, *15*, 365-373.
59. Damodaran, S.; Song, K. B., Kinetics of adsorption of proteins at interfaces: role of protein conformation in diffusional adsorption. *Biochimica et Biophysica Acta (BBA)-Protein Structure and Molecular Enzymology* **1988**, *954*, 253-264.
60. Drenckhan, W.; Saint-Jalmes, A., The science of foaming. *Advances in colloid and interface science* **2015**, *222*, 228-259.
61. Delahaije, R. J.; Hilgers, R. J.; Wierenga, P. A.; Gruppen, H., Relative contributions of charge and surface coverage on pH-induced flocculation of protein-stabilized emulsions. *Colloids and Surfaces A: Physicochemical and Engineering Aspects* **2016**, *25*, 390-398.
62. Guzey, D.; McClements, D. J., Impact of electrostatic interactions on formation and stability of emulsions containing oil droplets coated by  $\beta$ -lactoglobulin-pectin complexes. *Journal of Agriculture and Food Chemistry* **2007**, *55*, 475-485.
63. Dhayal, S. K.; Delahaije, R. J.; de Vries, R. J.; Gruppen, H.; Wierenga, P. A., Enzymatic cross-linking of  $\alpha$ -lactalbumin to produce nanoparticles with increased foam stability. *Soft matter* **2015**, *11*, 7888-7898.
64. Schwenzfeier, A.; Lech, F.; Wierenga, P. A.; Eppink, M. H. M.; Gruppen, H., Foam properties of algae soluble protein isolate: Effect of pH and ionic strength. *Food Hydrocolloids* **2013**, *33*, 111-117.
65. Kuropatwa, M.; Tolkach, A.; Kulozik, U., Impact of pH on the interactions between whey and egg white proteins as assessed by the foamability of their mixtures. *Food Hydrocolloids* **2009**, *23*, 2174-2181.
66. Miquelim, J. N.; Lannes, S. C.; Mezzenga, R., pH Influence on the stability of foams with protein-polysaccharide complexes at their interfaces. *Food Hydrocolloids* **2010**, *24*, 398-405.
67. Rullier, B.; Novales, B.; Axelos, M. A., Effect of protein aggregates on foaming properties of  $\beta$ -lactoglobulin. *Colloids and Surfaces A: Physicochemical and Engineering Aspects* **2008**, *330*, 96-102.
68. Ng, K. M., A Multidisciplinary Hierarchical Framework for the Design of Consumer Centered Chemical Products. *Computer Aided Chemical Engineering*, **2015**, *37*, 15-24.



69. Bernardo, F. P.; Saraiva, P. M., A conceptual model for chemical product design. *AIChE Journal* **2015**, *61*, 802-815.
70. Gani, R., Computer-aided methods and tools for chemical product design. *Chemical Engineering Research and Design* **2004**, *82*, 1494-1504.
71. Wibowo, C.; Ng, K. M., Product-centered processing: manufacture of chemical-based consumer products. *AIChE Journal* **2002**, *48*, 1212.
72. Bongers, P. M. M.; Almeida-Rivera, C.; Jacek, J.; Jan, T., Product driven process synthesis methodology. *Computer Aided Chemical Engineering* **2009**, *26*, 231-236.
73. Jankowiak, L.; Méndez Sevillano, D.; Boom, R. M.; Ottens, M.; Zondervan, E.; van der Goot, A. J., A process synthesis approach for isolation of isoflavones from okara. *Industrial & Engineering Chemistry Research* **2015**, *54*, 691-699.
74. Žderić, A. Extraction of key components from cellular material: aspects of product and process design. PhD, Eindhoven University of Technology, Eindhoven, 2015.
75. Monsanto, M. Separation of Polyphenols from Aqueous Green and Black Tea. PhD, Eindhoven University of Technology, Eindhoven, 2015.



---

## Effect of plant age on the quantity and quality of proteins extracted from sugar beet (*Beta vulgaris* L.) leaves

---

Effects of the developmental stage of leaves (e.g. young, mature or senescent) on their chemical composition have been described in literature. This study focuses on the variation in chemical composition and quantity and quality of proteins extracted from leaves due to variation in plant age (i.e. harvesting time), using leaves from sugar beets grown in field (Rhino, Arrival) and in greenhouse (Isabella). Within the same variety (Rhino-field, Arrival-field, Isabella-greenhouse), the protein content was similar for leaves from young and old plants ( $22\pm1$ ,  $16\pm1$ , and  $10\pm3\%$  w/w db, respectively). Variation in final protein isolation yield was mostly due to variation in nitrogen extractability (28-56%), although no consistent correlation with plant age was found. A significant effect of the plant age was observed on the quality (color) of the extracted proteins; i.e. brown (indicative of polyphenol oxidase activity) and yellow for extracts from old and young plants, respectively.

---

**Based on:** Kiskini, A; Vissers A., Vincken, J. P.; Gruppen, H.; Wierenga, P. A., Effect of plant age on the quantity and quality of proteins extracted from sugar beet (*Beta vulgaris* L.) leaves. *Journal of Agriculture and Food Chemistry* **2016**, 64, 8305-8314.

## INTRODUCTION

Leaves from various plants have long been considered as a source of protein for both food and feed applications (1) due to their nutritional value (e.g. adequate amounts of essential amino acids) (2), good techno-functional properties (e.g. high solubility at a wide pH range) (3) and high abundance in nature. For instance, in the Netherlands in 2011, the sugar beet cultivation area was 72,000 ha (4), which translates to approximately 2.2 Mt leaves. The quantity and quality of the proteins extracted from leaves depend on different factors, one of which is the overall chemical composition of the leaves. This composition has been shown to differ among leaves of different age (developmental stages) e.g. young, old or senescent (5-8). However, when leaves are obtained collectively during harvest of the plants, as for example in the case of sugar beet leaves, an array of leaves of different developmental stages is collected. Also, the harvesting time may vary, since, for instance, in Northern Europe the harvest of the sugar beets usually takes place from September until December. Therefore, when sugar beet leaves are to be used as a source of protein for food or feed applications, it is important to test whether harvesting time; i.e. the plant age, has an effect on the overall chemical composition of the whole foliage, and consequently on the protein quantity and quality of the proteins extracted.

Differences in the protein content of the whole foliage with varying plant age have been observed. In sugar beet leaves the protein content increased from 26.4% to 31.0% w/w dry weight basis (db) in leaves collected 60 and 100 days after sowing, respectively (8). For alfalfa leaves, it was reported that the protein content of the foliage initially increased with plant age by 24% and subsequently decreased by 19% (9).

The protein extractability can be hindered due to the presence of intact cell walls. It was reported that protein extraction from dehulled rapeseed meal was 33% lower when no cell wall degrading enzymes were used (10). Also, even after the cell wall opening pectins, which constitute a large part of cell walls of dicotyledon plants, can still hamper the protein isolation due to their interaction with proteins. Overall, it is expected that differences in the carbohydrate content will lead to differences in protein extractability. It has been shown that in sugar beet leaves the carbohydrate content decreased from 41% to 31% w/w db in leaves collected 60 days to 100 days after sowing, respectively (8).

Other compounds present in leaves, like phenolic compounds, are also expected to influence protein extractability (11). The naturally present phenolic compounds in leaves can, upon cell disruption, be oxidized by endogenous polyphenol oxidases (PPOs), such as catecholase and cresolase (12). This reaction leads to quinones that can polymerize with other phenolic compounds (13) or covalently link to proteins (14). The latter can potentially hinder protein extractability. The reaction products are dark colored, thus the color is an indication of protein modification. Protein modification can negatively affect the quality of the proteins, e.g. decrease their solubility. It has been shown that covalent linkage of enzymatically oxidized phenolic compounds to proteins, like lysozyme or  $\alpha$ -lactalbumin, significantly decreased protein solubility at pH values ranging between 3.0 and 5.0 (15).

Similar to proteins and carbohydrates, the content of phenolic compounds may also vary with plant age. For example, the total content of phenolic compounds in sugar beet leaves collected 100 days after sowing was approximately 1.5 times higher than that in leaves collected after 60 days (8). In contrast, in lettuce leaves it was reported that the phenolic compounds content in leaves collected 59 days after sowing was 8.5 times lower than in leaves collected 28 days after sowing, although at 73 days after sowing it was similar to that of 28 days. While the phenolic compounds content showed a fluctuation over time, the PPO activity determined in these leaves showed a constant increase with the lettuce age (14).

From the above, it is evident that the plant age has an effect on the chemical composition of the leaves. The aim of the present research is to determine the effect of plant age on the chemical composition of the sugar beet leaves and thereby its effect on the protein quantity and quality (color) of the extracted proteins. It is hypothesized that: (1) plant age affects the chemical composition of the sugar beet foliage, (2) the quantity of protein from sugar beet leaves obtained from old plants is lower than that from leaves from young plants and (3) in leaves from old plants there is higher PPO activity, which leads to brown color formation during protein extraction.

## MATERIALS AND METHODS

### Chemicals and sugar beet leaves

The sugar beet leaves were obtained either from sugar beets grown in a field (*Beta vulgaris* L. var. Rhino, var. Arrival) or grown in a greenhouse (*Beta vulgaris* L. var. Isabella) at Unifarm (Wageningen, The Netherlands). The seeds were provided by Royal Cosun (Breda, The Netherlands; purchased from Kws Saat, Einbeck, Germany). Chlorophyll *a* (purity of 90% w/w, based on HPLC as provided by the supplier) was purchased from Wako Pure Chemical Industries (Osaka, Japan). Gallic acid (purity of 98.5% based on GC as provided by the supplier), (+)-Catechin hydrate (purity of  $\geq 98\%$ , based on HPLC as provided by the supplier) and L-tyrosine (purity of  $\geq 98\%$  w/w, based on HPLC as provided by the supplier) were purchased from Sigma Aldrich (St. Louis, MO, USA). All other chemicals used were purchased from either Merck (Darmstadt, Germany) or Sigma-Aldrich.

### Growth conditions

**Field.** The sugar beet seeds (pelleted seeds containing fungicides and insecticides) were sown in April 2013 (*Beta vulgaris* L. var. Rhino) and April 2014 (*Beta vulgaris* L. var. Arrival). The plants were protected against weed and fungi. In both years, there was no need for pest control. In 2013, the sugar beet leaves (no stems) were collected 3 and 6 months after sowing and were denoted as LF<sub>3R</sub> and LF<sub>6R</sub>, respectively. In 2014, the collection of the leaves took place 3 and 8 months after sowing and the leaves were respectively denoted as LF<sub>3A</sub> and LF<sub>8A</sub>. The subscript indicates the age, in months, and the variety of the sugar beets. The leaves, at the different harvesting times, were collected from different spots in the field to ensure that leaves from regrowth were not used. Senescent leaves were discarded. The leaves collected in 2013 and 2014 were collectively denoted as field leaves (LF).



**Greenhouse.** Fifteen seeds of sugar beets (*Beta vulgaris* L. var. Isabella) were sown, each month from December 2012 to July 2013. Seeds were sown in pots (12 × 12 × 20 cm) containing normal soil for flowering plants. The plants were grown in these pots until their first leaf fall off. Next, they were transplanted to trays (40 × 30 × 25 cm) and grown until they had two true leaves. Eight healthy seedlings were then randomly selected and thinned to one per pot (25 × 25 × 25 cm). The plants were grown under a natural photoperiod, with a minimum of 16 h light exposure. In case of shorter natural photoperiod, artificial light was used (SON-T Agro, Philips, Eindhoven, The Netherlands). The humidity in the greenhouse was 65-75% and the temperature was set at 16-18 °C. The plants were watered with tap water twice a day. Pest was biologically controlled using swirski-mite (Koppert biological systems, Berkel en Rodernrijs, The Netherlands). All sugar beets were sown at different time points and harvested at the same time (September 2013) resulting in leaves ranging from 2 (LG<sub>2l</sub>) to 9 (LG<sub>9l</sub>) months. In this way, variations due to different storage times before analysis were avoided. The sugar beet leaves (no stems) that were collected from the sugar beets grown in the greenhouse were collectively denoted as greenhouse leaves (LG). Similarly to the collection of leaves from the field, senescent leaves were discarded. The LG<sub>9l</sub> leaves were mostly senescent and hence they were excluded from the analyses.

### Sugar beet leaves handling

After the sugar beets leaves were collected, the leaves were washed using tap water and stored at 4 °C until the excess water was completely drained off (not longer than 36 h). Part of the leaves was stored in vacuum sealed bags at -20 °C until further analysis. The rest of the leaves were freeze-dried. The freeze-dried leaves were ground in an ultra-centrifugal mill (Retsch ZM 200, Haan, Germany) at 6,000 rpm with a 0.5 mm or 0.2 mm sieve, for the leaves grown in the greenhouse and in the field, respectively. The freeze-dried powders were stored at -20 °C until further analysis.

### Protein isolation

**Sugar beet leaves grown in the field.** Frozen sugar beet leaves (13±2.4% w/w dry matter) were blended for 2 min in a household-type blender with 150 mM sodium phosphate buffer pH 8.0 containing 0.8 M NaCl, using a leaves to buffer ratio of 1:3 (w/w). In another experiment, LF<sub>6R</sub> were blended under the same conditions in the same buffer supplemented with 0.17% (w/v) Na<sub>2</sub>S<sub>2</sub>O<sub>5</sub> and denoted LF<sub>6R,SO3</sub>. The pH of the suspension was readjusted to 8.0 after supplementation of the Na<sub>2</sub>S<sub>2</sub>O<sub>5</sub>. The pulp obtained after blending the leaves was left for 1 h at 4 °C and subsequently filtered through a Büchner funnel (no filter paper). The filtrate was centrifuged (38,400 *g*, 4 °C, 30 min) and the supernatant (juice) obtained was subsequently dialyzed (MWCO 12,000-14,000 Da, Medicell International, London, UK) at 4 °C for 18-24 h against 35 mM sodium phosphate buffer pH 8.0 (LF<sub>3R</sub>, LF<sub>6R</sub>, LF<sub>3A</sub>, LF<sub>8A</sub>) or against the same buffer containing 0.13% (w/v) Na<sub>2</sub>S<sub>2</sub>O<sub>5</sub> (LF<sub>6R,SO3</sub>). Next, the dialyzed juices were further dialyzed against distilled water at 4 °C for 24 h. The pH of the dialyzed juice was lowered to 4.5 using 0.5 M HCl at room temperature. The acidified dialyzed juice was kept at 4 °C for at least 1 h and subsequently centrifuged (5,000 *g*, 4 °C, 10 min). The pellet obtained was re-dispersed in distilled water and solubilized by adjusting the pH to 8.0 using 0.5 M

NaOH at room temperature and subsequently freeze-dried. The obtained leaf soluble protein concentrates obtained were denoted as LSPC<sub>LF,3R</sub>, LSPC<sub>LF,6R</sub>, LSPC<sub>LF,6R,SO3</sub>, LSPC<sub>LF,3A</sub> and LSPC<sub>LF,8A</sub>. Extractions were performed in duplicate.

**Sugar beet leaves grown in the greenhouse.** A similar process as for field leaves was followed, albeit with some adaptations; i.e. freeze-dried ( $96.9 \pm 0.4\%$  w/w dry matter) instead of frozen leaves were used. The leaves were suspended in distilled water at 13% (w/w). From this point onwards, the same process that is described for the protein isolation from the leaves grown in field was followed. The leaf soluble protein concentrates obtained from sugar beet leaves grown in the greenhouse were denoted as LSPC<sub>LG,2I</sub>, LSPC<sub>LG,3I</sub>, LSPC<sub>LG,4I</sub>, LSPC<sub>LG,5I</sub>, LSPC<sub>LG,6I</sub>, LSPC<sub>LG,7I</sub>, LSPC<sub>LG,8I</sub>. Extractions were performed twice in two consecutive years.

Dialyzed juices obtained from frozen LG were used for the determination of the presence of colored compounds and PPO activity. The same process, as described for the dialyzed juices from field leaves, was followed. Extractions in the presence of Na<sub>2</sub>S<sub>2</sub>O<sub>5</sub> were not performed.

### Compositional analyses

For each analysis at least two independent samples were taken and each analysis was carried out at least in duplicate. The average and the standard deviation (SD) obtained from the two independent samples were calculated. All values were expressed on a dry weight basis (db).

**Dry matter content.** Dry matter content was determined gravimetrically by drying the samples at 105 °C overnight.

**Total nitrogen content.** Total nitrogen content (N<sub>T</sub>) was determined by the Dumas method using a Flash EA 1112 N analyzer (Thermo Fisher Scientific, Waltham, MA, USA), according to manufacturer's protocol. Methionine was used as standard for the quantification.

**Amino acid analysis.** Amino acid composition was determined based on ISO 13903:2005 method (15) adjusted for micro-scale. The amide nitrogen from asparagine and glutamine and nitrogen from aspartic acid and glutamic acid were not determined separately. Therefore, nitrogen recovered from these amino acids was calculated assuming that ASX (asparagine/aspartic acid) and GLX (glutamine/glutamic acid) were present as either 100% ASN/GLN or 100% ASP/GLU.

**Nitrogen-to-protein (N-prot) conversion factors.** Based on the amino acids analysis two N-protein (N-Prot) factors; i.e.  $k_p$  and  $k_a$  were determined, as described previously (16). The  $k_p$  is the ratio of the sum of amino acid residue weights determined by amino acid analysis to total nitrogen (N<sub>T</sub>) weight, determined by the Dumas method. The  $k_a$  is the ratio of the sum of amino acid residue weights to nitrogen weight from recovered amino acids. Given that the nitrogen recovered from asparagine/aspartic acid and glutamine/glutamic acid was calculated assuming that ASX and GLX were present as either 100% ASN/GLN or 100% ASP/GLU, two  $k_p$  and two  $k_a$  values were calculated for each sample. The values for  $k_a$  are presented as a range between a lower and an upper limit, calculated with ASX/GLX = 100% ASN/GLN and ASX/GLX = 100% ASP/GLU,

respectively. The values for  $k_p$  are presented as average between the values calculated with ASX/GLX = 100% ASN/GLN or 100% ASN/GLN because the standard deviations were found to be on average <0.2% of the average values. The  $k_p/k_a$  ratio represents the ratio of proteinaceous ( $N_{AA}$ ) over the total nitrogen ( $N_T$ ). The  $k_p$  calculated for the leaves was used as the N-Prot factor for the respective leaves, whereas the average  $k_p$  calculated for the LSPC<sub>LF,3R</sub> and LSPC<sub>LF,6R</sub> was used as the N-Prot factor for all LSPCs.

**Carbohydrate composition and total uronic acid content.** Carbohydrate content was determined as the sum of the uronic acid and the neutral carbohydrate contents. Freeze-dried leaves and LSPC (10-13 mg) were treated with 72% (w/w)  $H_2SO_4$  (1 h, 30 °C) followed by hydrolysis with 1 M  $H_2SO_4$  for 3 h at 100 °C. The suspensions were then centrifuged (16,000 *g*, 20 °C, 10 min) and the supernatants were used for uronic acid and neutral carbohydrate determinations. Uronic acid content was determined as described previously (17). A calibration curve with galacturonic acid (12.5-100  $\mu g/mL$ ) was used for quantification. Neutral carbohydrates were analyzed as free monosaccharides using high performance anion-exchange chromatography on a Dionex Ultimate 3000 system (Thermo Scientific, Sunnyvale, CA, USA) equipped with a CarboPac PA-1 column (2 mm  $\times$  250 mm ID) in combination with a CarboPac guard column (2 mm  $\times$  50 mm ID) and a pulsed amperometric detection, as described previously (18) with adaptations. The elution profile that was used (0.4 mL/min) was as follows: 0-35 min 100%  $H_2O$ , 35-50 min from 100% 0.1 M NaOH to 100% 1 M NaOAc in 0.1 M NaOH, 50-55 min 100% 1 M NaOAc in 0.1 M NaOH, 55-63 min 100% 0.1 M NaOH, 63-78 min 100%  $H_2O$ . From 0 to 35 min and from 63 to 78 min, a post column addition of 0.5 M NaOH at a flow rate of 0.1 mL/min was performed to detect and quantify the monosaccharides eluted. Arabinose, rhamnose, galactose, glucose, xylose and mannose (2-75  $\mu g/mL$ ) were used for the quantification. The total neutral carbohydrate content was calculated as the sum of the weight of the total anhydrous monosaccharides.

**Phenolic compounds content.** Phenolic compounds were extracted from freeze-dried leaves using 5 consecutive extractions of 30 min at 4 °C in 50% v/v aqueous MeOH containing 0.5% (v/v) acetic acid, at a leaves to extractant ratio of 1:10 (w/v) (19). In each extraction, the pellet was separated from the supernatant by centrifugation (8,000 *g*, 4 °C, 10 min). Fresh solvent was added to the solids after each centrifugation step. The supernatants obtained were combined and filtered (0.45  $\mu m$  cellulose filter), to yield the final extract. Phenolic compounds content was determined in the final extract using the Folin-Ciocalteu phenol reagent method (20) with adaptations. The extract (20  $\mu L$ ) was diluted with 1.58 mL distilled water and incubated with 100  $\mu L$  Folin-Ciocalteu reagent for 20 min. Subsequently, 300  $\mu L$   $Na_2CO_3$  (20% w/v) were added to the mixture and after 2 h incubation the absorbance at 725 nm was measured. A gallic acid calibration curve (0-1 g/L) was used for the quantification.

**Ash content.** Ash content was determined gravimetrically by incinerating the dried samples at 525 °C overnight.

**Lipid content.** Lipid content was determined gravimetrically using the Folch method (21) with adaptations. In detail, the freeze-dried samples were extracted twice using a MeOH/CHCl<sub>3</sub> (1:2 v/v) solution at room temperature. The washing of the combined extracts was done by addition of 5 mL of 0.88% (w/v) aqueous KCl solution. The weight of the lipid extract was determined after the solvents were evaporated using a rotary evaporator. From this weight the mass of chlorophyll *a* (described below) was subtracted to obtain the total lipid content.

**Lignin content.** Acid insoluble lignin was determined gravimetrically, as described previously (22).

**Chlorophyll *a* content.** Chlorophyll *a* content was determined after dissolving the lipid extract into 1 mL 90% (v/v) aqueous acetone. The absorbance of the solution was measured at 664 nm (23). For the quantification a calibration curve of chlorophyll *a* in 90% v/v aqueous acetone was used.

### Nitrogen recovery

To study the plant age effect on nitrogen extraction, the nitrogen extractability; i.e. the proportion of nitrogen that was recovered in the juice (nitrogen recovery in the juice%) was calculated as the amount of nitrogen in the juice divided by the amount of nitrogen in the respective pulp×100%. The pulp, rather than the frozen or the freeze-dried leaves, was used as the initial reference material for the nitrogen recovery calculation, to avoid any differences caused by leaf to leaf variation. To study the effect of plant age on nitrogen isolation, the recovery after dialysis and acid precipitation was calculated as the amount of nitrogen in the dialyzed juice or in the LSPC divided by the amount of nitrogen in the juice×100%.

### Protein composition

The protein composition was determined using SDS-PAGE under reducing conditions. All samples (freeze-dried LG and LF, LF Rhino juice, LF Rhino dialyzed juice, LF Rhino protein concentrates; 5.0 g protein/ L) were prepared according to the manufacturer's protocol. They were then applied to the gels (any kD, Mini-protean TGX precast protein gels, Bio-Rad Laboratories, Hercules, CA, USA). The proteins were separated on a Mini-protean II system (Bio-Rad Laboratories, Hercules, CA, USA) according to the manufacturer's protocol and visualized by staining the gels using Coomassie blue stain (InstantBlue, Expedeon, San Diego, CA, USA).

### Presence of colored compounds

The presence of colored compounds in the dialyzed juice was determined by measuring the absorbance from 250 to 750 nm in 1 cm quartz cuvettes using a UV-1800 Shimadzu spectrophotometer and UV Probe 2.00 software (Shimadzu, Kyoto, Japan).

### PPO activity assay

PPO-cresolase activity was determined by incubation of the dialyzed juice with tyrosine, while PPO-catecholase activity was determined by incubation of the dialyzed juice with catechin. The dialyzed juice (200 µL) was mixed with 100 µL tyrosine (2 mM in 0.1 M sodium phosphate buffer, pH 6.7) or catechin solution (2 mM in 0.1 M sodium

phosphate buffer, pH 6.7) in a 96-well plate. The formation of oxidation products after the addition of tyrosine was monitored at 520 nm (24) over 1200 min using a TECAN Infinite F500 spectrophotometer (Männedorf, Switzerland). The formation of oxidation products after the addition of catechin was monitored at 420 nm (25) over 300 min. The formation of oxidation products after the tyrosine addition was monitored over a longer period of time because prior experiments showed that in this case there is a long lag phase before the colored compounds are formed. Incubation of dialyzed juice with buffer was used to verify for autoxidation. Another control was performed by adding tyrosine or catechin to the buffer (0.1 M sodium phosphate buffer, pH 6.7). The initial reaction rates of cresolase and catecholase were calculated from the slopes of the linear segment (initial segment) of the absorbance *vs* time curves (corrected for the nitrogen content of the sample) and were expressed as  $\text{AU} \cdot \text{min}^{-1} \cdot (\text{mg N})^{-1}$ .

## RESULTS AND DISCUSSION

### Composition of the sugar beet leaves

The protein content did not considerably vary between the LF (field leaves) from young and old plants (**Table 2.1**). In the LG (greenhouse leaves), the protein contents for plants of 3-8 months were also quite constant (on average  $9.6 \pm 2.5\%$  w/w db) (**Figure 2.1**). Only the youngest plants (2 months old) had deviating high protein content ( $22.2 \pm 0.2\%$  w/w db) (**Figure 2.1**). Overall, the protein content in the LG (LG<sub>21</sub> excluded) was 41-59% lower than the protein content in the LF, which shows that the growth conditions have an effect on the protein content in the leaves. That was expected since it is known that environmental conditions; e.g. temperature, rainfall, light, can affect the growth response and thus the chemical composition of the plants (26). These data suggest that the protein content in the leaves depends on the growth conditions and possibly on the variety, but not on the plant age.

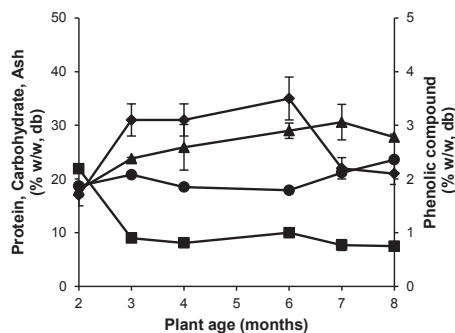


**Figure 2.1** Protein (■), carbohydrate (▲), ash (●) and phenolic compound contents (◆) in the greenhouse leaves. Error bars indicate SD. Error bars are not shown when SD is smaller than the size of the used marker.

**Table 2.1** Chemical composition (w/w% db) of field leaves (LF) and the corresponding protein concentrates (LSPCs)<sup>a</sup>.

Sample	Dry matter <sup>b</sup>	Protein <sup>c</sup>	Total carbohydrate	Lipids <sup>d</sup>	Chlorophyll <i>a</i>	Lignin	Ash	Phenolic compounds	Total
LF <sub>3R</sub>	11.3 (±0.3)	22.8 (±1.7)	19.2 (±0.7)	4.2 (±0.1)	0.3 (±0.1)	6.4 (±0.6)	16.4 (±0.1)	1.5 (±0.3)	70.8
LF <sub>6R</sub>	14.1 (±0.2)	21.7 (±1.5)	22.9 (±2.2)	8.0 (±1.0)	0.8 (±0.2)	10.1 (±0.6)	15.2 (±0.5)	2.7 (±0.1)	81.4
LF <sub>3A</sub>	10.6 (±0.4)	14.6 (±1.0)	31.4 (±0.9)	5.0 (±0.3)	0.3 (±0.1)	13.0 (±0.2)	14.0 (±1.0)	1.0 (±0.1)	79.3
LF <sub>8A</sub>	15.8 (±0.2)	16.6 (±2.6)	27.3 (±0.4)	7.7 (±0.4)	0.5 (±0.1)	15.8 (±0.3)	11.0 (±2.0)	1.5 (±0.1)	80.4
LSPC <sub>LF,3R</sub>	93.0 (±0.5)	75.0 (±4.4)	3.1 (±0.5)	4.2 (±0.1)	n.d. <sup>e</sup>	n.d.	1.3 (±0.4)	n.d.	83.6
LSPC <sub>LF,6R</sub>	91.8 (±1.4)	64.1 (±4.3)	3.8 (±1.2)	3.3 (±0.3)	n.d.	n.d.	2.0 (±0.6)	n.d.	73.2
LSPC <sub>LF,3A</sub>	95.0 (±0.8)	61.2 (±4.3)	3.7 (±0.2)	4.9 (±0.8)	n.d.	n.d.	1.0 (±0.0)	n.d.	70.8
LSPC <sub>LF,8A</sub>	94.4 (±1.3)	54.2 (±4.1)	5.1 (±0.4)	7.7 (±0.2)	n.d.	n.d.	2.0 (±0.0)	n.d.	69.0

<sup>a</sup> All data are expressed as average (from at least two independent samples) (±SD).<sup>b</sup> In w/w% fresh weight.<sup>c</sup> Determined as N<sub>T</sub>·k<sub>p</sub>.<sup>d</sup> Determined as CHCl<sub>3</sub>/MeOH soluble material, corrected for chlorophyll *a* content.<sup>e</sup> Not determined.

The amino acid composition did not differ between the leaves of different plant ages, both for LF and LG samples (**Table 2.2**). Based on the amino acid analysis, the two N-Prot factors k<sub>p</sub> and k<sub>a</sub> were determined. In the LF, the k<sub>p</sub> was 8-13% higher for young than for old plants (**Table 2.3**). For the LG, the k<sub>p</sub> varied between 4.12 and 4.57, while no clear effect of the plant age was identified. Overall, the average k<sub>p</sub> calculated for the sugar beet leaves was 4.41±0.26 for all leaves (**Table 2.3**). This value is similar to the average k<sub>p</sub> value (4.46±0.37) reported for other leafy materials (27). For k<sub>a</sub>, a minimal and a maximal value were calculated for each sample, assuming all ASX/GLX to be present as ASP/GLU or as ASN/GLN, respectively (**Table 2.3**). The k<sub>a</sub> factor was similar for all leaves tested (**Table 2.3**). The average k<sub>a</sub> factor (average lower limit and average upper limit) for all leaves (both LF and LG) was 22-43% higher than the average k<sub>p</sub>. This indicates the presence of substantial amounts of non-proteinaceous nitrogen (NPN), such as inorganic nitrogen, hormones, chlorophyll and nucleic acids. From the ratio N<sub>AA</sub>/N<sub>T</sub>, it was estimated that the leaves from old plants from Rhino and Arrival contain 24-46% and 43-150%, respectively, more NPN than the leaves from young plants (**Table 2.3**).



**Table 2.2** Amino acid profile (w/w% protein) and total amino acid (AA) content of field leaves (LF), greenhouse leaves (GH) and protein concentrates obtained from field Rhino leaves.

Sample	ASX <sup>a</sup>	THR	SER	GLN <sup>a</sup>	GLY	ALA	VAL	ILE	LEU	TYR	PHI	HIS	LYS	ARG	CYS	MET	PRO	total AA
LF <sub>3R</sub>	10.50 (±0.03)	5.20 (±0.01)	4.90 (±0.00)	12.09 (±0.05)	6.26 (±0.01)	6.56 (±0.02)	6.26 (±0.01)	4.93 (±0.01)	9.47 (±0.01)	4.40 (±0.00)	5.99 (±0.01)	3.09 (±0.01)	5.81 (±0.01)	5.44 (±0.02)	1.72 (±0.00)	2.22 (±0.02)	5.17 (±0.07)	24.68 <sup>a</sup> (±0.15)
LF <sub>6R</sub>	10.74 (±0.02)	5.20 (±0.01)	4.92 (±0.01)	12.03 (±0.02)	6.43 (±0.02)	6.30 (±0.01)	6.24 (±0.00)	4.85 (±0.01)	9.39 (±0.01)	4.52 (±0.04)	6.02 (±0.02)	3.10 (±0.01)	5.65 (±0.01)	5.44 (±0.00)	1.74 (±0.01)	2.21 (±0.00)	5.24 (±0.05)	23.69 <sup>a</sup> (±0.94)
LF <sub>3A</sub>	10.61 (±0.05)	5.17 (±0.01)	4.95 (±0.03)	11.49 (±0.07)	6.25 (±0.01)	6.59 (±0.02)	6.31 (±0.01)	4.95 (±0.01)	9.51 (±0.05)	3.96 (±0.03)	5.99 (±0.06)	2.96 (±0.03)	6.72 (±0.03)	5.28 (±0.03)	1.82 (±0.02)	2.14 (±0.05)	5.31 (±0.07)	16.12 <sup>a</sup> (±0.55)
LF <sub>8A</sub>	10.00 (±0.05)	4.96 (±0.01)	5.32 (±0.03)	11.21 (±0.03)	7.28 (±0.02)	6.39 (±0.02)	5.94 (±0.02)	4.79 (±0.00)	8.71 (±0.01)	4.69 (±0.01)	5.64 (±0.06)	3.49 (±0.02)	5.68 (±0.03)	5.27 (±0.03)	2.28 (±0.02)	2.09 (±0.05)	5.28 (±0.05)	18.07 <sup>a</sup> (±0.69)
LG <sub>21</sub>	10.35 (±0.02)	5.08 (±0.03)	4.76 (±0.00)	12.47 (±0.00)	6.02 (±0.02)	6.28 (±0.01)	6.23 (±0.00)	4.95 (±0.05)	9.50 (±0.01)	4.23 (±0.05)	6.05 (±0.01)	2.95 (±0.00)	6.76 (±0.00)	5.37 (±0.01)	1.57 (±0.02)	2.15 (±0.00)	5.28 (±0.04)	26.75 <sup>a</sup> (±0.60)
LG <sub>31</sub>	10.67 (±0.06)	4.96 (±0.03)	5.18 (±0.01)	11.64 (±0.06)	6.35 (±0.01)	6.09 (±0.01)	6.13 (±0.01)	5.09 (±0.00)	9.16 (±0.02)	4.17 (±0.02)	5.94 (±0.03)	3.31 (±0.09)	6.66 (±0.03)	4.83 (±0.03)	2.02 (±0.00)	2.00 (±0.01)	5.79 (±0.02)	10.93 <sup>a</sup> (±0.92)
LG <sub>41</sub>	10.69 (±0.08)	5.04 (±0.00)	5.24 (±0.04)	11.66 (±0.11)	6.34 (±0.03)	6.10 (±0.02)	6.14 (±0.07)	5.08 (±0.01)	9.15 (±0.07)	4.12 (±0.00)	5.83 (±0.13)	3.26 (±0.02)	6.71 (±0.01)	4.87 (±0.07)	2.04 (±0.03)	2.01 (±0.07)	5.73 (±0.07)	9.92 <sup>a</sup> (±0.42)
LG <sub>51</sub>	10.40 (±0.06)	5.05 (±0.01)	5.12 (±0.05)	11.79 (±0.06)	6.32 (±0.04)	6.08 (±0.01)	6.05 (±0.02)	4.97 (±0.00)	9.10 (±0.02)	4.28 (±0.02)	5.95 (±0.07)	3.32 (±0.01)	6.62 (±0.01)	5.39 (±0.10)	1.85 (±0.05)	2.08 (±0.01)	5.63 (±0.02)	6.53 <sup>a</sup> (±0.16)
LG <sub>61</sub>	10.51 (±0.07)	4.99 (±0.04)	5.20 (±0.00)	11.85 (±0.14)	6.38 (±0.05)	6.13 (±0.03)	6.04 (±0.06)	4.99 (±0.03)	9.17 (±0.05)	4.11 (±0.04)	5.96 (±0.11)	3.21 (±0.05)	6.66 (±0.01)	4.98 (±0.04)	2.07 (±0.01)	2.04 (±0.01)	5.70 (±0.08)	12.16 <sup>a</sup> (±0.03)
LG <sub>71</sub>	10.62 (±0.03)	4.97 (±0.00)	5.30 (±0.02)	12.15 (±0.05)	6.44 (±0.02)	6.03 (±0.03)	5.96 (±0.02)	5.94 (±0.00)	8.94 (±0.00)	4.18 (±0.06)	5.72 (±0.11)	3.32 (±0.03)	6.60 (±0.04)	4.76 (±0.08)	2.28 (±0.00)	1.96 (±0.03)	5.82 (±0.22)	9.37 <sup>a</sup> (±0.09)
LG <sub>81</sub>	10.59 (±0.04)	4.94 (±0.01)	5.29 (±0.00)	12.26 (±0.04)	6.47 (±0.02)	6.07 (±0.03)	6.03 (±0.00)	4.92 (±0.03)	9.01 (±0.04)	4.08 (±0.04)	5.77 (±0.02)	3.28 (±0.03)	6.64 (±0.04)	4.69 (±0.12)	2.34 (±0.03)	2.01 (±0.03)	5.62 (±0.15)	9.16 <sup>a</sup> (±0.15)
average (±SD)	10.52 (±0.21)	5.05 (±0.10)	5.17 (±0.19)	11.88 (±0.37)	6.41 (±0.31)	6.24 (±0.20)	6.12 (±0.13)	4.95 (±0.09)	9.19 (±0.26)	4.25 (±0.21)	5.90 (±0.14)	3.21 (±0.17)	6.50 (±0.38)	5.12 (±0.30)	1.99 (±0.26)	2.08 (±0.09)	5.57 (±0.25)	
LSPC <sub>LF,3R</sub>	10.10 (±0.07)	5.71 (±0.06)	4.14 (±0.03)	11.12 (±0.45)	5.56 (±0.04)	6.25 (±0.00)	6.56 (±0.00)	4.66 (±0.04)	9.50 (±0.05)	5.08 (±0.05)	5.97 (±0.04)	3.02 (±0.02)	6.97 (±0.01)	6.28 (±0.08)	1.58 (±0.02)	2.22 (±0.02)	5.29 (±0.00)	87.34 <sup>a</sup> (±0.16)
LSPC <sub>LF,6R</sub>	10.16 (±0.02)	5.50 (±0.00)	4.52 (±0.00)	11.30 (±0.00)	5.79 (±0.00)	6.17 (±0.00)	6.48 (±0.00)	4.77 (±0.00)	9.31 (±0.00)	4.90 (±0.00)	5.82 (±0.00)	2.97 (±0.00)	7.05 (±0.00)	6.21 (±0.00)	1.62 (±0.00)	2.25 (±0.00)	5.20 (±0.00)	74.39 <sup>a</sup> (±0.26)
average (±SD)	10.13 (±0.13)	5.60 (±0.15)	4.33 (±0.26)	11.21 (±0.19)	5.67 (±0.16)	6.21 (±0.06)	6.52 (±0.06)	4.72 (±0.07)	9.40 (±0.14)	4.99 (±0.13)	5.90 (±0.11)	2.99 (±0.03)	7.01 (±0.05)	6.24 (±0.04)	1.60 (±0.03)	2.24 (±0.02)	5.23 (±0.07)	

<sup>a</sup> No separate analysis of ASP/ASN and GLU/GLN.

**Table 2.3** Proteinaceous nitrogen and nitrogen-to-protein conversion factors  $k_a$  and  $k_p$  for different materials (LF, LG, LSPC)<sup>a</sup>

Sample	$N_{AA}/N_T$ (%) <sup>b,c</sup>	N-Prot factor $k_p$ <sup>d</sup>	N-Prot factor $k_a$ <sup>e</sup>
LF <sub>3R</sub>	75<x<87	4.72 ( $\pm 0.01$ )	5.40<y<6.31
LF <sub>6R</sub>	69<x<81	4.36 ( $\pm 0.01$ )	5.39<y<6.31
LF <sub>3A</sub>	79<x<92	4.95 ( $\pm 0.01$ )	5.39<y<6.28
LF <sub>8A</sub>	70<x<80	4.32 ( $\pm 0.01$ )	5.37<y<6.21
LG <sub>2l</sub>	66<x<77	4.15 ( $\pm 0.01$ )	5.39<y<6.31
LG <sub>3l</sub>	73<x<85	4.57 ( $\pm 0.01$ )	5.41<y<6.31
LG <sub>4l</sub>	66<x<77	4.16 ( $\pm 0.01$ )	5.40<y<6.30
LG <sub>5l</sub>	66<x<77	4.12 ( $\pm 0.01$ )	5.38<y<6.26
LG <sub>6l</sub>	68<x<79	4.29 ( $\pm 0.01$ )	5.40<y<6.30
LG <sub>7l</sub>	68<x<80	4.31 ( $\pm 0.01$ )	5.39<y<6.31
LG <sub>8l</sub>	72<x<84	4.53 ( $\pm 0.01$ )	5.40<y<6.32
<i>Average (<math>\pm SD</math>)</i>	<i>70 (<math>\pm 4</math>)&lt;x&lt;82 (<math>\pm 5</math>)</i>	<i>4.41 (<math>\pm 0.26</math>)</i>	<i>5.39(<math>\pm 0.01</math>)&lt;y&lt;6.29(<math>\pm 0.03</math>)</i>
LSPC <sub>LF,3R</sub>	85<x<99	5.33 ( $\pm 0.01$ )	5.39<y<6.24
LSPC <sub>LF,6R</sub>	82<x<95	5.13 ( $\pm 0.01$ )	5.38<y<6.23
<i>Average (<math>\pm SD</math>)</i>	<i>84 (<math>\pm 2</math>)&lt;x&lt;97 (<math>\pm 2</math>)</i>	<i>5.23 (<math>\pm 0.14</math>)</i>	<i>5.39(<math>\pm 0.01</math>)&lt;y&lt;6.23(<math>\pm 0.01</math>)</i>

<sup>a</sup> LF, field leaves; LG, greenhouse leaves; LSPC, protein concentrates.

<sup>b</sup> Proteinaceous nitrogen ( $N_{AA}$ ) as proportion (%) of total nitrogen ( $N_T$ ).

<sup>c</sup> Lower and upper limits represent values calculated with ASX/GLX = 100% ASP/GLU and ASX/GLX = 100% ASN/GNL, respectively.

<sup>d</sup>  $k_p$  is the average value of  $k_p$  calculated with ASX/GLX = 100% ASP/GLU and with ASX/GLX = 100% ASN/GLN.

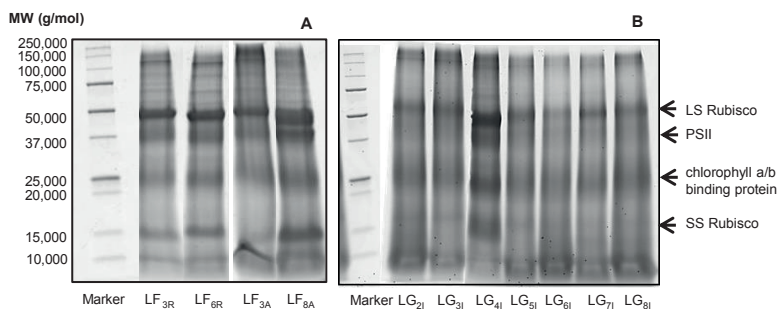
<sup>e</sup> Lower and upper limits represent values calculated with ASX/GLX = 100% ASN/GLN and ASX/GLX = 100% ASP/GLU, respectively.

The total carbohydrate content in LF Arrival was higher in LF<sub>3A</sub> than in LF<sub>8A</sub> (31.4 $\pm$ 0.9 vs 27.3 $\pm$ 0.4% w/w db), whereas in LF Rhino the carbohydrate content did not differ considerably between the two plant ages (**Table 2.1**). For the LG an increase from 18.0 $\pm$ 1.3% (for 2 months old plants) to 28.2 $\pm$ 3.1% w/w db (for 3-8 months old plants) was observed (**Figure 2.1**). The main monosaccharides present in all leaves after hydrolysis were glucose and uronic acids (**Table 2.4**), which are building blocks of cellulose and pectins, respectively.

**Table 2.4** Constituent monosaccharide composition (mol%) of field (LF) and greenhouse (LG) leaves.

Sample	Arabinose	Rhamnose	Galactose	Glucose	Xylose	Mannose	Uronic acid
LF <sub>3R</sub>	17	0	11	38	4	0	29
LF <sub>6R</sub>	18	0	10	43	3	0	26
LF <sub>3A</sub>	22	0	5	46	3	0	23
LF <sub>8A</sub>	22	0	8	44	3	0	23
LG <sub>2I</sub>	12	0	7	33	4	0	43
LG <sub>3I</sub>	15	0	4	35	5	0	41
LG <sub>4I</sub>	15	0	5	36	5	0	39
LG <sub>5I</sub>	16	0	6	42	5	0	30
LG <sub>6I</sub>	18	0	6	41	5	0	30
LG <sub>7I</sub>	19	0	6	36	6	0	34
LG <sub>8I</sub>	18	0	6	37	5	0	34

The overall protein composition was similar for the leaves of both plant ages (both Rhino and Arrival), as shown by SDS-PAGE under reducing conditions (**Figure 2.2A**). The most distinctive bands were observed around 50,000 and 15,000 g/mol, which are indicative of the large (LS ~ 52,000; Uniprot accession code Q4PLI7) and small (SS ~ 13,000; Uniprot accession code A0A0J8D2X9) Rubisco subunits (28). In addition, two less intense bands were observed at around 37,000 and 25,000 g/mol, which are indicative of respectively the photosystem II protein D1 (PSII) (Uniprot accession code A0A023ZQ82) and of the chlorophyll a/b binding protein (Uniprot accession code 049812) that have been identified in *Beta vulgaris* species) (28). In the greenhouse leaves the most distinctive bands were observed around 50,000 and 25,000 g/mol, whereas no bands were observed at 39,000 and 15,000 g/mol (with the exception of LG<sub>4I</sub>) (**Figure 2.2B**).

**Figure 2.2** SDS-PAGE gels stained by Coomassie blue of: (A) field leaves (LF) and (B) greenhouse leaves (LG).

For both LF Rhino and LF Arrival, the phenolic compounds content was on average 1.7 times higher in leaves obtained from old than in leaves obtained from young plants (**Table 2.1**). This is line with previous research (8). Similar to LF and to literature (8), the phenolic compounds content in leaves from older plants (LG<sub>3I</sub>–LG<sub>6I</sub>) was on average 2 times higher than that measured in leaves from younger plants (LG<sub>2I</sub>) (**Figure 2.1**). Interestingly, it was observed that with further increase in plant age (leaves from 7-8

months old plants) the analyzed phenolic compounds content decreased to the initial value measured, i.e. in leaves from 2 months old plants (**Figure 2.1**).

The ash content did not differ between the two plant ages, neither for LF Rhino nor for LF Arrival (**Table 2.1**). For the LG, an increase in the ash content from  $18.7 \pm 0.2\%$  to  $23.6 \pm 0.2\%$  w/w db was observed as the plant age increased (**Figure 2.1**).

For both LF Rhino and LF Arrival, the lipid and lignin contents increased with plant age (with 90 and 54% for lipids and with 58 and 22% for lignin, respectively). The chlorophyll  $\alpha$  content did not differ between the two plant ages for LF Arrival, whereas an increase from  $0.3 \pm 0.1\%$  in LF<sub>3R</sub> to  $0.8 \pm 0.2\%$  in LF<sub>6R</sub> (**Table 2.1**) was observed for LF Rhino.

In total, 71-81% of the total dry matter in the LF samples was annotated (**Table 2.1**). This incomplete mass balance cannot be explained. It should be noted that such incomplete analysis is often observed in literature (1, 29) and it should be taken into account when explaining variations in chemical composition among different samples.

### Nitrogen recovery

The nitrogen that was extracted in the juice; i.e. the nitrogen extractability of LF Rhino, was quite constant for both plant ages ( $53.0 \pm 5.0$  vs  $45.6 \pm 2.9\%$  for LF<sub>3R</sub> and LF<sub>6R</sub>, respectively, **Table 2.5A**). In contrast, for LF Arrival, a 39% decrease in the nitrogen extractability was observed as the plant age increased from 3 to 8 months (**Table 2.5B**). For the LG samples a decrease of even 50% was observed as the plant age increased from 2 to 5 months (**Table 2.5B**).

**Table 2.5** Nitrogen recovery % at each processing step for (A) field leaves (LF) and (B) greenhouse leaves (LG).

A	Recovered in:	LF <sub>3R</sub> <sup>a</sup>	LF <sub>6R</sub> <sup>a,b</sup>	LF <sub>3A</sub> <sup>a</sup>	LF <sub>8A</sub> <sup>a</sup>
<i>extraction</i>	juice	53.0 (±5.0)	45.6 (±2.9)	48.3 (±1.4)	29.3 (±3.8)
<i>isolation</i>	dialyzed juice	62.2 (±3.5)	63.9 (±3.2)	59.9 (±6.1)	57.7 (±2.9)
	LSPC	44.9 (±1.7)	50.9 (±0.4)	41.6 (±1.7)	42.8 (±4.3)

B	Recovered in:	LG <sub>2l</sub> <sup>c</sup>	LG <sub>3l</sub> <sup>c</sup>	LG <sub>4l</sub> <sup>c</sup>	LG <sub>5l</sub> <sup>d</sup>	LG <sub>6l</sub> <sup>c</sup>	LG <sub>7l</sub> <sup>c</sup>	LG <sub>8l</sub> <sup>c</sup>
<i>extraction</i>	juice	55.6 (±0.3)	44.4 (±4.2)	41.1 (±5.7)	27.7	40.1 (±7.4)	46.1 (±6.5)	46.1 (±6.0)
<i>isolation</i>	dialyzed juice	44.8 (±6.0)	55.5 (±6.1)	45.0 (±3.6)	44.4	52.3 (±2.3)	59.5 (±1.4)	62.0 (±5.5)
	LSPC	38.6 (±7.0)	45.2 (±7.1)	34.7 (±9.7)	34.3	43.5 (±1.8)	48.6 (±4.2)	n.d. <sup>e</sup>

<sup>a</sup> Average (±SD) of two repeated extractions in the same year.<sup>b</sup> Similar values were also obtained when proteins were extracted in the presence of sulfite.<sup>c</sup> Average (±SD) of two repeated extractions in two consecutive years.<sup>d</sup> Extraction was done once.<sup>e</sup> Not determined.

It must be noted that the absolute age of the plants grown in the field and in the greenhouse may not represent exactly the same developmental stage of the plant, given the fact that based on previous observations at Unifarm the growth of the sugar beets; i.e. time until harvest, in a greenhouse was faster than in a field. For the LG samples, it was observed that the nitrogen extractability increased again at higher plant age. Other researchers have also reported that the nitrogen extractability (nitrogen recovered in the juice/nitrogen in the pulp) from bean leaves initially decreased with plant age and subsequently increased (30). For other species, e.g. lucerne, the nitrogen extractability was shown to be constant (on average 78±5%) with age, whereas for sunflower leaves the nitrogen extractability showed a sharp decrease from 62% (leaves collected in July) to 22% (leaves collected in September) (30). Overall, it was shown that nitrogen extractability from leaves of different species changes with age, but not always in the same way (30). In this study, we also show that nitrogen extractability changes with age, even within the same species. Despite the variation in the nitrogen extractability, the nitrogen recovery in the dialyzed juice was quite constant with plant age (Table 2.5). This shows that, given the fact that the low molecular N-containing compounds were removed after dialysis, the protein recovery was quite constant with plant age. The nitrogen recovery in the subsequent stage (LSPC) was also quite constant with plant age, with the exception of LF Rhino for which the nitrogen recovery in LSPC<sub>LF,6R</sub> was 13% higher than in LSPC<sub>LF,3R</sub> (Table 2.5A).

### Chemical composition of the protein concentrates obtained from field leaves

In protein concentrates obtained from LF of both varieties, the protein contents did not differ between the two plant ages (**Table 2.1**). The  $k_p$  factors calculated for  $LSPC_{LF,3R}$  and  $LSPC_{LF,6R}$  were quite similar; on average  $5.23 \pm 0.14$  (**Table 2.3**). The  $k_a$  factors calculated for these samples ranged from  $5.39 \pm 0.01$  to  $6.23 \pm 0.01$  for both  $LSPC_{LF,3R}$  and  $LSPC_{LF,6R}$  (**Table 2.3**). It was observed that the  $k_a$  factor for the protein concentrates (LSPC) was 3–19% higher than the respective  $k_p$  factor, whereas for the leaves (LF) this difference was higher (22–43%), as discussed previously. This indicates that the isolation method leading to the concentrates indeed led to removal of NPN.

The total carbohydrate content in  $LSPC_{LF,8A}$  was higher than in  $LSPC_{LF,3A}$  ( $5.1 \pm 0.4$  vs  $3.7 \pm 0.2\%$  w/w db), whereas for LF Rhino protein concentrates the carbohydrate content was similar in both plant ages (on average  $3.5 \pm 0.5\%$  w/w db) (**Table 2.1**).

In protein concentrates obtained from LF Rhino, the lipid content was higher for leaves from young than for leaves from old plants (**Table 2.1**). For protein concentrates obtained from LF Arrival, the opposite was the case (**Table 2.1**). The ash content in  $LSPC_{LF,8A}$  was higher than in  $LSPC_{LF,3A}$ , whereas in protein concentrates from LF Rhino, the ash content was the same for both plant ages (**Table 2.1**).

Overall, it was shown that the chemical composition of  $LSPC_{LF,3R}$  was quite similar to the chemical composition of  $LSPC_{LF,6R}$  except for lipid content (**Table 2.1**). In contrast, the chemical composition of the protein concentrates obtained from LF Arrival differed between the two plant ages (**Table 2.1**).

### Protein composition of the protein concentrates obtained from field leaves

The overall protein composition was similar for the protein concentrates (from LF Rhino) of both plant ages, as shown by SDS-PAGE under reducing conditions (**Figure 2.3**). For all samples (juice, dialyzed juice and protein concentrate) the most distinctive bands were observed around 50,000 and 15,000 g/mol (large and small subunits of Rubisco, respectively) (28). This suggests that the isolation method did not lead to loss of Rubisco. The band at around 25,000 g/mol present in leaves was not apparent in this case. This indicates that the isolation method was adequate for the removal of the green color.

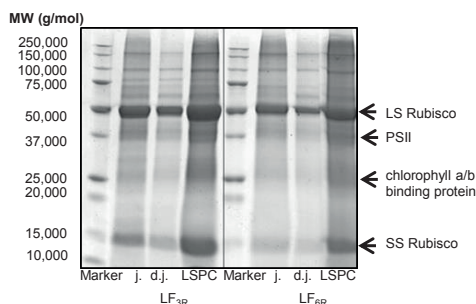


**Figure 2.3** SDS-PAGE gels stained by Coomassie blue of: j. = juice, d.j. = dialyzed juice, LSPC = protein concentrates from (Rhino) field leaves (LF).



### PPO-mediated browning in extracts of field and greenhouse leaves from old plants

A striking observation was that the juice obtained from leaves of old sugar beets ( $LF_{6R}$ ) was brown, whereas the juice from leaves of young sugar beets ( $LF_{3R}$ ) was yellow (Figure 2.4A inset). The same effect was observed for  $LF_{Arrival}$  and for  $LG$  (Figure 2.4A, B insets).

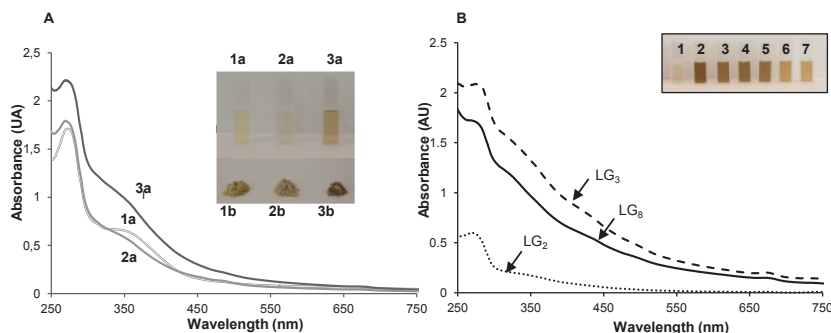


**Figure 2.4** (A) UV-vis spectra of the dialyzed juices obtained from the field leaves. (Inset) Cuvettes containing dialyzed juice from  $LF_{3R}$  (1a),  $LF_{6R,SO_3}$  (2a), and  $LF_{6R}$  (3a) and respective protein concentrates  $LSPC_{LF,3R}$  (1b),  $LSPC_{LF,6R,SO_3}$  (2b) and  $LSPC_{LF,6R}$  (3b). (B) UV-vis spectra of the dialyzed juices obtained from the greenhouse leaves. (Inset) Cuvettes containing dialyzed juices from 1 to 7,  $LG_{2I}$  to  $LG_{8I}$ .

The brown color observed in these juices was still present in the high molecular mass ( $>12,000$  g/mol) fraction after dialysis and acid precipitation (Figure 2.4A inset). Hence, it is stated that most of the brown color observed was associated with high molecular weight compounds. In another study, it was shown that the brown color observed during protein extraction from potato tubers was due to oxidized phenolic compounds (32). In the same study, it was also shown that most of the oxidized phenolic compounds were associated with high molecular weight compounds, which is in line with our observation. Therefore, it was hypothesized that the brown compounds observed in our study were formed by quinones, which were produced via PPO-mediated oxidation of the phenolic compounds. To test whether PPO activity (catecholase / cresolase activity) was indeed the reason for the brown color formation in the juices from the old plants, juice from  $LF_{6R}$  was prepared in the presence of sulfite. Sulfite is known to prevent enzymatic mediated browning, by inactivating the PPO and/or by formation of sulfo-adducts that do not contribute to browning (24). Indeed, in the presence of sulfite, the juice from the leaves of old plants ( $LF_{6R,SO_3}$ ) was not brown (Figure 2.4A), which indicates that the PPO activity was responsible for the brown color formation. The PPO activity was determined in the dialyzed juice of  $LF_{6R,SO_3}$  and surprisingly, after the removal of sulfite, the PPOs were still active (Figure 2.5A1, B1).

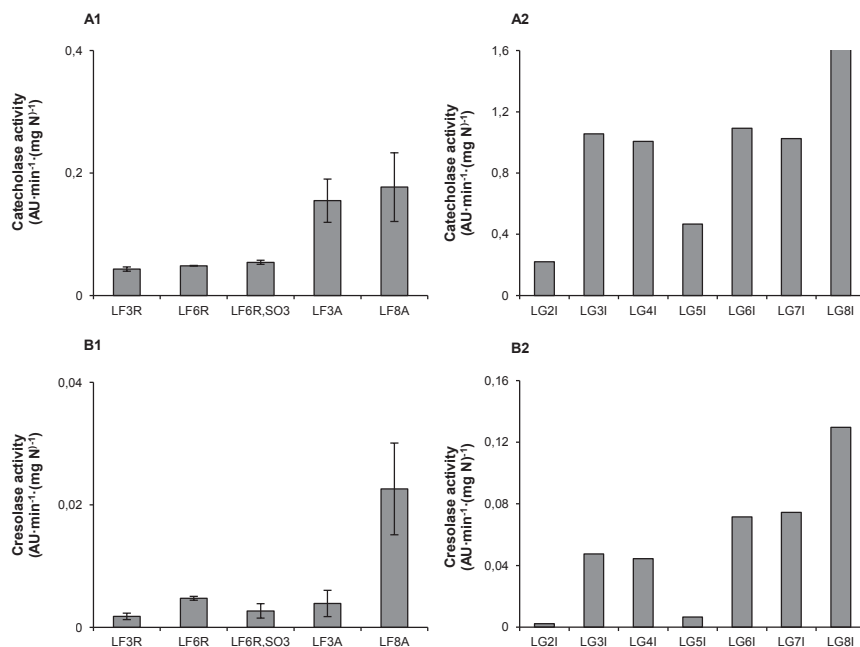


**Figure 2.5** Catecholase activity (on catechin) ( $\text{AU} \cdot \text{min}^{-1} \cdot (\text{mg N})^{-1}$ ) (A1, 2) and cresolase activity (on tyrosine) ( $\text{AU} \cdot \text{min}^{-1} \cdot (\text{mg N})^{-1}$ ) (B1, 2) activity measured in the dialyzed juice obtained from the field (LF) (A1, B1) and the greenhouse (LG) (A2, B2) leaves.

It has been shown previously that when chlorogenic acid was incubated with tyrosinase and sulfite, the enzyme was irreversibly inactivated, while no color development was observed (32). As discussed before, sulfite can lead to the formation of sulfo-adducts that do not contribute to browning. Hence, the latter is suggested to be the case in the present study.

Given the fact that the brown color formation in the (dialyzed) juices from the leaves of the old plants was attributed to PPO activity, the lack of brown color formation in the (dialyzed) juice of the leaves from young plants was consequently thought to be due to absence of PPO activity. Surprisingly, the catecholase activity measured in the dialyzed juice from leaves of young plants was similar to that in the dialyzed juice of leaves from old plants (**Figure 2.5A1**). The cresolase activity was higher in the dialyzed juice of leaves from old plants than in that of leaves from young plants ( $0.005 \text{ AU} \cdot \text{min}^{-1} \cdot (\text{mg N})^{-1}$  in  $\text{LF}_{6\text{R}}$  vs  $0.002 \text{ AU} \cdot \text{min}^{-1} \cdot (\text{mg N})^{-1}$  in  $\text{LF}_{3\text{R}}$  and  $0.023 \text{ AU} \cdot \text{min}^{-1} \cdot (\text{mg N})^{-1}$  in  $\text{LF}_{8\text{A}}$  vs  $0.004 \text{ AU} \cdot \text{min}^{-1} \cdot (\text{mg N})^{-1}$  in  $\text{LF}_{3\text{A}}$ ) (**Figure 2.5B1**). In the LG dialyzed juices, both the catecholase and the cresolase activity were higher in leaves from old plants than in leaves from young plants (**Figure 2.5A2, B2**). The values determined for  $\text{LG}_{5\text{I}}$  ( $0.47 \text{ AU} \cdot \text{min}^{-1} \cdot (\text{mg N})^{-1}$  and  $0.007 \text{ AU} \cdot \text{min}^{-1} \cdot (\text{mg N})^{-1}$ , for catecholase and cresolase activity, respectively) deviated very strongly from the values determined for the other samples ( $\text{LG}_{3\text{I}}$ – $\text{LG}_{4\text{I}}$  and  $\text{LG}_{6\text{I}}$ – $\text{LG}_{8\text{I}}$ ) and were, therefore, not included in further considerations. Interestingly, the cresolase activity measured in  $\text{LF}_{3\text{A}}$  (yellow juice and dialyzed juice) was similar to the cresolase activity measured in  $\text{LF}_{6\text{R}}$  (brown juice and dialyzed juice)

(**Figure 2.5B1**). This indicates that the cresolase activity itself does not explain the color difference between the juices of leaves from old and young plants. Furthermore, the catecholase activity in LG<sub>21</sub> dialyzed juice (yellow juice and dialyzed juice) was 1.2 - 4.4 times higher than the catecholase activity in the brown juices and dialyzed juices obtained from the field leaves. Thus, the PPO activity (cresolase and/or catecholase) *per se*, as determined with the typical methods used throughout literature, cannot explain the striking difference in color between the (dialyzed) juices and the LSPC from young and old plants.

Overall, it is concluded that the age of the sugar beets does not affect the protein content in the whole foliage. The nitrogen extractability varies with plant age, although no consistent correlation with plant age is found. The nitrogen recovery in the subsequent isolation stages is independent of plant age. Thus, the variation in the final yield of protein extraction is mostly due to the variation in nitrogen extractability. A significant effect of the plant age is observed on the quality (color) of the protein extracted from the sugar beet leaves; i.e. the protein extracted from leaves of older plants is brown, whereas the protein extracted from leaves from young plants is yellow.

## FUNDING

This work has been carried out within the framework of Institute for Sustainable Process Technology (ISPT).

## ACKNOWLEDGEMENTS

The authors would like to thank the Animal Nutrition group of Wageningen University for performing the amino acid analysis.

## REFERENCES

1. Edward, R.; Miller, R.; De Fremery, D.; Kunckles, B.; Bickoff, E.; Kohler, G., Pilot plant production of an edible white fraction leaf protein concentrates from alfalfa. *Journal of Agriculture and Food Chemistry* **1975**, *23*, 620-626.
2. Makkar, H. P. S.; Becker, K., Nutritional value and antinutritional components of whole and ethanol extracted Moringa oleifera leaves. *Animal Feed Science and Technology* **1996**, *63*, 211-228.
3. Betschart, A.; Kinsella, J. E., Extractability and solubility of leaf protein. *Journal of Agriculture and Food Chemistry* **1973**, *21*, 60-65.
4. <http://www.suikerunie.nl/Sustainability-number-of-beet-growers.aspx> (04/05/17)
5. Nordkvist, E.; Åman, P., Changes during growth in anatomical and chemical composition and in-vitro degradability of lucerne. *Journal of the Science of Food and Agriculture* **1986**, *37*, 1-7.
6. Byers, M.; Sturrock, J., The yields of leaf protein extracted by large-scale processing of various crops. *Journal of the Science of Food and Agriculture* **1965**, *16*, 341-355.
7. Tambari, U.; Aliero, B.; Muhammad, S.; Hassan, L., Interaction effect of season, habitat and leaf age on proximate composition of *Senna occidentalis* and *Senna obtusifolia* leaves

grown in Fadama and upland locations in Sokoto, Nigeria. *Nigerian Journal of Basic and Applied Sciences* **2015**, *23*, 39-44.

8. Biondo, P. B. F.; Boeing, J. S.; Barizão, É. O.; Souza, N. E. d.; Matsushita, M.; Oliveira, C. C. d.; Boroski, M.; Visentainer, J. V., Evaluation of beetroot (*Beta vulgaris* L.) leaves during its developmental stages: a chemical composition study. *Food Science and Technology* **2014**, *34*, 94-101.

9. Addy, T. O., Whitney, L.F., Chen, C.S., Mechanical parameters in leaf cell rupture for protein production. In *Leaf protein concentrates*, Telek, L. G., H. D., Ed. AVI Publishing Co., Inc.: 1983.

10. Rommi, K.; Hakala, T. K.; Holopainen, U.; Nordlund, E.; Poutanen, K.; Lantto, R., Effect of enzyme-aided cell wall disintegration on protein extractability from intact and dehulled rapeseed (*Brassica rapa* L. and *Brassica napus* L.) press cakes. *Journal of Agriculture and Food Chemistry* **2014**, *62*, 7989-7997.

11. Prigent, S. V.; Voragen, A. G.; Visser, A. J.; van Koningsveld, G. A.; Gruppen, H., Covalent interactions between proteins and oxidation products of caffeoylquinic acid (chlorogenic acid). *Journal of the Science of Food and Agriculture* **2007**, *87*, 2502-2510.

12. Pourcel, L.; Routaboul, J.-M.; Cheynier, V.; Lepiniec, L.; Debeaujon, I., Flavonoid oxidation in plants: from biochemical properties to physiological functions. *Trends in plant science* **2007**, *12*, 29-36.

13. Cheynier, V.; Owe, C.; Rigaud, J., Oxidation of grape juice phenolic compounds in model solutions. *Journal of Food Science* **1988**, *53*, 1729-1732.

14. Chutichudet, B.; Chutichudet, P.; Kaewsit, S., Influence of developmental stage on activities of polyphenol oxidase, internal characteristics and colour of lettuce cv. grand rapids. *American Journal of Food Technology* **2011**, *6*, 215-225.

15. ISO 13903:2005 (2005). *Animal Feeding stuff – Determination of amino acids content*, International organization for standardization, Geneva, Switzerland.

16. Mosse, J., Nitrogen-to-protein conversion factor for ten cereals and six legumes or oilseeds. A reappraisal of its definition and determination. Variation according to species and to seed protein content. *Journal of Agriculture and Food Chemistry* **1990**, *38*, 18-24.

17. Murciano Martínez, P.; Bakker, R.; Harmsen, P.; Gruppen, H.; Kabel, M., Importance of acid or alkali concentration on the removal of xylan and lignin for enzymatic cellulose hydrolysis. *Industrial Crops and Products* **2015**, *64*, 88-96.

18. Jurak, E.; Kabel, M. A.; Gruppen, H., Carbohydrate composition of compost during composting and mycelium growth of *Agaricus bisporus*. *Carbohydrate Polymers* **2014**, *101*, 281-288.

19. Narváez Cuenca, C. E.; Vincken, J. P.; Zheng, C.; Gruppen, H., Diversity of (dihydro) hydroxycinnamic acid conjugates in Colombian potato tubers. *Food Chemistry* **2013**, *139*, 1087-1097.

20. Slinkard, K.; Singleton, V. L., Total phenol analysis: Automation and comparison with manual methods. *American Journal of Enology and Viticulture* **1977**, *28*, 49-55.

21. Folch, J.; Lees, M.; Stanley, G. H. S., A simplified method for the isolation and purification of total lipides from animal tissues. *Journal of Biological Chemistry* **1957**, *226*, 497-509.

22. Kabel, M. A.; Bos, G.; Zeevalking, J.; Voragen, A. G. J.; Schols, H. A., Effect of pretreatment severity on xylan solubility and enzymatic breakdown of the remaining cellulose from wheat straw. *Bioresource Technology* **2007**, *98*, 2034-2042.

23. Jeffrey, S. t.; Humphrey, G., New spectrophotometric equations for determining chlorophylls a, b, c1 and c2 in higher plants, algae and natural phytoplankton. *Biochemie und Physiologie der Pflanzen* **1975**, *167*, 191-194.
24. Kuijpers, T. F. M.; Narváez Cuenca, C. E.; Vincken, J. P.; Verloop, A. J. W.; van Berkel, W. J. H.; Gruppen, H., Inhibition of enzymatic browning of chlorogenic acid by sulfur-containing compounds. *Journal of Agriculture and Food Chemistry* **2012**, *60*, 3507-3514.
25. Gowda, L. R.; Paul, B., Diphenol activation of the monophenolase and diphenolase activities of field bean (*Dolichos lablab*) polyphenol oxidase. *Journal of Agriculture and Food Chemistry* **2002**, *50*, 1608-1614.
26. Gupta, A. J.; Gruppen, H.; Maes, D.; Boots, J. W.; Wierenga, P. A., Factors causing compositional changes in soy protein hydrolysates and effects on cell culture functionality. *Journal of Agriculture and Food Chemistry* **2013**, *61*, 10613-10625.
27. Milton, K.; Dintzis, F. R., Nitrogen-to-Protein Conversion factors for tropical plant samples. *Biotropica* **1981**, *13*, 177-181.
28. UniProtKB <http://www.uniprot.org/> (08.05.2017),
29. Tamayo Tenorio, A.; Gieteling, J.; de Jong, G. A. H.; Boom, R. M.; van der Goot, A. J., Recovery of protein from green leaves: Overview of crucial steps for utilisation. *Food Chemistry* **2016**, *203*, 402-408.
30. Butler, J. B., An investigation into some causes of the differences of protein expressibility from leaf pulps. *Journal of the Science of Food and Agriculture* **1982**, *33*, 528-536.
31. Narváez Cuenca, C. E.; Vincken, J. P.; Gruppen, H., Quantitative fate of chlorogenic acid during enzymatic browning of potato juice. *Journal of Agriculture and Food Chemistry* **2013**, *61*, 1563-1572.
32. Kuijpers, T. F. M.; Gruppen, H.; Sforza, S.; van Berkel, W. J. H.; Vincken, J. P., The antibrowning agent sulfite inactivates *Agaricus bisporus* tyrosinase through covalent modification of the copper-B site. *FEBS Journal* **2013**, *280*, 6184-6195.

---

## Emulsion properties of sugar beet (*Beta vulgaris* L.) leaf and soybean (*Glycine max*) proteins

---

To apply novel proteins, e.g. sugar beet leaf proteins (LSPC), in emulsions an understanding is needed of the relation between system conditions (e.g. pH, I), protein molecular properties (e.g. protein radius, charge;  $\zeta$ -potential) and emulsion properties. Previously a model describing this relation was proposed for pure protein systems. A main parameter in this model is the critical protein concentration ( $C_{cr}$ ) at which a stable emulsion is formed. The aim of this study was to test whether this model can be applied to LSPC, and soy protein isolate (SPI). At pH 8.0 ( $I = 0.01$  M), the  $C_{cr}$  of LSPC was comparable to the  $C_{cr}$  of SPI (2.1 and 1.0 g/L, respectively). For both proteins the  $C_{cr}$  increased with decreasing  $\zeta$ -potential and was highest at a pH around the pI (i.e. lowest  $\zeta$ -potential). A critical  $\zeta$ -potential ( $\zeta_{cr} \sim 11$  mV) for both proteins was identified below which flocculation occurs. LSPC-stabilized emulsions were stable against flocculation at a wider pH range ( $pH \leq 3.0$  and  $pH \geq 5.5$ ) than SPI-stabilized emulsions ( $pH \geq 5.5$ ). For both proteins,  $C_{cr}$  was higher at pH 8.0 and high I (0.5 M) than at low I (0.01 M) (5.4 and 3.5 g/L, for LSPC and SPI, respectively). This relates to a higher protein adsorbed amount at the interface ( $\Gamma_{max}$ ) at high I. The predicted values for the formation and stability of emulsions (at  $\zeta > \zeta_{cr}$ ) by these impure protein systems based on the molecular properties of the dominant proteins, taking also into account the presence of charged carbohydrates, were close to the experimental values. Thus, the model developed to characterize the emulsion properties of pure protein can be applied to these mixed protein systems.

---

**Based on:** Kiskini, A.; Delahaije, R. J. B. M.; Wierenga, P. A.; Gruppen, H., Emulsion properties of sugar beet (*Beta vulgaris* L.) leaf and soybean (*Glycine max*) proteins (*submitted*)

## INTRODUCTION

There is a strong interest to use proteins from novel sources, such as plant leaves like sugar beet leaves, as ingredients in different food applications (e.g. emulsions). For this, the emulsion properties of these novel proteins need to be characterized. A complicating factor is that the emulsion properties depend on the molecular properties of the protein as well as the system conditions. This means that each novel protein should be tested under many different conditions to obtain a complete overview of its emulsion properties. Such an approach is impractical, and although it provides much data it does not give a clear overview. Recently, a new concept was developed that describes the efficiency of a protein to form an emulsion based on the critical protein concentration ( $C_{cr}$ ) needed to obtain stable emulsions (1-3). This  $C_{cr}$  depends on the system conditions, which in turn affect the molecular properties of the protein, e.g. protein radius, charge, exposed hydrophobicity. This concept was developed using purified proteins (e.g.  $\beta$ -lactoglobulin, ovalbumin) and has not been tested on less pure (plant) protein concentrates/isolates. The first aim of this study is to provide an overview of the emulsion properties of sugar beet leaf protein concentrate (LSPC) and soy protein isolate (SPI) under different system conditions; i.e. pH and ionic strength (I). The second aim is to test whether the recently developed concept (1) of characterization of the emulsion properties of pure protein systems could also be applied in more complex systems, such as LSPC and SPI.

The basis for the recently proposed concept is that above a certain protein concentration ( $C_p$ ), also referred to as protein-rich regime ( $C_p > C_{cr}$ ), the emulsion droplets obtained after homogenization will have a minimum size ( $d_{3,2min}$ ). This minimum size depends on the mechanical parameters (e.g. homogenization pressure) and the physical properties of the system (e.g. viscosity of the oil). At protein concentrations below the  $C_{cr}$ , there is not sufficient protein to cover the oil-water interface of all droplets within the timespan of formation, and as a result the emulsion droplets (partially) coalesce. This regime is referred to as the protein-poor regime. The  $C_{cr}$  can therefore be used as a quantitative parameter that describes the efficiency of a protein to form a stable emulsion.

The  $C_{cr}$  depends on the volume fraction of oil ( $\Phi_{oil}$ ), the adsorbed amount of protein ( $\Gamma_{max}$ ) that is needed to stabilize the interface, the minimum average droplet size ( $d_{3,2min}$ ) and the adsorption rate constant  $k_{adsorb}$  (4). It was shown that for pure protein stabilized emulsions the values of  $\Gamma_{max}$  and  $k_{adsorb}$  can be estimated from the protein charge (related to electrostatic interactions), the relative exposed hydrophobicity and the protein radius (4). In this way, the  $C_{cr}$  links the molecular, interfacial and emulsion properties and also helps to understand the effect of varying system conditions. For example, at pH 7.0,  $I = 0.01$  M and 10% (v/v) sunflower oil the  $C_{cr}$  of lysozyme, ovalbumin and  $\beta$ -lactoglobulin are  $> 25$  g/L,  $\sim 10$  g/L and  $\sim 2$  g/L, respectively (1). The difference in  $C_{cr}$  is due to the differences in the relative exposed hydrophobicity of these three proteins; 0.06, 0.19 and 1.00, respectively. The  $C_{cr}$  can be also used as a factor to describe the effect of system conditions on emulsion stability. For example, it was shown that the  $C_{cr}$  of a  $\beta$ -lactoglobulin-stabilized emulsion increased from  $\sim 2$  g/L to



~ 2.5 g/L with an increase of the ionic strength from 0.01 M to 0.2 M (1). This increase was attributed to a decrease of the effective protein radius due to a decrease in electrostatic repulsion between adsorbed proteins and the consequent decrease of the Debye layer. This decrease in electrostatic repulsion was experimentally confirmed by a decrease in  $\zeta$ -potential.

In mixed systems, such as protein concentrates or isolates other factors, such as the protein composition and the presence of charged carbohydrates, are expected to contribute to the emulsion properties. For example, for algae protein isolate (ASPI) the presence of charged carbohydrates was shown to be the reason for the stability against flocculation in the pH range 4.0 - 5.0 (4). In LSPC, a protein content of 64% (w/w dry basis, db) and a charged carbohydrates content of 1.9% (w/w db) were determined (5). Rubisco, which is a multimeric protein, consisting of 8 large and 8 small polypeptide chains, was identified as the main protein in LSPC (6). Soy protein isolate (SPI) also consists of a mixture of protein (83% w/w db) and other compounds (3). Soy protein consists of glycinin and  $\beta$ -conglycinin, which are both also multimeric proteins (3). Therefore, the aim of this study is to test whether the overall behavior of mixed/non-pure protein systems can be predicted based on molecular properties of the dominant proteins present in the systems. To test this, the recently developed concept (1) of characterization of the emulsion properties of pure protein systems will be applied. In addition, to obtain an overview of the emulsion properties of LSPC- and SPI-stabilized emulsions, the emulsion stability against flocculation of the emulsions produced at pH 8.0 and low ionic strength ( $I = 0.01$  M) will be determined by changing the system conditions after emulsification.

## MATERIALS AND METHODS

### Chemicals and sugar beet leaves

Sugar beets (*Beta vulgaris* L. var. Florena) were grown on a sandy field in Wageningen, The Netherlands. After collection of the sugar beets, the fresh leaves were manually separated from the stems. The leaves were then washed using tap water and stored at 4 °C, until the excess water was completely drained off (no longer than 36 h). Afterwards, the leaves were stored in vacuum sealed bags at -20 °C. Soy protein isolate (SPI; 64:36 (w/w) glycinin: $\beta$ -conglycinin,  $83.1 \pm 0.1\%$  w/w db protein ( $N_T$ -5.60) (3), based on Dumas analysis, as described previously (6) was produced at the Laboratory of Food Chemistry (Wageningen University, Wageningen, The Netherlands) as previously described (7). Sunflower oil was purchased from a local supermarket (Wageningen, The Netherlands). 8-anilino-1-naphthalenesulfonic acid (ANSA) ( $\geq 97\%$  purity, based on HPLC) and  $\beta$ -lactoglobulin (L-0130,  $\geq 90\%$  purity, based on PAGE) were purchased from Sigma-Aldrich (St. Louis, MO, USA). All other chemicals used were purchased from either Merck (Darmstadt, Germany) or Sigma-Aldrich.

### Protein isolation from sugar beet leaves

The protein was extracted from the frozen sugar beet leaves in 0.15 M sodium phosphate buffer pH 8.0 containing 0.8 M NaCl and 0.17% (w/v)  $Na_2S_2O_5$ , as described previously (5). The soluble proteins after centrifugation and subsequent dialysis were

isolated by acid precipitation at pH 4.5 using 0.5 M HCl. The pellet obtained was subsequently re-solubilized in distilled water at pH 8.0 and freeze-dried, yielding the leaf soluble protein concentrate (LSPC). LSPC contained  $69.3 \pm 0.3\%$  w/w db protein ( $N_T$ -5.23) (5), based on Dumas analysis, as described previously (5).

### **Preparation of LSPC and SPI dispersions and solutions**

LSPC and SPI were dispersed in 3.65 mM sodium phosphate buffer pH 8.0 without NaCl (final I = 0.01 M) or with 0.49 M NaCl (final I = 0.5 M) and stirred for at least 3 h at room temperature. The LSPC and SPI dispersions were termed LSPC<sub>tot</sub> and SPI<sub>tot</sub>, respectively. The LSPC<sub>tot</sub> and SPI<sub>tot</sub> at pH 8.0 and I = 0.01 M were centrifuged (5,000 *g*, 20 °C, 10 min). After centrifugation the obtained supernatants were filtered through a Büchner funnel using a Whatman paper filter (5-10 µm) (Sigma-Aldrich). The LSPC and SPI filtrates, which contained only the dissolved part of the sample, were termed LSPC<sub>sol</sub> and SPI<sub>sol</sub>, respectively. The ionic strength of one part of the LSPC<sub>sol</sub> and SPI<sub>sol</sub> was adjusted to 0.5 M by addition of NaCl. The samples were then stirred for at least 1 h at room temperature. The pH of the samples was periodically checked and re-adjusted to pH 8.0 by addition of 0.2 M NaOH when necessary. All concentrations given below for LSPC<sub>tot</sub>, SPI<sub>tot</sub>, LSPC<sub>sol</sub> and SPI<sub>sol</sub> are on protein basis ( $C_p$ ).

### **Gross chemical composition of proteins**

The gross chemical composition described by the dry matter, protein, total neutral monosaccharides and uronic acids content of LSPC<sub>tot</sub>, SPI<sub>tot</sub>, LSPC<sub>sol</sub> and SPI<sub>sol</sub> was determined as described elsewhere (6).

### **Quantification of exposed hydrophobicity**

Protein exposed hydrophobicity was determined using ANSA as a fluorescent probe, as described previously (8), with adaptations. LSPC<sub>sol</sub> and SPI<sub>sol</sub> ( $C_p$  = 0.5 g/L) and 2.4 mM ANSA solutions were made in 3.65 mM sodium phosphate buffer at pH 8.0. The maximum area of the fluorescence spectrum was corrected with the area of the buffer. The relative exposed hydrophobicity was expressed as the area obtained for the sample relative to the area obtained for a 0.5 g/L  $\beta$ -lactoglobulin solution in the same buffer.

### **Protein composition**

The protein composition of LSPC<sub>tot</sub>, SPI<sub>tot</sub>, LSPC<sub>sol</sub> and SPI<sub>sol</sub> was determined using SDS-PAGE under reducing conditions. The proteins were separated on a Mini-protean II system (Bio-Rad Laboratories, Hercules, CA, USA) according to the manufacturer's protocol and visualized by staining the gels using Coomassie blue stain (InstantBlue, Expedeeon, San Diego, CA, USA), as described elsewhere (6).

### **Molecular mass ( $M_w$ ) calculation**

Based on SDS-PAGE analysis of LSPC, Rubisco was found to be the most abundant protein in LSPC. Therefore, the  $M_w$  of LSPC was estimated as the  $M_w$  of Rubisco. Rubisco is typically present in a hexadecameric structure, consisting of 8 large (52,301 g/mol) (Uniprot accession code Q4PLI7) and 8 small (12,936 g/mol) (Uniprot accession code A0A0J8D2X9) (9) subunits. Therefore, the  $M_w$  of Rubisco was assumed to be 521,896 g/mol. The SPI used in this study consists of glycinin and  $\beta$ -conglycinin in a ratio of 64:36 (w/w) (3). At pH 7.6 and I = 0.5 M, glycinin is present as hexamer with a  $M_w$  of

320,000 - 360,000 g/mol (10, 11). At pH 7.6 and  $I = 0.03$  M glycine is predominantly present as hexamer, while a small part of it (15-20%) is present as trimer (12).  $\beta$ -conglycinin at pH > 5.0 and  $I = 0.5$  M is mainly present as trimer with a  $M_w$  of 180,000 g/mol, whereas at  $I < 0.1$  M, it is mainly present as hexamer (13). For calculations, the  $M_w$  of a hypothetical SPI molecule at pH 8.0 and  $I = 0.01$  M was estimated to be 328,160 g/mol and at  $I = 0.5$  M 282,400 g/mol.

### Protein solubility

To determine whether there is a protein concentration effect on protein solubility,  $LSPC_{tot}$  and  $SPI_{tot}$  were prepared by dispersing LSPC and SPI in 3.65 mM sodium phosphate buffer pH 8.0 (final  $I = 0.01$  M) at  $C_p = 1.5, 2.5, 5.0$  and  $10.0$  g/L. Next, the  $LSPC_{tot}$  and  $SPI_{tot}$  were stirred for at least 3 h at room temperature and then centrifuged (5,000  $g$ , 20 °C, 10 min). The protein concentration of the supernatants was determined using Dumas, as described previously (6). The protein solubility was defined as the protein concentration of the supernatant at each pH divided by the protein concentration of the sample at pH 8.0; initial protein concentration of  $LSPC_{sol}$  or  $SPI_{sol}$  (at pH 8.0). The latter was set to 100%. In the protein concentration range tested the solubility of LSPC and SPI was constant independent of the initial amount of dispersed protein.

The protein solubility as a function of pH was determined for  $LSPC_{tot}$  and  $SPI_{tot}$  (at  $C_p = 10.0$  g/L) and  $LSPC_{sol}$  and  $SPI_{sol}$  (obtained after centrifugation of  $LSPC_{tot}$  and  $SPI_{tot}$  at  $C_p = 10.0$  g/L) as previously described (14), with adaptations. The pH of the  $LSPC_{tot}$ ,  $SPI_{tot}$ ,  $LSPC_{sol}$  and  $SPI_{sol}$  at low ( $I = 0.01$  M) and high ( $I = 0.5$  M) ionic strength was adjusted (at room temperature) from pH 8.0 to 2.0 with 1 unit intervals, using 0.2 M HCl. Added amounts of HCl or NaOH and the actual pH values were recorded using a pH-stat unit (719 S Titrimo, Metrohm, Herisau, Switzerland). At each pH interval, the conductivity of the protein solutions was measured using a conductivity meter (Inolab conductivity meter level 1, WTW, Weilheim, Germany) and converted to the equivalent molar concentration of NaCl. The pH adjustment did not considerably influence the ionic strength of the solutions up to pH 3.0. After pH-adjustment, samples were kept at room temperature for at least 1 h. The samples were then centrifuged (5,000  $g$ , 20 °C, 10 min) and the protein concentration of the supernatants was determined using Dumas, as described previously (6).

Part of the  $LSPC_{sol}$  and  $SPI_{sol}$  (obtained after centrifugation of  $LSPC_{tot}$  and  $SPI_{tot}$  at  $C_p = 10$  g/L, pH 8.0 and  $I = 0.01$  M) was freeze-dried. These freeze-dried supernatants were then dispersed in 3.65 mM sodium phosphate buffer pH 8.0 (final  $I = 0.01$  M) at  $C_p$  similar as  $LSPC_{sol}$  and  $SPI_{sol}$ , stirred for at least 3 h at room temperature and centrifuged (5,000  $g$ , 20 °C, 10 min). The protein concentration of the supernatants was determined using Dumas, as described previously (6).

### Emulsification

For emulsification only the soluble part of LSPC and SPI at pH 8.0 and  $I = 0.01$  M ( $LSPC_{sol}$  and  $SPI_{sol}$ ) were used.  $LSPC_{sol}$  and  $SPI_{sol}$  were mixed with 10% (v/v) sunflower oil using an Ultra turrax Type T-25B (IKA, Staufen, Germany) at 9,500 rpm for 1 min. Next, the samples were homogenized by passing them 30 times through a Labhoscope 2.0

laboratory scale high-pressure homogenizer (Delta Instruments, Drachten, The Netherlands) at 15 MPa. During homogenization, the samples were cooled on ice-water. Subsequently, the emulsions were stored for 24 hours at 4 °C prior to further analysis. Prior to analysis, the emulsions were brought to room temperature. Three different sets of experiments were performed:

**Effect of protein concentration at pH 8.0, pH 5.0 and pH 3.0.** LSPC<sub>sol</sub> and SPI<sub>sol</sub> at different protein concentrations ( $C_p = 0.25 - 10.0$  g/L for LSPC<sub>sol</sub> and  $C_p = 0.6 - 9.2$  g/L for SPI<sub>sol</sub>) at pH 8.0 and  $I = 0.01$  M were prepared. After emulsification, the pH of the LSPC<sub>sol</sub>- and SPI<sub>sol</sub>-stabilized emulsions was re-adjusted to pH 8.0 using 0.2 M NaOH (if needed). Part of the LSPC<sub>sol</sub>- and SPI<sub>sol</sub>-stabilized emulsions ( $C_p = 0.25 - 10$  g/L for LSPC<sub>sol</sub> and  $C_p = 0.6 - 9.2$  g/L for SPI<sub>sol</sub>) at pH 8.0 and  $I = 0.01$  M was used to adjust the pH to 5.0 and 3.0 using 0.1 or 0.2 M HCl. The emulsions were further diluted by mixing 1 part 3.65 mM sodium phosphate buffer adjusted to respective pH with 1 part of emulsion.

**Effect of pH.** After emulsification, the pH of the LSPC<sub>sol</sub>- and SPI<sub>sol</sub>-stabilized emulsions ( $C_p = 10$  g/L for LSPC<sub>sol</sub> and  $C_p = 9.2$  g/L for SPI<sub>sol</sub>) at pH 8.0 and  $I = 0.01$  M, was adjusted to pH 2.0 - 7.0, with 1 unit interval, using 0.1 or 0.2 M HCl. The emulsions were further diluted by mixing 1 part 3.65 mM sodium phosphate buffer adjusted to respective pH with 1 part of emulsion.

**Effect of ionic strength (I).** After emulsification, the ionic strength of part of the LSPC<sub>sol</sub>- and SPI<sub>sol</sub>-stabilized emulsions ( $C_p = 0.25 - 10.0$  g/L for LSPC<sub>sol</sub> and  $C_p = 0.6 - 9.2$  g/L for SPI<sub>sol</sub>) at pH 8.0 and  $I = 0.01$  M was adjusted to 0.5 M. The ionic strength was adjusted by mixing 1 part of 3.65 mM sodium phosphate buffer containing 3.99 M NaCl (final  $I = 4.0$  M) pH 8.0 with 7 parts of the initial emulsion, and the pH was re-adjusted to pH 8.0 using 0.2 M NaOH (if needed).

### Determination of particle size

**Laser diffraction.** The average particle size (expressed as volume surface average diameter;  $d_{3,2}$ ) of the emulsions was measured using laser light diffraction (Mastersizer 3000, Malvern Instruments, Worcestershire, UK) equipped with a Hydro SM sample dispersion unit, as described previously (4). For each sample, five sequential measurements were performed and averaged.

The ( $d_{3,2}$ ) as a function of concentration was fitted using equations 3.1 and 3.2.

$$\text{For } C_p < C_{cr} \text{ (protein-poor regime): } d_{3,2} = \alpha \cdot \left( \frac{1}{C} - \frac{1}{C_{cr}} \right) + d_{3,2min} \quad (3.1)$$

$$\text{For } C_p \geq C_{cr} \text{ (protein-rich regime): } d_{3,2} = d_{3,2min} \quad (3.2)$$

in which  $C_p$  is the protein concentration (g/L),  $\alpha$  (L/g) and  $C_{cr}$  (critical concentration, g/L) are the fitting parameters and  $d_{3,2min}$  is the minimum average particle size ( $\mu\text{m}$ ).

**Diffusing wave spectroscopy (DWS).** As indication of the droplet size *in situ*, i.e. without dilution, DWS measurements were performed using forward laser scattering at 13° angle in a Zetasizer Nano ZSP (Malvern Instruments). The path length was 4 mm and the measurement position was set to 2.19 nm. Measurements were performed at

25 °C for 120 s and data obtained were averaged for five sequential runs. The averaged data were normalized by dividing all the values obtained by the maximum value measured. Normalized autocorrelation curves were fitted using equation 3.3 as described elsewhere (4):

$$g_2(t)-1 = e^{-\beta t^p} \quad (3.3)$$

in which  $g_2(t)$  is the autocorrelation function of multiple scattered light as function of time  $t$  and  $\beta$  and  $p$  are fitting parameters. The decay time ( $\tau_{1/2}$ ), which is defined as the time at which  $g_2(t)-1$  decayed to half of its initial value, was determined by fitting equation 3.3.

### Determination of theoretical total net charge of dispersions and solutions

The theoretical total net charge of LSPC was calculated based on the amino acid sequence of the large and small Rubisco subunit (1:1 large:small subunit ratio) (9). For SPI the amino acid composition of glycinin and  $\beta$ -conglycinin (64:36 (w/w) glycinin: $\beta$ -conglycinin ratio) was used (9). For SPI<sub>sol</sub> the theoretical total net charge was calculated both in the presence and in the absence of the basic subunits of the glycinin. In all cases, the contribution of the uronic acids present in the samples was taken into account. The  $pK_a$  value for uronic acids is 3.3 (15) and for aspartic acid, glutamic acid, lysine, arginine and histidine side chains 3.9, 4.3, 10.8, 12.5 and 6.0, respectively.

### Determination of $\zeta$ -potential

The  $\zeta$ -potential as a function of pH (pH 2.0 - 8.0, with 1 unit intervals) at  $I = 0.01$  M was determined with a Zetasizer Nano ZSP (Malvern Instruments) at 25 °C. Data were collected over three sequential readings and processed using the Smoluchowski model, as described elsewhere (16).

**Dispersions and solutions.** LSPC<sub>tot</sub> and SPI<sub>tot</sub> ( $C_p = 5.0$  g/L) and LSPC<sub>sol</sub> and SPI<sub>sol</sub> (obtained after centrifugation of the LSPC<sub>tot</sub> and SPI<sub>tot</sub> at  $C_p = 5.0$  g/L) were measured at 150 V.

**Emulsions.** LSPC<sub>sol</sub>- and SPI<sub>sol</sub>-stabilized emulsions ( $C_p = 10.0$  g/L for LSPC<sub>sol</sub> and  $C_p = 9.2$  g/L for SPI<sub>sol</sub>) were measured at 40 V, after being diluted 500 times in the respective buffers.

### Theoretical critical $\zeta$ -potential of emulsion droplets for flocculation

The theoretical critical  $\zeta$ -potential ( $\zeta_{cr}$ ) for flocculation was calculated using the DLVO theory, as described elsewhere (17). Based on the DLVO theory, the overall interaction potential ( $U_{tot}$ , J) between two protein stabilized emulsion droplets is the sum of the van der Waals interactions ( $U_{vdW}$ , J) and electrostatic interactions ( $U_e$ , J). The  $U_{vdW}$  and  $U_e$  were calculated based on equations 3.4 and 3.5, respectively (18).

$$U_{vdW} = -\frac{A}{6} \cdot \left( \frac{2 \cdot R^2}{4 \cdot R \cdot h} + \frac{2 \cdot R^2}{4 \cdot R^2 + 4 \cdot R \cdot h + h^2} + \ln \left( \frac{4 \cdot R \cdot h + h^2}{4 \cdot R^2 + 4 \cdot R \cdot h + h^2} \right) \right) \quad (3.4)$$

$$U_e = -2 \cdot \pi \cdot \epsilon_0 \cdot \epsilon_r \cdot R \cdot \Psi_0^2 \cdot e^{-kh} \quad (3.5)$$

in which  $A$  is the Hamaker constant ( $4.83 \cdot 10^{-21}$  J) (19),  $R$  is the droplet radius (m),  $h$  is the separation distance between the droplets (m),  $\epsilon_0$  is the dielectric constant of vacuum ( $8.85 \cdot 10^{-12}$  C<sup>2</sup>/J m),  $\epsilon_r$  is the relative refractive index of the medium (80),  $\Psi_0$  is the surface potential (V) and  $\kappa$  is the inverse Debye screening length (m).

The  $\kappa$  was calculated using equation 3.6.

$$\kappa = \sqrt{\frac{2 \cdot N_a \cdot e^2 \cdot I}{\epsilon_0 \cdot \epsilon_r \cdot \kappa_B \cdot T}} \quad (3.6)$$

in which  $N_a$  is the Avogadro constant ( $6.022 \cdot 10^{23}$  mol<sup>-1</sup>),  $e$  is the elementary charge ( $1.602 \cdot 10^{-19}$  C),  $I$  is the ionic strength (mol/m<sup>3</sup>),  $\kappa_B$  is the Boltzmann constant ( $1.38 \cdot 10^{-23}$  J/K) and  $T$  is the temperature (K). It was assumed that flocculation occurs when the primary maximum is below  $5 \kappa_B \cdot T$  or when the secondary minimum is below  $-5 \kappa_B \cdot T$  (19). Using this critical barrier of  $5 \kappa_B \cdot T$ , the  $U_{\text{tot}}$  vs  $\Psi_0$  for different values of  $\Psi_0$  was plotted. The theoretical critical  $\zeta$ -potential corresponds to the lowest  $\Psi_0$  such that  $U_{\text{tot}} \geq 5 \kappa_B \cdot T$ .

### Experimental maximum adsorbed amount ( $\Gamma_{\text{max, exp}}$ )

The experimental maximum amount of protein adsorbed at the oil-water interface

( $\Gamma_{\text{max, exp}}$  in mg/m<sup>2</sup>) was calculated using equation 3.7 (4).

$$\Gamma_{\text{max, exp}} = \frac{d_{3,2\text{min}} \cdot (1 - \Phi_{\text{oil}}) \cdot Q_H \cdot C_{\text{cr}}}{6 \cdot \Phi_{\text{oil}}} \quad (3.7)$$

in which  $\Phi_{\text{oil}}$  is the volume fraction oil (-),  $d_{3,2\text{min}}$  is the experimentally determined minimum droplet size ( $\mu\text{m}$ ),  $Q_H$  is the exposed hydrophobicity (-) and  $C_{\text{cr}}$  is the (critical) protein concentration (g/L).

### Theoretical maximum adsorbed amount for monolayer ( $\Gamma_{\text{max, theory}}$ )

To check whether the  $\Gamma_{\text{max, exp}}$  calculated by equation 3.7 corresponds to the theoretical maximum adsorbed amount of a monolayer ( $\Gamma_{\text{max, theory}}$ ), the  $\Gamma_{\text{max, theory}}$  (mg/m<sup>2</sup>) was calculated using equation 3.8 (4).

$$\Gamma_{\text{max, theory}} = \frac{M_w \cdot 10^3}{\pi \cdot R_{\text{eff}}^2 \cdot N_a} \cdot \theta_{\infty} \quad (3.8)$$

in which  $M_w$  is the molecular mass of the protein (g/mol),  $\theta_{\infty}$  (-) is the saturation coverage at the jamming limit, which was theoretically calculated to be 0.547 and 0.907 for non-diffusing and diffusing proteins, respectively (20, 21).  $R_{\text{eff}}$  is the effective radius of the protein (m), which was calculated from equation 3.9, as described elsewhere (4).

$$R_{\text{eff}} = R_p - \frac{1}{2} \cdot \ln \left( \frac{x}{R_p} \right) \cdot \kappa^{-1} \quad (3.9)$$

in which  $R_p$  is the hard-sphere protein radius (m), which was calculated from equation 3.10, as described elsewhere (4) and  $x$  (-) is a constant. The constant  $x$  for both LSPC and SPI was assumed to be similar as for  $\beta$ -lactoglobulin ( $1.77 \cdot 10^{-9}$ , at pH 7.0) (4), given that the  $\zeta$ -potential of LSPC, SPI and  $\beta$ -lactoglobulin are in the same range (-21.4, -24.1 and -21.2 mV, respectively).

$$R_p = \left( \frac{3 \cdot v \cdot M_w}{4 \cdot \pi \cdot N_a} \right)^{\frac{1}{3}} \quad (3.10)$$

in which  $v$  is the partial specific volume of the protein ( $0.73 \cdot 10^{-6} \text{ m}^3/\text{g}$ ) (22).

### Light microscopy

Light microscopy (20x magnification) (Axioscope A01, Carl Zeiss, Sliedrecht, The Netherlands) was used to distinguish between flocculation and coalescence after the emulsions were either diluted 1:1 with the respective buffer or with 0.5% (w/v) SDS in the respective buffer. In the case of droplet flocculation, the emulsion droplets (or flocculants) are expected to fall apart after the addition of SDS, whereas no effect of SDS is expected when droplet coalescence occurs.

## RESULTS AND DISCUSSION

### Characterization of LSPC and SPI in dispersions and in solutions

LSPC<sub>tot</sub> contained 69.3% (w/w db) protein and 5.1% (w/w db) carbohydrates; of which 3.1% (w/w db) neutral and 2.0% (w/w db) acidic monosaccharides (uronic acids) (**Table 3.1**). The ratio of uronic acids to protein was 0.03 w/w.

**Table 3.1** Gross chemical composition (% w/w dry basis) and uronic acids:protein ratio (w/w) of LSPC and SPI dispersions (LSPC<sub>tot</sub>, SPI<sub>tot</sub>) and solutions (LSPC<sub>sol</sub>, SPI<sub>sol</sub>) at pH 8.0 and I = 0.01 M.

Sample	Protein <sup>a</sup>	Neutral constituent monosaccharides	Uronic acids	Uronic acids:protein
LSPC <sub>tot</sub>	69.3 (± 0.3)	3.1 (± 0.1)	2.0 (± 0.1)	0.03
LSPC <sub>sol</sub>	62.8 (± 0.2)	4.6 (± 0.1)	3.9 (± 0.1)	0.06
SPI <sub>tot</sub>	83.1 (± 0.1)	2.9 (± 0.1)	0.7 (< 0.1)	0.01
SPI <sub>sol</sub>	63.1 (± 0.2)	4.7 (± 0.2)	1.2 (< 0.1)	0.02

<sup>a</sup> Determined as  $N_T \cdot k_p$ .

The main protein present in LSPC<sub>tot</sub> was Rubisco, as indicated by the dominant bands around 50,000 and 15,000 g/mol (9) (**Figure 3.1**). These gross composition values are in the same range as previous values reported for LSPC obtained from a different sugar beet variety (6). SPI<sub>tot</sub> contained 83.1% (w/w db) protein and 3.6% (w/w db) carbohydrates; of which 2.9% (w/w db) neutral and 0.7% (w/w db) acidic monosaccharides (**Table 3.1**). The ratio of uronic acids to protein was 0.01 (w/w). SPI<sub>tot</sub> mainly consisted of proteins with molar masses around 64,000 – 67,000, 50,000, 35,000, 20,000 and 11,000 g/mol. These are indicative of the  $\alpha/\alpha'$  subunits of  $\beta$ -conglycinin (Uniprot accession codes P13916, P11827), the  $\beta$  subunit of  $\beta$ -conglycinin (Uniprot accession code P25974), the acidic polypeptides of glycinin (except A5), the basic polypeptides of glycinin and the acidic polypeptide A5 of glycinin (Uniprot accession codes P04347, P04405, P04776, P11828) (9) (**Figure 3.1**).



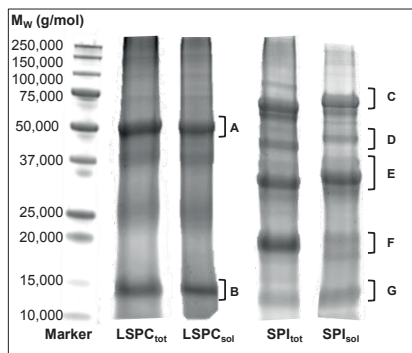


**Figure 3.1** SDS-PAGE gels of LSPC<sub>tot</sub>, LSPC<sub>sol</sub>, SPI<sub>tot</sub> and SPI<sub>sol</sub> under reducing conditions stained by Coomassie blue. Subscripts “tot” and “sol” indicate dispersions and solutions, respectively. In LSPC lanes the large (LS) (A) and the small (SS) (B) Rubisco subunits are indicated. In the SPI lanes the  $\alpha/\alpha'$  subunits of  $\beta$ -conglycinin (C),  $\beta$  subunit of  $\beta$ -conglycinin (D), the acidic polypeptides of glycinin (except A5) (E), the basic polypeptides of glycinin (F) and the acidic polypeptide A5 of glycinin (G) are indicated.

The solubility of LSPC and SPI, at pH 8.0 and  $I = 0.01$  M, was only ~45% and ~27%, respectively ( $C_p = 10.0$  g/L). When the soluble parts of LSPC and SPI were freeze-dried and re-dissolved ( $C_p = 10.0$  g/L) at pH 8.0 and  $I = 0.01$  M, the solubility of both samples was > 95%. The difference in solubility between LSPC (and SPI) in dispersions and in solutions was, therefore, suggested to be due to a difference in protein composition and/or gross chemical composition. This difference is postulated to result in formation of aggregates during freezing and freeze-drying of the starting material.

The most abundant proteins in the soluble parts (LSPC<sub>sol</sub> / SPI<sub>sol</sub>) were similar to the proteins present in the dispersions. The only difference was the lower intensity of the band at  $\pm 20,000$  g/mol for SPI<sub>sol</sub> compared to SPI<sub>tot</sub> (**Figure 3.1**). The main difference between the proteins present in dispersions and in solutions was the gross chemical composition (**Table 3.1**). Both LSPC<sub>sol</sub> and SPI<sub>sol</sub> were enriched in uronic acids; the ratio of uronic acids to protein was 2 times higher in the LSPC<sub>sol</sub> and SPI<sub>sol</sub> than in the respective starting materials (**Table 3.1**). This was also reflected in a shift of the  $\zeta$ -potential vs pH curve to lower pH values for the solutions compared to the dispersions (**Figure 3.2A, B**).

For LSPC<sub>sol</sub>, the lowest absolute charge (0 mV) was reached at pH 4.0, whereas for LSPC<sub>tot</sub> it was reached at pH 4.5 (**Figure 3.2A**). For SPI<sub>sol</sub> the lowest absolute charge (0 mV) was reached at pH 3.3, whereas for SPI<sub>tot</sub> it was reached at pH 4.5 (**Figure 3.2B**).

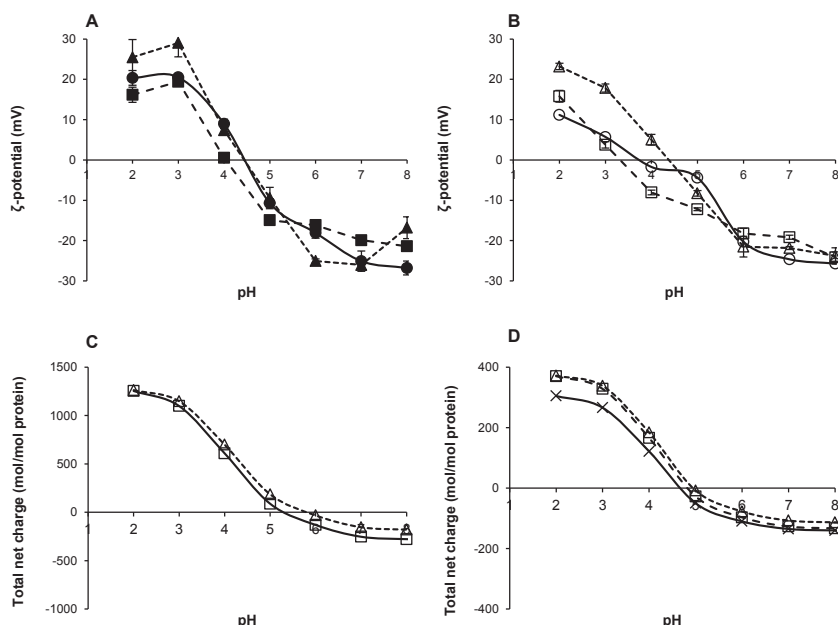


**Figure 3.2**  $\zeta$ -Potential (A, B) and total net charge (C, D) as a function of pH for LSPC (A, C; closed symbols) and SPI (B, D; open symbols) dispersions ( $\blacktriangle$ ,  $\triangle$ ), solutions ( $\blacksquare$ ,  $\square$ ) and emulsions ( $\bullet$ ,  $\circ$ ) at  $I = 0.01$  M. In panels A and B all markers are average values of three measurements with the error bars indicating SD. Error bars are not shown when SD is smaller than the size of the used marker. In panel D the markers ( $\times$ ) indicate the total net charge of SPI solution if we exclude the basic polypeptides of glycine.

Theoretical calculations of the total net charge of the protein mixtures (dispersions and solutions) support the suggested contribution of uronic acids (**Figure 3.2C, D**), although the experimental shift was more pronounced than the theoretical shift. Interactions between negatively charged carbohydrates and positively charged proteins have previously been reported, for example, for complexes of whey protein isolate and pectin and  $\beta$ -lactoglobulin and pectin (23, 24).

### pH dependent solubility of LSPC and SPI

At  $I = 0.01$  M ( $C_p = 10.0$  g/L), the solubility of  $LSPC_{tot}$  at pH 7.0 and at pH  $\leq 3.0$  was similar to the solubility at pH 8.0 (**Figure 3.3A**). For  $SPI_{tot}$  ( $C_p = 10.0$  g/L) the solubility at pH 6.0 - 7.0 and at pH  $< 3.0$  was similar to the solubility at pH 8.0 (**Figure 3.3B**).  $LSPC_{tot}$  had a minimum solubility at pH 5.0, and  $SPI_{tot}$  had a minimum solubility between pH 4.0 and 5.0. Given that for the emulsion formation only the soluble part was used, the solubility of both  $LSPC_{sol}$  and  $SPI_{sol}$  was also studied. The solubility of  $LSPC_{sol}$  (obtained from  $LSPC_{tot}$  at  $C_p = 10.0$  g/L) was close to 100% in the pH range from 6.0 to 8.0 and at pH  $< 3.0$  (**Figure 3.3A**), and it was lowest between pH 4.0 and 5.0. For  $SPI_{sol}$  the solubility was 100% between pH 6.0 and pH 8.0, and it was  $< 20\%$  at lower pH values (**Figure 3.3B**).

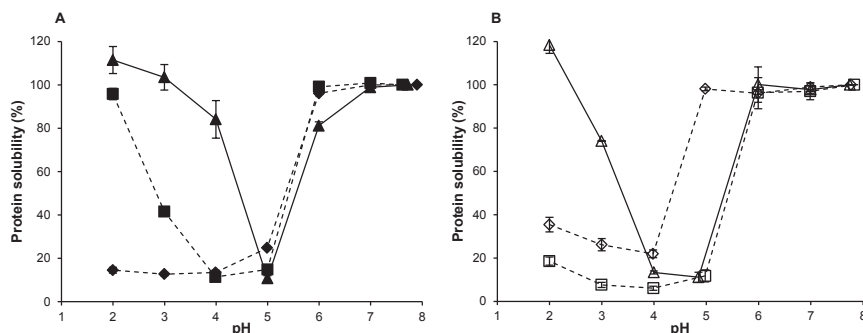


**Figure 3.3** Protein solubility as a function of pH for LSPC (A, closed symbols) and SPI (B, open symbols) dispersions ( $\blacktriangle$ ,  $\triangle$ ) and solutions ( $\blacksquare$ ,  $\square$ ) at  $I = 0.01$  M and dispersions ( $\bullet$ ,  $\circ$ ) and solutions ( $\blacklozenge$ ,  $\blacklozenge$ ) at  $I = 0.5$  M. All markers are average values with the error bars indicating SD, except for LSPC and SPI solutions at  $I = 0.5$  M ( $\bullet$ ,  $\circ$ ). Error bars are not shown when SD is smaller than the size of the used marker.

LSPC<sub>sol</sub> was 60 - 86% less soluble than LSPC<sub>tot</sub> in the pH range from 3.0 to 4.0 (**Figure 3.3A**). The main difference in solubility between SPI<sub>tot</sub> and SPI<sub>sol</sub> was seen at pH < 4.0, where SPI<sub>sol</sub> was 84 - 90% less soluble than SPI<sub>tot</sub> (**Figure 3.3B**). The difference in solubility between the dispersions and solutions is suggested to be caused by the enrichment of the solutions in uronic acids (**Table 3.1**), and the consequent shift of the apparent pI (**Figure 3.2A, B**). In literature there is a large deviation reported regarding the solubility of soy protein isolates (SPIs) at pH 3.0, ranging from 25 to 98% (solubility at pH 8.0 arbitrarily set at 100%) (25-28). Although, the uronic acids content of the SPIs was not reported in these studies, the results from our study indicate that a difference in the content of uronic acids might partially also explain the differences in solubility reported in literature.

At high ionic strength ( $I = 0.5$  M), the solubility of LSPC<sub>tot</sub> decreased gradually as a function of pH from 100% (arbitrary value) at pH 8.0 to  $16 \pm 2\%$  in the pH range from 2.0 to 4.0 (**Figure 3.3A**). For SPI<sub>tot</sub>, the solubility was 100% between pH 6.0 and pH 8.0, and it then decreased to a minimum value (21%) at pH 4.0.

At  $I = 0.5$  M for both LSPC<sub>sol</sub> and SPI<sub>sol</sub> the solubility as a function of pH was similar to that of the respective dispersions. This similarity between the solubility of the proteins (LSPC and SPI) in dispersions and in solutions at high ionic strength was expected given that the high ionic strength leads to charge screening and therefore the formation of less protein-uronic acid complexes. The main effect of the ionic strength on the solubility of LSPC (both LSPC<sub>tot</sub> and LSPC<sub>sol</sub>) as a function of pH was observed in the pH range from 2.0 to 3.0 (**Figure 3.3A**). In this pH range the solubility of LSPC (both LSPC<sub>tot</sub> and LSPC<sub>sol</sub>) at  $I = 0.5$  M was  $\sim 17\%$  whereas at  $I = 0.01$  M the solubility was  $\sim 100\%$  for LSPC<sub>tot</sub> and  $> 42\%$  for LSPC<sub>sol</sub>. For SPI (both SPI<sub>tot</sub> and SPI<sub>sol</sub>) the ionic strength had a pronounced effect on the protein solubility at pH 5.0 (**Figure 3.3B**). At this pH and at high ionic strength ( $I = 0.5$  M) the solubility of both SPI<sub>tot</sub> and SPI<sub>sol</sub> was  $> 76\%$ , whereas at pH 5.0 and  $I = 0.01$  M the solubility was  $\sim 12\%$ . This effect has been previously reported in literature (29). The effect of ionic strength on protein solubility can be due to a difference in the association state of the multimeric proteins. For

example, at pH 7.6 and  $I = 0.03$  M glycinin (64% of SPI) is mainly present as a hexamer, while a small part of it (15-20%) is present as a trimer (12).  $\beta$ -conglycinin (36% of SPI) at  $I = 0.5$  M is mainly present as a trimer, whereas at  $I < 0.1$  M, it is mainly present as a hexamer (13). Such an effect of ionic strength has been also shown for other leguminous proteins, such as helianthin (30). At pH 8.5 and  $I = 0.03$  M helianthin is present as 50% 11S and 50% 7S, whereas at pH 8.5 and  $I = 0.25$  M it is present as 70% 11S and 30% 7S. A change in the association state of the protein could possibly lead to a change in the interaction between the protein molecules and non-protein compounds, such as charged carbohydrates.

### **Characterization of LSPC<sub>sol</sub>- and SPI<sub>sol</sub>-stabilized emulsions**

**Effect of protein concentration on emulsion flocculation.** The average particle size or, in case of non-flocculated emulsions, the average droplet size was measured as  $d_{3,2}$  and indicated by the decay time ( $\tau_{1/2}$ ). For emulsions stabilized with both LSPC<sub>sol</sub> and SPI<sub>sol</sub>, prepared at pH 8.0 ( $I = 0.01$  M), the  $d_{3,2}$  decreased with increasing protein concentration (from 0.6 g/L to  $\sim 10$ g/L) (Figure 3.4A, C). At protein concentrations above the critical concentration (2.1 g/L and 1.0 g/L for LSPC<sub>sol</sub> and SPI<sub>sol</sub>, respectively), the  $d_{3,2}$  reached a minimum value of 0.6  $\mu$ m (Table 3.2; Figure 3.4A, C). These critical concentrations are 2.4 – 5.0 times lower than the  $C_{cr}$  reported for whey protein isolate (WPI) (17). For LSPC<sub>sol</sub>, at  $C_p < 0.6$  g/L macroscopic phase separation was observed. At the same time, a small  $d_{3,2}$  was measured. It was assumed that the combination of small droplets and macroscopic phase separation indicated that the protein concentration was too low to allow homogeneous emulsification. This means that, unlike previous observations on emulsion formation as function of protein concentration, three instead of two regimes should be distinguished. These regimes are demarcated by two critical concentrations.

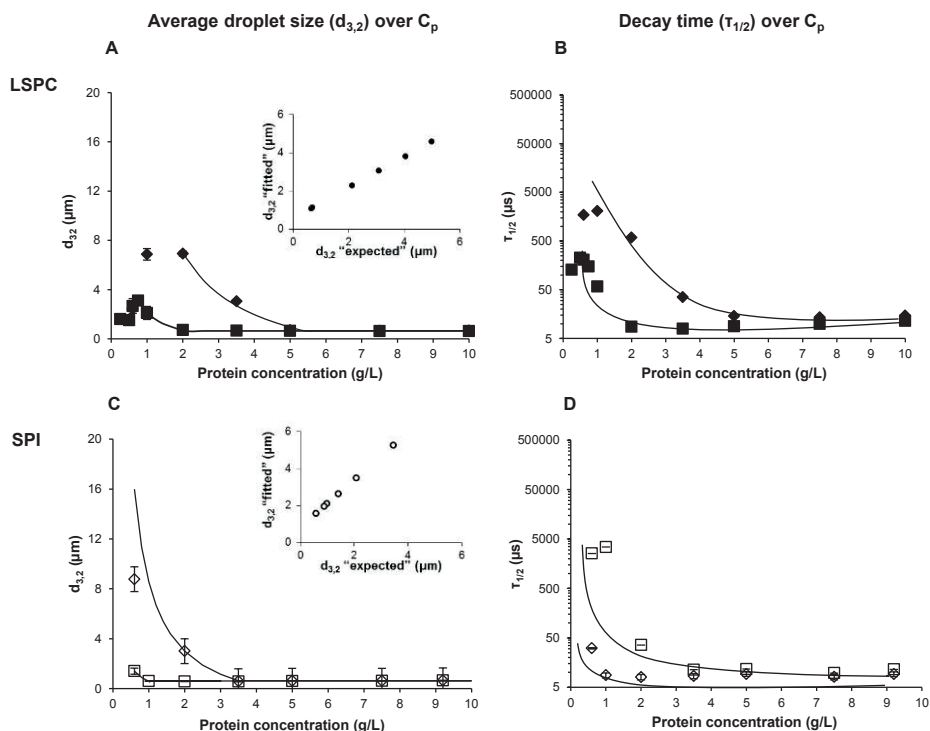


**Figure 3.4** Average droplet size ( $d_{3,2}$ ) (A, C) and decay time ( $\tau_{1/2}$ ) (B, D) as function of protein concentration of emulsions stabilized with LSPC<sub>sol</sub> (closed symbols) and SPI<sub>sol</sub> (open symbols) at pH 8.0 and  $I = 0.01$  M (■, □) or  $I = 0.5$  M (◆, ◇). All markers are average values of five measurements with the error bars indicating the SD. Error bars are not shown when SD is smaller than the size of the used marker. The lines represent the fit of the data calculated with equations 3.1 and 3.2 and the fitting parameters shown in **Table 3.2**. The lines for  $\tau_{1/2}$  (C) are guides to the eye. In panels A and C insets show the  $d_{3,2}$  obtained from the fitted data vs the expected  $d_{3,2}$ , based on equation 3.7 (using the  $\Gamma_{\max, \text{theory}}$ ),  $d_{3,2}$  for LSPC<sub>sol</sub> and SPI<sub>sol</sub>-stabilized emulsions at pH 8.0 and  $I = 0.01$  M

Below the first critical concentration ( $C_{\text{crEF}}$ ; critical concentration for emulsion formation) there is not enough protein to emulsify all oil, and macroscopic phase separation is observed. At higher concentrations, all oil is emulsified, and the  $d_{3,2}$  decreases with protein concentration, until the second critical concentration ( $C_{\text{cr}}$  or else  $C_{\text{crd3,2}}$ ) is reached. Above this concentration a minimum droplet size ( $d_{3,2\text{min}}$ ) is reached. This observation of 3 regimes was previously described for foam formation (32) but had not clearly been identified in the emulsion studies.

When the ionic strength of the emulsions was adjusted to 0.5 M, an increase in  $C_{\text{cr}}$  was observed (**Figure 3.4A, C**), from 2.1 to 5.4 g/L for LSPC<sub>sol</sub> and from 1.0 to 3.5 g/L for SPI<sub>sol</sub> (**Table 3.2**). This increase was larger than what was previously reported for other proteins, such as  $\beta$ -lactoglobulin, for which the  $C_{\text{cr}}$  increased from 2.0 g/L at  $I = 0.01$  M to 2.5 g/L at  $I = 0.2$  M (2).

**Table 3.2** Fitting parameters ( $\alpha$ ,  $d_{3,2 \min}$  and  $C_{cr}$ ) obtained by fitting equations 3.1 and 3.2 to the data shown in **Figures 3.4 and 3.5**.

			LSPC <sub>sol</sub>				SPI <sub>sol</sub>				
			0.01			0.5	0.01			0.5	
			3.0	5.0	8.0	8.0	3.0	5.0	8.0	8.0	
d <sub>3,2</sub> (C)fit	$C_p < C_{cr}$ :	$\alpha$									
	$\alpha \cdot \left( \frac{1}{C} - \frac{1}{C_{cr}} \right) + d_{3,2\min}$	d <sub>3,2min</sub> (μm)	8.8	11.8	2.9	20.2	7.3	6.9	11.1	11.1	
			2.6	3.7	0.6	0.7	8.5	8.7	0.6	0.6	
	$C_p \geq C_{cr}$ :	C <sub>cr</sub> (g/L)	5.0	>10.0	2.1	5.4	3.9	5.3	1.0	3.5	

**Effect of pH on emulsion flocculation.** When the pH of the emulsions was adjusted from pH 8.0 to 5.0 and 3.0 the  $C_{cr}$  increased for both LSPC<sub>sol</sub>- and SPI<sub>sol</sub>-stabilized emulsions (**Table 3.2**). In addition, the measured particle size ( $d_{3,2}$ ) at pH 5.0 and 3.0 was higher than at pH 8.0, even in the protein-rich regime (**Figure 3.5A, C**).

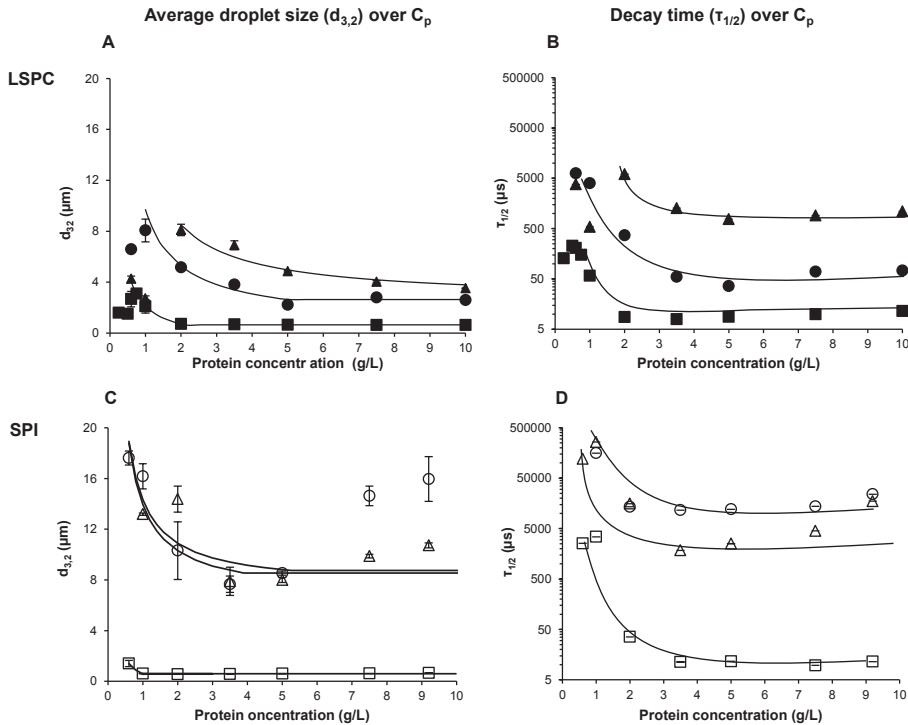


**Figure 3.5** Average droplet size ( $d_{3,2}$ ) (A, C) and decay time ( $\tau_{1/2}$ ) (B, D) as function of protein concentration of emulsions stabilized with LSPC<sub>sol</sub> (closed symbols) and SPI<sub>sol</sub> (open symbols) at I = 0.01 M and pH 3.0 ( $\bullet$ ,  $\circ$ ), pH 5.0 ( $\blacktriangle$ ,  $\triangle$ ) or pH 8.0 ( $\blacksquare$ ,  $\square$ ). All markers are average values of five measurements with the error bars indicating the SD. Error bars are not shown when SD is smaller than the size of the used marker. The lines for  $d_{3,2}$  (A, C) represent the fit of the data calculated with equations 3.1 and 3.2 and the fitting parameters shown in **Table 3.2**. The lines for  $\tau_{1/2}$  (B, D) are guides to the eye.

The increase in particle size was not due to coalescence but due to flocculation, as confirmed by microscopy (**Figure 3.6**). The flocculation was further confirmed (at  $C_p \sim 10$  g/L) by the decrease in particle size, as seen by microscopy, after addition of SDS to the emulsions (**Figure 3.6**). The flocculation corresponded to a decrease in charge, as shown by the  $\zeta$ -potential values (**Figure 3.2**), and a consequent decrease in electrostatic repulsion between the particles. The increase in  $C_{cr}$  with decreasing pH and the increase in  $d_{3,2}$  at pH around the pI was also shown for other proteins, such as WPI (17).

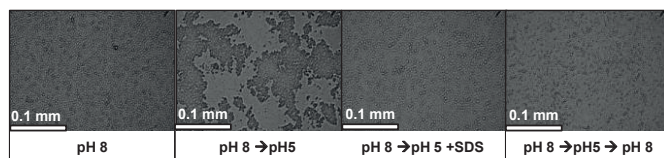


**Figure 3.6** Light microscopy pictures of emulsions stabilized with 10 g/L LSPC<sub>sol</sub> (10% v/v oil) at pH 8.0, after adjustment to pH 5.0, after adjustment to pH 5.0 and addition of SDS and after adjustment to pH 5.0 and readjustment to pH 8.0.

To further study the effect of charge on protein-stabilized emulsions, the pH of LSPC<sub>sol</sub>- and SPI<sub>sol</sub>-stabilized emulsions ( $I = 0.01$  M and  $C_p \sim 10$  g/L; protein-rich regime) was adjusted to values between pH 2.0 and 7.0. For LSPC<sub>sol</sub>-stabilized emulsions the particles flocculated between pH 4.0 - 5.0 (**Figure 3.7A, B**). For SPI<sub>sol</sub>-stabilized emulsions, flocculation was observed over a wider pH range (pH 2.0 - 5.0) (**Figure 3.7A, B**).

The flocculation corresponded to the pH range where LSPC<sub>sol</sub> and SPI<sub>sol</sub> had the lowest solubility (**Figure 3.3**) and where the charge of the emulsion particles was the lowest (**Figure 3.2A, B**). The transition from non-flocculated to flocculated emulsions occurred at an absolute  $\zeta$ -potential of  $\sim 11$  mV; the critical  $\zeta$ -potential ( $\zeta_{cr}$ ) (**Figure 3.7D**). This experimental  $\zeta_{cr}$  is similar to the theoretically calculated  $\zeta_{cr}$  ( $\sim 11$  mV) determined based on a critical barrier for flocculation of  $5 k_B T$  (19). In addition, this value is almost similar to the  $\zeta_{cr}$  value that was determined for WPI stabilized emulsions ( $\zeta_{cr} \sim 9$  mV) (17).



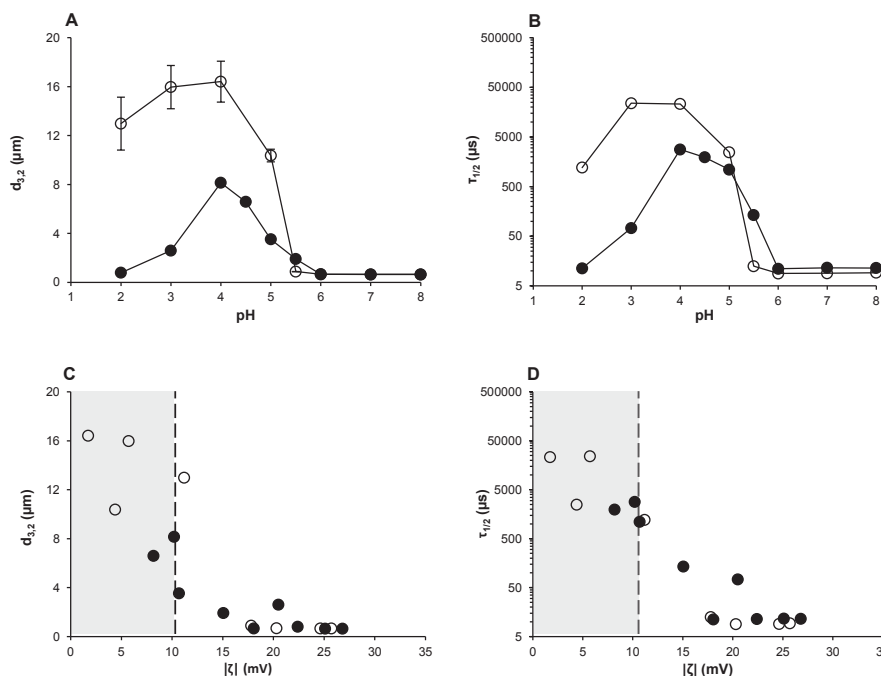


**Figure 3.7** Average droplet size ( $d_{3,2}$ ) (A, C) and decay time ( $\tau_{1/2}$ ) (B, D) of emulsions stabilized by LSPC<sub>sol</sub> (●) and SPI<sub>sol</sub> (○) at  $I = 0.01$  M as function of pH (A, B) and absolute  $\zeta$ -potential (C, D). All markers are average values of three (for  $\zeta$ -potential) or five (for  $d_{3,2}$  and  $\tau_{1/2}$ ) measurements. In panel A the error bars indicate SD. Error bars are not shown when SD is smaller than the size of the used marker. The grey area in panel C and D represent the  $\zeta < \zeta_{cr}$ .

**Link of  $C_{cr}$  to protein adsorbed amount on the interface.** Using the experimental data from the emulsions, estimates were obtained for the maximum adsorbed amount of protein needed to cover the oil-water interface. With increasing ionic strength, the  $\Gamma_{max, exp}$  at the interface increased from  $1.7 \text{ mg/m}^2$  to  $5.1 \text{ mg/m}^2$  for LSPC<sub>sol</sub> and from  $1.0 \text{ mg/m}^2$  to  $3.5 \text{ mg/m}^2$  for SPI<sub>sol</sub> (Table 3.3). By using the  $\Gamma_{max, exp}$  at low ( $I = 0.01$  M) and at high ( $I = 0.5$  M) ionic strength the  $R_{eff}$  at both ionic strengths was calculated (Table 3.3). It was found that the  $R_{eff}$  decreased with increasing ionic strength (Table 3.3). This explains the observation that the  $C_{cr}$  calculated from the experimental data, for both LSPC<sub>sol</sub> and SPI<sub>sol</sub> at high ionic strength was higher than at low ionic strength (Table 3.2).

**Table 3.3** Protein adsorbed amount at the interface derived from  $d_{3,2}$  ( $\Gamma_{\max, \exp}$ ) and based on theoretical calculations ( $\Gamma_{\max, \text{theory}}$ ) at pH 8.0. The parameters used for the calculations.

			Conditions	LSPC <sub>sol</sub>	SPI <sub>sol</sub>
From emulsions	Experimental values	Q <sub>H</sub> (-) <sup>a</sup>		0.9	1.1
		Φ <sub>oil</sub> (-)		0.10	0.10
		C <sub>cr</sub> (g/L)	I = 0.01 / 0.5 M	2.1 / 5.4	1.0 / 3.5
		d <sub>3,2,min</sub> (μm) <sup>a</sup>	I = 0.01 / 0.5 M	0.6 / 0.7	0.6 / 0.6
	Calculated data	Γ <sub>max, exp</sub> (mg/m <sup>2</sup> ) <sup>b</sup>	I = 0.01 / 0.5 M	1.7 / 5.1	1.0 / 3.5
		R <sub>eff</sub> (nm) <sup>c</sup>	I = 0.01 / 0.5 M	9.4 / 5.4	9.7 / 4.8
Constant	Literature values	M <sub>w</sub> (g/mol) <sup>d</sup>	I = 0.01 / 0.5 M	521,896 / 521,896	282,400 / 328,160
From adsorbed layer	Experimental data	Ψ <sub>0</sub> (V) <sup>a</sup>		-21.4·10 <sup>-3</sup>	-24.1·10 <sup>-3</sup>
	Calculated data	κ <sup>-1</sup> (nm) <sup>e</sup>	I = 0.01 / 0.5 M	3.1 / 0.4	3.1 / 0.4
		R <sub>p</sub> (nm) <sup>f</sup>	I = 0.01 / 0.5 M	5.3 / 5.3	4.6 / 4.3
		R <sub>eff</sub> (nm) <sup>c</sup>	I = 0.01 / 0.5 M	7.0 / 5.6	6.0 / 4.5
		Γ <sub>max, theory</sub> (mg/m <sup>2</sup> ) <sup>c</sup>	I = 0.01 / 0.5 M (θ <sub>∞</sub> = 0.547) (θ <sub>∞</sub> = 0.907)	3.1 / 4.9 5.1 / 8.1	2.6 / 4.0 4.3 / 6.6

<sup>a</sup>Experimental values.<sup>b</sup>Calculated data from equation 3.7.<sup>c</sup>Calculated data from equation 3.8.<sup>d</sup>Literature values.<sup>e</sup>Calculated data from equation 3.6.<sup>f</sup>Calculated data from equation 3.10

The values of  $\Gamma_{\max, \exp}$  at each ionic strength were in the same range as the theoretical maximum adsorbed amount ( $\Gamma_{\max, \text{theory}}$ ) derived from the molecular properties. For this calculation (equation 3.8) a monolayer with a saturation coverage ( $\theta_{\infty}$ ) of 0.547 was used (**Table 3.3**). To assess whether the theoretical maximum adsorbed amount ( $\Gamma_{\max, \text{theory}}$ ) could satisfactorily forecast the sensitivity of an emulsion towards flocculation, the expected  $d_{3,2}$  as a function of  $C_p$  was calculated based on equation 3.7. For both LSPC<sub>sol</sub>- and SPI<sub>sol</sub>-stabilized emulsions the expected  $d_{3,2}$  as a function of  $C_p$  was calculated at pH 8.0 and  $I = 0.01$  M. The values for  $d_{3,2}$  calculated based on the  $\Gamma_{\max, \text{theory}}$  were in close agreement to the experimentally measured values (**Figure 3.4A, C, insets**).

When the pH decreased from pH 8.0 to pH 5.0 and pH 3.0, the  $C_{cr}$  increased for both the LSPC<sub>sol</sub> and the SPI<sub>sol</sub>-stabilized emulsions. This higher  $C_{cr}$  at pH 5.0 and pH 3.0 corresponds to an increase in  $\Gamma_{\max, \exp}$  at these pH values (from 1.7 mg/m<sup>2</sup> to 17.5 and > 50 mg/m<sup>2</sup> for LSPC<sub>sol</sub> and from 1.0 mg/m<sup>2</sup> to 54.7 and 76.1 mg/m<sup>2</sup> for SPI<sub>sol</sub>; **Figure 3.8**). These values are much higher than the theoretical maximum adsorbed amount of an adsorbed monolayer ( $\Gamma_{\max, \text{theory}}$ ). Even in case of a closely-packed monolayer ( $\theta_{\infty} = 0.907$ ) with  $R_p = R_{eff}$ ,  $\Gamma_{\max, \text{theory}}$  equals 8.8 and 7.6 mg/m<sup>2</sup> for LSPC<sub>sol</sub> and SPI<sub>sol</sub>, respectively (**Figure 3.8**). Therefore, the higher adsorbed amount of protein determined at pH 5.0 and at pH 3.0 was ascribed to the formation of multilayers. This indicates that the theoretical model cannot be used to predict the adsorbed amount at pH values close to pI, or at  $\zeta < \zeta_{cr}$ . This accounts not only for complex systems but also for more pure protein systems, such as WPI (17). However, it needs to be noted that, as it was

shown in the present study, when  $\zeta < \zeta_{cr}$ , at any  $C_p$  (even in the protein-rich regime) there is emulsion flocculation. Therefore, under these conditions  $\zeta_{cr}$  should be used to predict the stability of an emulsion against flocculation, rather than  $C_{cr}$ .

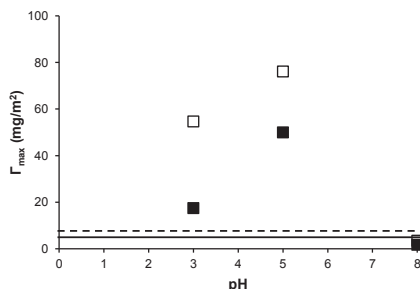


**Figure 3.8** Adsorbed amount ( $\Gamma_{max, exp}$ ) calculated from equation 3.7 as a function of pH for  $LSPC_{sol}$  (■) and  $SPI_{sol}$  (□) at  $C_p = C_{cr}$  and  $I = 0.01$  M. The lines represent the theoretical maximum adsorbed amount of a monolayer ( $\Gamma_{max, theory}$ , calculated from equation 3.8) using a saturation coverage ( $\theta_{\infty}$ ) of 0.907 and  $R_p = R_{eff}$  for  $LSPC_{sol}$  (dashed line) and  $SPI_{sol}$  (solid line).

**Effect of protein concentration on flocculation reversibility.** For pure protein systems, it was shown that the pH induced flocculation was reversible in the protein-rich regime (17). To determine whether this was also the case for less pure systems, the pH of  $LSPC_{sol}$ -stabilized emulsions ( $C_p = 1.0$  and  $10.0$  g/L) was re-adjusted from pH 5.0 and pH 3.0 to pH 8.0. For the  $LSPC_{sol}$ -stabilized emulsion at a low protein concentration ( $C_p = 1.0$  g/L), the flocculation was irreversible (**Figure 3.9**). At higher protein concentration ( $C_p = 10.0$  g/L), the flocculation was completely reversible. This was confirmed by microscopy (**Figure 3.6**) and by the fact that  $\tau_{1/2}$  decreased to the value originally observed at pH 8.0 (**Figure 3.9**).

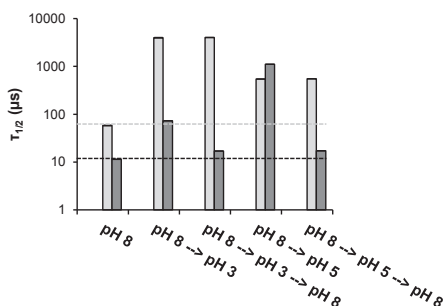


**Figure 3.9** Decay time ( $\tau_{1/2}$ ) for  $LSPC_{sol}$  stabilized emulsions at pH 8.0, pH 8.0  $\rightarrow$  pH 3.0, pH 8.0  $\rightarrow$  pH 3.0  $\rightarrow$  pH 8.0, pH 8.0  $\rightarrow$  pH 5.0, pH 8.0  $\rightarrow$  pH 5.0  $\rightarrow$  pH 8.0 at 1.0 g/L (■) and at 10.0 g/L (■). The dotted lines are guides to the eye.

At high concentrations, sufficient protein will be present to form a saturated adsorbed layer, even at pH close to the pI. At pH  $\sim$  pI, however, the lack of electrostatic repulsion will still result in flocculation. If the pH is then re-adjusted to the original pH, the flocculates will dissociate. At low protein concentrations this does not happen, since there is not enough protein to form a fully adsorbed layer at pH  $\sim$  pI. Consequently, the flocculation at low protein concentrations is not only caused by a lack of charge but

also by a lack of protein coverage. These results show that even in this respect, the complex systems behave in a similar manner as the 'simpler', pure protein-stabilized systems

## CONCLUSIONS

LSPC has emulsion properties comparable to the widely used plant protein SPI. Both LSPC- and SPI-stabilized emulsions show similar sensitivity to pH and ionic strength as the more simple/pure protein-stabilized emulsions; i.e. WPI. At pH 8.0, the values of  $C_{cr}$ ,  $\Gamma_{max}$ ,  $R_{eff}$  and  $d_{3,2}$  obtained from experimental values were close to those forecasted based on the molecular properties of the dominant proteins, taking also the charged carbohydrates into account. From this it was concluded that the model (equation 3.7 using  $\Gamma_{max, theory}$  instead of  $\Gamma_{max, exp}$ ) developed for pure protein-stabilized emulsions can also be used to forecast the properties of emulsions stabilized by more complex protein mixtures.

## FUNDING

This work has been carried out within the framework of Institute for Sustainable Process Technology (ISPT).

## REFERENCES

1. Delahaije, R. J.; Gruppen, H.; Giuseppin, M. L. F.; Wierenga, P. A., Towards predicting the stability of protein-stabilized emulsions. *Advances in Colloid and Interface Science* **2015**, *219*, 1-9.
2. Tcholakova, S.; Denkov, N.; Lips, A., Comparison of solid particles, globular proteins and surfactants as emulsifiers. *Physical Chemistry Chemical Physics* **2008**, *10*, 1608-1627.
3. Kuipers, B. J.; van Koningsveld, G. A.; Alting, A. C.; Driehuis, F.; Voragen, A. G.; Gruppen, H., Opposite contributions of glycinin- and  $\beta$ -conglycinin-derived peptides to the aggregation behavior of soy protein isolate hydrolysates. *Food Biophysics* **2006**, *1*, 178-188.
4. Delahaije, R. J.; Gruppen, H.; Giuseppin, M. L.; Wierenga, P. A., Quantitative description of the parameters affecting the adsorption behaviour of globular proteins. *Colloids and Surfaces B: Biointerfaces* **2014**, *123*, 199-206.
5. Schwenzfeier, A.; Wierenga, P. A.; Eppink, M. H.; Gruppen, H., Effect of charged polysaccharides on the techno-functional properties of fractions obtained from algae soluble protein isolate. *Food Hydrocolloids* **2014**, *35*, 9-18.
6. Kiskini, A.; Vissers, A.; Vincken, J. P.; Gruppen, H.; Wierenga, P. A., Effect of plant age on the quantity and quality of proteins extracted from sugar beet (*Beta vulgaris* L.) leaves. *Journal of Agriculture and Food Chemistry* **2016**, *64*, 8305-8314.
7. Kuipers, B. J.; van Koningsveld, G. A.; Alting, A. C.; Driehuis, F.; Gruppen, H.; Voragen, A. G., Enzymatic hydrolysis as a means of expanding the cold gelation conditions of soy proteins. *Journal of Agriculture and Food Chemistry* **2005**, *53*, 1031-1038.
8. Delahaije, R. J.; Wierenga, P. A.; van Nieuwenhuijzen, N. H.; Giuseppin, M. L.; Gruppen, H., Protein concentration and protein-exposed hydrophobicity as dominant parameters

- determining the effect of protein-stabilized oil-in-water emulsions. *Langmuir* **2013**, *29*, 11567-11574.
9. UniProtKB <http://www.uniprot.org/> (08/05/2017)
  10. Badley, R. A.; Atkinson, D.; Hauser, H.; Oldani, D.; Green, J. P.; Stubbs, J. M., The structure, physical and chemical properties of the soy bean protein glycinin. *Biochimica et Biophysica Acta - Protein Structure* **1975**, *412*, 214-228.
  11. Iyengar, R.; Ravestein, P., New aspects of subunit structure of soybean glycinin. *Cereal Chemistry* **1981**, *58*, 325-330.
  12. Lakemond, C. M.; de Jongh, H. H.; Hessing, M.; Gruppen, H.; Voragen, A. G., Soy glycinin: influence of pH and ionic strength on solubility and molecular structure at ambient temperatures. *Journal of Agriculture and Food Chemistry* **2000**, *48*, 1985-1990.
  13. Phillips, G. O.; Williams, P. A., *Handbook of hydrocolloids*. Elsevier: **2009**.
  14. Schwenzfeier, A.; Wierenga, P. A.; Gruppen, H., Isolation and characterization of soluble protein from the green microalgae *Tetraselmis* sp. *Bioresource Technology* **2011**, *102*, 9121-9127.
  15. Kohn, R.; Kovac, P., Dissociation constants of D-galacturonic and D-glucuronic acid and their O-methyl derivatives. *Chemicke zvesti* **1978**, *32*, 478-485.
  16. Delahaije, R. J.; Wierenga, P. A.; Giuseppin, M. L.; Gruppen, H., Improved emulsion stability by succinylation of patatin is caused by partial unfolding rather than charge effects. *Journal of Colloid Interface Science* **2014**, *430*, 69-77.
  17. Delahaije, R. J.; Hilgers, R. J.; Wierenga, P. A.; Gruppen, H., Relative contributions of charge and surface coverage on pH-induced flocculation of protein-stabilized emulsions. *Colloids and Surfaces A: Physicochemical and Engineering Aspects* **2016**, *25*, 390-398.
  18. Israelachvili, J. N., *Intermolecular and surface forces: revised third edition*. Academic press: **2011**.
  19. Delahaije, R. J.; Gruppen, H.; van Nieuwenhuijzen, N. H.; Giuseppin, M. L.; Wierenga, P. A., Effect of glycation on the flocculation behavior of protein-stabilized oil-in-water emulsions. *Langmuir* **2013**, *29*, 15201-15208.
  20. Reynaert, S.; Moldenaers, P.; Vermant, J., Interfacial rheology of stable and weakly aggregated two-dimensional suspensions. *Physical Chemistry Chemical Physics* **2007**, *9*, 6463-6475.
  21. Talbot, J.; Tarjus, G.; Van Tassel, P.; Viot, P., From car parking to protein adsorption: an overview of sequential adsorption processes. *Colloids and Surfaces A: Physicochemical and Engineering Aspects* **2000**, *165*, 287-324.
  22. Erickson, H. P., Size and shape of protein molecules at the nanometer level determined by sedimentation, gel filtration, and electron microscopy. *Biological procedures online* **2009**, *11*, 32.
  23. Ganzevles, R. A.; Zinoviadou, K.; van Vliet, T.; Cohen Stuart, M. A.; de Jongh, H. H., Modulating surface rheology by electrostatic protein/polysaccharide interactions. *Langmuir* **2006**, *22*, 10089-10096.
  24. Salminen, H.; Weiss, J., Effect of pectin type on association and pH stability of whey protein-pectin complexes. *Food Biophysics* **2014**, *9*, 29-38.
  25. Barac, M. B.; Pesic, M. B.; Stanojevic, S. P.; Kostic, A. Z.; Bivolarevic, V., Comparative study of the functional properties of three legume seed isolates: adzuki, pea and soy bean. *Journal of food science and technology* **2015**, *52*, 2779-2787.

26. Chen, S.; Zhang, N.; Tang, C. H., Influence of nanocomplexation with curcumin on emulsifying properties and emulsion oxidative stability of soy protein isolate at pH 3.0 and 7.0. *Food Hydrocolloids* **2016**, *61*, 102-112.
27. Jung, S.; Murphy, P. A.; Johnson, L. A., Physicochemical and functional properties of soy protein substrates modified by low levels of protease hydrolysis. *Journal of Food Science* **2005**, *70*, C180-C187.
28. Were, L.; Hettiarachchy, N.; Kalapathy, U., Modified soy proteins with improved foaming and water hydration properties. *Journal of Food Science* **1997**, *62*, 821-824.
29. Hermansson, A. M., Methods of studying functional characteristics of vegetable proteins. *Journal of the American Oil Chemists' Society* **1979**, *56*, 272-279.
30. González-Pérez, S.; Vereijken, J. M.; Merck, K. B.; van Koningsveld, G. A.; Gruppen, H.; Voragen, A. G., Conformational states of sunflower (*Helianthus annuus*) helianthinin: effect of heat and pH. *Journal of Agriculture and Food Chemistry* **2004**, *52*, 6770-6778.
31. Lech, F. J.; Delahaije, R. J.; Meinders, M. B.; Gruppen, H.; Wierenga, P. A., Identification of critical concentrations determining foam ability and stability of  $\beta$ -lactoglobulin. *Food Hydrocolloids* **2016**, *57*, 46-54.

---

## Foam properties of sugar beet (*Beta vulgaris* L.) leaf and soybean (*Glycine max*) proteins

---

The use of novel proteins, e.g. sugar beet leaf proteins (LSPC), in foams requires an understanding of the relation between system conditions, molecular and interfacial properties of the proteins, and their foam properties. In pure protein systems, a model was recently developed, where this relation was described using the critical concentrations that were needed to obtain maximal foam ability ( $C_{crFA}$ ) and minimal bubble size ( $C_{cr3,2}$ ). The aim of this study was to test whether this model could also be applied in more complex systems, e.g. LSPC. Soy protein isolate (SPI) was also tested as a control, given that it, similarly to LSPC, comprises a mixture of multimeric proteins and other non-protein compounds, e.g. charged carbohydrates. The  $C_{crFA}$  of LSPC and SPI were similar ( $0.2 \pm 0.1$  g/L) at pH 8.0 ( $I = 0.01$  M). For both LSPC and SPI, the  $C_{crFA}$  increased with decreasing pH. The critical soluble protein concentration was however constant ( $0.2 \pm 0.1$  g/L). At high ionic strength ( $I = 0.5$  M) both proteins were more efficient in foam formation than at low ionic strength ( $I = 0.01$  M), which was related to their faster adsorption at the interface. A minimum soluble protein concentration was needed to form stable foams. At pH 3.0 and 5.0 the foams were more stable than at pH 8.0. The improved foam stability at these pH values was possibly due to the formation of protein or protein-charged carbohydrate aggregates. Overall, the model developed for pure protein systems was found to be applicable to these mixed protein systems.

---

**Based on:** Kiskini, A.; Lech, F. J.; Delahaije, R. J. B. M; Gruppen, H.; Wierenga, P. A., Foam properties of sugar beet (*Beta vulgaris* L.) leaf and soybean (*Glycine max*) proteins (to be submitted).



## INTRODUCTION

Proteins from novel plant sources, such as leaves, have gained interest as alternatives to existing protein-ingredients in food products. A plethora of studies have been published focusing on the isolation of plant proteins and their characterization with respect to their techno-functional properties, e.g. foam properties (1-5). From such studies it becomes clear that foam properties depend on the system conditions. Therefore, to obtain a complete overview of the foam properties of a protein the effect of various system conditions (e.g. pH, I) should be studied. Such an approach is usually impractical. In addition, due to the fact that different methods for foam formation and/or foam determination are usually used in literature the comparison of data from different studies and/or the extrapolation to conditions different to ones presented in a study becomes challenging. This challenge could be tackled if the foam properties of a protein could be related to its molecular and/or interfacial properties. Given that the molecular properties of a protein can be also affected by the system conditions an understanding of the relation between system conditions, molecular and interfacial properties of the proteins, and their foam properties is then needed.

Recently, a model was developed for the description of the foam properties of pure proteins (6), based on an earlier model developed to describe the formation of pure protein-stabilized emulsions (7, 8). In this model (6) the foam properties of a protein, at given conditions (e.g. pH, I), are described as a function of the protein concentration ( $C_p$ ). There are two critical concentrations, denoted as  $C_{crFA}$  and  $C_{cr3,2}$  that demarcate the shift from the protein-poor to the protein-intermediate and the shift from the protein-intermediate to the protein-rich regime, respectively. In the protein-poor regime the foam ability (FA), e.g. the initial foam height, increases with increasing protein concentration up to a maximum value ( $FA_{max}$ ), reached when  $C_p = C_{crFA}$ . In this regime, the foam bubbles are large, but their mean radius ( $r_{3,2}$ ) decreases with increasing protein concentration. In the intermediate-protein regime no further increase in foam ability is observed, i.e.  $FA = FA_{max}$ . In this regime the  $r_{3,2}$  still decreases with increasing protein concentration until  $C_p = C_{cr3,2}$ . At  $C_p = C_{cr3,2}$  the  $r_{3,2}$  reaches a minimum value and thereafter becomes independent of protein concentration (protein-rich regime). The decrease of  $r_{3,2}$  is expected to decrease drainage rate and increase foam stability. For several proteins the foam stability was found to decrease in the protein-rich regime ( $C_p > C_{cr3,2}$ ) (6, 9) even though one might expect either a constant, or increasing foam stability with increasing protein concentration.

The critical concentrations ( $C_{crFA}$ ,  $C_{cr3,2}$ ) can be used to compare the effects of different system conditions. For example, the  $C_{crFA}$  for  $\beta$ -lactoglobulin at pH 7.0 was 0.25 g/L, whereas at pH 5.0 and 3.0 it was 0.45 and 0.75 g/L, respectively. Similarly, the  $C_{cr3,2}$  increased with a decrease in pH from 1.0 g/L at pH 7.0 to > 20 g/L at pH 5.0 (6). This increase in critical concentration corresponded to a decrease in adsorption rate, as measured by the change of surface pressure over time (6). Through this link, a link to molecular properties can be made, since the adsorption kinetics are linked to the molecular properties (e.g. exposed hydrophobicity, charge and radius) of the proteins (10). In this way, the determination of the critical concentrations provides a systematic

approach to characterize the foam properties of proteins, as well as a way to link these properties to the molecular properties of the protein.

In non-pure protein systems, such as in protein concentrates or isolates, other factors, e.g. the presence of charged carbohydrates, are expected to contribute to the foam properties. It was, for example, shown that for algae protein isolate (ASPI), removal of the naturally present charged carbohydrates resulted in a higher foam stability between pH 5.0 - 7.0 (11). In LSPC and SPI, a protein content of 69.3% and 83.1% (w/w dry basis, db) and a charged carbohydrates content of 2.0% and 0.7% (w/w db) were reported, respectively (chapter 3). The presence of charged carbohydrates in these samples affected the protein solubility of LSPC and SPI (chapter 3). Given that in many studies the solubility has been linked to the foam properties of a protein (1, 12), it is expected that the effects on solubility will also affect the foam properties of these mixed systems. Despite the complexity of these systems, it was shown that their emulsion stability could be closely forecasted based on the known (from literature) and measured molecular properties of the most dominant proteins, presence of charged carbohydrates and a small set of experiments (chapter 3).

The first aim of this study is to provide an overview of the foam properties of LSPC and SPI under different system conditions; i.e. pH and I. The second aim is to test whether the recently developed model for the characterization of the foam properties of pure protein systems (6) can be applied in more complex systems, such as LSPC and SPI.

## MATERIALS AND METHODS

### Chemicals and sugar beet leaves

Sugar beets (*Beta vulgaris* L. var. Florena) were grown on a sandy field in Wageningen, The Netherlands. After collection of the sugar beets, the fresh leaves were removed from the stems. The leaves were then washed using tap water and stored at 4 °C, until the excess water was completely drained off (no longer than 36 h). Afterwards, the leaves were stored in vacuum sealed bags at -20 °C. The proteins were extracted from the frozen sugar beet leaves in 0.15 M sodium phosphate buffer pH 8.0, containing 0.8 M NaCl and 0.17% (w/v) Na<sub>2</sub>S<sub>2</sub>O<sub>5</sub>, as described previously (13). The soluble proteins after centrifugation and subsequent dialysis were isolated by acid precipitation at pH 4.5 using 0.5 M HCl. The pellet obtained was subsequently re-solubilized in distilled water at pH 8.0 and freeze-dried, yielding the leaf soluble protein concentrate (LSPC). LSPC contained 69.3% (w/w db) protein (N·5.23), based on Dumas, as described previously (13), and 5.1% carbohydrates (w/w db); 3.1% (w/w db) neutral constituent monosaccharides and 2.0% (w/w db) uronic acids (chapter 3). The main protein present in LSPC was Rubisco (>80% of protein, as based on SDS-PAGE), with a molecular mass of 521,896 g/mol (chapter 3), as shown by SDS-PAGE. Soy protein isolate was produced at the Laboratory of Food Chemistry (Wageningen, The Netherlands), as described elsewhere (14). SPI contained 83.1% (w/w db) protein and 3.6% (w/w db) carbohydrates; 2.9% (w/w db) neutral constituent monosaccharides and 0.7% (w/w db) uronic acids (chapter 3). SPI consisted of glycinin and β-conglycinin in a ratio of 64:36 w/w (15). The

molecular mass of SPI was assumed to be 328,160 g/mol, based on the weight ratios of glycinin and  $\beta$ -conglycinin (*chapter 3*). All other chemicals used were purchased from either Merck (Darmstadt, Germany) or Sigma-Aldrich (St. Louis, MO, USA).

### Protein solubility

The solubility of LSPC and SPI ( $\text{LSPC}_{\text{sol}}$  and  $\text{SPI}_{\text{sol}}$ ) as a function of pH, at  $I = 0.01$  M, was determined, as previously described (*chapter 3*).

### Preparation of LSPC and SPI dispersions and solutions

Freeze-dried LSPC and SPI were dispersed in 3.65 mM sodium phosphate buffer ( $I = 0.01$  M) pH 8.0 and stirred for at least 3 h at room temperature. The LSPC and SPI dispersions ( $\text{LSPC}_{\text{tot}}$  and  $\text{SPI}_{\text{tot}}$ , respectively) at pH 8.0 and  $I = 0.01$  M were centrifuged (5,000 *g*, 20 °C, 10 min) and then filtered through a Büchner funnel using a Whatman paper filter (5-10  $\mu\text{m}$ ) (Sigma Aldrich), to produce stock solutions ( $\text{LSPC}_{\text{sol}}$  and  $\text{SPI}_{\text{sol}}$ , respectively). The protein concentrations of  $\text{LSPC}_{\text{sol}}$  and  $\text{SPI}_{\text{sol}}$  were determined using the Pierce® BCA protein assay using BSA as a standard. In the following sections, the protein concentration ( $C_p$ ) refers to the protein concentration at pH 8.0 and  $I = 0.01$  M. All experiments were performed at least in duplicate.

**Effect of protein concentration.**  $\text{LSPC}_{\text{sol}}$  and  $\text{SPI}_{\text{sol}}$  at different concentrations (0.01 - ~ 5.0 g/L) were prepared by diluting the stock solutions with 3.65 mM sodium phosphate buffer pH 8.0 (final  $I = 0.01$  M).

**Effect of ionic strength.** The ionic strength of  $\text{LSPC}_{\text{sol}}$  and  $\text{SPI}_{\text{sol}}$  stock solutions at pH 8.0 and  $I = 0.01$  M was adjusted to 0.5 M by addition of crystal NaCl. The samples were then stirred for at least 1 h at room temperature. The pH of the samples was periodically checked and re-adjusted to pH 8.0 by addition of 0.2 M NaOH, if necessary. Different concentrations (0.01 - ~ 5.0 g/L) of  $\text{LSPC}_{\text{sol}}$  and  $\text{SPI}_{\text{sol}}$  at  $I = 0.5$  M were prepared by diluting the stock solutions with 3.65 mM sodium phosphate buffer pH 8.0, containing 0.49 M NaCl (final  $I = 0.5$  M).

**Effect of pH.** The pH of  $\text{LSPC}_{\text{sol}}$  and  $\text{SPI}_{\text{sol}}$  stock solutions at pH 8.0 and  $I = 0.01$  M was adjusted to pH 5.0 or to pH 3.0 by addition of 0.2 M HCl. After pH adjustment the samples were stirred for at least 1 h at room temperature. Different concentrations (0.01 - ~ 5.0 g/L) of LSPC and SPI dispersions were prepared by diluting the samples in either 3.33 mM citric acid/sodium citrate buffer pH 5.0 (for pH 5.0,  $I = 0.01$  M) or in 10 mM citric acid/sodium citrate buffer pH 3.0 (for pH 3.0,  $I = 0.01$  M).

### Foam properties

$\text{LSPC}_{\text{sol}}$  and  $\text{SPI}_{\text{sol}}$  at pH 8.0 and  $I = 0.01$  M or  $I = 0.5$  M or dispersions at pH 3.0 or pH 5.0 and  $I = 0.01$  M (40 mL) at different concentrations (0.01 - ~ 5.0 g/L) were placed in the foam cell ( $d = 34$  mm) of an automated foam analyzer (FoamScan, Teclis IT-Concept, Longessaigne, France) at 24 °C and were allowed to equilibrate for 15 min at this temperature. Nitrogen was sparged through a metal frit into the sample in the closed foam cell, as described elsewhere (6). The  $\text{N}_2$  was sparged at a flow rate of 200 mL/min until a foam volume of 200 mL was reached. The foam volume was measured as a function of time by image analysis. The relative foam ability (FA) was expressed as the

foam volume of the sample after 60 s, divided by the maximum obtainable foam volume (183.3 mL) of a 10% SDS solution (pH 8.0, I = 0.01 M). The FA as a function of concentration was fitted with equation 4.1, adapted from (6)

$$FA(C_p)_{fit} = \frac{\alpha}{1 + e^{-\beta(C_p - \delta)}} \quad (4.1)$$

where FA is the foam ability (-),  $C_p$  is the protein concentration (g/L) and  $\alpha$ ,  $\beta$  and  $\delta$  are the fitting parameters. Based on  $FA(C_p)_{fit}$  a critical concentration ( $C_{crFA}$ ) (g/L) for foam ability was determined, as described in detail previously (6). This  $C_{crFA}$  corresponds to the  $C_p$  at which the foam volume (height) reaches its maximal value, under the pre-set conditions, and thereafter becomes independent of the  $C_p$ . In this study, the  $C_{crFA}$  was defined as the threshold beyond which the absolute rate of change of FA with respect to  $C_p$  was below 0.1%. The Sauter bubble radius ( $r_{3,2}$ ) was determined by analysis of images obtained at the end of sparging. The ( $r_{3,2}$ ) as a function of concentration was fitted using equations 4.2 and 4.3, adapted from (8).

$$\text{For } C_p < C_{cr3,2} \text{ (protein-poor regime): } r_{3,2}(C_p)_{fit} = \varepsilon \cdot \left( \frac{1}{C_p} - \frac{1}{C_{cr3,2}} \right) + r_{3,2min} \quad (4.2)$$

$$\text{For } C_p \geq C_{cr3,2} \text{ (protein-rich regime): } r_{3,2}(C_p)_{fit} = r_{3,2min} \quad (4.3)$$

where  $r_{3,2}$  is the Sauter mean bubble radius (mm) and  $\varepsilon$  and  $r_{3,2min}$  are the fitting parameters.  $C_{cr3,2}$  (g/L) is the critical protein concentration above which the Sauter bubble radius becomes independent of the protein concentration, as described in detail elsewhere (6). The foam stability was expressed as foam half-life time ( $t_{1/2}$ ), which is the time at which 50% of the foam volume at the end of sparging had disappeared.

### Interfacial properties

LSPC (0.6 g/L and 0.06 g/L) and SPI (0.6 g/L) solutions at pH 8.0 and I = 0.01 M or I = 0.5 M or dispersions at pH 3.0 or pH 5.0 and I = 0.01 M were used to determine the interfacial properties. All experiments were performed at room temperature. Surface pressure ( $\Pi$ ) and dilatational complex elastic modulus ( $E_d$ ) were determined using an automated drop tensiometer (Tracker, Teclis IT-Concept). The protein solutions or dispersions were placed in a syringe. A droplet (9  $\mu$ L) of sample hanging from the tip of a needle (G18, Sigma Aldrich) was formed by a computer controlled syringe monitored with a video camera. Surface pressure was calculated according to equation 4.4.

$$\Pi = \gamma_0 - \gamma_i \quad (4.4)$$

where  $\gamma_0$  is the equilibrium surface tension of the respective buffer (72.4 mN/m for I = 0.01 M and 71.8 mN/m for I = 0.5 M) and  $\gamma_i$  the surface tension (mN/m) at each measured time point. As an indication of adsorption kinetics, the initial adsorption rate in the first 20 s of adsorption ( $d\Pi/dt$ ) was used. For some samples, the  $d\Pi/dt$  only started to increase ( $\delta > 1$  mN/m) after a certain amount of time. This amount of time is referred to as lag time. Surface elasticity measurements were adapted from a previously described method (16) and performed using the automated drop tensiometer (Tracker, Teclis IT-Concept). The formed drop was subjected to sinusoidal changes in interfacial area (25 mm<sup>2</sup>) at 0.1 Hz frequency and 5% deformation. Each set of five sinuses were

followed by an equilibration phase of 60 s. The complex dilatational elastic modulus ( $E_d$ ), which consists of a storage modulus ( $E'$ ) and a loss modulus ( $E''$ ), was calculated from changes in surface tension and the surface area over the period of the sinusoidal oscillation. The phase angle ( $\delta$ ;  $\tan(\delta) = E''/E'$ ) was also determined. For all samples, the phase angles did not differ with concentration / pH / ionic strength, i.e.  $\tan(\delta)$  was  $11 \pm 3^\circ$  for  $\text{LSPC}_{\text{sol}}$  and  $8 \pm 2^\circ$  for  $\text{SPI}_{\text{sol}}$ . Therefore, only values for the complex modulus are shown.

An amplitude sweep was performed with deformations ranging between 1% and 30% at a constant frequency of 0.02 Hz to study the rheological response as a function of amplitude, as described previously (17). The rheological response is presented in the form of Lissajous plots ( $\delta\gamma$  vs  $\delta A$ ); difference in surface tension ( $\delta\gamma = \gamma - \gamma_1$ ) versus relative deformation ( $\delta A = A - A_1/A_1$ ), where  $\gamma$  and  $A$  are the surface tension and area of the deformed interface and  $\gamma_1$  and  $A_1$  are the surface tension and area of the non-deformed interface. The curves were then qualitatively analyzed based on their shape. An ellipsoidal shape of the curve indicates the absence of non-linearity in the response of the interface towards deformation. This indicates that the determination of the elastic modulus ( $E_d$ ) was reliable (17).

### Determination of $\zeta$ -potential

The pH of  $\text{LSPC}_{\text{sol}}$  and  $\text{SPI}_{\text{sol}}$  solutions (obtained after centrifugation of the 5.0 g/L  $\text{LSPC}_{\text{tot}}$  and  $\text{SPI}_{\text{tot}}$  at pH 8.0 and  $I = 0.01$  M) was adjusted from pH 8.0 to pH 2.0, with 1 unit intervals, using 0.2 M HCl. The  $\zeta$ -potential was determined with a Zetasizer Nano ZSP (Malvern Instruments, Worcestershire, UK) at 25 °C and 150 V. Data were collected over three sequential readings and processed using the Smoluchowski model, as described previously (18).

### Determination of protein exposed hydrophobicity

Protein exposed hydrophobicity was determined using ANSA as a fluorescent probe, as described previously (19), with adaptations.  $\text{LSPC}_{\text{sol}}$  and  $\text{SPI}_{\text{sol}}$  ( $C_p = 0.5$  g/L) and 2.4 mM ANSA solutions were made in 3.65 mM sodium phosphate buffer at pH 8.0. The maximum area of the fluorescence spectrum was corrected with the area of the buffer. The relative exposed hydrophobicity was expressed as the area obtained for the sample relative to the area obtained for a 0.5 g/L  $\beta$ -lactoglobulin solution in the same buffer.

## RESULTS AND DISCUSSION

### Effect of pH on the solubility of $\text{LSPC}_{\text{sol}}$ and $\text{SPI}_{\text{sol}}$

The effect of pH on the solubility of  $\text{LSPC}_{\text{sol}}$  and  $\text{SPI}_{\text{sol}}$  was described in detail in **Chapter 3**. In short, the solubility of  $\text{LSPC}_{\text{sol}}$  as a function of pH showed the typical U-shape curve with a minimum around pH 4.5 (**Figure 4.1**). At pH 5.0 only  $14.8 \pm 0.8\%$  of  $\text{LSPC}_{\text{sol}}$  stayed in solution, while at pH 3.0 the solubility was  $40.0 \pm 2\%$ . The solubility of  $\text{SPI}_{\text{sol}}$  was constant ( $97.8 \pm 1.9\%$ ) between pH 6.0 and pH 8.0 and the lowest solubility was observed in the pH range from 3.0 to 4.0 ( $6.9 \pm 0.2\%$ ) (**Figure 4.1**). The solubility of  $\text{SPI}_{\text{sol}}$  at pH 5.0 was  $11.7 \pm 2.8\%$ .

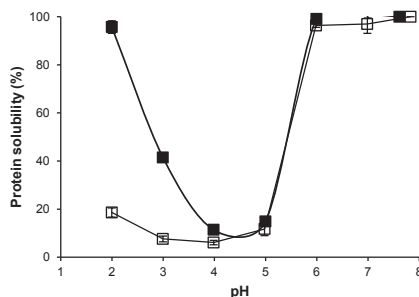


**Figure 4.1** Protein solubility as a function of pH for LSPC<sub>sol</sub> (■) and SPI<sub>sol</sub> (□) at  $I = 0.01$  M. All markers are average values with the error bars indicating SD. Error bars are not shown when SD is smaller than the size of the used marker.

### Effect of protein concentration and ionic strength on foam ability and $C_{crFA}$

The foam ability (FA) as a function of protein concentration was fitted with equation 4.1. The fitted data described the experimental data well (**Figure 4.2A, B**), so in further text, the fitted values for the  $C_{crFA}$  were used (**Table 4.1**). The FA of both LSPC<sub>sol</sub>- and SPI<sub>sol</sub>-stabilized foams at pH 8.0 ( $I = 0.01$  M) increased with increasing protein concentration up to a critical protein concentration ( $C_{crFA}$ ), above which the FA reached a plateau value (**Figure 4.2A, C**). The values of  $C_{crFA}$  at pH 8.0 and  $I = 0.01$  M were comparable for LSPC<sub>sol</sub> and SPI<sub>sol</sub> (0.2 g/L and 0.3 g/L, respectively; **Table 4.1**). For both LSPC<sub>sol</sub> and SPI<sub>sol</sub>, the slope of the FA-concentration curve at  $I = 0.5$  M was higher than at  $I = 0.01$  M (**Figure 4.2A, C**). This indicates that at higher ionic strength, both LSPC<sub>sol</sub> and SPI<sub>sol</sub> were slightly more efficient in foam formation than at lower ionic strength. This effect did, however, not result in a decrease of the  $C_{crFA}$  (**Table 4.1**). The fact that the  $C_{crFA}$  at  $I = 0.5$  M is similar to that at  $I = 0.01$  M might be an artifact of the experimental conditions ( $N_2$  was sparged until foam volume of 200 mL was reached).

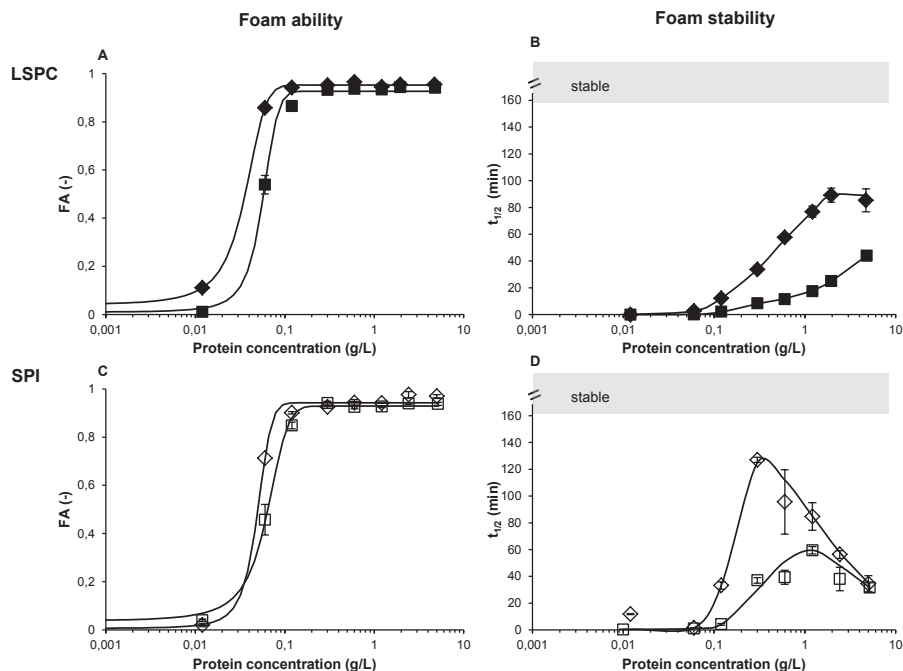


**Figure 4.2** A: Foam ability (A, C) and foam half-life time ( $t_{1/2}$ ; B, D) of  $\text{LSPC}_{\text{sol}}$  (closed symbols) and  $\text{SPI}_{\text{sol}}$  (open symbols) as function of protein concentration at pH 8.0 and ionic strength of 0.01 M (■, □) or 0.5 M (◆, ◇). The solid lines in A and C represent the fit of the data using equation 4.1 and the fitting parameters  $\alpha$ ,  $\beta$ , and  $\delta$  shown in **Table 4.1**. The solid lines in B and D are guides to the eye. All markers are average values with the error bars indicating SD. Error bars are not shown when SD is smaller than the size of the used marker. The grey area indicates that the samples did not reach the  $t_{1/2}$  within the timeframe (167 min) of the experiment.

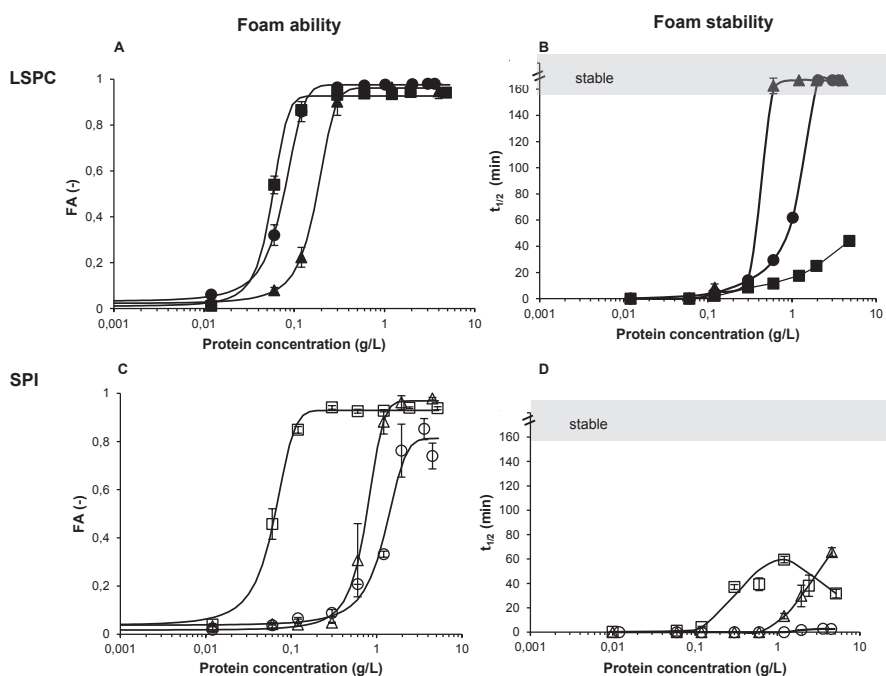


Table 4.1 Critical concentrations and fitting parameters for equations 4.1, 4.2 and 4.3.

		I	LSPC						SPI		
			0.01 M			0.5 M			0.01 M		
			3.0	5.0	8.0	3.0	5.0	8.0	3.0	5.0	8.0
FA(C <sub>p</sub> ) <sub>fit</sub>	Protein concentration in bulk	pH									
		α	0.97	0.96	0.93	0.95	0.97	0.93	0.81	0.97	0.93
		β	44.54	21.30	80.05	88.21	5.25	50.57	2.47	-	101.06
		δ	-0.08	-0.18	-0.06	-0.03	-	-0.06	-1.22	-	-0.05
	Soluble protein concentration	C <sub>crFA</sub> (g/L)	0.3	0.6	0.2	0.2	4.3	2.4	0.3	0.3	0.2
r3,2(C <sub>p</sub> ) <sub>fit</sub>	Protein concentration in bulk	S-C <sub>crFA</sub> (g/L)	0.1	0.1	0.2	0.2	0.3	0.3	0.3	0.3	0.2
		ε	0.03	0.13	0.06	0.02	0.43	0.13	0.43	0.13	0.05
		Γ <sub>3,2min</sub> (mm)	0.06	0.08	0.07	0.05	0.09	0.05	0.09	0.05	0.06
		C <sub>cr3,2</sub> (g/L)	3.9	1.2	5.0	0.5	> 5.0	5.0	> 5.0	5.0	2.5
	Soluble protein concentration	S-C <sub>cr3,2</sub> (g/L)	1.6	0.2	5.0	0.5	> 0.4	0.6	> 0.4	0.6	2.5

### Effect of pH on foam ability and $C_{crFA}$

At pH 5.0 and pH 3.0, the FA for both  $LSPC_{sol}$  and  $SPI_{sol}$  increased with increasing protein concentration up to a  $C_{crFA}$ , above which the FA levelled off (**Figure 4.3A, C**). The  $C_{crFA}$  for both proteins at pH 3.0 and pH 5.0 was higher than at pH 8.0 (**Table 4.1**). It should be noted that these values for  $C_{crFA}$  refer to the total protein concentration in the bulk. If only the soluble  $C_p$  of  $LSPC_{sol}$  and  $SPI_{sol}$  at pH 3.0 and pH 5.0 is taken into account, the  $C_{crFA}$  is similar ( $S-C_{crFA} = 0.2 \pm 0.1$  g/L) for both proteins and at all tested pH values (**Table 4.1**). This indicates that -in these cases- the minimum protein concentration of a protein to reach the maximum FA relates to the soluble protein concentration, and not to the total protein concentration. A relationship between protein solubility and foam ability has been previously described in literature (1, 12, 20).



**Figure 4.3** Foam ability (A, C) and foam half-life time ( $t_{1/2}$ ; B, D) of  $LSPC_{sol}$  (closed symbols) and  $SPI_{sol}$  (open symbols) as a function of protein concentration at pH 3.0 (●, ○), pH 5.0 (▲, △) or pH 8.0 (■, □) and ionic strength of 0.01 M. The solid lines in A and C represent the fit of the data using equation 4.1 and the fitting parameters  $\alpha$ ,  $\beta$ , and  $\delta$  shown in **Table 4.1**. The solid lines in B and D are guides to the eye. All markers are average values with the error bars indicating SD. Error bars are not shown when SD is smaller than the size of the used marker. The grey area indicates that the samples did not reach the  $t_{1/2}$  within the timeframe (167 min) of the experiment.

### Effect of protein concentration and ionic strength on $C_{cr3,2}$

At pH 8.0 and low ionic strength ( $I = 0.01$  M), the  $r_{3,2}$  for both  $LSPC_{sol}$  and  $SPI_{sol}$ -stabilized foams decreased with increasing protein concentration. This decrease continued until a critical protein concentration ( $C_{cr3,2}$ ). At  $C_p = C_{cr3,2}$ , the  $r_{3,2}$  reached a

minimum value ( $r_{3,2min}$ ), which at  $C_p > C_{cr3,2}$  was independent of  $C_p$  (**Figure 4.4A, C**). The  $C_{cr3,2}$  for LSPC<sub>sol</sub>- and SPI<sub>sol</sub>-stabilized foams was 5.0 g/L and 2.5 g/L, respectively (**Table 4.1**). At  $I = 0.5$  M, the  $C_{cr3,2}$  for LSPC<sub>sol</sub> was considerably lower than at  $I = 0.01$  M (0.5 g/L vs 5.0 g/L; **Table 4.1**). However, for SPI<sub>sol</sub>, no effect of ionic strength on  $C_{cr3,2}$  was observed (**Table 4.1**).

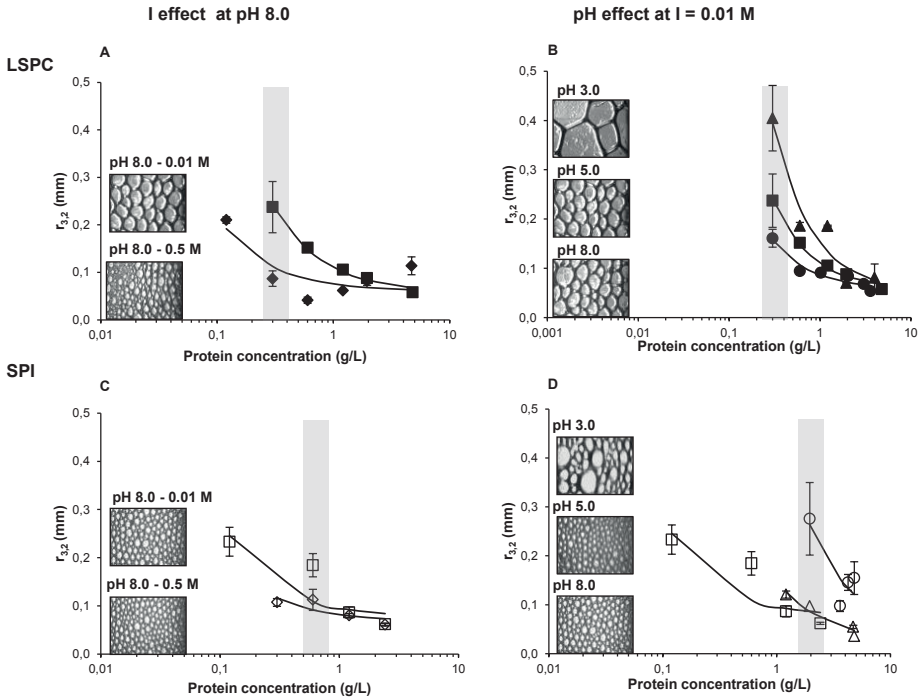


**Figure 4.4** Bubble radius ( $r_{3,2}$ ) as a function of protein concentration of LSPC<sub>sol</sub> (closed symbols) and SPI<sub>sol</sub> (open symbols) at (A, C): pH 8.0 and ionic strength of 0.01 M (■, □) or 0.5 M (◆, ◇) and at (B, D): pH 3.0 (●, ○), pH 5.0 (▲, △) or pH 8.0 (■, □) and ionic strength of 0.01 M. All markers are average values with the error bars indicating SD. Error bars are not shown when SD is smaller than the size of the used marker. Solid lines represent the fit of the data using equations 4.2 and 4.3 and the fitting parameters  $\epsilon$ ,  $C_{cr3,2}$  and  $r_{3,2min}$  shown in **Table 4.1**. Respective concentrations of bubbles shown in insets are indicated by the grey area.

#### Effect of protein concentration and ionic strength on foam stability

The foam stability (FS), indicated by  $t_{1/2}$ , of LSPC<sub>sol</sub> at pH 8.0 at both ionic strengths increased with increasing protein concentration (**Figure 4.2B**). The foam stability was higher at high ionic ( $I = 0.5$  M) than at low ( $I = 0.01$  M) strength. For example, at  $C_p = 5.0$  g/L ( $C_p > C_{cr3,2}$ ; protein-rich regime), the  $t_{1/2}$  for LSPC<sub>sol</sub> at  $I = 0.5$  M was approximately two times higher than at  $I = 0.01$  M (**Figure 4.5**). For SPI<sub>sol</sub>, at both ionic strengths tested, the FS initially increased up until a certain protein concentration and it then significantly decreased, even at  $C_p > C_{cr3,2}$  (**Figure 4.2D**). While typically such a decrease at higher protein concentrations is not expected, it has also been reported for other proteins, such as  $\beta$ -lactoglobulin (6) and  $\alpha$ -lactalbumin (9).

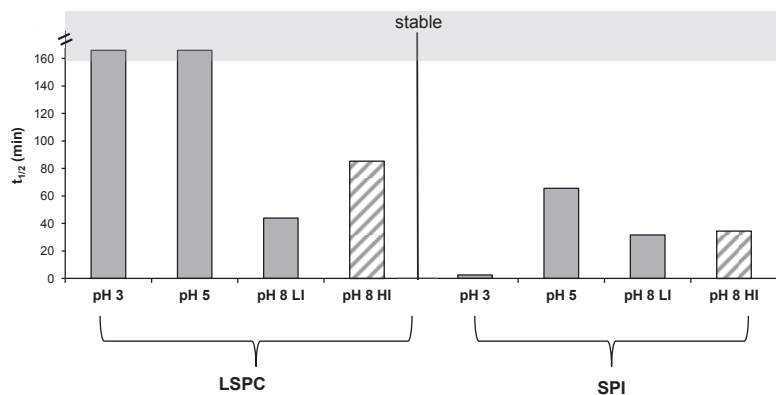


**Figure 4.5** Foam half-life times ( $t_{1/2}$ ) of foams stabilized with LSPC<sub>sol</sub> or SPI<sub>sol</sub> at pH 3.0, pH 5.0 and pH 8.0 and ionic strength of 0.01 M (solid) and 0.5 M (pattern) ( $C_p = 5.0$  g/L). The grey area indicates that the samples did not reach the  $t_{1/2}$  within the timeframe (167 min) of the experiment.

### Effect of pH on $C_{\text{cr}3,2}$

As expected, the  $r_{3,2}$  for both LSPC<sub>sol</sub> and SPI<sub>sol</sub> decreased with increasing protein concentration at all pH values tested (**Figure 4.4B, D**). For LSPC<sub>sol</sub>, the  $C_{\text{cr}3,2}$  at pH 8.0 (5.0 g/L) was higher than at pH 5.0 (1.2 g/L) and at pH 3.0 (3.9 g/L) (**Table 4.1**). For SPI<sub>sol</sub> the  $C_{\text{cr}3,2}$  at pH 8.0 was 2.5 g/L and at pH 5.0 and pH 3.0 it was 5.0 g/L and > 5.0 g/L, respectively (**Table 4.1**). If only the soluble concentration of the protein at pH 5.0 and at pH 3.0 is taken into account, then the minimum protein concentration ( $S\text{-}C_{\text{cr}3,2}$ ) required to form a stable foam ( $r_{3,2} = r_{3,2\text{min}}$ ), using LSPC<sub>sol</sub> at pH 5.0 and at pH 3.0, was 0.6 g/L and 1.2 g/L, respectively (**Table 4.1**). For SPI<sub>sol</sub>, the  $S\text{-}C_{\text{cr}3,2}$  at pH 5.0 was 0.6 g/L (**Table 4.1**). At pH 3.0, the  $r_{3,2\text{min}}$  was not reached within the protein concentrations tested. For both proteins, it was observed that the  $S\text{-}C_{\text{cr}3,2}$  was the lowest at pH close to their overall isoelectric point (LSPC<sub>sol</sub> pI: 4.5 and SPI<sub>sol</sub> pI: 3.3; **Figure 4.6**). This shows that unlike  $C_{\text{crFA}}$  the  $C_{\text{cr}3,2}$  is not only dependent on soluble protein.

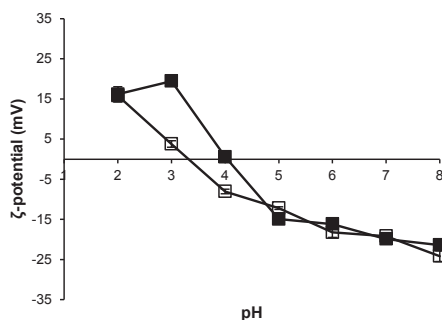


**Figure 4.6** ζ-potential as a function of pH for LSPC<sub>sol</sub> (■) and SPI<sub>sol</sub> (□) solutions at ionic strength of 0.01 M. All markers are average values with the error bars indicating SD. Error bars are not shown when SD is smaller than the size of the used marker.

### Effect of pH foam stability

The FS of LSPC<sub>sol</sub>-stabilized foams increased with increasing protein concentration at all pH values tested (**Figure 4.3B**). At  $C_p > 5.0$  g/L (protein-rich regime), LSPC<sub>sol</sub>-stabilized foams at pH 5.0 and pH 3.0 had higher FS than at pH 8.0 (**Figure 4.5**). Rubisco from spinach also showed higher foam stability at pH 5.5 and pH 3.0 than at pH 8.0 (22).

For SPI<sub>sol</sub>, the FS of the foams at pH 8.0 increased with increasing protein concentration up until  $C_p = 1.2$  g/L and then it decreased (**Figure 4.3D**). At pH 3.0, no stable foams could be obtained. In addition to the low  $t_{1/2}$  the  $r_{3,2min}$  was not reached, which shows that the protein-rich regime was not reached. This is postulated to be due to lack of sufficient soluble protein at this pH (i.e.  $C_{crr3,2}$  for SPI at pH 3.0  $>$  maximal  $C_p$  tested). At pH 5.0, the FS for SPI<sub>sol</sub>-stabilized foam increased with increasing protein concentration, even at  $C_p > C_{crr3,2}$ . At  $C_p = 5.0$  g/L (protein-rich regime), the FS of SPI<sub>sol</sub>-stabilized foam at pH 5.0 was 2 times higher than at pH 8.0 (**Figure 4.5**). These results are in contrast with literature, where the foam stability of soy protein isolates is typically minimal at pH 5.0 (22, 23). This apparent discrepancy might be due to the different methods used for foam formation and determination, the different composition of the samples used and/or the fact that the samples were tested at different protein concentrations.

Our data indicate that initially, a minimum soluble protein concentration is required to completely cover the air-water interface and form a stable foam. At pH 5.0 and at pH 3.0, it is postulated that aggregates are formed between proteins or proteins and charged carbohydrates present in the samples. These aggregates contribute to the higher FS at these pH values than at pH 8.0. Other researchers have also shown that non-aggregated proteins are essential to produce stable foams, while aggregates contribute to a better foam stabilization (20). Positive effects of the formed aggregates on the foam stability were previously reported, for example, for complexes of napin and pectin (24).

### Link of foam ability to interfacial and molecular properties

**Effect of ionic strength.** To determine whether the foam properties of LSPC<sub>sol</sub> and SPI<sub>sol</sub> can be linked to their interfacial properties, the  $E_d$  and  $\Pi$  of adsorbed layers formed from these solutions were determined at different ionic strengths. For LSPC<sub>sol</sub>, at  $C_p = 0.06$  g/L (pH 8.0), the  $E_d$ - $\Pi$  curves at  $I = 0.01$  M and  $I = 0.5$  M collapsed onto a single curve (**Figure 4.7A**). This suggests that the interactions between the adsorbed proteins at the air-water interface at low (0.01 M) and high (0.5 M) ionic strength are similar. Thus, differences at  $d\Pi/dt$  at low and high ionic strength can be taken as an indication of differences in adsorption kinetics. LSPC<sub>sol</sub> adsorbed faster at  $I = 0.5$  M than at  $I = 0.01$  M ( $d\Pi/dt = 45$  vs  $12$   $\mu\text{N}/(\text{m}\cdot\text{s})$ , respectively, **Figure 4.7B**), which might explain the higher foam ability of LSPC<sub>sol</sub> at  $I = 0.5$  M than at  $I = 0.01$  (**Figure 4.2A**). The faster adsorption at higher ionic strength was previously described for other proteins, e.g. algae soluble protein isolate, whey protein isolate and ovalbumin (25). In these cases this faster adsorption was attributed to a decreased electrostatic barrier for adsorption at the air-water interface (16).

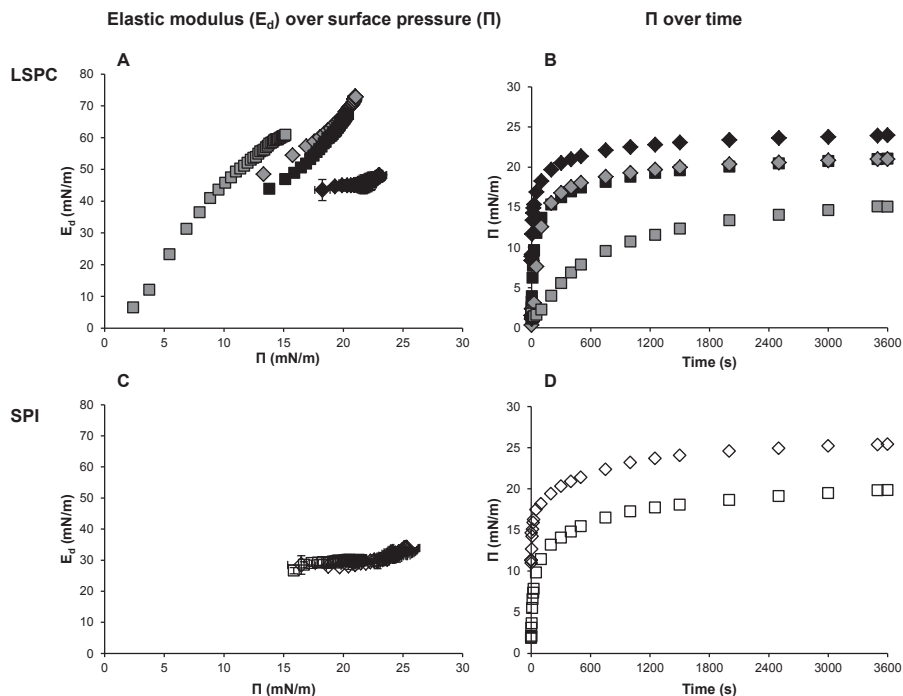


**Figure 4.7** Elastic modulus ( $E_d$ ) as a function of surface pressure ( $\Pi$ ) at the air-water interface (A, C) and  $\Pi$  as a function of time (B, D) of LSPC<sub>sol</sub> (at  $C_p = 0.06$  g/L grey closed symbols and  $C_p = 0.6$  g/L black closed symbols) and SPI<sub>sol</sub> (at  $C_p = 0.6$  g/L open symbols) at pH 8.0 and ionic strength of 0.01 M (■, ■, □) or 0.5 M (◆, ◆, ◇). All markers are average values with the error bars indicating SD. Error bars are not shown when SD is smaller than the size of the used marker.

For LSPC<sub>sol</sub>, at  $C_p = 0.6$  g/L (pH 8.0), the  $E_d$ - $\Pi$  curves at low and high ionic strength did not superimpose. This indicates a slight difference in the equation of state of adsorption for LSPC<sub>sol</sub>. The suggested difference in the equation of state of LSPC<sub>sol</sub> at different ionic strengths was also reflected in the behavior of these interfaces at larger amplitudes. At  $I = 0.01$  M, the interface showed a linear response (**Figure 4.8**). At  $I = 0.5$  M, the response was not analyzed since the bubble got expelled before the end of the experiment (data not shown). The difference in the equation of state might due to the contribution of non-protein compounds (e.g. charged carbohydrates) or to the presence of multiple types and/or forms of proteins (e.g. dissociated forms). This difference seems to be protein concentration dependent, given that at  $C_p = 0.06$  g/L, the  $E_d$ - $\Pi$  curves for LSPC<sub>sol</sub> at  $I = 0.01$  M and  $I = 0.5$  M did superimpose. The protein concentration-dependent effect of ionic strength on equation of state was not surprising. For other proteins, e.g.  $\beta$ -lactoglobulin, it has previously been reported that the effect of ionic strength on the dissociation state of the protein changed with the protein concentration (26).

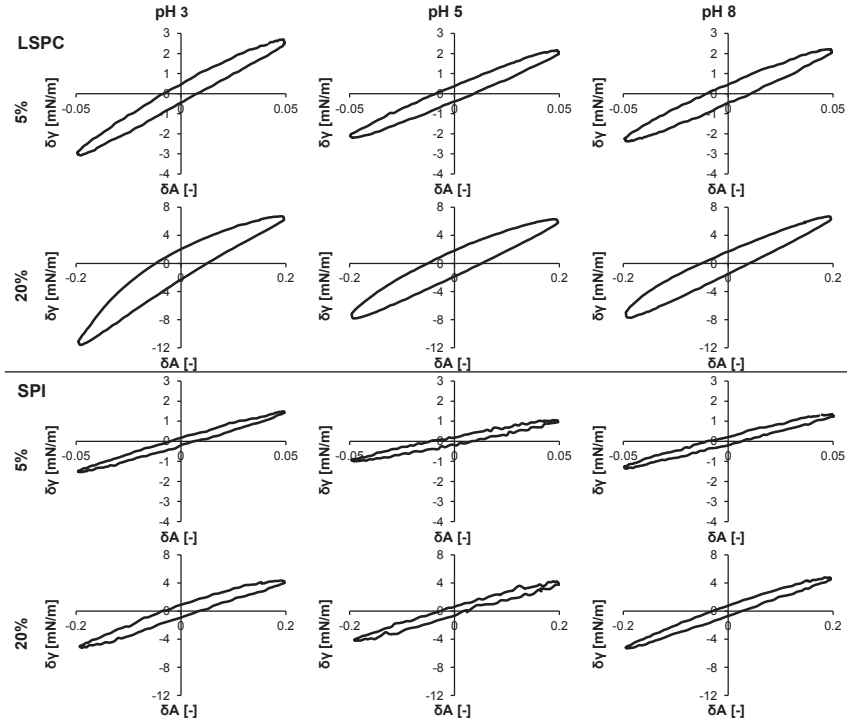


**Figure 4.8** Lissajous plots for  $\text{LSPC}_{\text{sol}}$  and  $\text{SPI}_{\text{sol}}$  at pH 8.0, pH 5.0 and pH 3.0 ( $I = 0.01$  M) and 5% and 20% deformation ( $C_p = 0.6$  g/L).

For  $\text{SPI}_{\text{sol}}$ , the  $E_d$  and  $\Pi$  were only determined at  $C_p = 0.6$  g/L (at both ionic strengths). For these samples, no effect of the ionic strength on the equation of state was observed (Figure 7C). The adsorption rate increased with increasing ionic strength (200 vs 300  $\mu\text{N}/(\text{m}\cdot\text{s})$  at  $I = 0.01$  M and  $I = 0.5$  M, respectively; **Figure 4.7D**). This difference was also reflected in a difference in foam ability; i.e. at  $C_p < C_{\text{crFA}}$ , the FA was higher at  $I = 0.5$  M than at  $I = 0.01$  M (at  $C_p > C_{\text{crFA}}$  the FA had reached its maximum value).

**Effect of pH.** For  $\text{LSPC}_{\text{sol}}$  ( $I = 0.01$  M and  $C_p = 0.06$  g/L), the  $E_d$ - $\Pi$  curves at pH 5.0 and at pH 8.0 overlapped (**Figure 4.9A**). This suggests that the interactions between the adsorbed proteins at the air-water interface at the different pH values are similar. Hence, the longer lag time (approximately 500 s) for  $\text{LSPC}_{\text{sol}}$  at pH 5.0 than at pH 8.0 is interpreted as a slower adsorption at this pH value (**Figure 4.9B**), which is suggested to be the cause of the lower foam ability of  $\text{LSPC}_{\text{sol}}$  under these conditions.

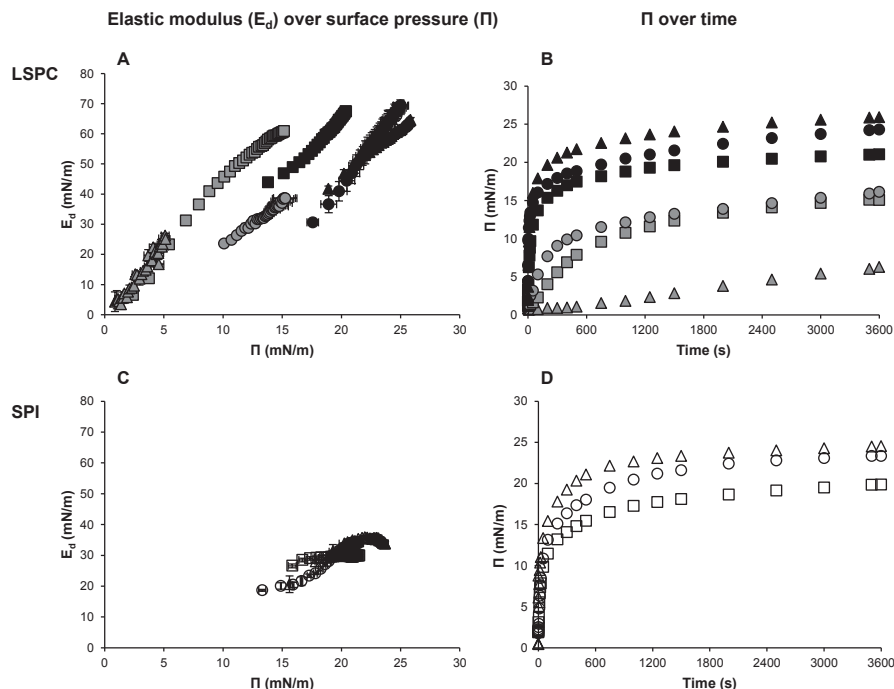


**Figure 4.9** Elastic modulus ( $E_d$ ) as a function of surface pressure ( $\Pi$ ) at the air-water interface (A, C) and  $\Pi$  as a function of time (B, D) of LSPC<sub>sol</sub> (at  $C_p = 0.06$  g/L grey closed symbols and  $C_p = 0.6$  g/L black closed symbols) and SPI<sub>sol</sub> (at  $C_p = 0.6$  g/L open symbols) pH 3.0 (●, ●, ○), pH 5.0 (▲, ▲, △) or pH 8.0 (■, ■, □) and ionic strength of 0.01 M. All markers in A and C are average values with the error bars indicating SD. Error bars are not shown when SD is smaller than the size of the used marker.

The slow adsorption at pH 5.0 is ascribed to the low solubility ( $14.8 \pm 0.8\%$ ) of LSPC<sub>sol</sub> at this pH (**Figure 4.1**). This shows that the interfacial properties, similarly to what was shown for the C<sub>crFA</sub>, relate to the soluble protein concentration and not to the total protein concentration. At pH 3.0 (both at  $C_p = 0.06$  g/L and 0.6 g/L) the  $E_d$ - $\Pi$  curve was shifted with respect to the curves at pH 8.0 and pH 5.0 (**Figure 4.9A**). The LSPC<sub>sol</sub> interface at pH 3.0 showed non-linear behavior (**Figure 4.8**).

In contrast, for SPI<sub>sol</sub> (at  $C_p = 0.6$  g/L), the  $E_d$ - $\Pi$  curves at pH 5.0 and pH 3.0 overlapped, and hence a similar equation of state is assumed (**Figure 4.9C**). The similar adsorption rates for SPI<sub>sol</sub> at pH 5.0 and pH 3.0 (**Figure 4.9D**) can explain the similar foam abilities for SPI<sub>sol</sub> at these pH values (**Figure 4.3C**). It needs to be noted that since the SPI<sub>sol</sub> interface showed non-linear behavior at pH 3.0, although less pronounced than LSPC<sub>sol</sub> (**Figure 4.8**), the values for  $E_d$  should be taken with caution.

## CONCLUSIONS

The foam ability, as expressed by the critical concentration of soluble proteins ( $S$ -C<sub>crFA</sub>) needed to produce foam, was constant as a function of pH, for both LSPC and SPI. At high ionic strength ( $I = 0.5$  M), both proteins were more efficient in foam formation



than at low ionic strength ( $I = 0.01 \text{ M}$ ). This was related to their faster adsorption at the interface. A minimum concentration was required to form stable foams. At pH 3.0 and 5.0, an enhanced foam stability was observed, which is postulated to be due to aggregates formed between proteins or proteins and charged carbohydrates. Less protein was required to form a stable foam at high than at low ionic strength. Overall, the foam ability and foam stability as a function of protein concentration for these protein mixtures showed a similar trend as that for pure protein-stabilized foams. Therefore, the use of critical protein concentrations to describe foam ability and foam stability, as developed for pure protein systems, can be applied to these mixed protein systems.

## FUNDING

This work has been carried out within the framework of Institute for Sustainable Process Technology (ISPT).

## REFERENCES

1. Wang, J.; Kinsella, J., Functional properties of alfalfa leaf protein: foaming. *Journal of Food Science* **1976**, *41*, 498-501.
2. Bora, P. S., Functional properties of native and succinylated lentil (*Lens culinaris*) globulins. *Food Chemistry* **2002**, *77*, 171-176.
3. Kabirullah, M.; Wills, R., Foaming properties of sunflower seed protein. *Journal of Food Science and Technology* **1988**, *25*, 16-19.
4. Martínez, K. D.; Sánchez, C. C.; Patino, J. M. R.; Pilosof, A. M., Interfacial and foaming properties of soy protein and their hydrolysates. *Food Hydrocolloids* **2009**, *23*, 2149-2157.
5. Lamsal, B.; Koegel, R.; Gunasekaran, S., Some physicochemical and functional properties of alfalfa soluble leaf proteins. *LWT-Food Science and Technology* **2007**, *40*, 1520-1526.
6. Lech, F. J.; Delahaije, R. J.; Meinders, M. B.; Gruppen, H.; Wierenga, P. A., Identification of critical concentrations determining foam ability and stability of  $\beta$ -lactoglobulin. *Food Hydrocolloids* **2016**, *57*, 46-54.
7. Tcholakova, S.; Denkov, N.; Lips, A., Comparison of solid particles, globular proteins and surfactants as emulsifiers. *Physical Chemistry Chemical Physics* **2008**, *10*, 1608-1627.
8. Delahaije, R. J.; Gruppen, H.; Giuseppin, M. L. F.; Wierenga, P. A., Towards predicting the stability of protein-stabilized emulsions. *Advances in Colloid and Interface Science* **2015**, *219*, 1-9.
9. Dhayal, S. K.; Delahaije, R. J.; de Vries, R. J.; Gruppen, H.; Wierenga, P. A., Enzymatic cross-linking of  $\alpha$ -lactalbumin to produce nanoparticles with increased foam stability. *Soft Matter* **2015**, *11*, 7888-7898.
10. Delahaije, R. J.; Gruppen, H.; Giuseppin, M. L.; Wierenga, P. A., Quantitative description of the parameters affecting the adsorption behaviour of globular proteins. *Colloids and Surfaces B: Biointerfaces* **2014**, *123*, 199-206.
11. Schwenzfeier, A.; Wierenga, P. A.; Eppink, M. H.; Gruppen, H., Effect of charged polysaccharides on the techno-functional properties of fractions obtained from algae soluble protein isolate. *Food Hydrocolloids* **2014**, *35*, 9-18.

12. Yasumatsu, K.; Sawada, K.; Moritaka, S.; Misaki, M.; Toda, J.; Wada, T.; Ishii, K., Whipping and emulsifying properties of soybean products. *Agricultural and Biological Chemistry* **1972**, *36*, 719-727.
13. Kiskini, A.; Vissers, A.; Vincken, J. P.; Gruppen, H.; Wierenga, P. A., Effect of plant age on the quantity and quality of the proteins extracted from sugar beet (*Beta vulgaris* L.) leaves. *Journal of Agriculture and Food Chemistry* **2016**, *64*, 8305-8314.
14. Kuipers, B. J.; van Koningsveld, G. A.; Alting, A. C.; Driehuis, F.; Gruppen, H.; Voragen, A. G., Enzymatic hydrolysis as a means of expanding the cold gelation conditions of soy proteins. *Journal of Agriculture and Food Chemistry* **2005**, *53*, 1031-1038.
15. Kuipers, B. J.; van Koningsveld, G. A.; Alting, A. C.; Driehuis, F.; Voragen, A. G.; Gruppen, H., Opposite contributions of glycinin- and  $\beta$ -conglycinin-derived peptides to the aggregation behavior of soy protein isolate hydrolysates. *Food Biophysics* **2006**, *1*, 178-188.
16. Wierenga, P. A.; Meinders, M. B.; Egmond, M. R.; Voragen, A. G.; de Jongh, H. H., Quantitative description of the relation between protein net charge and protein adsorption to air-water interfaces. *The Journal of Physical Chemistry B* **2005**, *109*, 16946-16952.
17. Wan, Z.; Yang, X.; Sagis, L. M. C., Contribution of long fibrils and peptides to surface and foaming behavior of soy protein fibril system. *Langmuir* **2016**, *32*, 8092-8101.
18. Delahaije, R. J. B. M.; Wierenga, P. A.; Giuseppin, M. L. F.; Gruppen, H., Improved emulsion stability by succinylation of patatin is caused by partial unfolding rather than charge effects. *Journal of Colloid and Interface Science* **2014**, *430*, 69-77.
19. Delahaije, R. J.; Wierenga, P. A.; van Nieuwenhuijzen, N. H.; Giuseppin, M. L.; Gruppen, H., Protein concentration and protein-exposed hydrophobicity as dominant parameters determining the flocculation of protein-stabilized oil-in-water emulsions. *Langmuir* **2013**, *29*, 11567-11574.
20. Rullier, B.; Novales, B.; Axelos, M. A., Effect of protein aggregates on foaming properties of  $\beta$ -lactoglobulin. *Colloids and Surfaces A: Physicochemical and Engineering Aspects* **2008**, *330*, 96-102.
21. Barbeau, W.; Kinsella, J., Physical behavior functional properties: Relationship between surface rheology and foam stability of ribulose 1, 5-bisphosphate carboxylase. *Colloids and Surfaces* **1986**, *17*, 169-183.
22. Barac, M. B.; Pesic, M. B.; Stanojevic, S. P.; Kostic, A. Z.; Bivolarevic, V., Comparative study of the functional properties of three legume seed isolates: adzuki, pea and soy bean. *Journal of Food Science and Technology* **2015**, *52*, 2779-2787.
23. Kempka, A.; Honaiser, T.; Fagundes, E.; Prestes, R., Functional properties of soy protein isolate of crude and enzymatically hydrolysed at different times. *International Food Research Journal* **2014**, *21*.
24. Schmidt, I.; Novales, B.; Boué, F.; Axelos, M. A., Foaming properties of protein/pectin electrostatic complexes and foam structure at nanoscale. *Journal of Colloid and Interface Science* **2010**, *345*, 316-324.
25. Schwenzfeier, A.; Lech, F.; Wierenga, P. A.; Eppink, M. H. M.; Gruppen, H., Foam properties of algae soluble protein isolate: Effect of pH and ionic strength. *Food Hydrocolloids* **2013**, *33*, 111-117.
26. Aymard, P.; Durand, D.; Nicolai, T., The effect of temperature and ionic strength on the dimerisation of  $\beta$ -lactoglobulin. *International Journal of Biological Macromolecules* **1996**, *19*, 213-221.

---

## Using product driven process synthesis in the biorefinery

---

The design of a biorefining process is challenging due to the high number of products that can be obtained from one feedstock, and the fact that some products can be negatively affected by processing conditions that are essential for other products. To facilitate this design, we propose the use of the product driven process synthesis methodology, with some adaptations. Four novel steps were introduced: (1) decomposition of the feedstock into its main compound classes, (2) identification of the potential uses of the compound classes found in the feedstock, based on the functionalities that they can deliver, (3) selection of the product-targets by evaluating their economic potential, and (4) identification of "critical tasks"; i.e. tasks that negatively affect the quantity and/or quality of each product during their separation. To illustrate how this new approach can be used in practice, a case study of a sugar beet leaves biorefinery is presented.

---

**Based on:** Kiskini, A.; Zondervan, E.; Wierenga, P. A.; Poiesz, E.; Gruppen, H., Using product driven process synthesis in the biorefinery. *Computers and Chemical Engineering* **2016**, 91, 257 – 268.

## INTRODUCTION

In the last fifteen years, the biorefinery concept has gained great momentum. The term biorefinery refers to the sustainable processing of a biomass into a spectrum of products and energy (1). By consequence, a biorefinery approach within the industry aims to optimize the yield of a range of components, rather than to maximize the yield of a single component. The latter implies that the focus of a biorefining process is both on compound classes present in high amounts in the feedstock (e.g. carbohydrates) that can lead to high-volume products (e.g. animal feed, fertilizers) and on compound classes present in low amounts in the feedstock (e.g. phenolic compounds) that can be sold for high prices (e.g. pharmaceuticals). By aiming at such a holistic exploitation of the use of the feedstock, the overall economic revenue of a biorefinery industry can be potentially higher than that of a traditional industry, focusing on the optimization of the production of only a single compound from the feedstock. For example, the cost for algae production is €0.40/kg algae (2). If the algae were only used for biodiesel production, the value of the biomass would be €0.20/kg algae, excluding the processing costs (2). That means that the production of algae only for biodiesel is not feasible. However, the total value of the biomass can reach up to €1.65/kg algae, if algae are used in biorefining (2). It is expected that the increase in sales price of the whole biomass, due to separation, will be higher than the added cost needed for the separation, leading to increased economic revenue. It needs to be noticed that this increase in revenue after biorefining is further increased due to the reduction in cost from handling the remaining waste streams.

Given the wide range of products that can be derived from a feedstock and the plethora of possible pathways that can lead to these products, it becomes evident that a systematic approach for the design of a biorefining process is needed. In the past, many systematic approaches have been developed to address the process design in biorefinery. A brief description of the recent advances of these systematic approaches in the context of biorefinery was presented by Ng *et al.* (3). The main focus of these approaches is the identification and selection of the optimum processing pathway given certain objectives. These objectives were typically related to process design aspects, such as yield maximization, energy minimization or economic performance. In some cases, environmental, health and safety aspects were also considered. However, to design an optimal biorefining process also the specific physico-chemical properties of the individual final products need to be considered. The latter has been the focus of product design methodologies. Thus, both product and process design methodologies need to be used. In the last years, a number of methodologies that integrate product and process design were published (3-7). The main idea behind these methodologies is that first the consumer wants are identified and translated into product specifications. Then, the process is designed in such a way that the final products meet these specifications. More precisely, Moggridge and Cussler (6) presented a template for chemical product and process design, where the whole procedure is decomposed into four sequential steps. The first three steps describe the product design starting from the identification of the customer needs, generation of ideas to meet the identified needs

and selection of best ideas, while the last step refers to the process design ("manufacture"). Based on this decomposition a framework for systematic chemical product design by using computer-aided methods and tools was developed (5). Wibowo and Ng (8) presented a systematic framework where the product manufacture was decomposed into two separate steps. The whole procedure consists of five main steps: "(1) product conceptualization, (2) identification of quality factors, (3) selection of ingredients and microstructure, (4) generation of process alternatives and (5) process and product evaluation". In this methodology heuristics, mathematical models and experimental data are used at each step to aid the decision making. More recently, Ng (3) presented a product-oriented, hierarchical framework for the design of chemical products. In this framework different disciplines, such as management, marketing, and chemical engineering are brought together and the design of the product is divided into three main phases: "(1) product conceptualization, (2) detail design and prototyping, (3) product manufacturing and launch". The product design was approached as a multi-objective optimization problem and the use of different tools, methods and databases is discussed. Also, Bernardo and Saraiva (4) showed an integrated approach for product and process design, they applied it to a cosmetic lotion case study. They showed that the approach that integrates process and product design seems to provide more optimal solutions than the solutions obtained when the two methodologies are used separately. More specifically for biorefinery, Ng *et al.* (9) developed recently a two-stage optimization approach for the selection of the optimal processing pathway that leads to a final product with specified properties. In their approach, first (first stage) the product properties ("product needs") are identified and then the final product ("mixture") is designed based on these properties. In the second stage, the optimal pathway that leads to the optimal mixture is identified using a super-structural optimization approach. The identification of the product properties is an important feature of this approach. In their approach the example of biofuel production was used. The product properties in this case were defined in terms of energy content, which is a well-known molecular property. The importance to introduce product properties into the process synthesis was highlighted as well by Gani and O'Connell (10). They used the example of phase equilibria. In this case, the intrinsic properties of the molecules are also well known and well described. Such concepts should be further developed to define more complex physico-chemical properties of the final products, to include, for instance, the structure of proteins or carbohydrates. In addition, the reactivity of the compounds should be taken into account, since chemical and physical changes of the compounds can change the final product properties.

In the present study we propose the use of the product driven process synthesis methodology (PDPS) to facilitate the product and process design in the biorefinery. PDPS was first introduced by Bongers *et al.* (11) as a structured approach towards the synthesis of a process in the food sector, where several raw materials are combined to produce one final product. The PDPS methodology was already successfully applied in a number of cases, as for instance the redesign of a production process for a bouillon cube (12). Recently, some attempts have been made to use the PDPS for the separation

of one compound from a feedstock, e.g., the isolation of isoflavones from okara (13), the separation of oleosomes from soybeans (14), the separation of polyphenols from tea (15). The use of PDPS in a separation process is not as straightforward as in the design of a structured product. The challenges that arise in this case were discussed by Jankowiak *et al.* (13). In short, the main challenges are due to the complexity induced by the interaction among the different compounds present in the feedstock, which hinders the isolation of pure compounds.

This study aims to further extend the application of PDPS to biorefinery by identifying steps that need to be adapted. A general description of the PDPS levels and the adaptations required to facilitate the use of PDPS in the biorefinery are presented. Emphasis is given to the complex physico-chemical properties of the final products. The manifold interactions of the various compounds/products during the processing and their effect on the products properties are also highlighted. Moreover, guidelines are provided to link the feedstock (input) composition to possible product (output) applications, and the functionalities that these products can deliver in food, feed or non-food matrices. A case study of a sugar beet leaves biorefinery is used as an example.

## THE PDPS METHODOLOGY

The PDPS methodology consists of 9 hierarchical levels (**Figure 5.1a**). The first 4 levels comprise the product design and the last 5 levels comprise the process synthesis (11). In the first three levels, the background of the project and the business context are defined (framing level), the consumer preferences (consumer wants level) are identified and they are then translated into tentative products attributes (product attributes level). At the next level (input-output level), the input; i.e. the ingredients required to construct the pre-defined product, is listed and the characteristics of the output (product) are described. As stated earlier, the next five levels deal with the process synthesis. The fundamental tasks that are required to go from the input to the output are defined in the task network (level 5). The mechanisms behind the selected tasks are defined in the mechanism and operational window (level 6). In principle, different outcomes (products) can be defined already at the “product attributes” level. At the “multi-product integration” level, overlaps derived from levels 4-6 can be identified and possibilities to combine the production of the final products are discussed. At the “equipment selection and design level”, the unit operations are selected and the conceptual design of the units and the final flow sheet are made. Ultimately, at the multi-product equipment integration level, the interaction of the various unit operations selected at the previous level is considered and optimized.

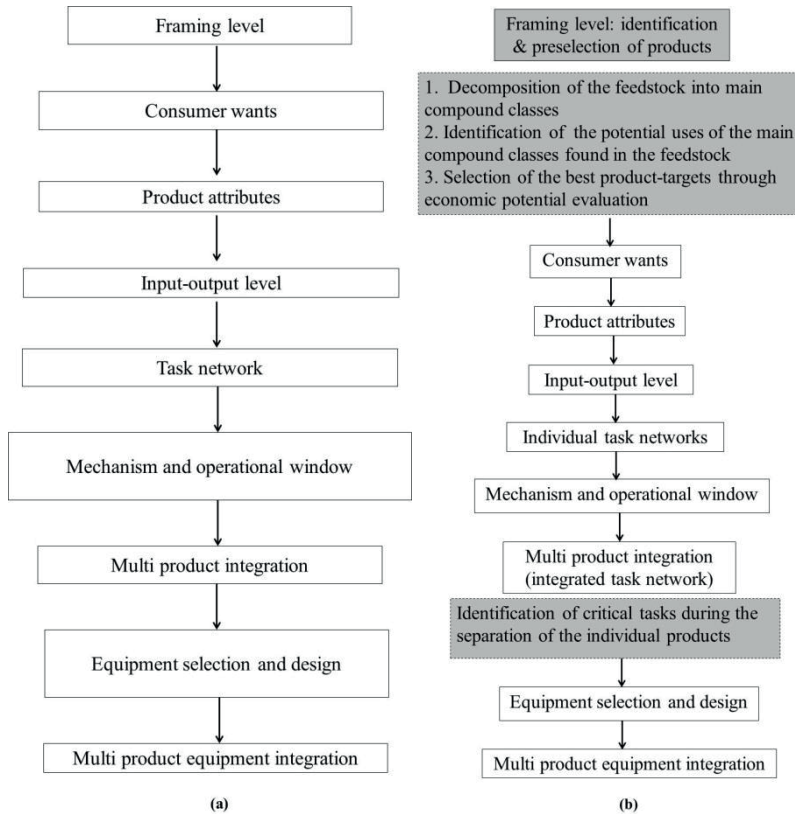


**Figure 5.1** (a) Levels of PDPS. (b) Levels of adapted PDPS.

## PDPS APPLICATION IN BIOREFINERY

### Framing level: identification and preselection of products

The framing level of the PDPS is the first activity of the product design stage. At this level, the general background of the project is described and the business context is set. Furthermore, in the framing level, the intention is to identify a number of market opportunities; i.e. product-targets. In biorefinery, the high number of the potential products that can be obtained from a single feedstock makes the identification and selection of the product-targets difficult. To facilitate this identification process we propose the addition of three novel, well-defined steps as part of the framing level; namely (1) decomposition of the feedstock into its main compound classes, (2) identification of the potential uses of the main compound classes found in the feedstock, and (3) selection of the best product-targets by evaluating the economic potential for each identified product-target (**Figure 5.1b**).

The identification of the potential uses of the main compound classes, which are present in the feedstock is typically done by a literature search, patent search or brainstorming in groups. To aid the identification process, 5 tables are developed that

contain information related to the compound classes; i.e. proteins, carbohydrates, lipids, phenolic compounds and minerals, typically found in agricultural feedstocks (**Table 5.1a-e**). Such information has not been comprehensively reported in the scientific literature. Therefore, the content of the tables should be seen as a first attempt to provide a systematic overview of the different functionalities and possible applications of (sub-)compound classes in food, feed and non-food areas. The different compound classes were further decomposed into subcompound classes, e.g. carbohydrates were segregated into pectins, cellulose, etc. The list was extended to include also similar compound classes that can be obtained from other sources, e.g. whey protein from cow milk, and are currently used in industry. Furthermore, a number of applications where the various compounds can be used, such as food applications, e.g. ice-creams, jams and non-food applications, e.g. cosmetics, biopesticides, are provided. The functionality that each compound class brings to each application, such as gelling, foaming, water binding, is described.



**Table 5.1** Example of compounds; (a) proteins, (b) carbohydrates, (c) lipids, (d) phenolic compounds, and (e) minerals, used in various commercial preparations and the link to specific functionalities that they deliver in these applications.

(a) PROTEINS	Subcompound classes	Functionality	Applications
	Food		
	Caseinates	Foam Emulsion Digestibility	Deserts
	Caseins		Bakery / Confectionary
	Egg white	Emulsion Gelling / Binding	Ice cream
	Egg yolk	Foam Emulsion Colour Foam Gelling Binding	Meat products Dressings Confectionary
	Meat proteins	Nutrition	
	Milk powder	Creamer (Whitening agent) Gelling / Binding	Coffee creamer
	Milk proteins	Digestibility (hydrolysates) Nutrition	Clinical nutrition
	Potato protein	Emulsion Nutrition	
	Soy proteins	Gelling / Binding Meat extender	Gels
	Soy proteins (hydrolysates)	Digestibility	Sports nutrition
	Whey protein	Foam Gelling / Binding	Vegetable whipped cream Confectionary Confectionary
		Emulsification	Confectionary
		Flavour enhancer Nutrition Foam	Sports nutrition
	Whole egg	Emulsification Gelling / Binding Nutrition	Mayonnaise Stabilisers (soups)
	Whole milk	Gelling / Binding	
	Feed		
	Soy proteins		General feed ingredient
	Non-Food		
	Soy proteins		Culture media

(b) CARBOHYDRATES	Subcompound classes	Functionality	Applications
	Food		
	Alginate Arabino-Galactan (Proteins) Gum Arabic (Arabino-Galactan) Arabinose Carageenan Cellulose Dextrans Glucose Fibers (General) Gos (Galactose) FOS (Fructose) Inulin (Fructose Polymer) Lactose Locust bean gum (Galactomannan) Monosachharides (Neutral Sugars) Pectin Xanthan Starch Sucrose Xanthan	Gelling Emulsifying / Foam Emulsifying / Foam Viscosifying Glycemic index lowering /Nutrition Gelling Gelling Water Binding Inert binding material Nutrition / Energy Delivery Water Binding Nutrition Nutrition Taste / Mouthfeel improvement Inert binding material Gelling Water Binding Emulsifying/Foam Water Binding Preservant ( $a_w$ lowering) Gelling Water Binding Emulsifying / Foam Viscosifying Gelling Taste Preservant ( $a_w$ lowering) Gelling	Desserts Flavour encapsulation Pharmaceuticals Jelly Jam Jam Pharmaceuticals Prebiotics Prebiotics Pharmaceuticals Fruit-Filling Sausage Ice-Cream Jam Jam Candy Coffee creamer Soups / Sauces Chocolate milk Sweetener Infused fruits Salad dressing
	Non-Food		
	(Anything) Cellulose Galacturonic acid Guar gum (Galactomannan) Lactose (Glucose+Galactose) Starch	Building blocks for chemicals Water binding Materials Building blocks for chemicals Stabilising of emulsions Building blocks for chemicals Water binding	Bio-ethanol Diapers Paper Bioplastics Cosmetics Bioplastics Diapers

	Subcompound classes	Functionality	Applications
(c) LIPIDS	<b>Food</b>		
	(Nut Oil)	Bulk liquid / texture	Ice-Cream
	Arachide Oil Carnabau Wax	Bulk liquid / texture Bulk liquid / texture	Candy
	Glucose-Monoesters	Emulsifier/ stabiliser	Whipped cream Pharmaceuticals
	Lecithin Linoleic Acid	Emulsifier/ stabiliser Health	
	Milk Fat	Emulsifier /stabiliser	Ice-Cream
	Mono- diglycerides	Bulk liquid/texture Emulsifier/stabiliser	
	Olive Oil Palm Oil	Bulk liquid / texture Bulk liquid / texture	Table / Cooking oil Frying fat
	Phospholipids Sterols	Emulsifier/ stabiliser Health	Spreads / Margarine/Shortening Margarine
	Sunflower $\omega$ 3- fatty acids	Bulk liquid / texture Health	Margarine
	<b>Non-food</b>		
	Lipids (General)	Building blocks for chemicals	Bio-fuel
	Coconut Fat	Texture	Cosmetics
	Linoleic Acid	Texture	Shampoo
	Rapeseed oil Stearic acid	Bulk liquid / texture Texture	Skin-care

	Subcompound classes	Functionality	Applications
(d) PHENOLIC COMPOUNDS	<b>Food</b>		
	Astaxanthin	Colorant	Beverages
	Beta-Carotene	Colorant	
	Chlorophyll	Antioxidants	
	Chlorophyll	Colorant	
	Epicatechin Gallate	Antioxidants	Margarine
	Epigallocatechin Gallate	Antioxidants	Dietary supplements
	Flavonoids	Antioxidants	
	Saponins	Antimicrobial Emulsifier	
	Theaflavin Tocopherols	Foaming Antioxidants Antioxidants	Root beers
	<b>Non-Food</b>		
	Phenolic compounds (General)	Chemicals Antioxidants	Biopesticides
	Phenol Formaldehyde		
	Resins	Plastics	Coatings Plants
	Saponins	Insecticide / Biocide  Chemicals	Livestock (control of ammonia emissions)

(c) MINERALS	Subcompound classes	Functionality	Applications
	Food		
	Al Br Ca  Ca Ca Lactate  I I K K K-Salts K-Salts Mg Mg-Salts Na NaCl NaCl NH <sub>3</sub>  Phosphates Phosphates Phosphates S S Vitamins Zn Zn	Health Electrolyte Anti-microbial / Preservative  Flavour Preservative  Texture modifier Flavour modifier Fertilizer Browning inhibitor Anti-microbial / Preservative Health Anti-oxidant/ Protective lining Health Health Electrolyte Antimicrobial / Preservative Flavour  Preservative Fertilizer Texture Modifier Flavour modifier Fertilizer Browning inhibitor Antimicrobial/Preservative Health	NaCl replacer  General in Food as taste enhancer/modifier Salted/Brined/Pickled Foods  Leavening acid Soft drinks  Wine Meat  Cans Fruits NaCl replacer  Salted/Brined/ Pickled Foods  Leavening acid Soft drinks  Wine Meat
	Non-Food		
	Fe		Fertilizer

A compound class can bring multiple functionalities to products. The composition, and thus the functionalities of compound classes, usually depend on their source (**Figure 5.2**). For example, sunflower protein is almost 100% soluble between pH 2.0 - 8.0 (*16*), whereas the solubility of alfalfa leaf protein is low between pH 3.0 - 5.0 (*17*) (**Figure 5.2**). The processing steps can affect both the purity and the intrinsic properties of a compound class (**Figure 5.2**). For example, the solubility of a protein extracted from algae highly depends on the presence of "co-passengers" ; i.e. other non-protein compound classes present in the final protein concentrate/isolate. The proteins present in a crude protein isolate from algae, which contains 39% w/w "co-passengers", are 100% soluble at pH 6.0, whereas the proteins in the algae juice, which contains 76% w/w "co-passengers", are only 50% soluble at the same pH (*18*). Furthermore, the method used to isolate a compound class can influence its functionality. For instance, the use of heat during protein isolation from leaves leads to protein denaturation, and subsequently to loss of protein solubility (**Figure 5.2**).

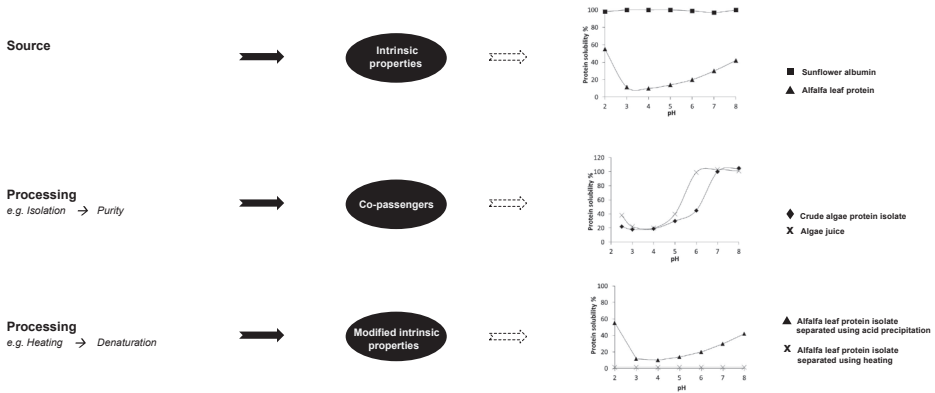


**Figure 5.2** Example of effect of source and processing on the functional properties (solubility) of proteins (reproduced and adapted from (16-18)).

Even a subcompound class can deliver multiple functionalities to products. The reason for this is that each subcompound class consists of chemically different molecules. It is quite often the case that different subcompound classes are incorrectly assumed to be similar, and thus have the same techno-functionalities. To continue with the example of proteins, given that proteins are mostly seen as a source of amino acids, differences in techno-functionalities are not acknowledged. There is, however, a large variability in subcompound classes of proteins (e.g. albumins, globulins). These subcompound classes, although they might derive from the same source, they exhibit different techno-functionalities. Moreover, individual compounds (e.g.  $\beta$ -lactoglobulin) from one source (e.g. caprine milk) can be chemically different from the same type of compound from another source (e.g. bovine milk). This is important for proteins, but the situation for the compound classes of minerals and vitamins is less complex. For example, vitamin C from orange juice is chemically exactly the same as vitamin C from blueberry juice. Yet, specifically for the compounds classes of proteins and carbohydrates the differences in functionality between similar subcompound classes from different sources need to be taken into account.

To facilitate the selection process of the potential product-targets a first rough evaluation of the economic potential (EP) is proposed as a third step. The economic potential at this stage is based on the revenues from the sales of the products and on the cost of raw materials. It can be calculated from equation 5.1, based on Cussler and Moggridge (6).

$$EP = \sum \frac{\text{productsales}}{\text{year}} - \frac{\text{raw materialcost}}{\text{year}} \quad (5.1)$$

The product sales/year for each product-target is calculated from equation 5.2:

$$\frac{\text{product sales}}{\text{year}} = t_{\text{operational}} \cdot Q \cdot C_{\text{solids}} \cdot C_{\text{product}} \cdot Y \cdot p \quad (5.2)$$

in which  $t_{\text{operational}}$  is the operational time (h/year),  $Q$  the feed flow rate (t/h),  $C_{\text{solids}}$  the solids content in the feed (w/w %),  $C_{\text{product}}$  the product content in the feed (w/w % on dry matter basis),  $Y$  the yield of the separation process (%) and  $p$  the sales price (€/t).

To estimate the sales prices of these products, open source literature can be used. Of course, it is important to realize that the sales prices depend on the quantity in which the products are sold as well as the market in which the products are sold. For example, in case of phenolic compounds, ferulic acid may be sold as a bulk chemical for which the price is typically around €3/kg (for markets of around 25 kt/year). It can also be sold for food applications. In this case, prices of €8-264/kg have been reported (19). Moreover, the sales prices are also determined by the functionality that a (sub-)compound class delivers to a final product. For example, soluble proteins can be used in food products (e.g., as emulsifiers) and can reach a price of €5/kg, and insoluble proteins can be used either in food as meat extenders or in animal feed as a protein source, and can reach a price of €0.75/kg (2). **Table 5.1a-e** can be used as a tool to guide a user in the direction of the product-targets, based on their potential functionalities. The calculation of the EP at this stage does not take into account the processing costs. At this stage, the EP is a rough estimate, which does not include processing costs. The reason is that the processing costs can only be estimated after the final integrated task network has been designed. The EP calculation at this point serves to exclude products that have negative EP, even without considering the processing costs.

### Consumer wants

The second level of the PDPS refers to the consumers wants; i.e. consumer preferences. The focus of the biorefinery is to provide ingredients or components that will be used by other industries to be converted into final products for food/feed or non-food applications. This means that a business-to-business approach is followed. Consumer wants can be obtained using different tools, such as interviews of focus groups, sensory panels (in case of food products), input from lead customers or analyses of similar products currently available on market (competitors' analysis).

### Product attributes

An important step at this level is the translation of the qualitative product properties, expressed by the consumer as "consumer wants", into quantitative product attributes. Rule-based methods, such as the quality function deployment (20), which also makes use of the house-of-quality, can be used as tools to facilitate this translation. These methods provide a structured environment to map the qualitative attributes (consumer wants) and to relate them to quantitative product attributes. The main challenge is to identify the quantitative correlation between the quality characteristics and the physico-chemical properties of the products. Since there are no generic rules that can be applied, this quantitative correlation is typically identified by using experimental data and domain knowledge, e.g. literature. For example, recently Dubbelboer *et al.* (21) developed models to link consumer-liking to physical properties and product formulations of a mayonnaise. More precisely, in this work qualitative sensory

attributes, such as mouth feel and spreadability, were recorded by trained tasting panels for different products. For the different products, quantitative attributes (physical properties and composition) were determined experimentally. The sensory attributes were then correlated to the quantitative attributes by statistical methods and surrogate models. In this specific study, a neural network approach was followed. The surrogate models were verified and validated and were subsequently used to optimize the product in terms of sensory attributes.

### **Input-output level**

The input of the process refers to the feedstock and its composition. A complete characterization of the input; i.e. a compositional analysis of the feedstock is required. The output refers to the products of the process and their specifications. The specifications refer both to the physical characteristics and the techno-functional properties of the products. In biorefinery, these properties are strongly dependent on the composition (purity) of the products (output). This in turn depends on the composition of the feedstock (presence and variety of compounds in the feedstock) and the processing conditions. Overall, in this step the specifications of the products need to be related to their composition (purity). To establish these relations domain knowledge (literature) and/or experimental data are needed.

### **Individual task networks**

At this level individual task networks are defined for each separate product. Each task network describes the necessary tasks needed to go from the feedstock (input) to each and every pre-selected product (output) separately. Since in biorefinery the outcome is not a structured product but a compound class, mainly separation tasks, e.g. cell wall disruption, transfer of a component from one phase to another, are identified. For each product, a set of alternative task networks is generated by changing the sequence or the combination of different tasks. For example, for the extraction of polyphenols from tea leaves the sequence of tasks can be either (a) size reduction, cell wall disruption, separation or (b) cell wall disruption, separation, size reduction (14).

### **Mechanism and operational window**

After designing and selecting the most promising task networks, the mechanisms that can be used for each task need to be defined. For each task, there are different mechanisms that can be considered. For example, cell wall disruption can be achieved using pulsed electric fields, enzymes, or shear. The desired mechanism then needs to be selected and the operational window; i.e. the range of the values of the process variables, needs to be specified.

### **Multi-product integration (integrated task network)**

At this level, the individual task networks that were designed for the separation of each separate product need to be combined. The combination of the separate task networks into one integrated task network is quite challenging. The challenge stems from the fact that tasks needed to separate a product "a", with a specific functionality, might affect the functionality of a product "b". For example, a heating task that is required for the extraction of phenolic compounds from leaves, leads to protein denaturation and thus

loss of protein functionality (e.g. decrease in solubility). In addition, the processing steps can affect both the purity and the intrinsic properties of a compound class (product), as discussed in the “framing level”.

We propose the addition of a novel step before designing the integrated task network; namely the identification of the “critical tasks”; i.e. the tasks that negatively affect the quantity and/or quality of each selected product (**Figure 5.1b**). After the identification of the critical tasks for each product, a pre-design of the integrated task network can be made. In case that any of the critical tasks, identified for each product, is part of the integrated task network, some action needs to be taken. More precisely, three of the following actions can be taken: (1) the sequence of the tasks in the integrated task network has to be organized in such a way that the critical task for each product takes place after this product has been separated, (2) the operational window related to the critical task can be adjusted accordingly, or (3) the critical task has to be replaced by another task.

It needs to be noted here that given that no thermodynamic models are available for the complex food systems, experimental data are required to actually quantify the effect of each critical step on the final products. These data can later be used to formulate mathematical functions, and thus the whole process design can be approached as a multi-objective optimization problem. Such an approach has been recently presented by Murillo-Alvarado *et al.* (22) for the optimization of the processing pathways in biorefineries.

After the integration of the task networks, the PDPS levels can be re-iterated. Such re-iteration contributes in defining the whole process more in depth, while it reduces the risk of fixated errors. For example, the economic potential (EP) can now be determined taking into account also the extraction costs. In this way, products that lead to a negative EP due to high extraction costs can be excluded, while other products that can be obtained- perhaps side-streams of the pre-selected products- may be considered.

## **CASE STUDY**

A sugar producing company wants to expand its business in the field of biorefinery by exploiting the leaves remaining on the field after the sugar beets have been harvested. Thus, in this case the raw material (input) is already preselected. Furthermore, the company has already decided that they want to follow a business-to-business (B2B) model, and therefore the final products (output) will be the compounds extracted from the leaves.

### **Framing level: identification and preselection of products**

**General background of the project.** Sugar beet leaves are currently not used in industry. After the sugar beets are harvested, the sugar beet leaves are embedded in the soil. It is commonly assumed that the leaves provide essential nutrients (fertilizer) that can be used by the crops sown in the field after the sugar beets are harvested. Based on this, there have been suggestions that 30-40% of the leaves should be left on



the field. However, only a small part of the nitrogen from the sugar beet leaves are recovered in the crops (5% (23) to 27% (24). This shows that sugar beet leaves embedded in the soil give only a small value as a fertilizer. Therefore, even if a part of the leaves are left on the field, commercial fertilizers are used to provide the needed nutrients. In consequence, a plethora of potentially valuable compounds, such as proteins, carbohydrates, phenolic compounds, lipids and minerals, which are present in the sugar beet leaves are left unexploited. These compounds could be extracted from the leaves and further used in various applications, thereby creating an opportunity to increase the value of the feedstock. The choice will be left to the final producer whether or not to leave this small part of the leaves on the field.

In the Netherlands, in 2011, the sugar beet cultivation area was 72,000 ha (25). This translates to approximately 5.6 Mt beets (26) and 2.2 Mt leaves per year. These values illustrate the possible significance of the exploitation of the sugar beet leaves. To allow for a cost efficient total process, a regional approach is needed. At local level, the leaves should be dried, preferably using mild, low-tech methods, to reduce the volume of the feedstock. The dried leaves can be then transported to a centralized processing factory where the actual (high-tech) biorefining takes place. It needs to be noted here that the seasonal character of the sugar beet leaves harvest might create a risk in terms of economies of scale. This risk can be minimized by using the same processing unit for different feedstocks that are available in different seasons.

**Identification and preselection of products.** *Decomposition of the feedstock into its main compound classes.* Based on experimental analyses at our lab, the following compounds classes were identified in sugar beet leaves (leaves and stems): protein 31%, carbohydrates 26%, lignin 8%, ash 15%, lipids 8%, phenolic compounds 3%, chlorophyll 0.8% (expressed in w/w % on dry matter basis, db). Lignin is mentioned separately from the phenolic compounds because lignin is an insoluble polymer of a phenolic compound.

*Identification of the potential uses of the main compound classes found in the feedstock.* To identify the potential uses of the main compound classes present in sugar beet leaves, we used the information presented in **Table 5.1a-e**. For this case study, we pre-selected proteins and carbohydrates, due to their high abundance in the feedstock and the great variety of applications in which they can be used. Protein can be used both in food and feed applications, while carbohydrates in this case were only considered for non-food applications. Phenolic compounds were pre-selected as product-targets because of the increasing interest in phenolic compounds as antioxidants and the tentative high sales price that they can reach.

*Selection of the best product-targets.* For the selection process of the potential product-targets a first rough evaluation of the economic potential for protein, carbohydrates and phenolic compounds was made. To estimate the sales prices of these products open source literature was used. An average sales price for proteins for food applications was assumed to be €5/kg, while an average sales price for proteins for feed applications was assumed to be €0.75/kg (2). The sales price for carbohydrates

(chemical building block) was assumed to be €1/kg. In case of phenolic compounds, e.g. ferulic acid, the sales price ranges between €8-264/kg (19). We here assumed a sales price of €8/kg. Of course, it is important to realize that the sales prices depend on the quantity in which the products are sold as well as the market in which the products are sold. For illustrative purposes three tentative scenarios are presented.

- Scenario 1: All protein is sold for food applications (€5/kg), carbohydrates are sold as chemicals (€1/kg) and ferulic acid as chemical (€8/kg).
- Scenario 2: 20% of protein is sold for food applications (€5/kg), 80% of protein is sold for feed applications (€0.75/kg), carbohydrates are sold as chemicals (€1/kg) and ferulic acid as chemical (€8/kg)
- Scenario 3: All protein is sold for feed applications (€0.75/kg) carbohydrates are sold as chemicals (€1/kg) and ferulic acid as chemical (€8/kg).

The EP was calculated using equation 5.1. The EP derived from scenario 1 was 2-3 times higher than the EP derived from scenario 2, and 4-5 times higher than the EP derived from scenario 3. However, scenario 1 considers that all proteins present in sugar beet leaves have the techno-functional properties required for food applications. In practice this is not the case. For example, only 20% of proteins present in algae can be extracted and have the solubility required for food applications (18). Scenario 3 had a lower EP than scenario 2. However, the extraction (processing) costs for scenario 2 are expected to be higher than the extraction costs for scenario 3. It is expected that the higher EP in scenario 2 (1-2 times higher than EP derived from scenario 3) will be sufficient to counter the increase in cost. Therefore, scenario 2 was selected as the optimum scenario.

The exact processing costs could be estimated in later stages, when the final integrated task network has been designed. The information of those later levels should then be included again at this level, thereby iterating through the PDPS levels. The product-targets defined in this level are:

- Protein for food applications.
- Protein for feed applications.
- Phenolic compounds for non-food applications.
- Carbohydrates for non-food applications.

### **Consumer wants**

The products that are produced here are aimed to be alternatives to existing products. The aim of the company is to enter into existing markets. Thus, the consumer wants were extrapolated from the characteristics of similar products already in market (competitor analysis) and the input of the lead customers. As an example, the resulting consumer wants for the protein for food applications, which in our case is a foam agent for coffee, are:

- Low price.
- No green color.
- No grassy odor and taste.
- Easily dissolved.
- Foams well.

- Powder.

In addition to consumer wants the legislation related to these products, in the country where the products are going to be sold, was taken into account.

### Product attributes

Based on the consumer wants the product attributes were defined. The house of quality was used to document the qualitative properties of the output and to relate them to quantitative product characteristics. An example is given for the protein-based foam agent for coffee. One of the consumer requirements was a product with no grassy flavor. The grassy flavor is an off-flavor that can be assessed using a sensory panel. In our case, we specified that a product is acceptable if it receives a score >4 (0: grassy off-flavor – 5: no grassy off-flavor) by a trained panel. Using a similar approach all the consumer wants were translated into product attributes (**Figure 5.3**).

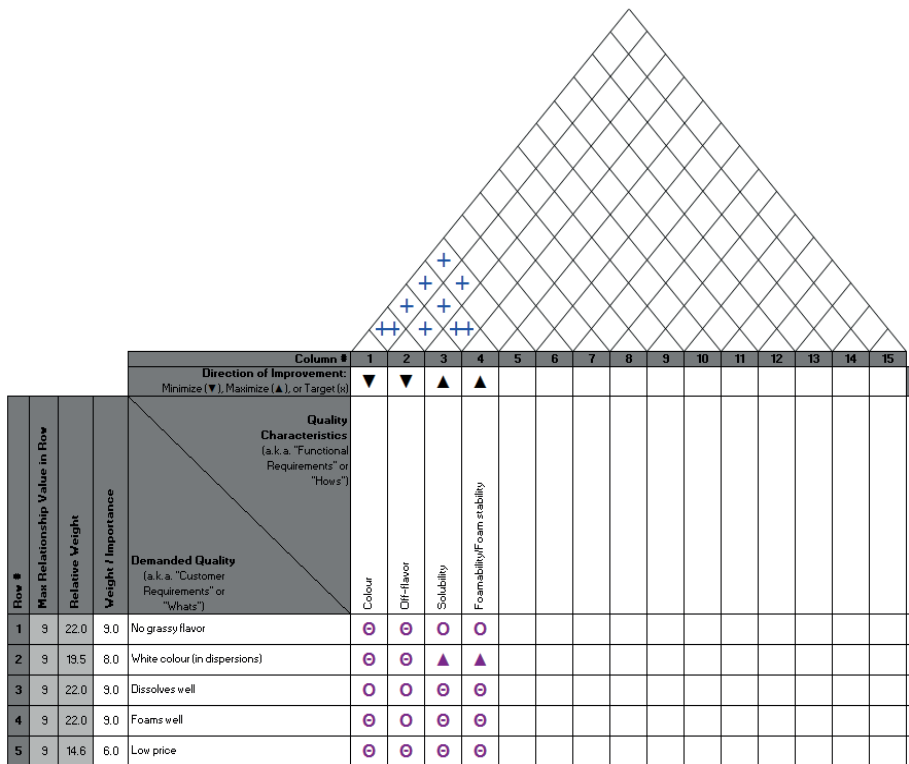


**Figure 5.3** Example of house of quality for sugar beet leaf protein-based foam agent for coffee and correlation of quality characteristics to target values. Symbols used: ⊖ strong relationship, ⊖ moderate relationship, ▲ weak relationship, ++ strong positive correlation, – negative correlation.

### Input-output level

**Input.** The sugar beet leaves (leaves and stems) were the input of the process. Given that the feedstock is a heterogeneous mixture of different compound classes we needed to define the input in more details. Thus, the input of our process was: protein

(31% w/w db), carbohydrates (26% w/w db), lignin (8% w/w db), ash (15% w/w db), lipids (8% w/w db), phenolic compounds (3% w/w db) and chlorophyll (0.8% w/w db).

**Output.** The output of the process was:

- Protein-based foam agent for coffee.
- Protein for feed.
- Phenolic compounds for chemical industry.
- Carbohydrates for bulk chemical industry.

The specifications for each product were defined by using domain knowledge and literature to actually translate the product attributes into product characteristics. As an example, we here show how the product attributes that were determined for the protein-based foam agent for coffee were translated into product specifications. The first product attribute that was determined in the previous level was the color (white color required). This was translated in absence in the final product of chlorophyll (green color) (27) and absence of oxidized polyphenols (brown color) (28). There should not be any off-flavors in the product. This was translated into absence of hexanal. The requirement of high solubility was translated into absence of oxidized polyphenols bound to proteins (29) and absence of denatured proteins. The latter was further translated into no use of a heating step during the extraction (17). Lastly, a high foam ability and foam stability was required for the product. This was translated into the absence of low-molecular weight surface active components such as free fatty acids (fat), or saponins (30). Similarly, for the other products the exact specifications were determined (Figure 5.4).

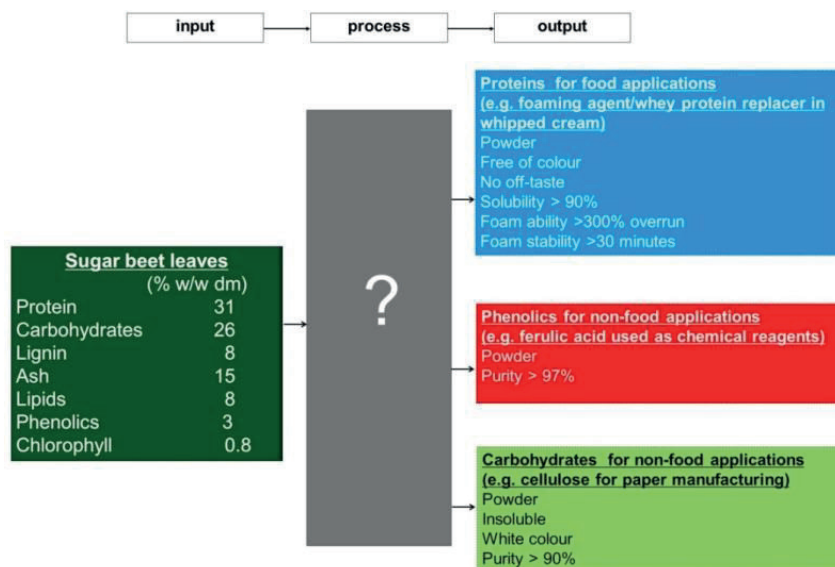


**Figure 5.4** Input-output level in the case of sugar beet leaves biorefinery.

### Individual task networks

The main tasks needed to convert the input into each specified output (identified in the previous levels) were defined, and then separate task networks were built for each of the products (output). For illustrative reasons, the main tasks required for the extraction of proteins from sugar beet leaves are described. The main tasks in this case include: cell wall disruption, separation (extraction), evaporation (**Figure 5.5a**). Another alternative is shown in **Figure 5.5b**. In this case, the sequence of tasks is as follows: evaporation, cell wall disruption, separation (extraction), evaporation.

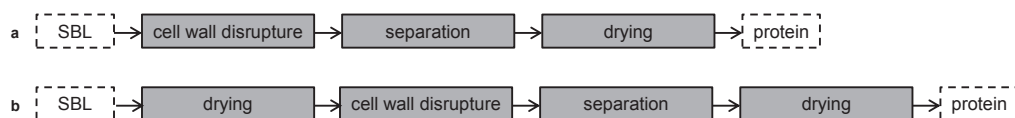


**Figure 5.5** Two alternative task networks for the separation of proteins from sugar beet leaves.

### Mechanism and operational window

In this level, the different mechanisms needed to fulfil the tasks presented in the task networks were defined. For example, in the case of the size reduction different mechanisms were identified, such as cutting, impact or ultrasound. For the extraction of the proteins from the other compound classes, a number of mechanisms, e.g. solubility, chemical affinity or molecular size were also identified. Similarly, for the other tasks different mechanisms were identified. As an example, a final task network for the extraction of proteins from sugar beet leaves is presented in **Figure 5.6a** (27). Shortly, the sugar beet leaves are macerated (cell wall disruption) and then mixed with  $\text{Na}_2\text{SO}_3$ . The solids (indicated as pellet in **Figure 5.6a**) are separated by pressing (separation) from the juice (indicated as supernatant in **Figure 5.6a**) and are subsequently discarded. The pH of the juice is subsequently lowered to 5.3 using HCl (decrease pH). At this pH, the chlorophyll containing fraction of the sugar beet leaves protein precipitates (indicated as pellet in **Figure 5.6a**). This precipitate is separated by filtration from the soluble fraction (indicated as pellet in **Figure 5.6a**) and can be used as protein for feed. The soluble protein fraction (indicated as supernatant in **Figure 5.6a**), which is obtained after this separation, is acidified to pH 4.5 with HCl (decrease pH). The obtained pellet is dried (evaporation) to yield a white protein powder. The task networks for the separation of phenolic compounds (**Figure 5.6b**) and carbohydrates (**Figure 5.6c**) from sugar beet leaves were based on protocols used for the separation of these compounds from tea leaves (15) and corn stover (31), respectively. After selecting the mechanisms and designing the task networks, the operational window for each mechanism was specified. For example, in our case gravity was selected as one of the mechanisms for the separation of soluble proteins from the insoluble fraction. Time and centrifugal speed were the variables that could be controlled. The operational window for the time was defined from 20 – 30 min and the operational window for the centrifugal force was defined from 9,000 to 40,000 *g*.

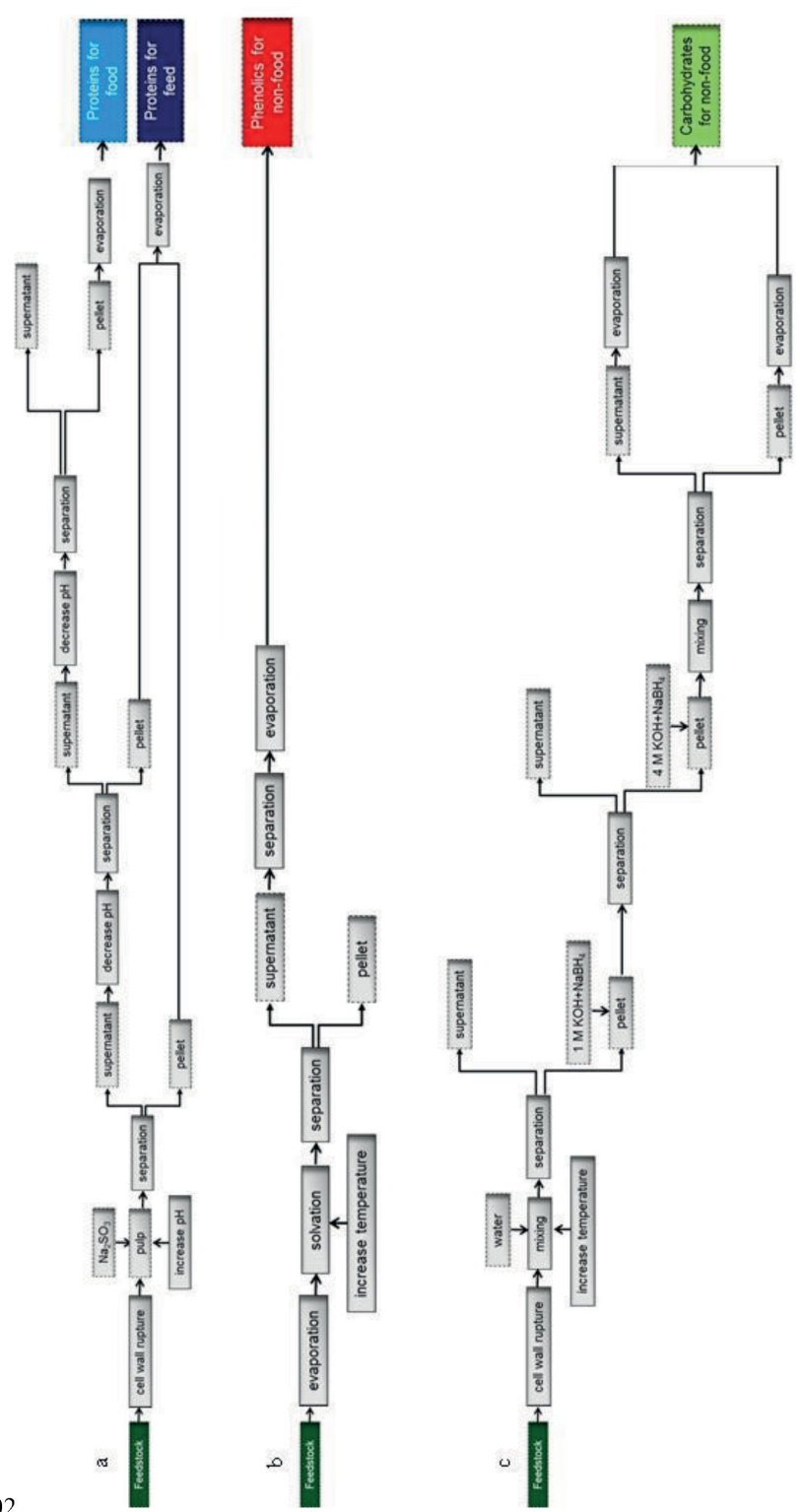


**Figure 5.6** Examples of individual task networks for the separation of proteins (a), phenolic compounds (b) and carbohydrates (c) from different feedstocks.

### Multi-product integration (integrated task network)

The task networks that were designed for the separation of proteins, phenolic compounds and carbohydrates were combined into one integrated task network. To do that, we first identified the critical tasks for each of our products (**Table 5.2**).

**Table 5.2** Example of critical tasks during the separation of proteins, carbohydrates and phenolic compounds from sugar beet leaves and their expected effects.

Compounds	Critical steps	Effect
Proteins	Heating pH>8.5	Denaturation (loss of solubility) Denaturation / chemical modification
Carbohydrates	Heating/ pH>10	Depolymerization (low water binding capacity)
Phenolic compounds	Heating/ pH>8.5	Oxidation / Polymerization

As discussed in the “multi-product integration” section, three different approaches can be taken to circumvent negative effects of the concurrent separation of different compounds. In this example, the first approach was to separate the leaves from the stems. This separation resulted in a carbohydrate rich stream (stems) and a protein and phenolic compounds rich stream (leaves). The benefit of this separation was that the alkaline conditions used for the extraction of carbohydrates will not negatively affect the proteins and the phenolic compounds. A second approach was to (re-)define the operational window of critical tasks. In our example, heating will improve extraction of phenolic compounds, but it can also lead to protein denaturation. Based on literature, the denaturation temperature of Rubisco, which is the major protein in leaves, is around 76 °C. Therefore, the maximum temperature used in our process was set 70 °C. Following a similar though process, an integrated multi-product task network was designed (**Figure 5.7**).

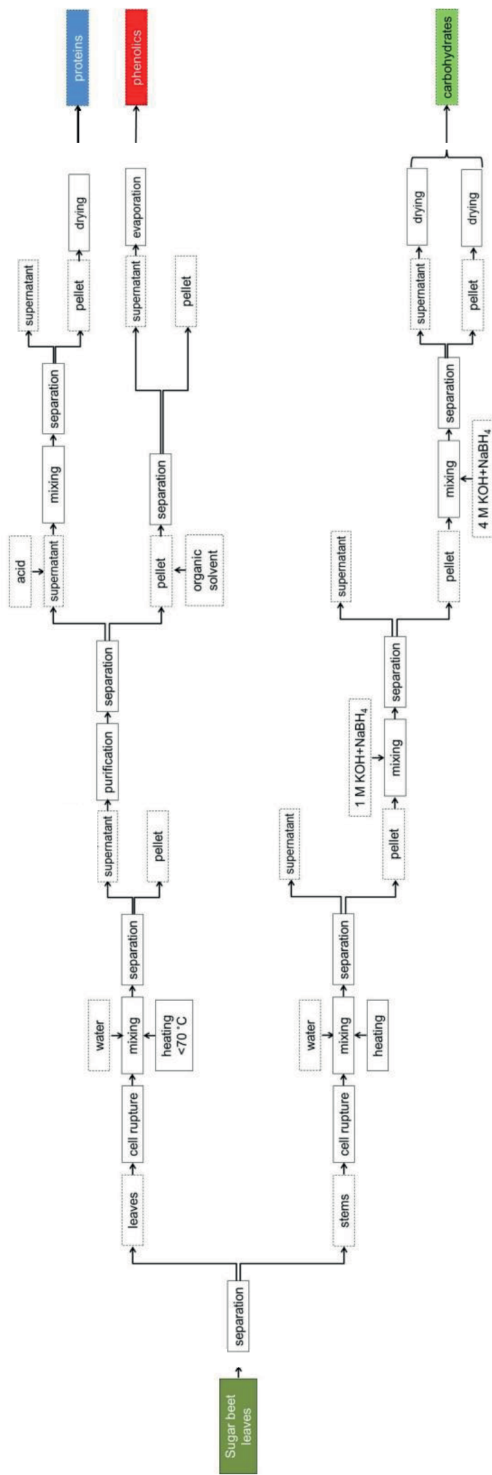


**Figure 5.7** Example of an integrated task network for the separation of proteins, phenolic compounds and carbohydrates from sugar beet leaves.



## CONCLUSIONS

To facilitate the application of PDPS methodology to a biorefining process, three novel steps have now been added to the framing level: (1) decomposition of the feedstock into main compound classes, (2) identification of potential uses of the main compound classes found in the feedstock and (3) selection of the best product-targets, by evaluating the economic potential that they can offer. Each compound class consists of different specific compounds with their own functionality. Since *a priori*, the exact compounds present in the feedstock and their functionality is not known, we developed 5 tables that contain information related to the main compound classes usually found in the feedstock; i.e., proteins, carbohydrates, lipids, phenolic compounds, minerals, and the functionalities that they can deliver to different matrixes. Information related to various applications of the different (sub-)compound classes in food, feed, and no-food areas is also provided. Such information is often not presented in scientific literature, and thus the content of the tables should be seen as a first attempt to provide a systematic overview of the different functionalities and possible applications of (sub-) compound classes in different areas. Given that the functionality of the compounds will be affected by process conditions, an extra step is proposed at this stage. This step involves the identification of the "critical tasks"; i.e. tasks that negatively affect the quantity and/or quality of each product during their separation. A case study of a sugar beet leaves biorefinery is presented to illustrate the use of PDPS in biorefinery.

## FUNDING

This work has been carried out within the framework of ISPT (Institute for Sustainable Process Technology).

## ACKNOWLEDGEMENTS

Dr Cristhian Almeida-Rivera is gratefully acknowledged for his critical feedback on the manuscript. We dedicate this paper to the late Prof. Dr Peter Bongers, who developed the PDPS methodology.

## REFERENCES

1. Van Ree, R.; Annevelink, E. Status Report Biorefinery **2007**.
2. Wijffels, R. H.; Barbosa, M. J.; Eppink, M. H. M., Microalgae for the production of bulk chemicals and biofuels. *Biofuels, Bioproducts and Biorefining* **2010**, *4*, 287-295.
3. Ng, K. M., A Multidisciplinary hierarchical framework for the design of consumer centered chemical Products. *Computer Aided Chemical Engineering*, **2015**, *37*, 15-24.
4. Bernardo, F. P.; Saraiva, P. M., A conceptual model for chemical product design. *AIChE Journal* **2015**, *61*, 802-815.
5. Gani, R., Computer-aided methods and tools for chemical product design. *Chemical Engineering Research and Design* **2004**, *82*, 1494-1504.
6. Moggridge, G. D.; Cussler, E. L., An introduction to chemical product design. *Chemical Engineering Research and Design* **2000**, *78*, 5-11.

7. Wibowo, C.; Ng, K. M., Product-centered processing: manufacture of chemical-based consumer products. *AIChE Journal* **2002**, *48*, 1212.
8. Wibowo, C.; Ng, K. M., Product-oriented process synthesis and development: creams and pastes. *AIChE Journal* **2001**, *47*, 2746.
9. Ng, L. N.; Andiappan, V.; Chemmangattuvalappil, N. G.; Ng, D. K. S., A systematic methodology for optimal mixture design in an integrated biorefinery. *Computers & Chemical Engineering* **2015**, *81*, 288-309.
10. Gani, R.; O'Connell, J. P., Properties and CAPE: from present uses to future challenges. *Computers & Chemical Engineering* **2001**, *25*, 3-14.
11. Bongers, P. M. M.; Almeida-Rivera, C.; Jacek, J.; Jan, T., Product driven process synthesis methodology. *Computer Aided Chemical Engineering*, **2009**, *26*, 231-236.
12. Gupta, S.; Bongers, P., Bouillon cube process design by applying product driven process synthesis. *Chemical Engineering and Processing: Process Intensification* **2011**, *50*, 9-15.
13. Jankowiak, L.; Méndez Sevillano, D.; Boom, R. M.; Ottens, M.; Zondervan, E.; van der Goot, A. J., A process synthesis approach for isolation of isoflavones from okara. *Industrial & Engineering Chemistry Research* **2015**, *54*, 691-699.
14. Žderić, A. Extraction of key components from cellular material: aspects of product and process design. PhD, Eindhoven University of Technology, Eindhoven, **2015**.
15. Monsanto, M. Separation of Polyphenols from Aqueous Green and Black Tea. PhD, Eindhoven University of Technology, Eindhoven, **2015**.
16. González Pérez, S.; Vereijken, J. M.; Van Koningsveld, G. A.; Gruppen, H.; Voragen, A. G., Physicochemical properties of 2S albumins and the corresponding protein isolate from sunflower (*Helianthus annuus*). *Journal of food science* **2005**, *70*, C98-C103.
17. Betschart, A. A., Nitrogen solubility of alfalfa protein concentrate as influenced by various factors. *Journal of Food Science* **1974**, *39*, 1110-1115.
18. Schwenzfeier, A.; Wierenga, P. A.; Gruppen, H., Isolation and characterization of soluble protein from the green microalgae *Tetraselmis* sp. *Bioresource Technology* **2011**, *102*, 9121-9127.
19. Quitmann, H.; Fan, R.; Czermak, P., Acidic, organic compounds in beverage, food and feed production. *Advances in Biochemical Engineering/Biotechnology* **2014**, *143*, 91-141.
20. Benner, M.; Linnemann, A.; Jongen, W.; Folstar, P., Quality function deployment (QFD) - can it be used to develop food products? *Food Quality and Preference* **2003**, *14*, 327-339.
21. Dubbelboer, A.; Janssen, J.; Krijgsman, A.; Zondervan, E.; Meuldijk, J., Integrated product and process design for the optimization of mayonnaise creaminess. *Computer Aided Chemical Engineering*, **2015**, *37*, 1133-1138.
22. Murillo-Alvarado, P. E.; Ponce-Ortega, J. M.; Serna-González, M.; Castro-Montoya, A. J.; El-Halwagi, M. M., Optimization of pathways for biorefineries involving the selection of feedstocks, products, and processing steps. *Industrial & Engineering Chemistry Research* **2013**, *52*, 5177-5190.
23. Widdowson, F. V., Results from experiments measuring the residues of nitrogen fertilizer given for sugar beet, and of ploughed-in sugar beet tops, on the yield of following barley. *The Journal of Agricultural Science* **1974**, *83*, 415-421.
24. Abshahi, A.; Hills, F.; Broadbent, F., Nitrogen utilization by wheat from residual sugarbeet fertilizer and soil incorporated sugarbeet tops. *Agronomy Journal* **1984**, *76*, 954-958.

25. <http://www.suikerunie.nl/> Number of beet growers and area under cultivation
26. FAOSTAT Production of sugar beets in Netherlands. (21/08/2015)
27. Merodio, C.; Sabater, B., Preparation and properties of a white protein fraction in high yield from sugar beet (*Beta vulgaris* L) leaves. *Journal of the Science of Food and Agriculture* **1988**, *44*, 237-243.
28. Edwards, M., Product engineering: Some challenges for chemical engineers. *Chemical Engineering Research and Design* **2006**, *84*, 255-260.
29. Prigent, S. V.; Voragen, A. G.; Visser, A. J.; van Koningsveld, G. A.; Gruppen, H., Covalent interactions between proteins and oxidation products of caffeoylquinic acid (chlorogenic acid). *Journal of the Science of Food and Agriculture* **2007**, *87*, 2502-2510.
30. Lech, F. J.; Meinders, M. B.; Wierenga, P. A.; Gruppen, H., Comparing foam and interfacial properties of similarly charged protein–surfactant mixtures. *Colloids and Surfaces A: Physicochemical and Engineering Aspects* **2015**, *473*, 18-23.
31. Van Dongen, F.; Van Eylen, D.; Kabel, M., Characterization of substituents in xylans from corn cobs and stover. *Carbohydrate Polymers* **2011**, *86*, 722-731.



---

## General Discussion

---

The aim of this thesis was to study the biorefinery of sugar beet leaves, with a special focus on the isolation of proteins. The research was therefore divided into three sub-aims. The first sub-aim was to determine whether there is a variability in the chemical composition of the leaves, and thus in the quantity and quality of the extracted proteins (LSPC) due to pre-harvest conditions (plant age). The protein content in the leaves was constant, although the content of other chemical compounds (e.g. carbohydrates, phenolic compounds) varied among the leaves of different plant ages. This variation in the chemical composition did not lead to a consistent with plant age effect on the quantity of the proteins isolated, although it significantly and consistently affected the color (quality) of the extracted proteins. The protein extract obtained from leaves of young plants was yellow, whereas the protein extract from leaves of old plants was brown (indicative of polyphenol oxidase activity) (**Chapter 2**). The second sub-aim was to evaluate the variability of the techno-functionality of LSPC due to system conditions. LSPC stabilized emulsions showed flocculation in the pH range from 3.0 to 5.5, which corresponds to a critical  $\zeta$ -potential ( $\zeta_{cr}$ ) below 11 mV. At high ionic strength ( $I = 0.5$  M) more protein was required to form an emulsion, which was stable against flocculation, than at low ionic strength ( $I = 0.01$  M). This was related to a higher protein adsorbed amount ( $\Gamma_{max}$ ) at the interface at high ionic strength. Regarding the foam properties it was observed that a constant soluble protein concentration was required for the foams to reach (a pre-set) maximum foam volume at all tested pH values (pH 3.0, 5.0 and 8.0). At pH 3.0 and 5.0, and as long as there was sufficient soluble protein to initially form a stable foam, LSPC foams were more stable than at pH 8.0. That was possibly due to aggregation of proteins or complexation of proteins and charged carbohydrates. At high ionic strength ( $I = 0.5$  M) LSPC was more efficient in foam formation than at low ionic strength ( $I = 0.01$  M). This was related to the faster adsorption of the proteins at the interface. An important result of this work was that it was shown that the techno-functional properties of LSPC could be closely forecasted using the models that have been developed for pure protein systems, by using the molecular properties of Rubisco

(dominant protein present in LSPC) and taking into account the presence of charged carbohydrates. The effect of protein concentration on the emulsion and foam properties of LSPC was similar as for pure protein systems, such as  $\beta$ -lactoglobulin (**Chapters 3, 4**). The third sub-aim was to extend current product and process synthesis approaches to enable the design of a biorefining process. For that the product driven process synthesis (PDPS) methodology, earlier developed for structured products, was used as a basis and the required adaptations were presented (**Chapter 5**).

Overall, this thesis describes the effect of pre-harvest (plant age), post-harvest (extraction with and without sulfite) and system conditions (pH, I) on the quantity and/or quality of proteins isolated from sugar beet leaves, alongside with a systematic approach for product and process design in a biorefinery. To obtain this overview a number of experimental techniques for the isolation of LSPC were employed, after several alternative techniques were tested. A summary as well as a discussion on the consideration of these techniques are described in this chapter. In addition, a number of research questions that arose during this project and were not addressed in the previous chapters are covered in the following sections.

## **EXTRACTION OF SOLUBLE PROTEINS**

### **Cell disruption methods**

In literature, as described in **Chapter 1**, many cell rupture methods, such as pressing, dry milling, and blending have been used for the extraction of proteins from leaf tissues (1-4). A relatively novel method for cell rupture is the use of pulsed electric field (PEF). Pulsed electric field is based on the electro-mechanical instability caused to (plant) cells upon application of external electrical fields (5). The intracellular material can then be released via diffusion (6, 7) or by applying an external force, e.g. pressing (8-11).

In this project blending was used as the cell rupture method for sugar beet leaves after several alternatives were also tested. The alternative cell rupture techniques that were tested include: dry grinding (Retsch ZM 200, Haan, Germany) in combination with blending, blending in combination with beadmilling (DYNO®-Mill, Type MULTI LAB, Willy A. Bachofen AG Maschinenfabrik, Muttenz, Switzerland), pressing (hydraulic press), PEF (EL-CRACK HPV30, DIL, Quakenbrück, Germany) in combination with pressing and PEF in combination with blending. The nitrogen recovery (% g nitrogen in extracted juice / g nitrogen in leaves) is shown in **Figure 6.1**.

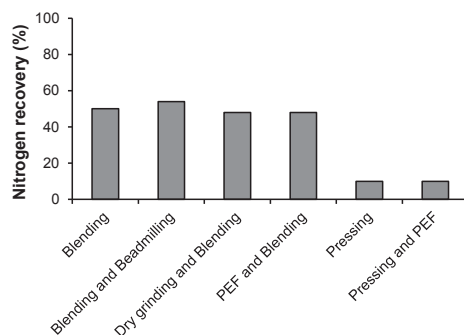


**Figure 6.1** Nitrogen recovery % obtained after different cell disruption methods.

The nitrogen recovery was slightly higher after blending in combination with beadmilling than after blending (50% vs 54% for blending and blending in combination with beadmilling, respectively). Dry grinding in combination with blending did not lead to any differences in nitrogen recovery. PEF in combination with pressing was similar to the nitrogen recovery obtained after pressing the leaves, and was even lower than after blending. Furthermore, the combination of PEF with blending did not increase the nitrogen recovery as compared to blending alone. The fact that PEF in combination with either pressing or blending did not yield any improvement in the extraction recovery, as shown for other tissues, e.g. sugar beets (8), might be due to the difference in the structure of the tissues tested. More specifically, for hard tissues compared to the soft leafy tissues, any extra softening of the tissue before pressing would lead to higher juice extractability. Thus, given the soft structure of the sugar beet leaves, PEF seems not to add any extra benefit when used as pre-treatment for nitrogen recovery. Overall, based on these data blending was shown to lead to a similar nitrogen recovery when used alone or in combination with any other method. Therefore, blending was selected as the main cell disruption method in this project.

## Isolation methods

**Removal of green color.** One of the main challenges in protein isolation from leaves and algae is the removal of green color, which is due to the presence of chlorophyll. In this project, high speed centrifugation (38,000 *g*, 30 min) was shown to be efficient for the removal of green color during protein isolation from sugar beet leaves. Another method, typically reported in literature, for the removal of green color is heating of the extracted leaf juice at  $T = 50 - 60\text{ }^{\circ}\text{C}$  followed by centrifugation (12-14). To test whether this method could also efficiently remove the green color during protein isolation from sugar beet leaves a number of experiments were performed (**Figure 6.2**). In these experiments proteins were extracted from frozen sugar beet leaves after blending the leaves in a household-type blender with 150 mM sodium phosphate buffer pH 8.0 containing 0.8 M NaCl and 0.17% (w/v)  $\text{Na}_2\text{S}_2\text{O}_5$ , as described in **Chapter 2**. The filtrate that was obtained after filtration through a Büchner funnel was denoted as filtrate 8. Filtrate 8 was then divided into two equal parts and treated as follows: (1) centrifuged at 38,400 *g*, 30 min, 4  $^{\circ}\text{C}$  (Juice<sub>8HiSpC</sub>) and (2) heated at 50  $^{\circ}\text{C}$  for 10 min (after the

temperature in the extracted juice had reached 50 °C) and then centrifuged at 9,000 *g*, 10 min, 4 °C min (Juice<sub>8HtC</sub>).

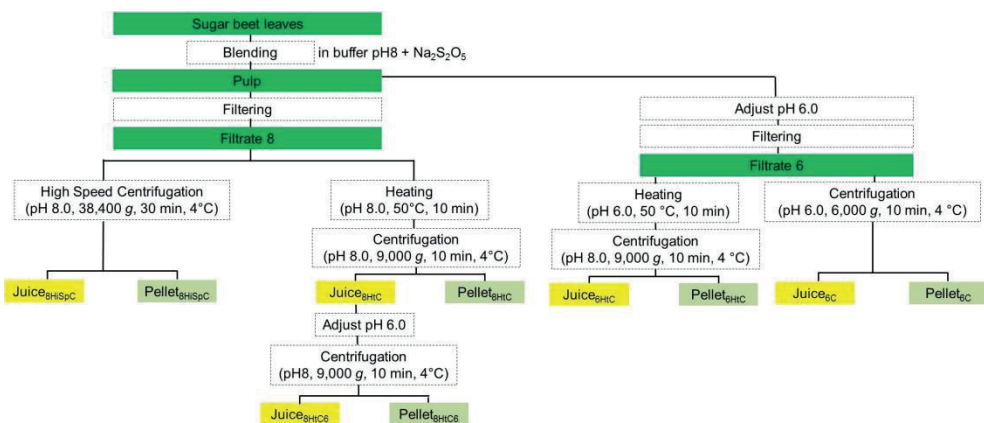


**Figure 6.2** Schematic representation of the different methods used for the removal of green color during protein isolation from sugar beet leaves.

The juice obtained after high speed centrifugation (Juice<sub>8HtSpC</sub>) was yellow, whereas the juice obtained after heating and mild centrifugation (Juice<sub>8HtC</sub>) was green (**Figure 6.3**). The color of the juices was also determined spectrophotometrically. For Juice<sub>8HtC</sub> three distinctive peaks in the absorbance spectra at ~ 479, ~ 620 and ~673 nm, indicative for the presence of chlorophyll  $\alpha$  and  $\beta$  (15), were observed. The fact that no green color removal was achieved after heating at 50 °C and centrifugation is in contrast with literature (12-14). This apparent discrepancy between our data and other reports was hypothesized to be due to the fact that in our case the extracted juice was at pH 8.0, whereas in the vast majority of literature, the extracted juice is at its natural pH (~ 6.0). To test this, the pH of the pulp was adjusted to pH 6.0 and the same process as described for Juice<sub>8HtC</sub> was followed. After heat treatment at 50 °C and mild centrifugation the obtained juice (Juice<sub>6HtC</sub>) showed no absorbance at the characteristic for chlorophyll wavelengths. These data suggest that the pH of the extracted juice during heating plays a dominant role in green color removal. Other researchers have also highlighted the significant effect of pH during green color removal from leaves (16). To test whether the pH (pH 6.0) could be sufficient for the removal of the green color, without the need of a heating step, the filtrate at pH 6.0 was mildly centrifuged (9,000 *g*, 10 min) (**Figure 6.2**). The obtained juice after this process (Juice<sub>6C</sub>) showed a significant reduction in the absorbance at all the characteristic for chlorophyll  $\alpha$  and  $\beta$  wavelengths (**Figure 6.3**). However, no complete color removal was achieved. These data suggest that (mildly) acidic conditions *per se* do not lead to efficient green color removal, and therefore a heating step is needed. The latter is believed to lead to a destabilization of the chloroplastic membranes, which can then be obtained after mild centrifugation.



As shown in this project, high speed centrifugation can also efficiently remove the green color from the extracted leaf juices. In addition, a higher nitrogen recovery was obtained after extraction of proteins from sugar beet leaves at pH 8.0 than at pH 6.0 (data not shown). Other researchers have also reported an approximately 5 times increase in protein extractability from sweet potato leaves at pH 8.0 than at pH 6.0 (17). Therefore, high speed centrifugation at pH 8.0 was used in this project for the green color removal during protein extraction from sugar beet leaves.

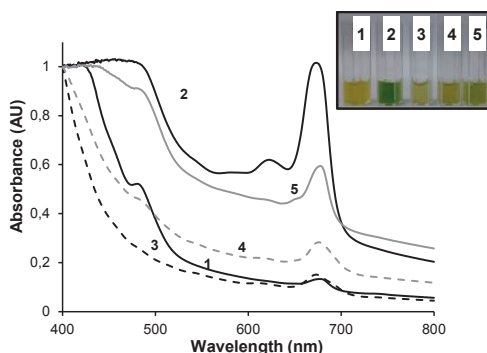


**Figure 6.3** UV spectra of the sugar beet leaf juices obtained using different conditions: (1) Juice<sub>8HiSp</sub>, (2) Juice<sub>8HiC</sub>, (3) Juice<sub>8HiC6</sub>, (4) Juice<sub>6HiC</sub>, (5) Juice<sub>6C</sub>. Inset: cuvettes containing the respective the sugar beet leaf juices.

### POLYPHENOL OXIDASE (PPO)-MEDIATED BROWN COLOR FORMATION

In literature it is often reported that the age of the leaves leads to differences in the chemical composition and protein extractability from leaves (18-20). One of the main questions in this thesis was whether this variability in the chemical composition of the leaves and the protein extractability is also observed when leaves (mainly mature) are collected at different time points or else when leaves are collected from plants of different ages. In **Chapter 2**, some differences were reported between leaves from young and old plants with regard to the chemical composition and protein extractability. The most striking difference between protein extracts obtained from leaves of young and old plants was the color. The protein extracts obtained from leaves of young plants were yellow whereas protein extracts obtained from leaves of old plants were brown. This observation was independent of year of harvest or growing conditions (field or greenhouse) (**Figure 6.4**).

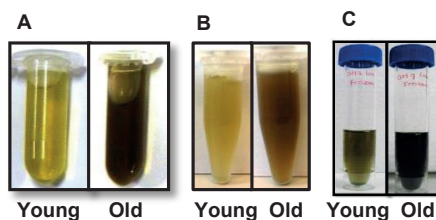


**Figure 6.4** Juice extracted from leaves obtained from young and old sugar beets grown in a field A) *Beta vulgaris* var. Isabella (collected at 2012), B) *Beta vulgaris* var. Rhino (collected at 2013) and in a greenhouse C) *Beta vulgaris* var. Isabella (collected at 2013).

In **Chapter 2**, we showed that the observed brown color formation was due to polyphenol oxidase (PPO) activity, which is a known, major quality problem in the processing of fruits and vegetables (21-23). However, it was also shown that in the protein extracts obtained from leaves of young plants, although no brown color formation was observed, there were active PPOs present and substantial amounts of phenolic compounds. Therefore, the main question that arose from this observation, and which has not been addressed in the previous chapters, was whether PPO activity determination and phenolic compounds quantification *per se* can explain or predict the brown color formation in plant extracts. To answer this question, additional experiments were performed and published separately (24). In this work, the phenolic compounds present in leaves of both plant ages were fractioned and quantified individually. The quantification of individual phenolic compounds revealed differences in phenolic composition between the two plant ages. In particular, the ratio of non-substrates (for PPO) to substrates (for PPO) was 8:1 in leaves from young plants and 3:1 in leaves from old plants. In addition, the PPO activity was determined using the endogenous phenolic compounds that were obtained from the sugar beet leaves. The main conclusion was that the PPO activity and presence of substrate phenolic compounds alone did not explain the difference in color between the protein extracts obtained from young and old plants. It was shown that after oxidation of substrate phenolic compounds into quinones, both substrate and non-substrate phenolic compounds can participate in non-enzymatic continuation reactions; i.e. (coupled oxidation and oxidation coupling, as explained in **Figure 6.5**. These non-enzymatic continuation reactions were the main drivers for brown color formation.

In short, the following mechanism is proposed (**Figure 6.5A**). Let's assume a system where a substrate phenolic compound; e.g. caffeic acid ester (CafAe) and one non-substrate phenolic compound; e.g. ferulic acid (FerA) are present. Initially, monomeric CafAe is enzymatically oxidized into a quinone. Subsequently, there are two continuation reactions in which this quinone can participate. The first continuation reaction is oxidative coupling, in which the quinone is attacked by nucleophiles. Nucleophiles present in this example are CafAe and FerA. The nucleophilic attack on the quinone yields a dimer, such as (CafAe)<sub>2</sub> or CafAe-FerA. Thereby, the quinone is reduced into a *o*-diphenolic dimer. This *o*-diphenolic dimer has potential to be oxidized. Due to its size, it is more likely that this *o*-diphenolic dimer will be re-oxidised through coupled oxidation (second continuation reaction), than through enzymatic oxidation (25). In this

reaction, the enzymatically formed quinone of monomeric CafAe can oxidize the dimer and be reduced into a monomeric CafAe again (**Figure 6.5A**). For CafAe-FerA dimer only the CafAe will be oxidized. These oxidized dimers can participate in further oxidative coupling reactions.

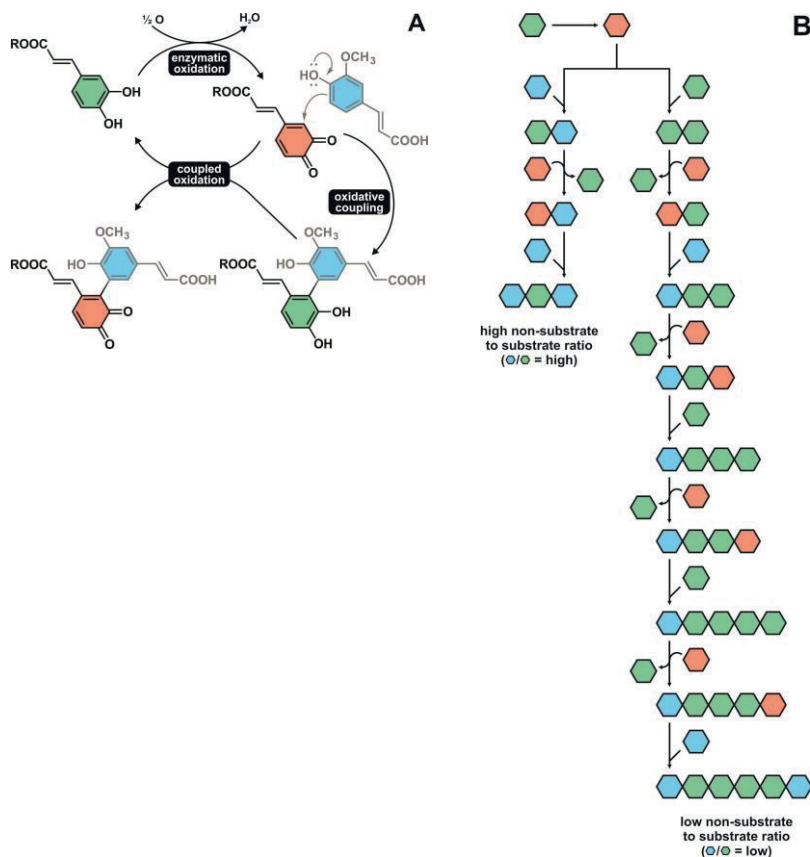


**Figure 6.5** (A) Proposed mechanism of enzymatic oxidation of a caffeic acid ester, followed by oxidative coupling to ferulic acid, and subsequent coupled oxidation. (B). Schematic representation of coupled oxidation and oxidative coupling reactions at high and low non-substrate-to-substrate ratio (adapted from (24)).

The oxidative coupling and coupled oxidation reactions can comprise various cycles, the number of which depends on the ratio of non-substrates-to-substrates phenolic compounds present in the mixture. The elongation of phenolic compounds by subsequent cycles of oxidative coupling and coupled oxidation are schematically shown in **Figure 6.5B**. It was demonstrated that at high non-substrate-to-substrate ratio the brown color formation is inhibited. In the previous example, that means that mainly CafAe-FerA dimers will be formed. Due to the relatively low CafAe concentration, all CafAe is consumed after a few reaction cycles and connected to non-substrate

phenolics. This results in small oligomers without an extensive conjugated system, which show no significant absorbance in the visible wavelength range (400-800 nm) (26). At low non-substrate-to-substrate ratio, e.g. low ratio of FerA:CafAe, there is increased probability of (CafAe)<sub>2</sub> formation, which can then undergo multiple cycles of coupled oxidation and oxidative coupling (**Figure 6.5B**). This leads to the formation of products with increased size, which show absorbance in the visible wavelength range. The fact that small oligomers without an extensive conjugated system do not show absorbance at the wavelengths typically used when PPO activity is determined colorimetrically (27, 28) underlines the fact that colorimetric assays might lead to underestimation of the actual PPO activity, and thus oxygen consumption assays, as used in (24), should be preferred. Besides non-substrate phenolic compounds (nucleophiles) other nucleophiles, such as free amino acids, that are present in leaves can also participate in oxidative coupling and thus increase the likelihood for browning. To this end, it needs to be noted that as shown in **Table 2.3**, the non-protein nitrogen content is higher in leaves from old plants than in leaves from young plants. This might also indicate that higher amounts of free amino acids are present in leaves from old plants, which can lead to higher PPO-mediated browning.

Overall, it was demonstrated that besides the PPO activity, it is the ratio between non-substrates-to-substrates phenolic compounds that drive enzymatic browning, rather than the absolute quantities of phenolic compounds. The latter emphasizes the importance of detailed compositional analysis of individual phenolic compounds to accurately predict or explain PPO-mediated brown color formation in plant extracts.

### **PPO-MEDIATED BROWN COLOR FORMATION AND EFFECT ON PROTEIN SOLUBILITY**

PPO-mediated browning is a major challenge not only when extracting proteins from leaves but also from other plant tissues, such as potato tubers (29, 30), or sunflower seeds (31). As discussed above, quinones that are formed after the oxidation of phenolic compounds by PPOs can polymerize with other phenolic compounds (32) or covalently link to proteins (33). The reaction products are dark colored, thus the color is an indication of protein modification. Protein modification can negatively affect the quality of the proteins, e.g. decrease their solubility, as it was shown for various proteins, e.g.  $\alpha$ -lactalbumin and lysozyme (33).

To test the effect of PPO activity on protein physico-chemical properties, the extraction was performed in absence or presence of sulfite (**Chapter 2**). The solubility of LSPC (10 g protein/L) isolated in the presence (LSPC<sub>LF6R,SO3</sub>) or absence (LSPC<sub>LF6R</sub>) of sulfite, as described in **Chapter 2**, was studied as a function of pH at I = 0.01 M. The solubility of both LSPC<sub>LF6R,SO3</sub> and LSPC<sub>LF6R</sub> was determined as described in **Chapter 3** and expressed as the protein concentration of the supernatant at each pH divided by the initial protein concentration of the dispersion (10 g protein/L). At pH 8.0 (I = 0.01 M) the solubility of LSPC<sub>LF6R</sub> at pH 8.0 was 1.4 times lower than the solubility of LSPC<sub>LF6R,SO3</sub> (**Figure 6.6**). This shows that the postulated PPO-induced protein modification, as

indicated by the brown color formation, led to a decrease in the initial protein solubility. Surprisingly, apart from the 1.4 times initial lower solubility at pH 8.0, LSPC<sub>LF6R</sub> and LSPC<sub>LF6R,SO3</sub> showed a similar solubility pattern as a function of pH.

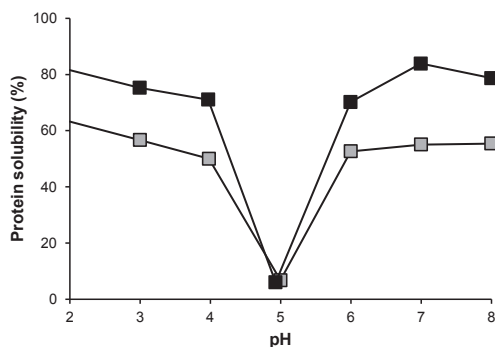


**Figure 6.6** Protein solubility of LSPC<sub>LF6R</sub> (■) and LSPC<sub>LF6R,SO3</sub> dispersions (10 g/L) (□) (as described in **Chapter 3**) at pH 8.0 ( $I = 0.01$  M).

The molecular weight ( $M_w$ ) distribution of the soluble part of LSPC<sub>LF6R</sub> and LSPC<sub>LF6R,SO3</sub> was further studied using size exclusion chromatography (SEC) an Äkta Micro equipped with a Superdex 200 PC 3.2/30 column (GE Healthcare, Uppsala, Sweden). LSPC<sub>LF6R</sub> showed a higher than LSPC<sub>LF6R,SO3</sub> absorption in the void volume ( $> 67$  kDa) at 280 nm (**Figure 6.7**), even though similar soluble protein concentration for both samples was used. This increase in absorbance in this area (high molecular weight compounds) can be due to binding of the PPO-induced quinones to proteins. However, the absorbance at 400 nm was only slightly higher for LSPC<sub>LF6R</sub> than for LSPC<sub>LF6R,SO3</sub>. Absorbance at this UV-vis range has been previously reported for proteins modified with oxidized phenolics (34). These data suggest that there is a binding of oxidized phenolics to proteins. However, no conclusions can be drawn whether this binding is covalent or non-covalent.

Given that LSPC<sub>LF6R,SO3</sub> also showed absorbance at 400 nm it cannot be excluded that even in the presence of sulfite during protein extraction there might be protein modification. This is not surprising given that in **Chapter 2** it was shown that the PPO from sugar beet leaves is not irreversibly inactivated in the presence of sulfite. Furthermore, in model incubations of tyrosinase with chlorogenic acid in the presence of NaHSO<sub>3</sub> it was shown that, although no color development (at 400 nm) was observed, there was still some initial PPO activity (35). That indicates that given that sulfite acts in a rather slow way there is time for PPO-induced quinones formation, which can subsequently bind to proteins.

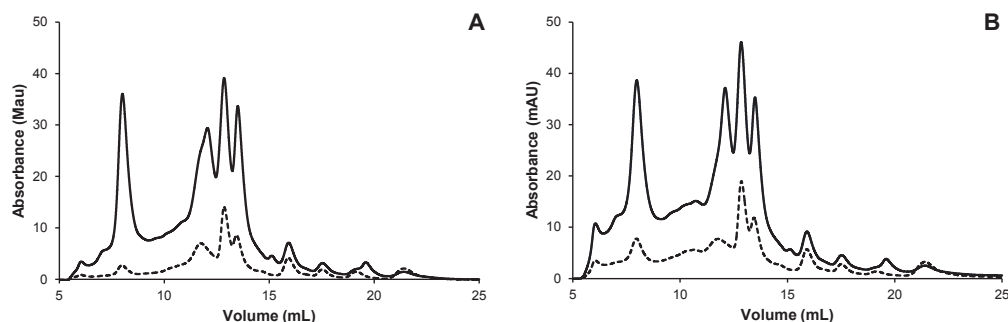


**Figure 6.7** Molecular weight distribution of (A) LSPC<sub>LF6R,SO3</sub> and (B) LSPC<sub>LF6R</sub>. All profiles were monitored at 280 nm (solid lines) and at 400 nm (dotted lines).

Determination of the protein modification by the *o*-phthalaldehyde (OPA) method for both LSPC<sub>LF3R</sub> and LSPC<sub>LF3R,SO3</sub>, as described elsewhere (36), showed that there was no lysine modification in any of the samples. This indicates that either the binding of proteins that was observed by SEC was non-covalent or that quinones preferentially bind to other amino acids, e.g. cysteine (37), histidine (38) and methionine (39). Treatment of the samples with SDS and subsequent determination of the molecular weight distribution could elucidate whether the binding is covalent or not.

Overall, these data indicate that there is a binding of oxidized phenolics to proteins. This binding might occur even in the presence of sulfite. However, the effect of protein modification due to oxidized phenolics binding in case of sugar beet leaves is not as pronounced as was shown for other proteins, e.g.  $\alpha$ -lactalbumin and lysozyme (33).

## TECHNO-FUNCTIONAL PROPERTIES

### Protein solubility and foam properties

In **Chapter 4**, it was shown that the soluble protein concentration, and not the total protein concentration, determines the foam ability of the protein concentrates/isolates. As shown, in **Figure 6.8**, indeed the foam ability of SPI solutions prepared at pH 3.0, pH 5.0 and pH 8.0 ( $I = 0.01$  M) as a function of the soluble protein concentration superimposed.

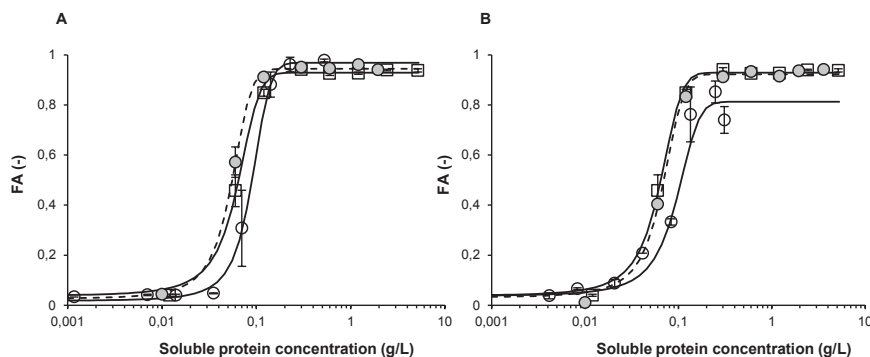


**Figure 6.8** Foam ability (FA) of SPI as a function of soluble protein concentration at pH 8.0 ( $\square$ ) (A, B), at pH 5.0 (A) and at pH 3.0 (B) with ( $\bullet$ ) and without removal of insoluble aggregates (only the soluble protein concentration, based on solubility data, is considered for the graph) ( $\circ$ ). All markers are average values with the error bars indicating SD. Error bars are not shown when SD is smaller than the size of the used marker.

Regarding the foam stability, in **Chapter 4**, it was shown that there is a minimum concentration of soluble protein needed to form stable foams. Above this concentration, it was shown that, for LSPC, the foam stability at pH 3.0 and at pH 5.0 was higher than at pH 8.0 (**Figure 4.3B**). For SPI at pH 3.0, no stable foams were obtained (**Figure 4.3D**). In this case the maximal total protein concentration tested was 5.0 g/L, which corresponds to 0.35 g/L of soluble protein at pH 3.0. Therefore, the fact that no stable foam was obtained for SPI at pH 3.0 was postulated to be due to the low concentration of soluble protein. At pH 5.0 SPI showed higher foam stability than at pH 8.0 at similar soluble protein concentrations (**Figure 6.9A**). This enhancement in foam stability was postulated to be due to the formation of aggregates between proteins or proteins and charged carbohydrates.

To test whether the aggregates contribute to the improvement of foam stability, further experiments were performed. In these experiments SPI was prepared at pH 5.0 and at pH 3.0 and after equilibration for at least 1 h at the respective pH the insoluble material was removed by centrifugation. In this case, it was observed that the foam stability at pH 5.0 as a function of the soluble protein concentration followed the same trend as the foam stability pH 8.0 (**Figure 6.9A**). This observation further supports our postulation that the aggregates contribute to an improvement in foam stability. Interestingly, when only the soluble part of SPI at pH 3.0 was used for foam formation a significantly higher foam stability was observed at pH 3.0 than at pH 8.0 (**Figure 6.9B**). This observation in combination with the fact that at  $C_p = 0.3$  g/L the foam stability at pH 8.0 was 37 min, whereas at the same soluble  $C_p$  at pH 3.0 the foam stability was only 3 min indicate that in the case of SPI the presence of aggregates at pH 3.0 negatively affected the foam stability. The fact that the aggregates showed a negative effect on the foam stability of SPI, whereas they positively affected the foam stability of LSPC was not surprising, given that the role of protein aggregates in literature is controversial. In some cases, aggregates were shown to enhance foam stability (40), whereas in some

other cases they showed a destabilizing effect (41). Many factors, such as the size of the particle, its structure and density influence the foam stabilizing ability of aggregates.

Another reason for the observed difference in foam stability between the soluble fractions of SPI at pH 3.0 and pH 8.0 might be a difference in the association state of SPI under different conditions. For example, it was shown that SPI at pH 3.8 and  $I = 0.03\text{ M}$  is present in the 7S form, whereas at pH 7.6 it is present in the 11S form (42). A difference in structure between SPI at pH 8.0 and at pH 3.0 is expected to lead to different behavior of the proteins at the air-water interface, as was also shown by the non-linear to deformation behavior of SPI at pH 3.0 (**Figure 4.8**). A positive effect of the dissociation of glycinin on foam stability was previously reported (43).

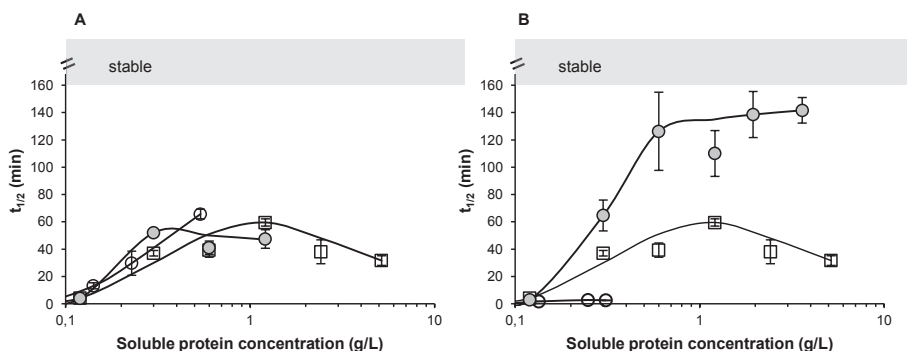


**Figure 6.9** Foam half-life time ( $t_{1/2}$ , min) of SPI as a function of soluble protein concentration at pH 8.0 ( $\square$ ) (A, B), at pH 5.0 (A) and at pH 3.0 (B) with ( $\bullet$ ) and without removal of insoluble aggregates (only the soluble protein concentration, based on solubility data, is considered for the graph) ( $\circ$ ). All markers are average values with the error bars indicating SD. Error bars are not shown when SD is smaller than the size of the used marker.

### The use of critical concentrations to describe emulsions and foams

The techno-functional properties; i.e. emulsion and foam properties, of a protein depend on the system conditions as well as the molecular properties of the protein. That implies that there are two big challenges when it comes to novel proteins:

(1) To define “the window of opportunity” for a novel protein, or in other words the potential uses of the protein, an extensive study of the techno-functional properties under various conditions is required.

(2) Comparison of the techno-functional properties of different proteins under only one set condition might lead to “false negatives”. For example, as shown in **Chapter 4**, at pH 8.0 ( $I = 0.5\text{ M}$ ) and  $C_p = 0.3\text{ g/L}$  SPI-stabilized foam is 4 times more stable than LSPC-stabilized foam under the same conditions (**Figure 4.2**). From this, one can conclude that SPI is a better foam stabilizing agent. However, at higher protein concentration, e.g. at  $C_p \approx 5.0\text{ g/L}$ , LSPC shows 2 times higher foam stability than SPI (**Figure 4.2**).

To tackle these challenges an understanding is needed of the relation between system conditions, protein molecular properties and techno-functional (emulsion and foam) properties.



For emulsions, a model describing this relation was proposed for pure protein systems (44). A main parameter in this model is the critical protein concentration ( $C_{cr}$ ) at which a stable emulsion is formed. The  $C_{cr}$  depends on the volume fraction of oil ( $\Phi_{oil}$ ), the adsorbed amount of protein ( $\Gamma_{max}$ ) that is needed to stabilize the interface and the adsorption rate constant  $k_{adsorb}$  (44). It was shown that the  $\Gamma_{max}$  and the  $k_{adsorb}$  can be approximated by the protein charge (related to electrostatic interactions), the relative exposed hydrophobicity and the protein radius. In the case of protein concentrates/isolates the challenge stems from the fact that they typically consist of a mixture of (multimeric) proteins and other compounds, e.g. carbohydrates, which can in turn also influence the emulsifying behavior of the system.

With the study and description of foam and emulsion properties of the LSPC several important steps were made. Firstly, in **Chapters 3** it was shown that the average droplet size ( $d_{3,2}$ ) of the LSPC-stabilized emulsions decreased as function of protein concentration. This decrease continued until a critical protein concentration, above which  $d_{3,2}$  became independent of the protein concentration. This decrease of  $d_{3,2}$  with protein concentration has been previously reported for more pure protein systems such as  $\beta$ -lactoglobulin (45) (**Figure 6.10**). A main outcome of **Chapter 3**, is that for LSPC-stabilized emulsions the values of  $C_{cr}$ ,  $\Gamma_{max}$ ,  $R_{eff}$  and  $d_{3,2}$  obtained from experimental data were close to those forecasted based on the molecular properties of the dominant proteins (Rubisco). The same observation was also made for SPI-stabilized emulsions. Thus, the emulsion properties of novel and/or non-pure protein systems, under various system conditions, can be in the future relatively easily forecasted by determining only a small set of quantifiable parameters (e.g. exposed hydrophobicity, protein radius) and by collecting only a small set of experimental data (e.g. determining the  $d_{3,2}$  for a small set of  $C_p$ ).

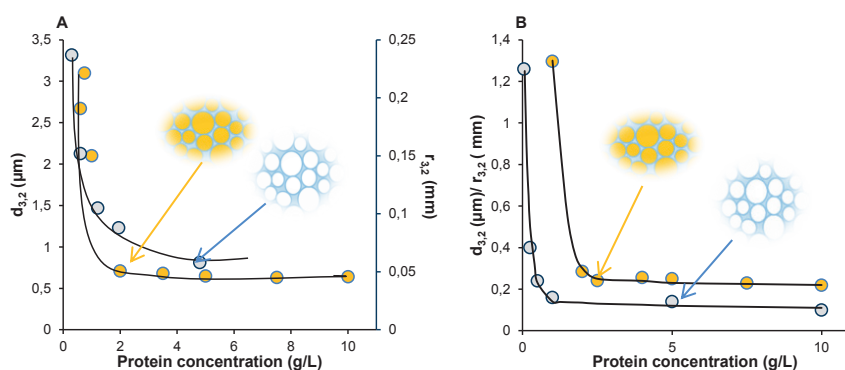


**Figure 6.10** Average droplet size ( $d_{3,2}$ ) of emulsions ( $\Phi = 0.1$ ) and bubble radius ( $r_{3,2}$ ) of foams as a function of protein concentration. (A) Stabilized with LSPC at pH 8.0 and  $I = 0.01$  M (**Chapters 3, 4**) and (B) Stabilized with  $\beta$ -lactoglobulin at pH 7.0 and  $I < 0.02$  M (reproduced and adapted from (45, 46). The lines are guides to the eye.

The concept developed for emulsions has been extended to foams (47). One of the benefits of using this approach is that by identifying the  $C_{cr,3,2}$ , we can at least

compare foams with an initial similar foam structure. That is because at  $C_{ccr3,2}$  the mean bubble radius reaches its minimum size ( $r_{3,2min}$ ). This means that the subsequently determined foam stability is at least minimally influenced by any differences in the initial foam structure.

In **Chapter 4**, it was shown that LSPC-stabilized foams show a similar to pure protein systems behavior (e.g. FA increases and  $r_{3,2}$  decreases with protein concentration) (**Figure 6.10**). However, there were also some differences between pure protein systems and our proteins. These were mostly seen in the sensitivity of changes in pH. In the mixed protein systems (LSPC/SPI) charged carbohydrates were present. The presence of charged carbohydrates in the system was shown to have a big effect on the foam properties. For example, at pH 5.0 (close to the pI of Rubisco) LSPC-stabilized foams showed higher foam stability than at pH 8.0. This was postulated to be due to contribution of protein and/or protein-charged carbohydrates aggregates. A link was shown between the interfacial properties and the foam ability e.g. for LSPC foams the faster adsorption at high ionic strength led to higher foam ability at high than at low ionic strength (**Figure 4.2A, 4.7B**).

## THE USE OF PDPS IN BIOREFINERY

The benefit of using the model approach of foam and emulsion properties as described above has several advantages. The main advantage is that it allows the description of the techno-functional properties of the proteins in a quantitative way. In addition, it allows for prediction of the techno-functional properties of the proteins by linking them to the molecular characteristics of the proteins. This is a feature that can then be used in the design of the biorefinery process.

In **Chapter 5**, we showed that the design of a biorefining process is challenging due to the high number of products that can be obtained from one feedstock, and the fact that some products can be negatively affected by processing conditions that are essential for other products. To facilitate this design the use of the product driven process synthesis (PDPS) methodology was reviewed (**Chapter 5**). One of the main adaptations in PDPS was the introduction of the products "functionalities". For instance, the focus is not only on the highest yield of proteins, in general, but on the highest yield of water soluble proteins. At its current state the adapted PDPS comprises of a hierarchical list of steps that describe the design of a biorefining process starting from the raw material and moving towards the final products. In other words, it can be used as a guideline, or else as a qualitative tool, for the design of a biorefining process.

The main question that remains is whether the adapted PDPS could be further expanded to provide also quantitative outcomes. Indeed, the last step of the adapted PDPS, which describes the "multi product integration (integrated task network)" could be approached as a multi-objective optimization problem. However, this approach is challenging due to: (1) the different effects of the various system conditions on the functionalities of the final products and (2) the interaction among the different compounds present in the feedstock, which hinders the isolation of pure compounds. For example, let's assume that the aim is to simultaneously maximize the yield of water

soluble protein (i.e. the focus is also on the functionality) and the yield of carbohydrates. These yields depend, for example (in the simplest form), on the temperature (T) used during the extraction. These relationships can be described, for example, using equations 6.1 and 6.2.

$$\text{Yield(solubleprotein)} = f(T, \alpha) \quad (6.1)$$

$$\text{Yield(carbohydrates)} = g(T, \beta) \quad (6.2)$$

where the parameters  $\alpha$  and  $\beta$  describe the effect of temperature on the respective yields.

To translate the “multi product integration (integrated task network)” step into a multi-objective optimization problem not only the values of these parameters are needed but also the exact functional form that describes the corresponding relationships (*viz.* the functions  $f$  and  $g$ ). To do that, typically a relatively large number of experiments are needed.

In **Chapter 2**, the effect of plant age on the quantity and quality of the protein isolated from sugar beet leaves was described. This is an example of an experiment where the parameter values (effect of plant age) were elicited. In **Chapter 3**, the emulsion properties of the sugar beet leaf proteins were described as function of the protein concentration. For that, equation 3.7 (**Chapter 3**) was used. This is an example of an experiment where the functional form of the relationship between the  $C_{cr}$ , the volume fraction of oil ( $\Phi_{oil}$ ), the adsorbed amount of protein ( $\Gamma_{max}$ ) that is needed to stabilize the interface, the minimum average droplet size ( $d_{3,2min}$ ) and the adsorption rate constant  $k_{adsorb}$  was determined. Such models (as described in **Chapter 3**) can be in the future added in PDPS as part of the “multi product integration (integrated task network)”. With this we can provide quantitative parameters that can be used in the PDPS as descriptors for the quality of the final products.

## SUGAR BEET LEAVES BIOREFINERY

The main focus of this project was on the isolation of proteins from sugar beet leaves. However, to further increase the economic revenue from the exploitation of sugar beet leaves a biorefinery approach, as discussed in **Chapter 5**, needs to be followed. In **Chapter 5** a case study of a sugar beet leaves biorefinery was presented. In this case study some examples of potential final products were discussed. Other alternatives have also been reported in literature. For example, sugar beet leaves can be used for the isolation of both soluble (as described in this thesis) and insoluble proteins. Thylakoid membranes and cellulose-rich fibres obtained from sugar beet leaves can be used as emulsions stabilizers (48, 49). Furthermore, the stems of the leaves have also great potential as a source of various compounds (**Table 6.1**).

**Table 6.1.** Chemical composition (w/w% db) of stems obtained from sugar beets grown in a greenhouse <sup>a</sup>.

Sample	Dry matter <sup>b</sup>	Protein <sup>c</sup>	Neutral carbohydrates	Uronic acids	Lipids <sup>c</sup>	Ash	Phenolic compounds
SG <sub>2I</sub>	7.9 (±0.6)	19.5 (±0.9)	13.5 (±2.9)	11.5 (±1.5)	4.2 (±0.1)	19.0 (±0.5)	2.0 (< 0.1)
SG <sub>3I</sub>	19.7 (±0.7)	3.0 (±0.1)	27.0 (n.d.) <sup>d</sup>	11.5 (±0.2)	8.0 (±1.0)	16.0 (±0.2)	2.9 (±0.1)
SG <sub>4I</sub>	19.9 (±0.1)	2.0 (<0.1)	29.6 (±0.2)	10.0 (±1.0)	5.0 (±0.3)	13.2 (±0.1)	2.1 (<0.1)
SG <sub>5I</sub>	12.3 (±4.9)	3.8 (±0.1)	46.3 (±0.9)	9.7 (<0.1)	7.7 (±0.4)	9.1 (< 0.1)	2.5 (±0.1)
SG <sub>6I</sub>	13.9 (±0.9)	2.8 (±0.1)	43.0 (<0.1)	10.4 ±1.1	4.2 (±0.1)	10.4 (±0.2)	2.3 (±0.2)
SG <sub>7I</sub>	18.2 (±0.2)	2.7 (<0.1)	37.4 (±0.6)	11.7 (±1.0)	3.3 (±0.3)	13.9 (±0.1)	2.6 (±0.1)
SG <sub>8I</sub>	14.6 (±2.4)	3.2 (±0.1)	36.9 (±0.3)	12.3 (±0.6)	7.7 (±0.2)	15.5 (±0.2)	2.8 (< 0.1)

<sup>a</sup> All data are expressed as average (from at least two independent samples) (±stdev).<sup>b</sup> In w/w% fresh weight.<sup>c</sup> Determined as N<sub>T</sub>·k<sub>p</sub> of respective leaves (**Chapter 2**).<sup>d</sup> Not determined<sup>e</sup> Determined as CHCl<sub>3</sub>/MeOH soluble material

As shown, in the case study described in **Chapter 5**, the stems can be separated from the leaves (blades) and further used as, for example, source of fibres, while the leaves can be used as a protein source. The separation of stems from leaves does not lead to significant losses in protein recovery given that leaves (blades) contribute approximately 69% to the total protein recovery. In addition, the presence of stems during protein extraction hinders the separation of the extracted juice from the insoluble material after centrifugation (process described in **Chapter 2**), due to the formation of an unstable pellet. However, in case that a pressing step is used for the extraction of soluble proteins, the stems can facilitate the separation of juice from solids, as they form a filter-like fibres layer around the screws. Apart from the various products that can be obtained from sugar beet leaves, the produced waste streams can be returned to the field and be used as fertilizers. In this case the economic revenue from sugar beet leaves biorefinery can be further increased due to the reduction in cost from handling the remaining waste streams.

## CONCLUDING REMARKS

Sugar beet leaves, which are currently a side stream of the sugar beets (*Beta vulgaris* L.) cultivation can be used for the extraction of various compounds, such as phenolic compounds, carbohydrates and proteins. With respect to protein extraction and isolation, the collection of the leaves can be performed after or simultaneously with the harvest of the beets, given that the time of harvest does not affect the protein content in the leaves. However, plant age has a significant effect on the color of the extracted proteins, which is due to PPO-mediated browning. This challenge can be tackled by the

use of sulfite during protein extraction, which prevents PPO-mediated browning. The proteins isolated from sugar beet leaves consist mainly of Rubisco. The sugar beet leaf protein concentrates (LSPC) show similar to other leaf proteins solubility behavior as a function of pH. In terms of emulsion properties, LSPC-stabilized emulsions are stable in a wider pH range than emulsions stabilized by other plant proteins, such as soy protein isolates. Regarding foam properties, the soluble protein concentration and not the total protein in the bulk determines the foam ability of LSPC. The presence of charged carbohydrates in LSPC is postulated to contribute to its improved foam stability at low pH values (pH 3.0 and 5.0). Lastly, although LSPC is complex mixture of different proteins and other non-protein compounds, its emulsion properties can be forecasted based on the molecular properties of the most dominant protein in it and taking into account the presence of charged carbohydrates. To do that models earlier developed for pure protein stabilized systems can be used. As such, the potential uses of LSPC, and of other novel proteins, in food applications can be determined by performing a small set of experiments.

## References

1. Aletor, O.; Oshodi, A. A.; Ipinmoroti, K., Chemical composition of common leafy vegetables and functional properties of their leaf protein concentrates. *Food chemistry* **2002**, *78*, 63-68.
2. Ghazi, A.; Metwali, S.; Atta, M. B., Protein isolates from Egyptian sweet potato leaves. *Food / Nahrung* **1989**, *33*, 145-151.
3. Devi, A. V.; Rao, N.; Vijayaraghavan, P., Isolation and composition of leaf protein from certain species of Indian flora. *Journal of the Science of Food and Agriculture* **1965**, *16*, 116-120.
4. Schwenzfeier, A.; Wierenga, P. A.; Gruppen, H., Isolation and characterization of soluble protein from the green microalgae *Tetraselmis* sp. *Bioresource Technology* **2011**, *102*, 9121-9127.
5. Töpfl, S., Pulsed Electric Fields (PEF) for Permeabilization of cell membranes in food-and bioprocessing-applications, process and equipment design and cost analysis. **2006**.
6. Zderic, A.; Zondervan, E., Polyphenol extraction from fresh tea leaves by pulsed electric field: A study of mechanisms. *Chemical Engineering Research and Design* **2016**, *109*, 586-592.
7. Coustets, M.; Joubert-Durigneux, V.; Hérault, J.; Schoefs, B.; Blanckaert, V.; Garnier, J.-P.; Teissié, J., Optimization of protein electroextraction from microalgae by a flow process. *Bioelectrochemistry* **2015**, *103*, 74-81.
8. Bouzrara, H.; Vorobiev, E., Beet juice extraction by pressing and pulsed electric fields. *International Sugar Journal* **2000**, *102*, 194-200.
9. Eshtiaghi, M.; Knorr, D., High electric field pulse pretreatment: potential for sugar beet processing. *Journal of Food Engineering* **2002**, *52*, 265-272.
10. Polikovskiy, M.; Fernand, F.; Sack, M.; Frey, W.; Müller, G.; Golberg, A., Towards marine biorefineries: Selective proteins extractions from marine macroalgae *Ulva* with

pulsed electric fields. *Innovative Food Science & Emerging Technologies* **2016**, *37*, 194-200.

11. Lebovka, N. I.; Praporscic, I.; Vorobiev, E., Enhanced expression of juice from soft vegetable tissues by pulsed electric fields: consolidation stages analysis. *Journal of Food Engineering* **2003**, *59*, 309-317.

12. Edwards, R. H.; Miller, R. E.; De Fremery, D.; Knuckles, B. E.; Bickoff, E.; Kohler, G. O., Pilot plant production of an edible white fraction leaf protein concentrate from alfalfa. *Journal of Agriculture and Food Chemistry* **1975**, *23*, 620-626.

13. Jwanny, E. W.; Montanari, L.; Fantozzi, P., Protein production for human use from sugarbeet: Byproducts. *Bioresource Technology* **1993**, *43*, 67-70.

14. Hernandez, A.; Martinez, C.; Alzueta, C., Effects of alfalfa leaf juice and chloroplast-free juice pH values and freezing upon the recovery of white protein concentrate. *Journal of Agriculture and Food Chemistry* **1989**, *37*, 28-31.

15. Smith, E. L., The chlorophyll-protein compound of the green leaf. *The Journal of general physiology* **1941**, *24*, 565-582.

16. Lundborg, T., Fractionation by centrifugation of leaf proteins from *Brassica napus*, *Brassica oleracea*, *Helianthus annuus* and *Atriplex hortensis* as a function of pH and temperature. *Physiologia Plantarum* **1980**, *48*, 251-260.

17. Ghazi, A.; Metwali, S.; Atta, M., Protein isolates from Egyptian sweet potato leaves. *Molecular Nutrition & Food Research* **1989**, *33*, 145-151.

18. Biondo, P. B. F.; Boeing, J. S.; Barizão, É. O.; Souza, N. E. d.; Matsushita, M.; Oliveira, C. C. d.; Boroski, M.; Visentainer, J. V., Evaluation of beetroot (*Beta vulgaris* L.) leaves during its developmental stages: a chemical composition study. *Food Science and Technology* **2014**, *34*, 94-101.

19. Chutichudet, B.; Chutichudet, P.; Kaewsit, S., Influence of developmental stage on activities of polyphenol oxidase, internal characteristics and colour of lettuce cv. grand rapids. *American Journal of Food Technology* **2011**, *6*, 215-225.

20. Arkcoll, D. B.; Festenstein, G. N., A preliminary study of the agronomic factors affecting the yield of extractable leaf protein. *Journal of the Science of Food and Agriculture* **1971**, *22*, 49-56.

21. Chow, Y. N.; Louarme, L.; Bonazzi, C.; Nicolas, J.; Billaud, C., Apple polyphenoloxidase inactivation during heating in the presence of ascorbic acid and chlorogenic acid. *Food chemistry* **2011**, *129*, 761-767.

22. Marri, C.; Frazzoli, A.; Hochkoeppler, A.; Poggi, V., Purification of a polyphenol oxidase isoform from potato (*Solanum tuberosum*) tubers. *Phytochemistry* **2003**, *63*, 745-752.

23. Jolivet, S.; Arpin, N.; Wichers, H. J.; Pellon, G., *Agaricus bisporus* browning: a review. *Mycological Research* **1998**, *102*, 1459-1483.

24. Vissers, A.; Kiskini, A.; Hilgers, R. J.; Marinea, M.; Wierenga, P. A.; Gruppen, H.; Vincken, J. P., Enzymatic browning in sugar beet leaves (*Beta vulgaris* L.): Influence of caffeic acid derivatives, oxidative coupling and coupled oxidation. *Journal of Agriculture and Food Chemistry* **2017**, *65*, 4911-4920.

25. Tanaka, T.; Mine, C.; Inoue, K.; Matsuda, M.; Kouno, I., Synthesis of theaflavin from epicatechin and epigallocatechin by plant homogenates and role of epicatechin quinone in the synthesis and degradation of theaflavin. *Journal of Agriculture and Food Chemistry* **2002**, *50*, 2142-2148.
26. Uchida, K.; Ogawa, K.; Yanase, E., Structure determination of novel oxidation products from epicatechin: thearubigin-like molecules. *Molecules* **2016**, *21*, 273.
27. Kuijpers, T. F. M.; Narváez Cuenca, C. E.; Vincken, J. P.; Verloop, A. J. W.; van Berkel, W. J. H.; Gruppen, H., Inhibition of enzymatic browning of chlorogenic acid by sulfur-containing compounds. *Journal of Agriculture and Food Chemistry* **2012**, *60*, 3507-3514.
28. Gowda, L. R.; Paul, B., Diphenol activation of the monophenolase and diphenolase activities of field bean (*Dolichos lablab*) polyphenol oxidase. *Journal of Agriculture and Food Chemistry* **2002**, *50*, 1608-1614.
29. Walter Jr, W. M.; Purcell, A. E., Effect of substrate levels and polyphenol oxidase activity on darkening in sweet potato cultivars. *Journal of Agriculture and Food Chemistry* **1980**, *28*, 941-944.
30. Narváez Cuenca, C. E.; Kuijpers, T. F. M.; Vincken, J. P.; de Waard, P.; Gruppen, H., New insights into an ancient antibrowning agent: Formation of sulfophenolics in sodium hydrogen sulfite-treated potato extracts. *Journal of Agriculture and Food Chemistry* **2011**, *59*, 10247-10255.
31. González Pérez, S.; Merck, K. B.; Vereijken, J. M.; van Koningsveld, G. A.; Gruppen, H.; Voragen, A. G., Isolation and characterization of undenatured chlorogenic acid free sunflower (*Helianthus annuus*) proteins. *Journal of Agriculture and Food Chemistry* **2002**, *50*, 1713-1719.
32. Cheynier, V.; Owe, C.; Rigaud, J., Oxidation of grape juice phenolic compounds in model solutions. *Journal of Food Science* **1988**, *53*, 1729-1732.
33. Prigent, S. V.; Voragen, A. G.; Visser, A. J.; van Koningsveld, G. A.; Gruppen, H., Covalent interactions between proteins and oxidation products of caffeoylquinic acid (chlorogenic acid). *Journal of the Science of Food and Agriculture* **2007**, *87*, 2502-2510.
34. Rawel, H. M.; Czajka, D.; Rohn, S.; Kroll, J., Interactions of different phenolic acids and flavonoids with soy proteins. *International Journal of Biological Macromolecules* **2002**, *30*, 137-150.
35. Kuijpers, T. F.; Narváez Cuenca, C. E.; Vincken, J. P.; Verloop, A. J.; van Berkel, W. J.; Gruppen, H., Inhibition of enzymatic browning of chlorogenic acid by sulfur-containing compounds. *Journal of Agriculture and Food Chemistry* **2012**, *60*, 3507-3514.
36. Wierenga, P. A.; Meinders, M. B.; Egmond, M. R.; Voragen, F. A.; de Jongh, H. H., Protein exposed hydrophobicity reduces the kinetic barrier for adsorption of ovalbumin to the air– water interface. *Langmuir* **2003**, *19*, 8964-8970.
37. Felton, G.; Broadway, R.; Duffey, S., Inactivation of protease inhibitor activity by plant-derived quinones: complications for host-plant resistance against noctuid herbivores. *Journal of Insect Physiology* **1989**, *35*, 981-990.
38. Hurrell, R.; Finot, P.; Cuq, J., Protein-polyphenol reactions. *British Journal of Nutrition* **1982**, *47*, 191-211.

39. Vithayathil, P. J.; Murthy, G. S., New reaction of *o*-benzoquinone at the thioether group of methionine. *Nature* **1972**, *236*, 101-103.
40. Wierenga, P. A.; van Norél, L.; Basheva, E. S., Reconsidering the importance of interfacial properties in foam stability. *Colloids and Surfaces A: Physicochemical and Engineering Aspects* **2009**, *344*, 72-78.
41. Rullier, B.; Novales, B.; Axelos, M. A., Effect of protein aggregates on foaming properties of  $\beta$ -lactoglobulin. *Colloids and Surfaces A: Physicochemical and Engineering Aspects* **2008**, *330*, 96-102.
42. Lakemond, C. M.; de Jongh, H. H.; Hessing, M.; Gruppen, H.; Voragen, A. G., Soy glycinin: influence of pH and ionic strength on solubility and molecular structure at ambient temperatures. *Journal of Agriculture and Food Chemistry* **2000**, *48*, 1985-1990.
43. Wagner, J. R.; Guéguen, J., Surface functional properties of native, acid-treated, and reduced soy glycinin. 1. Foaming properties. *Journal of Agriculture and Food Chemistry* **1999**, *47*, 2173-2180.
44. Delahaije, R. J.; Gruppen, H.; Giuseppin, M. L. F.; Wierenga, P. A., Towards predicting the stability of protein-stabilized emulsions. *Advances in Colloid and Interface Science* **2015**, *219*, 1-9.
45. Delahaije, R. J.; Gruppen, H.; Giuseppin, M. L.; Wierenga, P. A., Quantitative description of the parameters affecting the adsorption behaviour of globular proteins. *Colloids and Surfaces B: Biointerfaces* **2014**, *123*, 199-206.
46. Lech, F. J.; Delahaije, R. J.; Meinders, M. B.; Gruppen, H.; Wierenga, P. A., Identification of critical concentrations determining foam ability and stability of  $\beta$ -lactoglobulin. *Food Hydrocolloids* **2016**.
47. Lech, F. J.; Delahaije, R. J.; Meinders, M. B.; Gruppen, H.; Wierenga, P. A., Identification of critical concentrations determining foam ability and stability of  $\beta$ -lactoglobulin. *Food Hydrocolloids* **2016**, *57*, 46-54.
48. Tenorio, A. T.; de Jong, E.; Nikiforidis, C.; Boom, R.; van der Goot, A., Interfacial properties and emulsification performance of thylakoid membrane fragments. *Soft matter* **2017**, *13*, 608-618.
49. Tenorio, A. T.; Gieteling, J.; Nikiforidis, C.; Boom, R.; van der Goot, A., Interfacial properties of green leaf cellulosic particles. *Food Hydrocolloids* **2017**, *71*, 8-16.



---

## Summary

---

To ensure sustainability in food processing the current large volumes of side or waste streams need to be valorized. For instance, sugar beet leaves (SBL), which are a side stream of the sugar beets cultivation, are embedded in the soil after sugar beets have been harvested. In consequence, a plethora of potentially valuable compounds, such as proteins, carbohydrates, phenolic compounds, lipids and minerals, which are present in the SBL, are left unexploited. The general aim of this thesis was to study the biorefinery of SBL, with a special focus on the isolation of proteins. To this end, the research was divided in three sub-aims. These were: 1) to determine whether there is variability in the chemical composition of the leaves due to pre-harvest conditions (plant age), 2) to evaluate the variability of the techno-functionality of leaf soluble protein concentrate (LSPC) due to system conditions and 3) to extend current product and process synthesis approaches to enable the design of biorefining process.

**Chapter 1** provides an overview of the methods and techniques developed for, as well as the challenges encountered when, extracting proteins from leaves. Several studies showed that the quantity and quality (e.g. color) of extracted leaf protein concentrates/isolates can be significantly affected by agronomical and environmental conditions as well as time of harvest. These effects depend on the tested species. These studies furthermore showed that the recovery of the extracted proteins as well as their techno-functional properties, e.g. solubility, depend on the protein extraction method that is used. Moreover, the techno-functionality of the extracted proteins was shown to be influenced by the system conditions, e.g. pH and ionic strength (I), and the sample composition, e.g. presence of charged carbohydrates. Based on this, it became apparent that in order to define the window of opportunity of a novel protein concentrate/isolate, the latter needs to be tested under various conditions. In addition, understanding these effects is essential in designing a process (biorefining process), which aims to optimize the yield of a range of compounds (with good techno-functional properties) rather than to maximize the yield of one single compound.

From **Chapter 1** it became evident that the time of harvest can affect both the quantity and the quality of the extracted leaf proteins. Given that these effects are species dependent, the first aim of this thesis was to evaluate these effects specifically on SBL. **Chapter 2** focuses on the variation in chemical composition and quantity and quality of proteins extracted from SBL due to variation in plant age; i.e. harvesting time. To this end, SBL collected at different time points were used. SBL from sugar beets grown both in field (varieties: Rhino, Arrival) and in greenhouse (variety: Isabella) were tested. It was shown that within the same variety (Rhino-field, Arrival-field, Isabella-greenhouse) the protein content was similar for SBL from young and old plants ( $22\pm1$ ,  $16\pm1$ , and  $10\pm3\%$  w/w db, respectively). Although no consistent correlation with plant

age was found, a variation in final protein isolation recovery was observed. This variation was mostly due to variation in nitrogen extractability (28-56%). A significant effect of the plant age was observed on the quality (color) of LSPC; i.e. brown (indicative of polyphenol oxidase- PPO- activity) for LSPC from old plants and yellow for LSPC from young plants

Based on the results from **Chapter 2**, a standardized method for the extraction of proteins from SBL was developed and used in the rest of the thesis. In this method sodium disulfite was used during protein extraction to inhibit PPO-mediated browning. The LSPC obtained after using this extraction method was yellowish and consisted mainly of protein (69.3% w/w db (N-5.23)) and carbohydrates (5.1% w/w db; half of which was charged carbohydrates). The main protein present in LSPC was Rubisco. The solubility of LSPC as a function of pH showed a typical, for leafy proteins, U-shape curve with a minimum solubility at pH 4.5. In **Chapter 3**, the emulsion properties of LSPC were determined under various system conditions. To be able to extrapolate regarding the emulsion properties of LSPC to conditions that were not tested we tried to link the molecular properties of LSPC to its emulsion properties. To this end, a model that was recently developed to describe this link for pure-protein systems was applied. It was shown that at pH 8.0 ( $I = 0.01$  M) the minimal protein concentration of LSPC needed to form a stable emulsion ( $C_{cr}$ ) was comparable to the  $C_{cr}$  of soy protein isolate (SPI), which was used as a control. The  $C_{cr}$  increased with decreasing  $\zeta$ -potential and was highest at a pH around the pI; i.e. lowest  $\zeta$ -potential. A critical  $\zeta$ -potential ( $\zeta_{cr} \sim 11$  mV) for both LSPC and SPI was identified, below which flocculation occurs. LSPC-stabilized emulsions were stable against flocculation at a wider pH range ( $pH \leq 3.0$  and  $pH \geq 5.5$ ) than SPI-stabilized emulsions ( $pH \geq 5.5$ ). For both proteins,  $C_{cr}$  was higher at pH 8.0 and high ionic strength (0.5 M) than at low ionic strength (0.01 M). This was related to a calculated higher protein adsorbed amount at the interface ( $\Gamma_{max}$ ) at high ionic strength. Thus, the emulsion properties of both protein concentrates/isolates could be linked to their molecular properties. A main outcome from this study was that the experimentally determined  $d_{3,2}$  (at  $\zeta > \zeta_{cr}$ ) was in close agreement to the theoretically calculated  $d_{3,2}$ . For the calculation of the  $d_{3,2}$  the molecular characteristics (molecular mass, exposed hydrophobicity) of the most dominant proteins in the protein concentrate/isolate were used. Overall, it was concluded that the emulsion properties even of complex/non-pure systems, such as LSPC and SPI can be closely forecasted based on the molecular properties of their dominant proteins, taking also into account the presence of charged carbohydrates, and a small set of experiments.

To further evaluate the window of opportunity for LSPC, its foam properties were evaluated. Based on the results from **Chapter 3**, the emulsion properties of LSPC could be linked to its molecular properties. Thus, the hypothesis that was tested in **Chapter 4** was that also the foam properties of LSPC can be linked to its molecular properties. It was then expected that the approach recently developed to characterize the foam properties of pure-protein systems under various system conditions can be successfully applied even to more complex systems, such as LSPC and SPI. In this approach, the foaming properties of a protein are described using two critical protein concentrations;

the  $C_{crFA}$ , which is the minimal protein concentration ( $C_p$ ) needed to obtain maximal foam ability and  $C_{cr3,2}$ , which is the minimal  $C_p$  needed to obtain minimal bubble size. It was shown that, as observed for pure-protein systems, the foam ability of LSPC increased with  $C_p$  at all conditions tested. Furthermore, if only the soluble  $C_p$  is taken into consideration it was observed that the soluble  $C_{crFA}$  was constant as a function of pH, for both LSPC and SPI. At high ionic strength ( $I = 0.5$  M) both proteins were more efficient in foam formation than at low ionic strength ( $I = 0.01$  M). This was related to their faster adsorption at the interface. A minimum  $C_p$  was required to form stable foams. At pH 3.0 and 5.0 LSPC had higher foam stability than at pH 8.0. This was postulated to be due to the formation of aggregates between proteins or between proteins and charged carbohydrates. At high ionic strength less protein was required to form stable foams than at low ionic strength. Overall, the foam ability and foam stability as a function of  $C_p$  for these protein mixtures showed a similar trend as for pure protein-stabilized foams. Therefore, it was concluded that the use of critical protein concentrations to describe foam ability and foam stability, as developed for pure protein systems, can be applied to these mixed protein systems.

In **Chapters 3** and **4** it was shown that the emulsion and foam properties of LSPC are comparable to these of the widely used plant protein SPI, and in some cases LSPC showed functional properties comparable to these of whey protein isolates. Thus, overall SBL have a great potential as a source of functional proteins. However, to further increase the economic revenue from the exploitation of SBL a biorefinery approach needs to be followed. The design of a biorefining process is challenging due to the high number of products that can be obtained from one feedstock, and the fact that some products can be negatively affected by processing conditions that are essential for other products, as was highlighted in **Chapters 2, 3** and **4**. The knowledge acquired through the previous studies was used to adapt an existing product and process synthesis methodology. In particular, the product driven process synthesis (PDPS) methodology, which was earlier developed for structured products, was adapted to extend its use in biorefinery (**Chapter 5**). Four novel steps were introduced in the original PDPS: (1) decomposition of the feedstock into its main compound classes, (2) identification of the potential uses of the compound classes found in the feedstock, based on the functionalities that they can deliver, (3) selection of the product-targets by evaluating their economic potential, and (4) identification of "critical tasks"; i.e. tasks that negatively affect the quantity and/or quality of each product during their separation. To illustrate how this new approach can be used in practice, a case study of a sugar beet leaves biorefinery was presented.

In **Chapter 6**, the main conclusions obtained in the previous chapters were discussed with respect to data from other studies presented in literature. Typically, pressing is used for the extraction of proteins from leaves. In this thesis, it was found that blending leads to protein recovery higher than pressing alone or pressing in combination with pulsed electric field. In the majority of studies dealing with the extraction of leafy proteins a heating step at 50 – 60 °C is applied, which is suggested to remove the green color. In **Chapter 2**, it was shown than centrifugation of the extracted

juice (pH 8.0) at 38,400 *g* was adequate for the removal of green color in the case of SBL. A number of experiments were also performed to test the effect of heating at 50 °C and different pH values (pH 8.0 and pH 6.0) on green color removal during protein extraction from SBL. It was shown that green color removal after heating could only be achieved at pH 6.0, which indicates that the pH of the extracted juice plays a more significant role than the actual heating step for the green color removal. Furthermore, the effect of PPO on brown color formation and protein modification was addressed. It was shown in further experiments with SBL that the phenolic compounds that are not substrates for PPO also contribute to PPO- mediated browning. This shows that to accurately predict or explain PPO-mediated brown color formation in plant extracts it is important to obtain a detailed compositional analysis of individual phenolic compounds. Moreover, the role of charged carbohydrates in emulsions and foams stability was discussed. In previous chapters, it was shown that the use of the models/ approaches developed for the description of pure protein stabilized emulsions and foams can be used in more complex systems, such as LSPC and SPI. The use of these models/approaches reduce the number of experiments needed to satisfactorily define the window of opportunity of a novel protein.

---

# Acknowledgements

---

Most people would think that doing a PhD means that you put an order in the disorder (“ataxia”) of your thoughts and as such you become an expert in your field. For me though the PhD increased the entropy in my mind and in my life and made me realize that chaos has even larger dimensions. And for that I am grateful, and I would like to thank everyone that contributed in the amplification of “my” entropy and to reach this realization.

Allereerst wil ik mijn promotor Harry en mijn co-promotor Peter bedanken! Harry, heel erg bedankt voor alle constructieve discussies die we hebben gevoerd tijdens dit hele project. Ik ben me er van bewust dat ik niet de makkelijkste AIO uit je carrière was. Ook al gingen jouw Nedelandse charme en mijn Griekse spirit niet altijd hand in hand, onze samenwerking wierp altijd haar vruchten af. Hoe jij FCH aanstuurt, je oprechte betrokkenheid in alle lopende projecten en de begeleiding die je biedt aan al je studenten, ongeacht of het een bachelor student of een AIO is, maken jou een unieke leider en daarvoor heb je mijn eeuwige waardering. Peter I have forgotten already how many times I told you “I hate you for being right” and that’s my way of telling you how much I appreciate your constructive comments even on the 32<sup>nd</sup> version of our first article! I will never (never, never, never!) forget our endless meetings face-to-face, by phone, skype or even smoke signs at any point of the day or from any place of the world. Having you as a supervisor taught be that there is not only left or right but sometimes you need to go up or down to reach your goal! All-in-all Peter Alexander Wierenga thank you!

I would like to thank Jean-Paul for all the useful feedback and the diligent support throughout the project. Your positive attitude and your way of giving the harshest comments in the smoothest manner make the life of every PhD student a bit “sweeter”. Special thanks to my supervisor from Eindhoven (currently in Bremen) Edwin Zondervan. Edwin, you introduced me to another way of thinking and you showed me that there are so many ways to approach a problem. Your drawings to help me map my thoughts during our meetings are one of the most valuable lessons that I also used later to help my students.

The support of the ISPT could not go unacknowledged. Not only did ISPT supported the project financially but also organized high quality courses and conferences that helped all the partners (and especially the PhD students) to expand their network and to broaden their perspectives. My special thanks go also to Daniella for her tireless assistance to all my minor and major problems. Moreover, I would like to thank all our project partners and project leaders - Olivera, Nasim, Ardjan<sup>†</sup> - for keeping us all on track. Olivera I have an extra reason to thank you...for giving my cv a second look and inviting me for the first (the toughest until now!) interview! This project also gave me the opportunity to closely collaborate with COSUN. Edwin (Poesz) thanks so much for your diligent help, your assistance wherever and whenever needed and your great hospitality when working at COSUN. Tjerk thanks a million for running all the PEF experiments with me, for staying late at the lab for me and for reaching all the stuff from

the top shelves for me ;). Arjen I will never forget you on my first day (or should I say first few hours) at FCH when you showed up with four garbage bags full of sugar beet leaves that you had to collect in the rain so that I could start my experiments on time! Thanks a lot!!!! Of course I would like to thank “my ladies” –Aleksandra, Annewieke and Laura- the other three PhD students (Dr-s by now!) for all the help during the project, the fruitful discussions and the fun times we had during all this –not always MILD- DISCLOSURE of our PhD sub-projects.

Many thanks to my students: Dane, Bertus, Anita, Yorán, Luuk, Jessica who not only helped me with my (our!) project but also helped me to grow as a person through mentoring them. I hope I didn’t disappoint you (a lot!) through my sometimes nasty –though always good intended- comments and I wish you all the best for your future steps. Also, thanks to all the technicians, especially Rene (my lab’s technician!) for all the introductions to the new equipment but also for helping me out with equipment problem-solving and keeping everything running smoothly in the lab. The kind help from Unifarm is also gratefully acknowledged.

A HUGE “thank you” goes to Jolanda! Strange enough (this is ironic) Jolanda’s absence never goes unnoticed! Jolanda, you never stop to amaze me with your knowledge about everything, your exceptional organizational skills and your great memory! You are the neck of FCH, as nicely put in the movie “My big fat Greek wedding” (“the man is the head of the family but the woman is the neck”).

Many thanks to all my FCH colleagues who I can call friends by now! I truly think that there is no FCH-student that didn’t volunteer to run some of my samples or to help me with one or another equipment or to brainstorm about my - rarely ;) - weird data! When the time came for me to produce big amounts of sugar beet leaf proteins the whole FCH got involved. And it was then that I realized that if you want to produce large amounts of samples you either need pilot scale equipment or large scale friends. And I am lucky enough to have INDUSTRIAL scale friends! Overall, if there is one thing I learned in FCH this is: once an FCH-er always an FCH-er!

An enormous thanks to all my officemates all these years. The PhD office is a sacred place. What happens in the office stays in the office (well, most of the times!). Surrender, Annewieke, Red, Edita, Suzanne, Bianca, Sylvia thanks for sharing all the nice moments (experiments that worked out, articles that got accepted...) and the not-that-nice moments with me! Thanks for being patient with me when I was on the phone (rarely ;) ) or when I wanted to share my frustrations or when I was chewing my gum really loud while writing before meeting a deadline! Thanks for bringing me coffee and water and food when it felt there is no time to do anything else but writing! You are the best officemates ever!

Thanks to all my protein buddies - Anja, Surrender, Frederik, Roy, Emma, Yuxi, Claire, Yunus, Sergio, Hugo- for all the constructive feedback and great ideas that helped my research go forward. Roy thanks for sharing without any complaint (!) your lab-table with me, for helping me with the emulsion- and not only- experiments! You are the most annoying good person I ever met! Surrender mou thanks so much for always being there for me! For our long discussions during our night shifts, for teaching me “how to keep my hands away from the fire” (although I still don’t always do it) and for letting me be a small part of your great family. Surrender, Soumi and Bihu you are my dearest family. My dear friend Frederik how many long

discussions did we have about foam and proteins and oral presentations and travelling and our plans for the future? How many times did you guide me through the phone on how to fix the foam scan? How many nights did we decide to stay awake to explore the cities during our PhD trips? For all these and for being a real friend I thank you! My dear co-author Anne, I couldn't have asked for a better person to work with! Your patience, positive attitude and the fact that you can keep calm even under the most stressful situations are only a few of the characteristics that I admire on you! The sugar beet leaves project was so much more pleasant when shared with you! Thank you for everything! My little one (Annewieke) thanks so much for - without ever complaining (!) - answering my enzymatic browning questions for a million times, for keeping notes for me during our project meetings, for helping me decrypt Harry's handwriting, for trying to teach me how to make nice stukjes and for being there for me all these years!

My "el trio de la muerte" (Elisabetta, Patricia, Carla) nothing would have been the same without you around at FCH and in my life in general! I honestly don't know where to start...scientific discussions, co-authoring articles, brainstorming about "further" experiments and set-up of theses, coffee breaks, dinners, long weekends, holidays...the list is endless and sometimes it feels (for the people around us) that us four together is like having the Pandora's box open (:p), thus the name Eli's mother gave us couldn't describe us any better!

My dear Carla I also need to THANK YOU for accepting (although I don't remember giving you the option to refuse) to be my paranymph. You saved my sanity million times, you helped me meet deadlines and made me laugh even at the hardest times! Siempre estare agradecido! Muchas gracias! Καλή μου Σύλβια είσαι το άτομο που μπήκε πιο πρόσφατα από όλους στη ζωή μου κι όμως έχεις κατακτήσει ήδη εξέχουσα θέση! Είσαι πάντα εκεί να με ακούς να διαμαρτύρομαι, να γκρινιάζω, να περηφανεύομαι και με ένα μοναδικό τρόπο νιώθω ότι ξέρεις πως νιώθω πριν καν μιλήσω! Νομίζω ότι όχι άδικα σε λένε Kalli-Angel (= good angel)! Και φυσικά σε ευχαριστώ πολύ πολύ που είσαι το «παρανυφάκι» μου!

Φιλάκι σ'ευχαριστώ πολύ που με αντέχεις όλα αυτά τα χρόνια, που είσαι η φωνή της λογικής και που είσαι διατεθειμένη να μου πας κόντρα όταν πιστεύεις πως κάνω λάθος όταν κανένας άλλος δεν τολμά! Είσαι πραγματικά ατρόμητη! Menfil and son (Μενέλαε, Φιλίω και Ορέστη) you just make my day!!! Κοπελιά (Μαρία Νικηφόρου) σε ευχαριστώ τόσο πολύ για τις άπειρες ώρες κουβέντας σε ευρύ φάσμα θεμάτων: από τις σπουδές και τη δουλειά μέχρι τη ζωή στην Ολλανδία και στην Ελλάδα και ως το τί ρούχα να βάλω στην ορκωμοσία! Είσαι πάντα η αντικειμενικά δίκαιη Μαρία Νικηφόρου! Mijn lieve Desiree, bedankt voor jouw steun en jouw positieve energie! Jij bent de beste leraar en de liefste koubara! Συγκάτοικος και Edwin thank you so much for being such a great friend and for ALWAYS being there for us! Διπλανούλα μου, Πέτρο και Αγγελική σας ευχαριστώ πολύ για όλα τα χρόνια που είστε δίπλα μου. Ποιος να το περίμενε ότι ένα Erasmus στη Βιέννη και ένα κουτί μπισκότα με γέμιση πορτοκάλι θα μας έφερναν σήμερα εδώ! «Μανούλα» (Στέλλα), Δημήτρη, Θέμη και Υρώ ευχαριστώ πολύ που είστε τόσο χρόνια στη ζωή μου και με ακούτε αγόγγυστα να μιλάω για ψωμάκια χωρίς γλουτένη και «γρουμπαλάκια» και με αντέχετε ακόμη! Φίλη μου (Νατάσα), Σταύρο και μικρή Αύρα σας ευχαριστώ πολύ που όλα αυτά τα χρόνια για ό,τι και αν χρειαστεί είστε πάντα «μόνο ένα τηλεφώνημα» μακριά! Λίτσα μου σ'ευχαριστώ τόσο πολύ για όλη τη θετική σου ενέργεια και το τραγουδάκι σου («καλή επιτυχία») πριν από κάθε μεγάλη στιγμή!

Φυσικά τεράστιες ευχαριστίες για τους γονείς μου και την αδερφή μου, Εβίτα! Χωρίς αυτούς τίποτα δε θα ήταν δυνατό! Το ξέρω ότι δεν είμαι το πιο εύκολο παιδί που υπάρχει και ώρες ώρες (πάντα!) θαυμάζω την υπομονή σας! Θα είμαι για πάντα ευγνώμων για όλα τα εφόδια που μου δώσατε: από τις «Καλοκαιρινές διακοπές» που μου παίρνατε κάθε καλοκαίρι για να μην ξεχνάω τί είχα μάθει όλη την προηγούμενη χρονιά στο σχολείο και τα φροντιστήρια ξένων γλωσσών που με στέλνατε γιατί είχα κλίση στις ξένες γλώσσες μέχρι τα ταξίδια στο εξωτερικό για να «ανοίξουν τα μάτια μου»! Αδερφή μου με ξέρεις όσο κανείς άλλος. Συγγνώμη που συχνά σου κάνω τη ζωή δύσκολη και σε ευχαριστώ τόσoooooo πολύ που αγόγγυστα με υπομένεις όλα αυτά τα χρόνια!

αλεξάνδρα



---

## About the author

---

### CURRICULUM VITAE



Alexandra Kiskini was born on November 11<sup>th</sup> 1981 in Trikala, Greece. She has studied Food Science and Technology, with a specialization in Food Processing and Food Engineering, at the Agricultural University of Athens (AUA), Greece. In 2004, she moved to Vienna, as an Erasmus exchange student, to complete part of her BSc thesis at the University of Natural Resources and Life Sciences, Austria. In 2007, she obtained her first Research MSc in Food Technology and Nutrition also from AUA, Greece. Later, she worked as a researcher at Kaplanidis Mills S.A. in collaboration with the University of Thessaly, on developing sports nutrition supplements, while she was teaching various courses at the department of Food Technology at the Technological Educational Institute of Thessaly. In 2011, she acquired her second Research MSc in Nutrition and Metabolism from Maastricht University, The Netherlands. Afterwards, she started working at the Laboratory of Food Chemistry as a PhD student under the supervision of Prof. Dr Harry Gruppen and Dr Peter Wierenga. The results of her PhD research are presented in this thesis. Currently, Alexandra is working as a visiting researcher at the Laboratory of Neurobiology, Physiology & Behavior at the University of California, Davis.

Alexandra can be contacted at: [alexkisk@gmail.com](mailto:alexkisk@gmail.com)

## LIST OF PUBLICATIONS

1. Kiskini, A., Lech F. J., Delahaije R. J. B. M., Gruppen H., Wierenga, P. A., Foam properties of sugar beet (*Beta vulgaris* L.) leaf and soybean (*Glycine max*) proteins. *to be submitted*.
2. Kiskini A., Delahaije R. J. B. M., Wierenga, P. A., Gruppen H., Emulsion properties of sugar beet (*Beta vulgaris* L.) leaf and soybean (*Glycine max*) proteins. *submitted*.
3. Vissers, A.; Kiskini, A.; Hilgers, R. J.; Marinea, M.; Wierenga, P. A.; Gruppen, H.; Vincken, J. P., Enzymatic browning in sugar beet leaves (*Beta vulgaris* L.): Influence of caffeic acid derivatives, oxidative coupling and coupled oxidation. *Journal of Agriculture and Food Chemistry* **2017**, *65*, 4911-4920.
4. Kiskini, A.; Vissers, A.; Vincken, J. P.; Gruppen, H.; Wierenga, P. A., Effect of plant age on the quantity and quality of proteins extracted from sugar beet (*Beta vulgaris* L.) leaves. *Journal of Agriculture and Food Chemistry* **2016**, *64*, 8305-8314.
5. Kiskini, A.; Zondervan, E.; Wierenga, P. A.; Poiesz, E.; Gruppen, H., Using product driven process synthesis in the biorefinery. *Computers & Chemical Engineering* **2016**, *91*, 257-268.
6. Kiskini, A.; Hamer, H. M.; Wall, B. T.; Groen, B. B.; de Lange, A.; Bakker, J. A.; Senden, J. M.; Verdijk, L. B.; van Loon, L. J., The muscle protein synthetic response to the combined ingestion of protein and carbohydrate is not impaired in healthy older men. *Age* **2013**, *35*, 2389-2398.
7. Kiskini, A.; Difilippo, E., Oligosaccharides in goat milk: structure, health effects and isolation. *Cellular and Molecular Biology* **2013**, *59*, 25-30.
8. Kerasioti, E.; Stagos, D.; Jamurtas, A.; Kiskini, A.; Koutedakis, Y.; Goutzourelas, N.; Pournaras, S.; Tsatsakis, A. M.; Kouretas, D., Anti-inflammatory effects of a special carbohydrate-whey protein cake after exhaustive cycling in humans. *Food and Chemical Toxicology* **2013**, *61*, 42-46.
9. Wall, B. T.; Hamer, H. M.; de Lange, A.; Kiskini, A.; Groen, B. B.; Senden, J. M.; Gijzen, A. P.; Verdijk, L. B.; van Loon, L. J., Leucine co-ingestion improves post-prandial muscle protein accretion in elderly men. *Clinical nutrition* **2013**, *32*, 412-419.
10. Pennings, B.; Groen, B. B.; van Dijk, J.-W.; de Lange, A.; Kiskini, A.; Kuklinski, M.; Senden, J. M.; van Loon, L. J., Minced beef is more rapidly digested and absorbed than beef steak, resulting in greater postprandial protein retention in older men. *The American journal of clinical nutrition* **2013**, *98*, 121-128.
11. Hamer, H. M.; Wall, B. T.; Kiskini, A.; de Lange, A.; Groen, B.; Bakker, J. A.; Gijzen, A. P.; Verdijk, L. B.; Van Loon, L., Carbohydrate co-ingestion with protein does not further augment post-prandial muscle protein accretion in older men. *Nutrition and Metabolism (Lond)* **2013**, *10*, 15.
12. Kerasioti, E.; Kiskini, A.; Veskoukis, A.; Jamurtas, A.; Tsitsimpikou, C.; Tsatsakis, A. M.; Koutedakis, Y.; Stagos, D.; Kouretas, D.; Karathanos, V., Effect of a special

carbohydrate -protein cake on oxidative stress markers after exhaustive cycling in humans. *Food and Chemical Toxicology* **2012**, *50*, 2805-2810.

13. Kiskini, A.; Kapsokefalou, M.; Yanniotis, S.; Mandala, I., Effect of iron fortification on physical and sensory quality of gluten-free bread. *Food and bioprocess technology* **2012**, *5*, 385-390.
14. Schoenlechner, R.; Mandala, I.; Kiskini, A.; Kostaropoulos, A.; Berghofer, E., Effect of water, albumen and fat on the quality of gluten-free bread containing amaranth. *International journal of food science & technology* **2010**, *45*, 661-669.
15. Kiskini, A.; Kapsokefalou, M.; Yanniotis, S.; Mandala, I., Effect of different iron compounds on wheat and gluten-free breads. *Journal of the Science of Food and Agriculture* **2010**, *90*, 1136-1145.
16. Kiskini, A.; Argiri, K.; Kalogeropoulos, M.; Komaitis, M.; Kostaropoulos, A.; Mandala, I.; Kapsokefalou, M., Sensory characteristics and iron dialyzability of gluten-free bread fortified with iron. *Food chemistry* **2007**, *102*, 309-316.

## OVERVIEW OF COMPLETED TRAINING ACTIVITIES

### ***Discipline specific activities***

#### Conferences and meetings

- PSE2015/ESCAPE2015<sup>†</sup>, Copenhagen, Denmark, 2015
- 15<sup>th</sup> Food Colloids Conference<sup>†</sup>, Karlsruhe, Germany, 2014
- 6<sup>th</sup> workshop on Leaf senescence<sup>†</sup>, Versailles, France, 2013

#### Courses

- PDPS course (TU/e), Eindhoven, The Netherlands, 2013
- Industrial proteins (VLAG), Wageningen, The Netherlands, 2013
- Advanced food analysis<sup>†</sup> (VLAG), Wageningen, The Netherlands, 2013
- Reaction kinetics in food science (VLAG), Wageningen, The Netherlands, 2012
- Biorefinery for biomolecules, (VLAG), Wageningen, The Netherlands, 2012

#### ***General courses***

- Carousel (WSG), Wageningen, The Netherlands, 2014
- Career perspectives (WSG), Wageningen, The Netherlands, 2014
- Open innovation (ISPT), Amersfoort, The Netherlands, 2014
- Voice matters-Voice and presentation skills training (WSG), Wageningen, The Netherlands, 2014
- Scientific writing (WSG), Wageningen, The Netherlands, 2013
- Project and time management (WSG), Wageningen, The Netherlands, 2013
- Interpersonal communication for PhD students (WSG), Wageningen, The Netherlands, 2012
- PhD competence assessment (WSG), Wageningen, The Netherlands, 2012
- PhD introduction week (VLAG), Venlo, The Netherlands, 2012

#### ***Optionals***

- Food Chemistry PhD trip, Germany, Denmark, Sweden, Finland<sup>†‡</sup>, 2014
- Food Chemistry PhD trip, Singapore and Malaysia<sup>†‡</sup>, 2012
- Food Chemistry PhD presentations, Wageningen, The Netherlands, 2011-2016
- Food Chemistry BSc/MSc students presentations and colloquia, Wageningen, The Netherlands, 2011-2016

#### ***Used symbols and abbreviations:***

- <sup>†</sup>Poster presentation; <sup>‡</sup> Oral presentation
- VLAG: Graduate School for Nutrition, Food Technology, Agrobiotechnology and Health Science
- TU/e: Technical University of Eindhoven
- WSG: Wageningen Graduate School
- ISPT: Institute for Sustainable Process Technology

The work described in this thesis was performed at the Laboratory of Food Chemistry, Wageningen University & Research. This research was sponsored by the Institute for Sustainable Process Technology (ISPT), project number: FO-10-06.

Financial support from Wageningen University for printing this thesis is gratefully acknowledged.

Cover design by Christina Kiskini

Printed by Proefschrift-AIO, the Netherlands

Alexandra Kiskini, 2017

